

THE STRUCTURE AND STABILITY OF SIMPLE TRI-IODIDES

by

ANTHONY JOHN THOMPSON FINNEY B.Sc. (Hons.)

submitted in fulfilment of the requirements

for the Degree of

Doctor of Philosophy

UNIVERSITY OF TASMANIA

HOBART

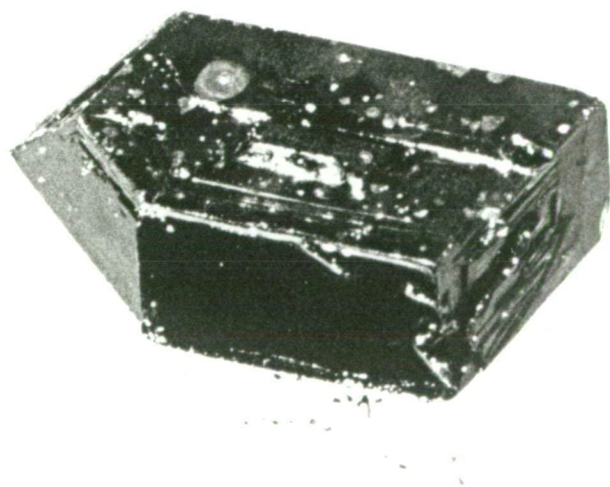
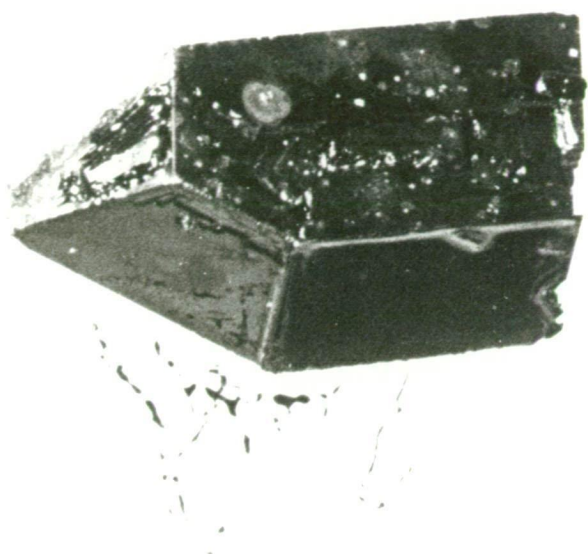
OCTOBER, 1973

Conferred April 1974

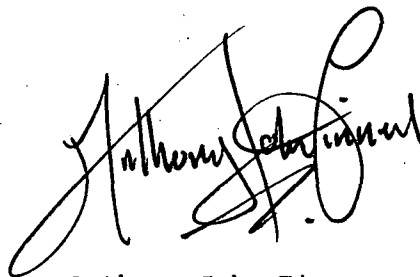
Frontispiece (reproduced as Plate 6 - 1, Chapter 1) - two

views of a large single crystal of $\text{KI}_3 \cdot \text{H}_2\text{O}$. The dimensions

of this specimen were approximately 3.0 cm x 1.5 cm x 0.5 cm.



This thesis contains no material which has been accepted for the award of any other degree or diploma in any University, and to the best of my knowledge and belief, this thesis contains no copy or paraphrase of material previously published or written by another person, except where reference is made in the text of this thesis.

A handwritten signature in black ink, appearing to read 'Anthony John Finney', with a large, stylized flourish at the end.

Anthony John Finney

Contents

	page
Abstract	(iv)
Acknowledgements	(vii)
Chapter 1 - The Structure and Stability of Simple Tri-iodides	1
Chapter 2 - The Theoretical Basis of X-Ray Structural Analysis	32
Chapter 3 - The Crystallographic Program Suite	50
Chapter 4 - The Refinement of the Structure of NH_4I_3	94
Chapter 5 - The Solution of the Structure of RbI_3	115
Chapter 6 - The Solution of the Structure of $\text{KI}_3 \cdot \text{H}_2\text{O}$	135
Chapter 7 - Discussion of the Inter-relation of Structure and Stability	201
Bibliography	255
Appendix A - Programming Details	267
Appendix B - Density Determinations	286
Appendix C - Derivation of the Unit Cell Constants of $\text{KI}_3 \cdot \text{H}_2\text{O}$	292
Appendix D - I_3^- force constant Calculation	299
Appendix E - Publications	311

THE STRUCTURE AND STABILITY OF SIMPLE TRI-IODIDES

Abstract

In this work the simple tri-iodides are regarded as being those in which the crystal lattice contains only cations, tri-iodide anions and possibly solvate molecules. The alkali metal tri-iodides CsI_3 and $\text{KI}_3 \cdot \text{H}_2\text{O}$ exemplify compounds of this type; polyiodides like the penta-iodide $(\text{CH}_3)_4\text{NI}_5$ or the hepta-iodide $(\text{C}_2\text{H}_5)_4\text{I}_7$, in which it is known that the anionic group is made up of I_3^- units accompanied by iodine molecules, are not encompassed by this study. In the solid state the simple tri-iodides exhibit a wide range of stability, and the probable causes underlying this range in behaviour are reviewed against existing knowledge concerning the crystalline structure and current models of the anion bonding of these compounds. The presence of solvate molecules in the lattice has a profound effect upon the stability of the simple tri-iodides; also among the unsolvated species there is a range in stability which can be attributed to differences in the electrostatic environment experienced by the anion. This sensitivity to electrostatic environment is reflected in small differences in the geometric configuration of the anion among the unsolvated tri-iodides as revealed by crystal structure analysis.

As the number of accurately known simple tri-iodide structures is small, the structure of NH_4I_3 was refined and the structure of RbI_3 and the hydrated species, $\text{KI}_3 \cdot \text{H}_2\text{O}$, were determined by the X-ray crystallographic method. A preliminary to this work, made necessary by the unusual features of the only available computing facilities, was the development of a complete integrated suite of crystallographic programs. Using the single crystal X-ray diffraction technique in conjunction with this program suite the accuracy with which the geometry of the I_3^- group

in NH_4I_3 is known was significantly improved. The structural analysis of RbI_3 proved that this compound was isostructural with CsI_3 , as had been anticipated on the basis of the known isomorphism of these two tri-iodides. In the case of $\text{KI}_3 \cdot \text{H}_2\text{O}$, the structure differs from that of the unsolvated simple tri-iodides (which all crystallize with unit cells having centrosymmetric orthorhombic symmetry) in that this compound possesses a noncentrosymmetric monoclinic cell. However, both $\text{KI}_3 \cdot \text{H}_2\text{O}$ and the unsolvated tri-iodides share the same planar structural motif defined by the relative arrangement of cations and anions in the cell.

On the basis of the extended body of structural data made available by the examination of these compounds, it was shown that the stability of the simple tri-iodides can be qualitatively and quantitatively related to two effects. The first of these is the stabilizing influence of electronic interactions between neighbouring I_3^- groups within the planar structure motif. The second is the destabilizing influence of any asymmetry in the electrostatic field experienced by the terminal atoms of the anion. The stability of the unsolvated species is determined by the balance struck between these two effects. It is suggested that in the case of the solvated simple tri-iodides, the presence of solvate molecules leads to a reduction in the destabilizing effect due to crystal field asymmetry, and that for this class of compounds their stability is largely conditioned by the strength of cation-solvate and solvate-solvate interactions.

The crystal chemistry of this class of compounds can be systematized by regarding the common simple tri-iodide structural motif as a variant of the structure of solid iodine on the one hand, and the penta-iodide structure on the other. Further, for those very stable tri-iodides which are solvated by organic molecules of moderate size so that

the charged species interpenetrate a continuous hydrogen-bonded organic substructure, the dominance of their behaviour by the solvate-solvate interaction appears to be accompanied by the severe modification or loss of the structural motif.

Acknowledgements

It is a pleasure to acknowledge my indebtedness to my supervisor, Dr. G.H. Cheesman; firstly, for introducing me to the problems of polyhalogen chemistry, and secondly for his sustained encouragement, advice and valued criticism throughout the extended period occupied by this work. Thanks are also due to my colleague, Mr. W.F. Donovan, for many useful discussions concerning the development of the crystallographic program suite in particular, and the art of X-ray structural analysis in general. At the same time I would like to acknowledge helpful discussions held with past and present members of the staff of the Chemistry Department of the University of Tasmania, and also to thank Professor H. Bloom for making it possible for this project to be undertaken in this Department.

I am also indebted to the staff of the Hydro-University Computing Centre; in particular to its Director, Mr. J. Boothroyd, for his deep interest in the special problems of crystallographic computer programming. In this connection I would like to acknowledge the hospitality and assistance given to me by Dr. B. Gatehouse and the members of the crystallographic group at the Department of Chemistry, Monash University.

These acknowledgements would be incomplete without reference to the help given at various stages during this project by the members of the workshop staff of the Chemistry Department. I would also like to record my indebtedness to Mrs. H. Hen for her assistance with the preparation of the graphic material included in this work, and to

Mrs. B. Dix who has cheerfully undertaken the demanding task of typing the text.

Lastly, I gratefully acknowledge the understanding support given throughout this project by my wife and children; this work is respectfully dedicated to them in recognition of a display of tolerance beyond the call of family duty.

A.J. Finney, October 1973.

Chapter 1 - The Structure and Stability of Simple Tri-iodides

	page
1 - 1 Introduction and Historical Perspective	2
1 - 2 Polyiodide Stability	5
1 - 3 Stability and Solvation	8
1 - 4 Polyiodide Structural Data	15
1 - 4 - 1 CsI_3	15
1 - 4 - 2 NH_4I_3	15
1 - 4 - 3 $(\text{C}_2\text{H}_5)_4\text{NI}_3$	15
1 - 4 - 4 $(\text{C}_6\text{H}_5)_4\text{AsI}_3$	16
1 - 4 - 5 $(\text{C}_5\text{H}_5)_2\text{FeI}_3$	17
1 - 4 - 6 CsI_4	17
1 - 4 - 7 $(\text{CH}_3)_4\text{NI}_5$	18
1 - 4 - 8 $(\text{C}_2\text{H}_5)_4\text{NI}_7$	18
1 - 4 - 9 $(\text{CH}_3)_4\text{NI}_9$	20
1 - 4 - 10 $\text{K}_2\text{I}_4 \cdot 6(\text{CH}_3\text{CONHCH}_3)$	22
1 - 4 - 11 $\text{HI}_3 \cdot 2(\text{C}_6\text{H}_5\text{CONH}_2)$	22
1 - 4 - 12 $\text{HI}_5 \cdot 2(\text{C}_{10}\text{H}_{13}\text{O}_2\text{N})$	23
1 - 5 Polyiodide Bonding in relation to Stability and Structure	24
1 - 6 The Aim of this Work	28

1 - 1 Introduction and Historical Perspective

Observations which suggested that halogen or interhalogen molecules would interact with halides to form a complex species were made from the beginnings of modern chemistry. In 1814 Gay-Lussac made the following comment -

"All of the hydroiodates (iodides in modern terminology) have the property of dissolving iodine abundantly, thereby becoming strongly coloured reddish-brown. But they only retain the iodine with very feeble force; for they give it up on boiling or evaporation in air; moreover, the iodine does not change the neutrality of the hydroiodates (iodides) and the reddish-brown colouration of the liquid, similar to that of other solutions of iodine, is a new proof of the feebleness of the combination"
(Gay-Lussac [1814]).

In 1819 Pelletier and Caventou [1819] described a new compound, which they named 'hydroiodure ioduré', formed by the addition of iodine to strychnine. This compound was in all probability strychnine polyiodide, $C_{21}H_{23}O_2N_2I_3$. Their work, published in *Annales de chimie et de physique*, has some significance as it is the first report of a polyhalogen complex in the literature. The first account of a polyhalogen complex of an inorganic cation was published in 1839 in a series of four papers by Filhol [1839a, 1839b, 1839c, 1839d] in which he described the preparation and reactions of the compound potassium tetrachloroiodate, $KICl_4$. In 1860 Baudrimont [1860] advanced evidence against the existence of compound formation between iodine and potassium iodide in aqueous solution. He observed that dissolved iodine could be completely removed from solutions of iodine in aqueous potassium iodide by repeated extraction with carbon disulphide. The same view was taken by Dossios and Weith [1869] who determined the solubility of iodine in strong solutions of potassium iodide. They

observed that the solubility of iodine increased with increasing strength of the potassium iodide solution, and conversely that free iodine was precipitated when such strong solutions were diluted. They regarded this as proof that true compound formation did not take place.

Tilden [1850] and Jorgensen [1856a] subsequently reported a number of new solid alkaloid tri-iodides; and Jorgensen [1856b], in seeking an explanation for the enhanced solubility of iodine in solutions of potassium iodide, advanced the hypothesis that this behaviour (and the results of the extraction experiments) could be explained by assuming partial dissociation of the complex in solution. As a consequence, any removal of iodine from the solution would result in a shift of the equilibrium, leading to the eventual complete dissociation of the compound.

The reservations held concerning the existence of the tri-iodide species were at least partially removed by Johnson's report in 1877 of the preparation of crystalline potassium tri-iodide by the slow evaporation of an iodine saturated solution of potassium iodide, and his further description in 1878 (Johnson [1878]) of the preparation by the same technique of ammonium tri-iodide. The determination of the freezing-point depression of potassium iodide solutions by iodine made in 1890 by Noyes and Le Blanc [1890] showed that in solution the complex carried only one negative charge, but did not allow the exact formula of the anionic species to be determined. The two lines of evidence for the existence of the I_3^- complex, the solution studies on the one hand and the preparative work on the other, were finally drawn together by Jakowkin [1894, 1895, 1896]. He showed, as a result of extensive quantitative distribution experiments, that the complex in solution has the formula I_3^- . The work of many chemists since has shown that a large number and variety of polyhalogen compounds can be formed by the union of halides with halogens or interhalogens. The literature concerning this family

of compounds is now voluminous, and a number of reviews in this field have been published (Grinell-Jones [1930], Cremer and Duncan [1931a, 1931b, 1932, 1933], Gmelin [1933], Sidgwick [1950], Wiebenga *et alii* [1961], Rundle [1963], Stepin *et alii* [1965] and most recently Popov [1967]).

The generalized formula $X_p Y_q Z_h^\pm$ may be used to represent polyhalogen ions, X , Y and Z denoting either identical or different halogen atoms. The sum $p+q+h$ is in most cases an odd number equal to or less than nine (the 'odd-number rule'). The majority of polyhalogen ions known are anionic, and in the past these have been described as addition products resulting from the action of a halide ion acting as a Lewis base upon a halogen or interhalogen molecule or molecules behaving as Lewis acids. However, cationic polyhalogen species have recently been reported, and these cannot be accommodated in this simple scheme. The cationic polyhalogens have been reviewed in detail elsewhere (Gillespie and Morton [1971], and as they stand outside the scope of this work, they will not be considered further.

With the possible exception of the polyastatides (Appelman [1960]), the polyiodides - with which this study is primarily concerned - are the most stable representatives of the class of polyhalide complexes. It is interesting to note that apart from the polybromide $KBr_6 \cdot 1.5 H_2O$ (Harris [1932]), all the examples of the breakdown of the 'odd-number rule' are found among the polyiodides. The first of these to be reported, CsI_4 , was accepted with considerable reluctance. This was only completely dispelled when an X-ray structural determination (Havinga *et alii* [1954]) demonstrated that the compound should be more properly formulated as the dimer Cs_2I_8 , the I_8^{--} anion being interpreted as a loose assemblage of I_3^- ions and iodine molecules. That this formulation is the correct one is supported by the observation (Hubard

[1942] that Cs_2I_8 is diamagnetic. By analogy, the diamagnetic polyiodide $\text{LiI}_4 \cdot 4\text{H}_2\text{O}$ reported by Cheesman and Nunn [1964] may perhaps be expected to have the formula $[\text{Li}(\text{H}_2\text{O})_4]_2\text{I}_8$. In the case of the hydrated sodium polyiodides $\text{NaI}_4 \cdot 2\text{H}_2\text{O}$ and $\text{NaI}_2 \cdot 3\text{H}_2\text{O}$ (Cheesman *et alii* [1940]), these may equally well be regarded as double salts ($\text{NaI}_3 \cdot \text{NaI}_5 \cdot 4\text{H}_2\text{O}$ and $\text{NaI} \cdot \text{NaI}_3 \cdot 6\text{H}_2\text{O}$). However it must be noted that Briggs *et alii* [1941] have raised doubts concerning the precise formulation of these species, and these may not be resolved until structural determinations have been carried out. In any event, the 'odd-number rule' must evidently be treated with caution, as polyiodide formation exhibits a variety of phenomena which require something more than simple valence considerations for their explanation.

1 - 2 Polyiodide Stability

All polyiodides dissociate on exposure to the atmosphere to the iodide and iodine (plus solvent, if solvated) under normal conditions of temperature and pressure. For some, like $\text{KI}_3 \cdot \text{H}_2\text{O}$ for example, this process is very rapid, going to completion in a matter of minutes. For others, of which $(\text{CH}_3)_4\text{NI}_3$ affords an example, decomposition is very slow and can only be detected after the passage of some weeks. The compounds can be stored indefinitely at equilibrium with their dissociation products in sealed containers.

A measure of the stability of the polyiodides can be gained from the data of Ephraim [1917], who measured the temperature at which the dissociation pressure of iodine over the polyiodides of caesium and rubidium reached one atmosphere. He found this temperature to be 250°C and 192°C respectively. His dissociation pressure/temperature data for these two compounds is represented as a $\ln p$ versus $1/T^\circ\text{K}$ plot in Figure 1 - 1.

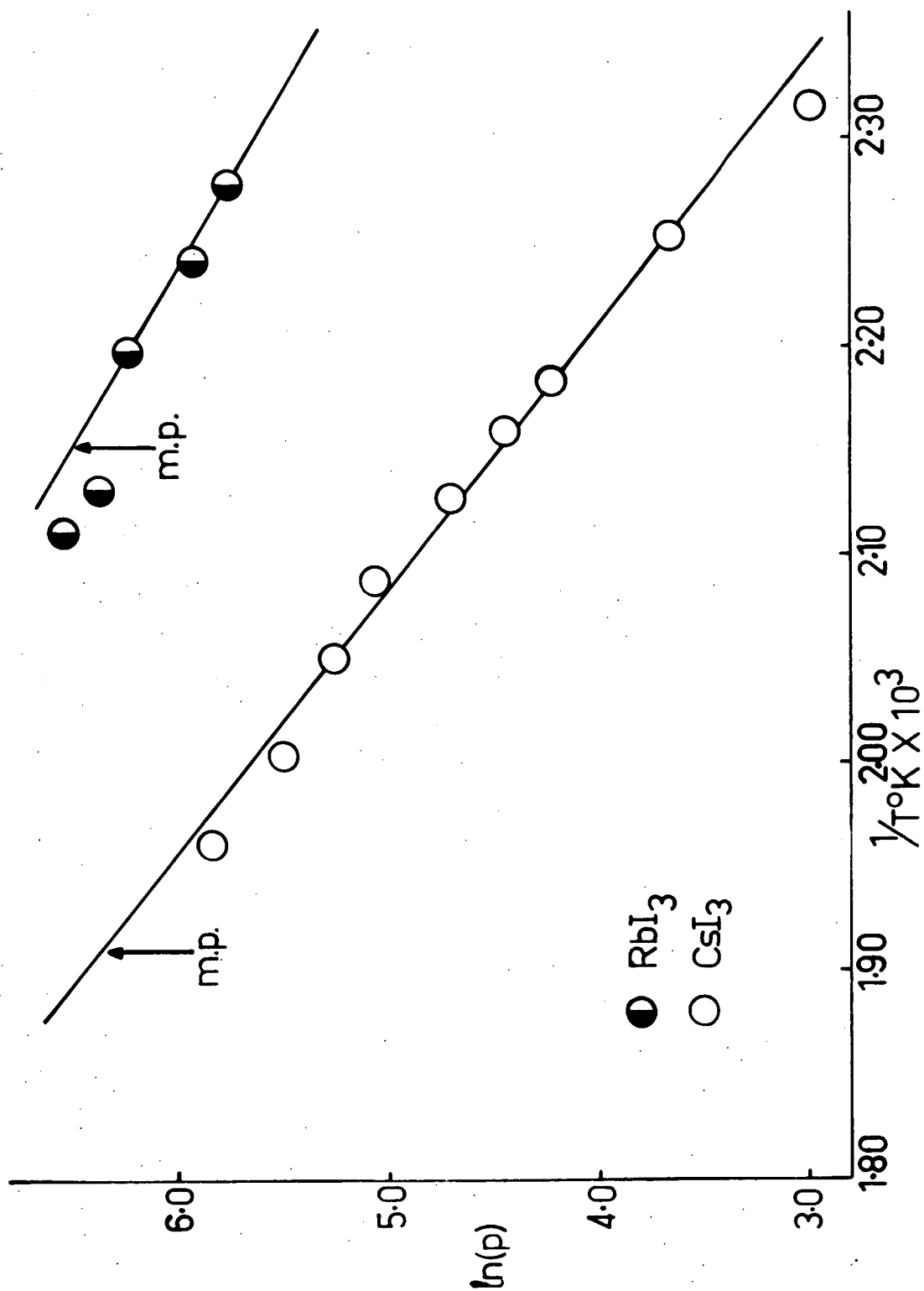


Figure 1 - 1, $\ln p$ versus $1/T^\circ\text{K}$ for CsI_3 , RbI_3
(taken from Ephraim [1917]).

Another and perhaps more precise measure of the relative stability of the polyiodides was devised by Cremer and Duncan [1931b]. Polyhalide salts were suspended in carbon tetrachloride, in which solvent both the parent halide and the derived polyhalogen compound are insoluble. The determination of free halogen in solution after equilibration gave an indication of the stability of the polyhalide in question. In Table 1 - 2 their results for the tri-iodide species are presented.

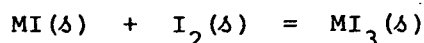
Table 1 - 1

Concentration of halogen in equilibrated polyhalide salt - CCl_4 System

Cation	Concentration (eq/litre)
Cs	0.00075
Rb	0.0059
NH_4	0.0120

The results presented in Table 1 - 1 indicate the instability of the polyiodides under normal conditions of temperature and pressure. They also show that the size of the cation has a pronounced effect on the stability of the tri-iodide species, and Cremer and Duncan [1931b] have shown that a parallel trend is exhibited by the mixed trihalides IBr_2^- , ICl_2^- and IBrCl^- . It appears that this characteristic reflects both the weakness of the bonding within the anionic polyiodide group and its sensitivity to its immediate environment. For example; caesium tri-iodide, CsI_3 , is easily prepared from aqueous solution as an anhydrous, black crystalline solid which is stable up to 115°C , at which temperature decomposition occurs with loss of iodine. On the other hand, the analogous potassium compound can be prepared only as a relatively unstable, highly deliquescent hydrate, which melts incongruently at 30°C .

The influence on stability of the size of the cation can also be seen in the trend of the thermodynamic data determined from electrochemical measurements for the reaction:



In Figure 1 - 2 the values of ΔG° and ΔH° determined by Topol [1967] at 25°C for this reaction for caesium, rubidium and ammonium have been plotted against r_+ , the cation radius. Here r_+ is taken (Cotton and Wilkinson [1972]) as 0.97, 1.33, 1.43, 1.48, and 1.68 Å for Na^+ , K^+ , NH_4^+ , Rb^+ and Cs^+ respectively. From the trend of the points plotted in this Figure, it can be seen that the thermodynamic data are in complete accordance with the results of the vapour pressure and solution studies. Extrapolation of the trend indicates that in the case of sodium it is highly probable that both ΔG° and ΔH° are positive, while in the potassium system the values are probably close to zero. Such a conclusion is not at variance with the observation that unsolvated potassium and sodium polyiodides are not formed at 25°C. As the same study reports ΔG° to be only slightly dependent on temperature in these systems, it is not likely that unsolvated forms would be stable at reduced temperatures.

The effect of cation size on polyiodide stability is also reflected in the behaviour of the larger polyiodide ions; for example, the large anion I_9^- does not form a solid unsolvated compound with the caesium cation. However, it can form stable unsolvated crystalline compounds with large singly-charged organic cations; as for example with the tetramethylammonium and trimethylphenylammonium cations.

1 - 3 Stability and Solvation

Historically, the sensitivity to the crystalline environment displayed by polyiodide anions has complicated the characterization of this group of

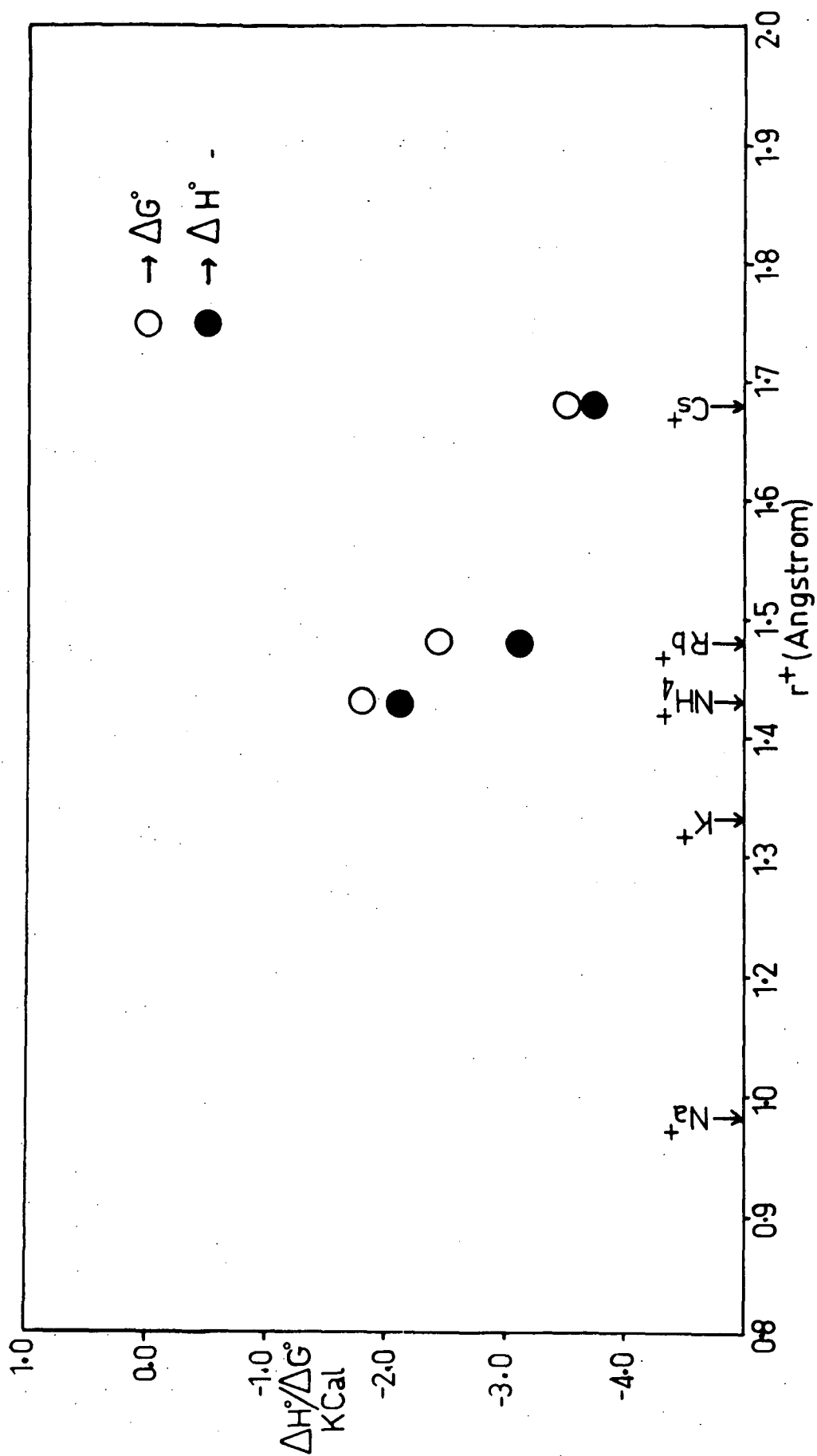


Figure 1 - 2, ΔG° and ΔH° versus r_+ for CsI_3 , RbI_3 and NH_4I_3 (taken from Topol [1967]).

compounds. The contrasting histories of ammonium and potassium tri-iodide are illustrative of the problems which have been encountered in this field. Both these compounds were first described by Johnson [1877, 1878]. The existence of ammonium tri-iodide was generally accepted, but the potassium polyiodide became, for more than half a century, the subject of much controversy and some acrimonious debate (Bancroft *et alii* [1931]). In 1931 the question of this compound's existence was finally resolved by Grace [1931]. He recognized the possibility of hydration, and by a careful phase study of the system $KI-I_2-H_2O$ at $0^\circ C$ clearly demonstrated the formation of the hydrate $KI_3 \cdot H_2O$ at this temperature. In this work Grace made a key contribution to the understanding of polyhalide chemistry, as he showed that many of the anomalous and previously puzzling properties of polyhalides could be understood if the hypothesis of solvation were accepted (Grace [1933]). In view of the long period which elapsed between the initial description and final confirmation of the existence of a tri-iodide of potassium, in contrast to the ammonium compound, it is perhaps ironic that as a result of a subsequent detailed study of the $NH_4I-I_2-H_2O$ system, Briggs *et alii* [1940] demonstrated the existence of a previously unsuspected ammonium tri-iodide trihydrate. This hydrated compound melted incongruently at $7^\circ C$ to give the unsolvated form discovered by Johnson [1878].

Water is not the only molecule which is known to stabilize poly-iodide structures. In fact, a considerable range of organic molecules are known which will also perform this function. It includes benzene, benzonitrile, acid amides, certain formic and oxalic esters, imides and anilides, and certain quasi alkaloids. Representative compounds of this type are given in Table 1-2. It should be noted that these compounds can be distinguished from those polyiodides in which the structure is stabilised by large organic cations.

TABLE 1 - 2

Polyiodides crystallizing with organic solvate molecules

Compound	Reference
$2\text{CsI}_9 \cdot 3(\text{benzene})$	Foote & Bradley (1933)
$\text{HI}_3 \cdot 4(\text{benzonitrile})$	Martin (1932)
$\text{LiI}_3 \cdot 4(\text{benzonitrile})$	"
$\text{NaI}_3 \cdot 2(\text{benzonitrile})$	"
$\text{KI}_3 \cdot 2(\text{benzonitrile})$	"
$\text{K}_2\text{I}_4 \cdot 6(\text{N-methylacetamide})$	Toman, Honzl & Jecny (1965)
$\text{HI}_3 \cdot 2(\text{benzamide})$	Moore & Thomas (1914)
$\text{NaI}_3 \cdot 3(\text{benzamide})$	Reddy, Knox & Robin (1963)
$\text{NaI}_5 \cdot 4(\text{diethyloxalate})$	Skrabal & Flach (1919)
$\text{KI}_3 \cdot 2(\text{diethylmethylorthoformate})$	"
$\text{CaI}_6 \cdot 6\text{H}_2\text{O} \cdot 6(\text{succinimide})$	Snook (1967)
$\text{HI}_5 \cdot 2(\text{phenacetin})$	Emery (1926)
$\text{HI}_3 \cdot 2(\text{trephenin})$	"
$\text{HI}_3 \cdot 2(\text{methacetin})$	"
$2\text{HI}_5 \cdot 3(\text{antipyrine})$	Emery & Palkin (1916)
$\text{HI}_4 \cdot 1(\text{pyramidone})$	"

On the basis of these data it is possible to make the following generalization: within the family of polyiodide compounds the requirement for some solvate molecule to stabilize the polyiodide anion sufficiently to allow the formation of solid crystalline compounds under normal laboratory conditions becomes apparent when the cation is small or when the anion is large. The numerous solvated polyiodides of H^+ , Li^+ , Na^+ , and K^+ cited above furnish examples of the first situation, and the benzene solvated caesium enneaiodide is an example of the second. In the case of the doubly solvated calcium hexaiodide it is possible that both conditions are present. The question that then arises concerns the nature of the role, or roles other than simple cation solvation, performed by these solvate molecules which makes it possible for solid crystalline polyiodide compounds to be formed when one or other or both of these circumstances prevail.

This question may best be considered against the background of the available information concerning the structures exhibited by the polyiodides and the conclusions concerning the nature of the bonding in the polyiodide anion which have been drawn from this information. The structural information available for the polyiodides has been gained in its entirety by the application of the X-ray diffraction technique. In fact, certain of the triiodides were among the first compounds to be examined by this technique when it was still relatively novel (Bozorth and Pauling [1925]). As the number of polyiodide compounds which have been subjected to X-ray crystallographic structural analysis is not large, and the reports are somewhat scattered in the literature, the results of the structural determinations are given in some detail below and the crystallographic data are gathered together in Table 1 - 4.

TABLE 1-4

Structural Data for Polyiodides

Compound	Space Group	Cell Dimensions Å°	Molecules/Cell	Reference
CsI_3	Pnma	a = 11.09 b = 6.86 c = 9.98	4	Bozorth & Pauling (1925) Tasman & Boswijk (1955) Runsink, Swen-Walstra & Migchelsen (1972)
NH_4I_3	Pnma	a = 10.819 b = 6.640 c = 9.662	4	Mooney (1935) Cheesman & Finney (1970)
$(\text{C}_2\text{H}_5)_4\text{NI}_3^- \text{ (I)}$	Cmca	a = 14.207 b = 15.220 c = 14.061	4	Migchelsen & Vos (1967)
$(\text{C}_2\text{H}_5)_4\text{NI}_3^- \text{ (II)}$	Pnma	a = 14.522 b = 13.893 c = 15.156	4	Migchelsen & Vos (1967)
$(\text{C}_6\text{H}_5)_4\text{AsI}_3$	P2/n	a = 15.34 b = 7.63 c = 10.63 $\beta = 93.4^\circ$	2	Mooney-Slater (1958) Runsink, Swen-Walstra & Migchelsen (1972)
$(\text{C}_5\text{H}_5)_2\text{FeI}_3$	$\text{R}\bar{3}\text{m}$	a = 8.522 c = 17.05	1	Bernstein & Herbstein (1968)
CsI_4	$\text{P}2_1/\text{a}$	a = 11.19 b = 9.00 c = 10.23 $\beta = 114^\circ$	4	Havinga, Boswijk & Wiebenga (1954)
$(\text{CH}_3)_4\text{NI}_5$	C2/c	a = 13.34 b = 13.59 c = 8.90 $\beta = 107^\circ$	4	Hach & Rundle (1951) Brockema, Havinga & Wiebenga (1957)

TABLE 1-4 cont.

Compound	Space Group	Cell Dimensions Å°	Molecules/Cell	Reference
$(C_2H_5)_4NI_7$	Abam	a = 11.5 b = 15.66 c = 12.37	4	Havinga & Wiebenga (1955)
$(CH_3)_4NI_9$	$P2_1/n$	a = 11.60 b = 15.00 c = 13.18 $\beta = 95^\circ$	4	James, Hach, French & Rundle (1955)
$K_2I_4 \cdot 6(CH_3CONHCH)_3$	$P\bar{3}1c$	a = 12.2 c = 15.2	4	Toman, Honzl & Jecny (1965)
$HI_3 \cdot 2(C_6H_5CONH_2)$	$P\bar{1}$	a = 20.828 b = 9.885 c = 9.588 $\alpha = 95^\circ$ $\beta = 101^\circ$ $\gamma = 94^\circ$	4	Reddy, Knox & Robin (1964)
$HI_5 \cdot 2(C_{10}H_{15}O_2N)$	$P\bar{1}$	a = 12.441 b = 10.67 c = 5.87 $\alpha = 103.3^\circ$ $\beta = 103.7^\circ$ $\gamma = 87.3^\circ$	1	Herbstein & Kapon (1972)

1 - 4 Polyiodide Structural Data

1 - 4 - 1 Caesium tri-iodide, CsI_3

Preliminary investigation by R.M. Bozorth & L. Pauling (1925)

Structural determination by H.A. Tasman & K.H. Boswijk (1955)

Refinement by J. Runsink *et alii* (1972)

This compound crystallizes in space group *Pnma* with cell dimensions $a_0 = 11.09$, $b_0 = 6.86$, $c_0 = 9.98 \text{ \AA}$. Individual tri-iodide ions can be discerned lying in layers which also contain the caesium cation. These layers are at right angles to the *b*-axis and cut it at $y = \frac{1}{4}$ and $y = \frac{3}{4}$. The tri-iodide group is asymmetric with interbond distances of 2.82 and 3.10 \AA ; the interbond angle is 176° . The average non-bonded inter-iodine distance is 4.34 \AA .

1 - 4 - 2 Ammonium tri-iodide, NH_4I_3

Initial determination by R.C.L. Mooney (1935)

Refinement by the author (1969) (see Chapter 4)

This compound is isomorphous and isostructural with CsI_3 , but has a slightly smaller cell: $a_0 = 10.819$, $b_0 = 6.640$, $c_0 = 9.662 \text{ \AA}$. The asymmetric tri-iodide group has interiodine distances of 2.791 and 3.113 \AA . The anion is linear to within 0.1° , and there is one tri-iodide - nitrogen distance significantly shorter than the others, which may be evidence for a form of hydrogen bonding with the possibility of rotation or torsion of the ammonium group about the N-H...I axis.

1 - 4 - 3 Tetraethylammonium tri-iodide, $(\text{C}_2\text{H}_5)_4\text{NI}_3$

Structural determination by T. Mighelsen and A. Vos (1967)

Tetraethylammonium tri-iodide crystallizes from methanolic solution in two distinct crystalline modifications. Both forms have orthorhombic symmetry and contain eight formula units in the unit cell. Modification

I belongs to space group $Cmca$ with cell dimensions $a_o = 14.207$, $b_o = 15.220$ and $c_o = 14.061 \text{ \AA}$; and modification II belongs to $Pnma$ with dimensions $a_o = 14.522$, $b_o = 13.893$ and $c_o = 15.156 \text{ \AA}$. Both forms have two crystallographically independent tri-iodide groups and in both cases these are situated on mirror planes. The arrangement of the tri-iodide anions within these planes or layers in both compounds is similar, but the stacking of the layers is different. In modification II the layers are almost exactly superimposed, but in I the successive layers suffer a shift of half a cell translation in the y direction. In both modifications the cations lie in holes formed by the eight I_3^- groups.

In modification I the special position occupied by the tri-iodide ion has $2/m$ symmetry and the ion is thus linear and symmetric. The interiodine distance in the two independent I_3^- groups is 2.928 and 2.943 \AA respectively, but the authors do not regard the difference in length to be significant. In the case of modification II the two independent tri-iodide ions are asymmetric and non-linear with interiodine distances of 2.912, 2.961 \AA and 2.892, 2.981 \AA , and interbond angles of 177.7° and 179.5° respectively. In this case the dimensional differences are judged to be significant.

1 - 4 - 4 Tetraphenylarsonium tri-iodide, $(C_6H_5)_4AsI_3$

Structural determination by R.C.L. Mooney-Slater (1958)

Refinement by Runsink *et alii* (1972)

This compound crystallizes in the monoclinic space group $P2_1/n$ with two molecules in the cell of dimensions $a_o = 15.34$, $b_o = 7.63$, $c_o = 10.63 \text{ \AA}$, $\beta_o = 93.4^\circ$. Tri-iodide groups can again be recognized in this compound in planes perpendicular to the b -axis. These planes lie at $y = \pm 1/6$ and effectively sandwich the cations which are disposed with the arsenic atoms in the plane at $y = 0$. There are fewer cation-

anion contacts across the unpopulated space between the layers than within these layers, which probably accounts for the pronounced cleavage exhibited by the crystals of this compound. The tri-iodide units are well separated with an average interionic distance of 5.79 \AA . The tri-iodide anion is symmetric with an interiodine distance of 2.90 \AA , but is bent with an interbond angle of 176° . The average carbon-iodine distance agrees well with that observed in tetraphenylarsonium iodide.

1 - 4 - 5 Ferricinium tri-iodide, $(C_5H_5)_2FeI_3$

Structural determination by T. Bernstein & F.H. Herbstein (1968)

This interesting compound crystallizes in the rhombohedral space group $R\bar{3}m$, with cell dimensions (referred to hexagonal axes) of $a_o = 8.522$, $c_o = 17.05 \text{ \AA}$. In the cell, each tri-iodide anion is surrounded by a rhombohedral cage of eight ferricinium cations. The anion is assumed to be linear and symmetric, with an interiodine distance of 2.93 \AA , but there is some indication from the thermal parameters of the iodine atoms that the structure could well be built up from a disordered arrangement of slightly bent asymmetric tri-iodide ions. There is clear evidence that the cyclopentadiene rings are rotationally disordered, but it is not possible on the X-ray evidence to distinguish between intramolecular 'free' rotation of the rings or a disordered arrangement of rigid ions.

1 - 4 - 6 Caesium tetraiodide, CsI_4

Structural Determination by E.E. Havinga *et alii* (1954)

This compound crystallizes in the monoclinic space group $P2_1/a$ with four molecules of CsI_4 in the cell which has dimensions $a_o = 11.19$, $b_o = 9.00$, $c_o = 10.23 \text{ \AA}$, $\beta_o = 114^\circ$. From the structural analysis it can be seen that the anionic group is most reasonably interpreted as a

loose assemblage of I_3^- ions and iodine molecules to form I_8^{2-} ; this requires the compound to be formulated as Cs_2I_8 . The I_8^{2-} group is very nearly planar and roughly Z-shaped; the important interiodine distances and bond angles are shown in Figure 1 - 3. From this figure it can be seen that the tri-iodide units are asymmetric and bent, and that the I - I distance in the iodine molecule does not differ greatly from the value of 2.70 Å° observed for solid iodine (Townes and Dailey [1952]). The shortest interionic distance is 3.9 Å° and the minimum cation-anion distance agrees with the sum of the ionic radii of Cs^+ and I^- .

1 - 4 - 7 Tetramethylammonium penta-iodide, $(CH_3)_4NI_5$

Structural determination by R.J. Hach & R.E. Rundle (1951)

Refined by B.J. Broekema *et alii* (1957)

Tetramethylammonium penta-iodide crystallizes in the monoclinic system, space group $C2/c$, with unit cell dimensions $a_0 = 13.34$, $b_0 = 13.59$, $c_0 = 8.90$ Å°, $\beta_0 = 107^\circ$. The iodine atoms form planar V-shaped I_5^- ions arranged in almost square nets. These nets are approximately parallel to 001 and are separated by 4.3 Å°. The cation nitrogen lies in the same plane as the net at the intersection of the net diagonals. The I_5^- group is planar to within 0.2 Å° and the arms of the V are linear to within 4°; the angle between the arms is 95°. The two independent interiodine distances within the ionic group are 2.81 and 3.17 Å°. The shortest non-bonded interiodine distance is 3.55 Å°.

1 - 4 - 8 Tetraethylammonium hepta-iodide, $(C_2H_5)_4NI_7$

Structural determination by E.E. Havinga & E.H. Wiebenga (1955).

The space group of this compound is either $Abam$ or the noncentrosymmetric $Aba2$. The compound crystallizes with four molecules in the

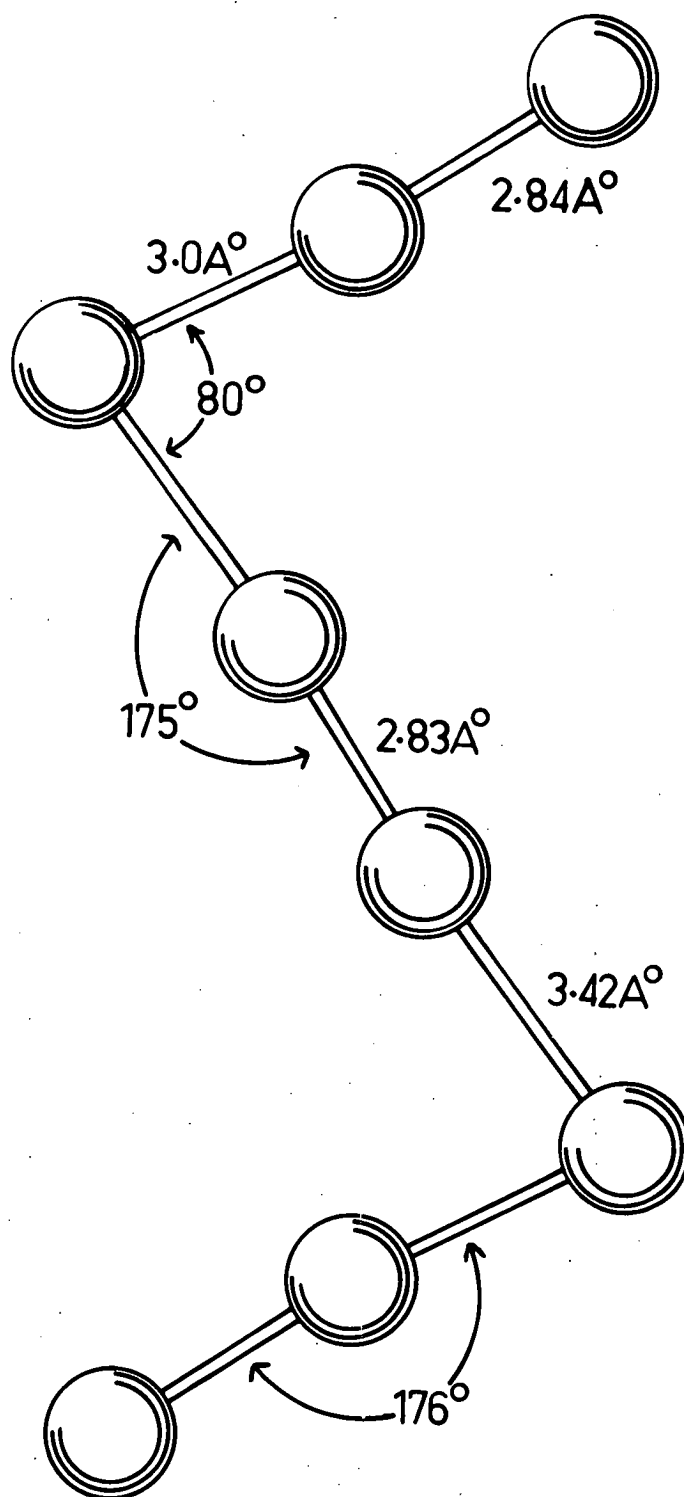


Figure 1 - 3, Interiodine distances and angles for the I_8^{2-} anion.

cell of dimensions $a_0 = 11.5$, $b_0 = 15.66$, $c_0 = 12.37$ Å°. The structure consists of I_3^- ions and iodine molecules, with the tetraethylammonium cation occupying holes in the structure. The authors consider that as the shortest distance between the iodine molecules and the tri-iodide groups is 3.47 Å°, there is no evidence for the existence of the I_7^- group in this compound and that it consequently should be described by the formula $(C_2H_5)_4NI_3 \cdot 2I_2$. The interiodine distance in the iodine molecules is 2.76 Å°; whichever space group is the correct one, the tri-iodide unit must be symmetric with an interiodine distance of 2.91 Å°. Space group *Abam* imposes the constraint that the tri-iodide group must be linear.

1 - 4 - 9 Tetramethylammonium ennea-iodide, $(CH_3)_4NI_9$

Structural determination by W.J. James *et alii* (1955)

This polyiodide crystallizes in the monoclinic system, space group $P2_1/n$. Four molecules are accommodated in the cell of dimensions $a_0 = 11.60$, $b_0 = 15.0$, $c_0 = 13.18$ Å°, $\beta_0 = 95^\circ$. The arrangement of iodine atoms in the structure is reminiscent of that in $(CH_3)_4NI_5$, in that five-ninths of the iodine atoms occur in layers, within which they are grouped into V-shaped I_5^- units. These sheets are separated by a distance of 9.1 Å° and between these sheets are found the tetramethylammonium cation and the six iodine molecules which surround the cation with their molecular axes perpendicular to the layers of I_5^- units. The interiodine distance in the molecular groups between the layers is 2.67 Å°, and the separation between the molecular group and the iodine atoms at one end of the arm of the V-shaped I_5^- group is either 3.24 or 3.43 Å°. The I_5^- group is slightly different in shape from that found in tetramethylammonium penta-iodide; the significant bond distances and bond angles are shown in Figure 1 - 4 (the molecular iodine groups lie above and below the iodine atom which has been line-shaded in that

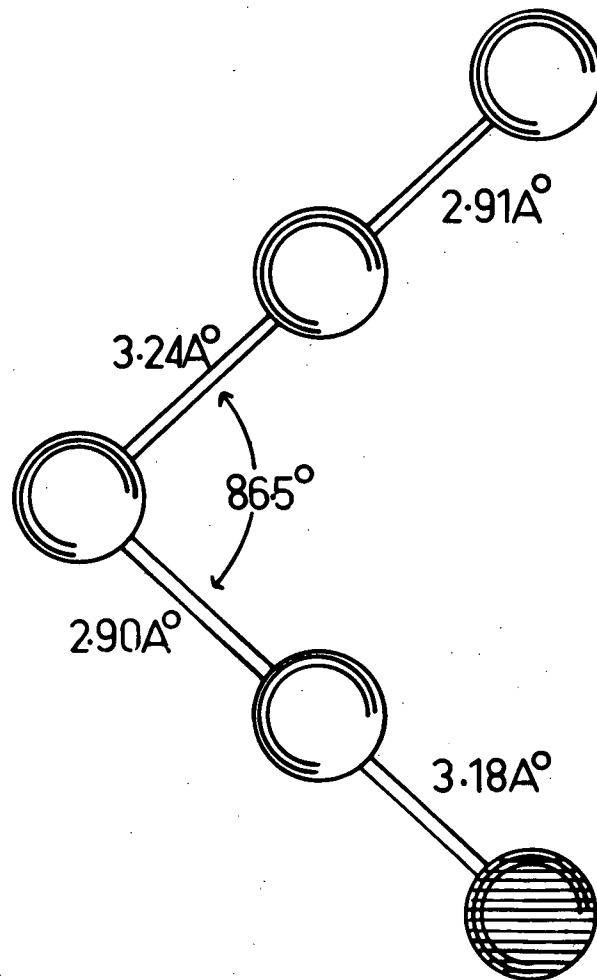
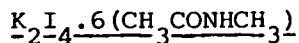


Figure 1 - 4, The I_5^- group of $(CH_3)_4NI_9$.

Figure).

1 - 4 - 10 Dipotassium tetra-iodide hexa-(N-methylacetamide),



Structural determination by K. Toman *et alii* (1964).

The crystals of this solvated polyiodide are trigonal, space group $P\bar{3}1c$ with a unit cell (referred to hexagonal axes) with dimensions $a_0 = 12.2$, $c_0 = 15.2 \text{ \AA}$. The cell contains two stoichiometric units with I_3^- ions and I^- ions alternating in arrays parallel to the c-axis. The planar N-methylacetamide molecules are so arranged that each iodide ion is in the centre of a trigonal cage of six -NH groups, and each potassium cation is similarly caged by six carbonyl oxygens. There is evidence that the tri-iodide ion is avoided by the -NH groups as the iodide ion to nitrogen separation is 3.74 \AA , while the distance between the nitrogen and the terminal iodine of the tri-iodide group is 4.01 \AA . The symmetry of the space group requires the tri-iodide anion to be both symmetric and linear. However, as in the case of ferricinium and tri-iodide, an examination of the thermal parameters of the I_3^- iodines indicates that the structure may be partially disordered. The authors consider that a bent and possibly asymmetric tri-iodide ion may statistically satisfy the symmetry requirements of the space group by random rotation about the trigonal axis or by end-for-end orientation disorder, or both. The interiodine distance, assuming a linear and symmetric unit, is 2.945 \AA ; the distance between I_3^- and I^- ions in the axial direction is 4.64 \AA .

1 - 4 - 11 Hydrogen tri-iodide di-(benzamide), $\text{HI}_3 \cdot 2(\text{C}_6\text{H}_5\text{CONH}_2)$

Structural determination by T.M. Reddy *et alii* (1964)

This hydrogen polyiodide solvated by benzamide molecules crystallizes in the triclinic system, space group $P\bar{1}$, with four molecules in the

cell $a_o = 20.828$, $b_o = 9.885$, $c_o = 9.588$ Å°, $\alpha_o = 95^\circ$, $\beta_o = 101^\circ$, $\gamma_o = 94^\circ$. The structure consists of arrays of dimerized benzamide molecules which form long channels in which the tri-iodide ions are aligned as two parallel chains 4.6 Å° apart. The two crystallographically distinct tri-iodide ions in the unit cell are both bent, with a bond angle of 177° , and are both slightly asymmetric. Bond lengths in both cases are 2.921 and 2.943 Å°. The distance between neighbouring tri-iodide ions in the chains is 3.8 Å°, suggesting at least a partial polymerization of these groups, a suggestion which may be supported by the fact that the chains are linear to within 16° . The position of the hydrogen cation was not determined in this analysis, and the possibility that the cationic group may in fact be H_3O^+ does not seem to have been explored - such an hypothesis has the merit of providing this compound with a cation of reasonable size and does not do violence to the available analytic data for this compound.

1 - 4 - 12 Hydrogen penta-iodide di-(phenacetin) $HI_{5.2}(C_{10}H_{13}O_2N)$

Structural determination by F.H. Herbststein & M. Kapon (1972)

As is the case with the previously described solvated hydrogen polyiodide, this compound crystallizes in the triclinic system, space group $P\bar{1}$ with one molecule in the cell with dimensions $a_o = 12.441$, $b_o = 10.67$, $c_o = 5.87$ Å°, $\alpha_o = 103.3^\circ$, $\beta_o = 103.7^\circ$, $\gamma_o = 87.3^\circ$. The structure is composed of parallel sheets of organic molecules and polyiodide ions. The latter contain zigzag chains of alternate iodine molecules and symmetric I_3^- ions. The bond length of the tri-iodide ion is 2.907 Å°, and that of the iodine molecule is 2.748 Å°. The distance between the terminal atoms of the tri-iodide ion and the iodine molecule is 3.550 Å°, commensurate with the spacing (3.50 Å°) found in crystalline iodine.

The phenacetin molecules are inclined at about 83° to the poly-

iodide sheet. The acidic protons are assumed to be associated with the neutral organic molecules, linking neighbours by symmetrical hydrogen bonds between symmetry related carbonyl groups. This interpretation is supported by the carbonyl oxygen-carbonyl oxygen separation across the symmetry centre of 2.44 \AA , which is less than the van der Waal's diameter of oxygen (2.80 \AA).

In the absence of analytic data, it is not possible to determine whether the assignment of the acidic protons to the phenacatin molecules is the correct interpretation, or rather that, as in the case of $\text{HI}_3 \cdot 2(\text{CH}_5\text{CONH}_2)$, the compound contains the H_3O^+ cation. In either case the possibility cannot be rejected on the basis of the published information; the implications of this hypothesis are discussed further in Chapter 7, Section 7 - 5.

1 - 5 Polyiodide Bonding in Relation to Stability and Structure

From this body of structural data the following generalizations can be made concerning polyiodide anions in the solid state. First, the anions are catenated assemblages of iodine atoms which are either linear - as in the case of the tri-iodide ion - or involve bond angles close to ninety degrees - as in the case of the I_8^{2-} ion. Second, the bond distances are always some 5 to 15% greater than twice the covalent radius of iodine (1.33 \AA) (Cotton and Wilkinson [1973]). Third, together with the iodine molecule, both the I_3^- and the I_5^- ions act to some extent as 'building blocks' out of which the more complex anions are assembled. Fourth, a common feature of the structures so far determined is the disposition of the polyiodide anions in layers or rows within the unit cell. This, and the mutual orientation of the tri-iodide ion in the structures containing the I_3^- entity, is reminiscent of the structure of solid iodine (Townes and Dailey [1952]).

Attempts to explain the bonding of polyiodides from an electro-

static point of view have been made (van Arkel and de Boer [1928], Havinga [1957]), but they fail to explain satisfactorily the observed anion geometries. The I_3^- ion bonding was discussed from the standpoint of molecular orbital theory by Pauling [1940], and a molecular orbital model for this anion involving 5d and 6s orbitals was advanced by Kimball [1940]. This model was criticised by Pimentel [1951]; he pointed out that the energy required to promote an electron from a halogen d-orbital is considerable, and that this is compensated by the energy of hybridization is an assumption of questionable validity. His alternative model, also proposed independently by Hach and Rundle [1951], treats the bonding as arising from the delocalization of the valency p-electrons to form a simple sigma bond between halogen centres.

This ps -bonding model was later extended in a simple one-electron LCAO-MO form by Havinga and Wiebenga [1959] to all polyhalides and interhalogens. Their treatment satisfactorily predicts all observed bond-angles and configurations with the exception of the interhalogen compound IF_7 . Subsequent more elaborate SCF-MO calculations have been carried out on a number of polyhalogen species and all demonstrate the adequacy of this model to account for the observed properties of these compounds subject to the limitations of such treatments when applied to atomic systems involving a large number of electrons. In view of the very large number of electrons involved in the polyiodide cases, the results of such treatments are remarkably good.

In 1959 Mooney-Slater observed that, regardless of the nature of the bonding of the tri-iodide ion, the configuration of the I_3^- species was sensitive to its crystallographic environment, the anion being long and markedly asymmetric in the relatively unstable ammonium tri-iodide and short and symmetric in the more stable tetraphenylarsonium tri-iodide. With the crystallographic data available at that time (which included those structures already described in which I_3^- units are assoc-

iated with iodine molecules to form I_8^{2-} , I_7^- , etc.) she showed that there appeared to be a systematic relationship between the overall length of the I_3^- anion and the degree of asymmetry in the bond lengths. This systematic relationship was compared to the behaviour of the H_3^+ molecule-ion system by Slater [1959], who attributed the dependence of configuration of the anion upon its surroundings to 'environmental pressure', ascribing the symmetry of I_3^- in $(C_6H_5)_4AsI_3$ to the crowding of the anion by the bulky tetraphenylarsonium cation.

This interpretation was later challenged by Rundle [1961] who related the observed configurations of the I_3^- ion to the balance struck in particular crystalline environments between the tendency of coulombic interactions between the cation and the anion to favour an asymmetric form and the opposing tendency of bonding interactions to favour a symmetric arrangement of iodine atoms. Rundle observed that the trend towards greater stability and more symmetric anion geometry which accompanies an increase in cation size runs in the expected direction, as the coulombic influence would decrease as the cationic radius increased.

This latter interpretation can be accommodated within the framework of the p -sigma model of polyiodide bonding. The valency electrons of iodine are well screened from the nuclear charge by the large number of electrons in orbitals of lower principal quantum number. Consequently, when a polyiodide anion is formed, the valency p -electrons readily delocalize, creating a weakly sigma-bonded entity. The other consequence of the screening effect is the ease with which external fields can distort or polarize the valency electron distribution over the anion. Any such distortion is accompanied by a change in the equilibrium configuration, and as this change is expressed as a lengthening of one or other of the I - I bonds, it is accompanied by a decrease in the stability of the complex. Thus in a crystalline environment a polyiodide anion can only be stable if its bonding electron distribution is protected from

severe electrostatic disruption. This effect has been examined in some detail by Brown and Nunn [1966] who, by a series of SCF-MO one electron calculations, showed that the free tri-iodide ion should be linear and symmetric, but that in the CsI_3 lattice the crystal field distorts the electron distribution so that the anion configuration of minimum energy is an asymmetric one with calculated bond lengths close to those determined for the CsI_3 structure.

The inference that the asymmetry of the tri-iodide ion in a given structure reflects the asymmetry of the electrostatic environment rather than the size of the cation has been elegantly substantiated by the study made by Migchelsen and Vos [1967] of the two modifications of $(\text{C}_2\text{H}_5)_4\text{NI}_3$ (see Section 1 - 4 - 3). In the case of the two crystallographic modifications of this compound the effects of change in cation size cannot arise; however, modification I of this compound exhibits two independent and symmetric tri-iodide ions which differ in total length, in contrast to modification II which possesses two independent asymmetric anions with the same total length. Migchelsen and Vos also carried out calculations similar to those performed by Brown and Nunn; these showed that in the case of modification I there was no potential difference due to external charges between the terminal iodines of the symmetric anions. However, in modification II potential differences of the order of 0.1 - 0.35 volt existed between the terminal iodines of the two asymmetric anions present in this form of $(\text{C}_2\text{H}_5)_4\text{NI}_3$. The variation of ΔV , the potential difference relative to the central iodine, with Δd , the difference in bond length, for a number of structures calculated from results presented in their study is given in Table 1 - 3 and Figure 1 - 5.

Table 1 - 3

Variation of potential difference (ΔV) with bond length difference (Δd)

Compound	Δd (Angstrom)	ΔV (volts)
$(C_2H_5)_4NI_3$ (I)	0.000	0.000
	0.000	0.000
$(C_6H_5)_4AsI_3$	0.000	0.000
$(C_2H_5)_4NI_3$ (II)	0.049	0.102
	0.089	0.357
CsI_3	0.210	1.266

These data indicate that there is a systematic relationship between the asymmetry of the electric field experienced by the tri-iodide ion and the asymmetry of the equilibrium configuration adopted by the ion under this field.

1 - 6 The Aim of this Work

The stability of solid unsolvated tri-iodides would appear, from the evidence assembled above, to be a function of the asymmetry of the electrostatic environment experienced by the anion in the crystalline lattice. Insofar as this asymmetry is determined by the size of the cation, the stability trend of the unsolvated tri-iodides of singly charged cations can be understood. It is also reasonable to expect the same principle to govern the stability of the more complex poly-iodide anions (I_5^- , I_9^- , etc.) in the solid state. Further, it is a reasonable hypothesis to assume that the major role of solvate molecules in those polyiodides which cannot be crystallized in an unsolvated form is to create a crystalline environment in which the asymmetry of the crystal fields in the vicinity of the anion is sufficiently small for the compound to be stable under normal conditions.

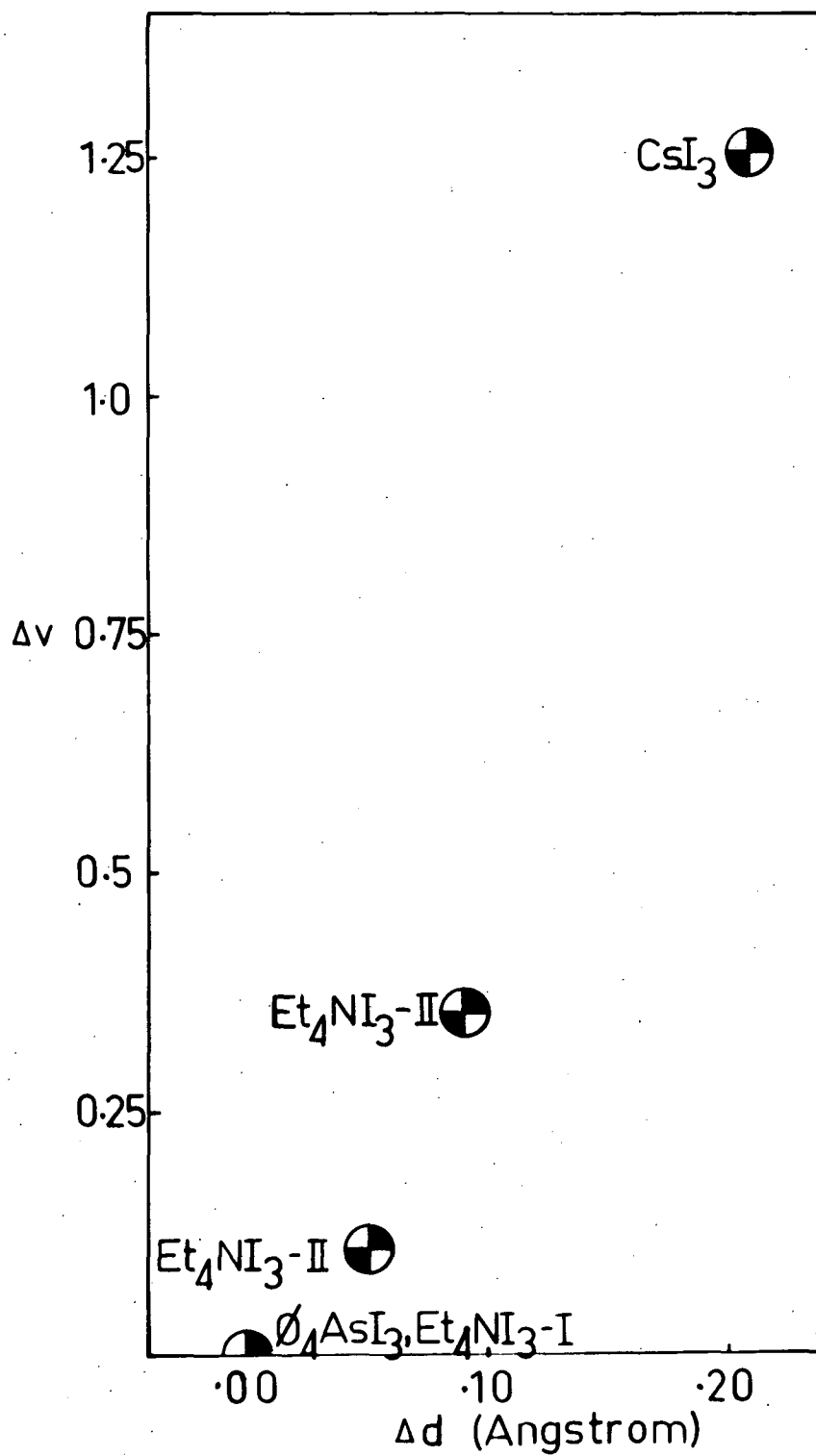


Figure 1 - 5, ΔV (volts) versus Δd (Angstrom units) for a number of tri-iodides, calculated from the data of Migchelsen and Vos [1967].

The major objective of this work was to examine this hypothesis critically in the light of the known deficiencies of simple crystal field theory as applied in the field of transition metal chemistry, and to test it by comparing the structure of a solvated alkali tri-iodide with that of the unsolvated tri-iodides. The solvated tri-iodide chosen for this comparative study was the potassium compound, $\text{KI}_3 \cdot \text{H}_2\text{O}$. This choice was made for a number of reasons: perhaps the most important being that $\text{KI}_3 \cdot \text{H}_2\text{O}$ is the most stable of the hydrated polyiodides. Further, this compound is presumed to be a tri-iodide on the basis of both analytic data and phase studies; in this respect it stands in sharp contrast to the hydrated sodium and lithium tri-iodides. The presence of tri-iodide anions within the structure would simplify the comparison of this crystalline environment with that of the unsolvated tri-iodides which are already known to contain discrete I_3^- units. Also, the solvate molecule is water, and there is in existence a considerable body of information concerning the roles performed by water molecules in other crystalline compounds which could be drawn on for comparison.

The solution of the structure of $\text{KI}_3 \cdot \text{H}_2\text{O}$ occupies a central place in this study, but in addition an attempt has been made to extend the number of accurately known unsolvated tri-iodide structures by the refinement of the structure of NH_4I_3 and the solution of the structure of RbI_3 . Further, it was hoped that as a result of this examination a simple model which would represent the response of the I_3^- ion to its crystallographic environment could be developed, and that in the light of this model a better understanding of the systematic structural chemistry of both the solvated and unsolvated tri-iodides could be gained.

Subsidiary objectives which grew out of this work were to develop a suite of crystallographic computer programs which could be conveniently

used with the available computing facilities, and also to test the applicability of the direct methods of crystal structure solution to the case of an inorganic compound which possesses a significant systematic relationship among its atomic parameters.

Chapter 2 - The Theoretical Basis of X-Ray Structural Analysis

	page
2 - 1 Diffraction of X-rays by Crystals	33
2 - 2 X-ray Scattering by Atoms	35
2 - 3 The Structure Factor	36
2 - 4 The Electron Density Distribution	38
2 - 5 The Phase Problem	39
2 - 6 The Patterson Method	41
2 - 7 The Direct Methods	45

2 - 1 Diffraction of X-rays by Crystals

The theory of the interaction of X-radiation with matter in the crystalline state has been exhaustively reviewed elsewhere (James [1948]); for this reason the discussion given here concentrates on the application of X-ray diffraction to the determination of crystal structures.

In 1912 von Laue suggested that if in fact X-radiation possessed wave-like properties, then the interatomic spacing of crystalline substances should be of the right order of magnitude for a crystal to act as a diffraction grating for X-rays. The first observation of X-ray diffraction was made in the same year by Friedrich and Knipping when they irradiated a single crystal of copper sulphate pentahydrate with an X-ray beam. This observation gave the first clear proof of the wave character of X-rays, and von Laue showed that the results of the diffraction experiment could be described in terms of diffraction from a three-dimensional diffraction grating (Laue, Friedrich and Knipping [1912]). As a result of these experiments W.L. Bragg developed a treatment of X-ray diffraction in terms of reflection of the incident X-ray beam by the lattice planes of the crystal (Bragg [1912]) and he derived the simple reflection law

$$n\lambda = 2d \cos \Omega \quad (\Omega = 90^\circ - \theta)$$

which now bears his name, and where d is the interplanar spacing, θ the angle of incidence, λ the X-ray wavelength and n an integer specifying the order of reflection.

It should be noted that the formulation of Bragg's Law rests on the assumption that the electron density can be assumed to be resident in the lattice planes of the crystal, whereas it is now known that electron density is distributed throughout the volume of the unit cell. The

derivation is, however, valid as it can be shown that scattering from electron density which does not occupy a rational lattice plane may be treated to yield a resultant as if the scattering took place in that plane. The nature of the electron density distribution in the unit cell volume controls the magnitude of these resultants, and gives rise to the differing intensities of reflection observed for different lattice planes.

If Bragg's Law is recast in the form

$$\sin \theta = n\lambda/2d$$

it can be seen that $\sin \theta$ is proportional to the reciprocal of the interplanar spacing, d . This was the point of departure for the development by Ewald [1921] of the concept of the *reciprocal lattice*. This concept was further developed and applied by Bernal [1926] to the problem of interpreting X-ray diffraction patterns, and now provides one of the most convenient tools available for the study of the diffraction of X-rays by crystals. The most significant property which adapts it to this purpose is that in the reciprocal lattice distances are measured in reciprocal units, d^* ($=1/d$), these quantities having the advantage of being directly proportional to $\sin \theta$. Thus

$$\sin \theta = n \lambda d^*$$

The reciprocal lattice, which may be considered to exist in a continuum (*reciprocal space*) defined by its coordinate system, is described by the edges a^* , b^* , c^* and interaxial angles α^* , β^* , γ^* of the reciprocal cell. These bear the same relationship to the reciprocal lattice as do the unit cell elements a , b , c , α , β , γ to the lattice of the real crystal. Conventionally, reciprocal quantities are designated by starred symbols to distinguish them from the analogous real or *direct* quantities. The relationship between the direct and reciprocal cell elements can be compactly expressed in vector notation for the general (triclinic) case as follows:-

$$a^* = (\underline{b}) \times (\underline{c}) / (\underline{a} \cdot \underline{b} \times \underline{c})$$

$$b^* = (\underline{c}) \times (\underline{a}) / (\underline{a} \cdot \underline{b} \times \underline{c})$$

$$c^* = (\underline{a}) \times (\underline{b}) / (\underline{a} \cdot \underline{b} \times \underline{c})$$

As the reciprocal space metric is directly proportional to $\sin \theta$, the direction of a reflection from the crystal plane with Miller indices hkl can be vectorially specified by the reciprocal lattice point h reciprocal cell units in the a^* -axial direction, k units in the b^* -axial direction and l units in the c^* -direction. Thus all reflections from the crystal planes can be associated with their corresponding reciprocal lattice points, and further, the reciprocal lattice possesses the entire symmetry of the direct lattice to which it is related; these two properties make possible the convenient discussion and treatment of reflection data in reciprocal lattice notation.

2 - 2 X-ray scattering by Atoms

It was implicit in the discussion in Section 2 - 1 that X-rays are scattered by the extranuclear electrons of the atoms which make up the crystal. For convenience, in describing the scattering behaviour of crystals, the unit of amplitude is taken to be the amplitude of the X-ray wavelet scattered by a single electron. On this basis, for a 'reflection' from a given lattice plane, the amplitude of the wave scattered by a single cell of the crystal (the *structure factor*) will be the sum of the appropriately phased amplitudes of the wavelets scattered by each electron in the cell. This form of the structure factor is not very useful in view of the large number of electrons usually involved and the limitations which exist regarding a precise knowledge of their position, even when the details of the structure are known. A more useful approach is to make use of the knowledge gained from atomic structure theory (Hartree [1927], [1957]) regarding the spatial distribution of the specific number of electrons

associated with each atom, and to group together the components of the structure factor so that each group is associated with one atom in the cell.

Using this approach, a detailed knowledge of electron position is not necessary. All that is required is a good description of the average spatial distribution of the electron cloud with respect to the atomic centre. Each group of terms in the structure factor then represents the appropriately phased contribution made by the electrons of each atom to the amplitude of the wave scattered by the cell. The scattering power of an atom, usually designated f , is measured in the same units as the structure factor, namely, the scattering power of a single electron. The maximum value that can therefore be attained by f for a given atom is equal to the atomic number Z . If the scattering electrons were concentrated at the atomic core - a 'point atom' - there would be no variation of f with scattering angle (normally expressed in terms of $(\sin \theta)/\lambda$). However, as atoms have an extended electronic structure, f decreases from an initial value of Z with increasing $(\sin \theta)/\lambda$, due to the destructive interference of the wave fronts scattered by each electron in the electron cloud. The detailed behaviour of f as a function of $(\sin \theta)/\lambda$, derived from atomic structure calculations, is available in the literature (Thomas and Umedu [1957], Henry and Lonsdale [1965]) for most elements in a number of valency states.

2 - 3 The structure factor

As outlined above, the structure factor F_{hkl} for a reflection from the lattice plane with Miller indices (Miller [1839, 1863]) hkl can be written as the sum of phased contributions from each atom in the unit cell. In exponential notation, this would be

$$F_{hkl} = \sum_j f_j e^{-i\phi_j}$$

where f_j is the scattering power at $(\sin \theta_{hkl})/\lambda$ of the j th atom in the cell, and ϕ_j is the phase of the structure factor. This can also be written as the explicit function

$$F_{hkl} = \sum_j f_j e^{-i2\pi(hx_j + ky_j + lz_j)}$$

where x_j, y_j, z_j are the fractional coordinates of the j th atom. Some computational convenience is gained by expressing the structure factor as the sum of real and imaginary components:

$$F_{hkl} = \sum_j f_j \cos \phi_j + i \sum_j f_j \sin \phi_j$$

Again, this can be written as an explicit function of the fractional coordinates:

$$\begin{aligned} F_{hkl} = & \sum_j f_j \cos 2\pi(hx_j + ky_j + lz_j) \\ & + i \sum_j f_j \sin 2\pi(hx_j + ky_j + lz_j) \end{aligned}$$

In those cases where the crystal possesses a centre of symmetry, that is, every atom at x, y, z is accompanied by another in the cell at $-x, -y, -z$, the expression for the structure factor may be simplified to

$$F_{hkl} = 2 \sum_j f_j \cos 2\pi(hx_j + ky_j + lz_j)$$

due to the cancellation of the imaginary component from symmetry related atoms. In this centrosymmetric case, as the atoms occur in pairs (except for an atom occupying the centre of symmetry, in which case it is its own centrosymmetric mate and must be treated specially) the summation need only be carried out over half the contents of the unit cell. In general, the presence of symmetry elements will simplify the general expression for F_{hkl} . A listing of the modified forms of the structure

factor expression for each of the 230 space groups is contained in Volume I of the *International Tables for X-ray Crystallography* (Henry and Lonsdale [1965]).

2 - 4 The Electron Density Distribution

Any periodic function $f(x)$ of unit period can be written as

$$f(x) = \sum_{h=-\infty}^{\infty} F(h) e^{-2\pi i h x}$$

where h is integral and $F(h)$ are the coefficients of the Fourier series for the function $f(x)$. The electron density distribution in the crystal is periodic in three dimensions as a consequence of the crystal being built up by the three-dimensional repetition of identical structural units. A Fourier series for the electron density distribution, $\rho(xyz)$, over the unit period specified by the unit cell can be written in a manner entirely analogous to that for the one-dimensional example given above. The Fourier coefficients in this case are the structure factors, F_{hkl} , so that

$$\rho(xyz) = \frac{1}{V} \sum_h \sum_k \sum_l F_{hkl} e^{-2\pi i (hx+ky+lz)} .$$

Here $\rho(xyz)$ represents the electron density (in units of electrons per unit volume) at the point xyz in the unit cell. This expression for the electron density in real space in terms of the structure factors in reciprocal space bears a close relationship to the exponential form of the expression for the structure factor in terms of atomic electron density distributions given in Section 2 - 3. The two expressions differ, however, in that the transformation in one direction is associated with a positive exponential term, while the reverse transformation is associated with a negative term. The choice of which transformation direction is to be associated with which sign is arbitrary, but the

choice, once made, must be maintained. In this work the convention adopted by the *International Tables for X-ray Crystallography* (Henry and Lonsdale [1965]) has been followed in which the negative sign is associated with the Fourier transformation from reciprocal to direct space.

By noting that the structure factor is a complex quantity which may be split into phase and magnitude components,

$$F_{hkl} = |F_{hkl}| e^{2\pi i \alpha_{hkl}}$$

the three dimensional Fourier series for the electron distribution in the unit cell can be given the alternative form where $2\pi i \alpha_{hkl}$ is the phase angle of the structure factor under consideration. The electron density expression can then be written as

$$\rho(xyz) = \frac{1}{V} \sum_h \sum_k \sum_l |F_{hkl}| e^{2\pi i \alpha_{hkl}} e^{-2\pi i (hx+ky+lz)}$$

which can be simplified to

$$\rho(xyz) = \frac{1}{V} \sum_h \sum_k \sum_l |F_{hkl}| e^{-2\pi i (hx+ky+lz - \alpha_{hkl})}$$

2 - 5 The Phase Problem

As shown in the previous section, an expression can be written for the electron density distribution in the unit cell in terms of the phase and magnitude of the structure factors F_{hkl} . The fundamental difficulty of the technique of structure solution by diffraction methods is the *phase problem*, namely, that the diffraction process using incoherent X-ray sources and current methods for recording reflections yields information about the relative magnitudes of the structure factors, but cannot disclose their relative phases. It is the existence of this problem which prevents the technique from being reduced to a straightforward computational task, for when both the magnitude and phases of

the structure factors are known the electron density distribution in the unit cell may be computed directly. At present the phase problem must be solved before the distribution of electron density can be determined by computation.

A solution of the phase problem will consist of a set of predicted phases - ideally, one for each observed structure factor magnitude. For such a solution to be accepted as the correct one, the electron density distribution calculated from it must meet a number of criteria:-

- (a) The electron density must be real, positive and continuous everywhere in the unit cell.
- (b) It must be concentrated in approximately spherical regions (atoms).
- (c) Once the atoms have been identified, the structure so revealed must be consistent with the existing body of knowledge concerning the structures of chemical compounds, with interatomic distances and angles variable only within limits established by previous experience. (Naturally the exercise of this criterion involves an element of judgement, otherwise novel structures would never be discovered).

The exact status of these criteria should be noted. It can be proved that any electron density distribution in the unit cell generates a diffraction pattern which is unique in its distribution of phase and magnitude among the structure factors. However, in proceeding from the diffraction pattern to the electron density distribution, it has not yet been demonstrated that the *necessary* constraints, which must be obeyed (a - c above) by the solution to the phase problem, are also *sufficient* to guarantee a unique solution. At present, it can only be shown that criterion (a) in isolation is not sufficient to ensure the unique nature of the solution. None the less, the three criteria

taken together are very restrictive, and the probability of arriving at a solution to the phase problem which conforms to all three and which generates an incorrect electron distribution is judged to be vanishingly small.

The first stage in the solution of the phase problem is the generation of a *phasing model*. This is a model of the electron density distribution which yields phases sufficiently correct for a convergent process of model improvement to be initiated. This process will normally consist of a cyclic alternation of structure factor calculations and Fourier syntheses, in the course of which the positions of all the atoms in the unit cell are discovered. When this stage is complete, a semi-automatic process of least-squares refinement of all atomic parameters may be commenced.

A number of techniques useful for the development of a phasing model are available to the crystallographer. These include trial-and-error methods, the anomalous dispersion technique, the method of isomorphous replacement, the heavy-atom and Patterson techniques, and the more recently developed 'direct' methods. Each technique has its own strengths and weaknesses, and consequently its own area of special utility. In the field of inorganic structure determination, the method involving the interpretation of the Patterson function is usually employed. However, the applicability of direct methods has also been investigated as a result of their successful use for the solution of organic structures. In the following sections these two methods are outlined.

2 - 6 The Patterson Method

In 1935, Patterson (Patterson [1934, 1935a, 1935b]) showed that the Fourier synthesis prepared by using the squared moduli of the structure factors, $|F_{hkl}|^2$, could give direct information about the structure. As the $|F_{hkl}|^2$ are independent of phase, and are directly related to the

observed diffraction intensities, no preliminary assumptions concerning the structure need be made. The maxima in the Patterson function $P(uvw)$ correspond to vectors between all possible pairs of atoms in the crystal structure, with all vectors referred to a common origin. Thus, if atoms are located in the crystal at positions x_i, y_i, z_i and x_j, y_j, z_j , the Patterson function will display a peak at u_h, v_h, w_h , such that

$$u_h = x_i - x_j$$

$$v_h = y_i - y_j$$

$$w_h = z_i - z_j$$

The height of any such peak will be roughly proportional to the product of the number of electrons in the two atoms inter-related by the vector in question.

For a compound having n atoms in the unit cell, the Patterson synthesis will have n^2 peaks, each representing one of the n vectors from each of the n atoms in the cell. As n of these vectors are of zero length, representing the vector from each atom to itself, these are concentrated as a large peak at the origin. The remaining $n^2 - n$ non-zero vectors are represented by peaks distributed throughout the cell volume, with heights proportional to the product of the peak heights of the inter-related atoms.

It was first shown by Langmuir and Wrinch (Langmuir and Wrinch [1938]) that in principle it is possible to recover the atomic distribution from the vector set represented by the Patterson function. Even though both real and hypothetical examples of different atomic distributions which give rise to the same vector set are known, (Pauling and Shappell [1930], Minzer [1949], Gurrido [1951], Hoseman and Bagchi [1953]), such *homometric* structures are exceptional. The practical difficulties in solving structures from their Patterson functions arise

not from the possibility of homometric structure ambiguities, but rather from the overlap of peaks in Patterson space as a consequence of their finite size. The Patterson synthesis for a compound containing a moderate number of atoms will display $n^2 - n$ non-origin peaks in the volume of the unit cell, and these in most cases will overlap to give some featureless regions of vector density. The severity of this problem can be reduced by modifying the coefficients of the synthesis, so that the scattering behaviour of the atoms approximates to that of point atoms. The 'sharpened' Patterson function so produced will contain approximations to point-vector peaks, with a consequent reduction in overlap.

A fundamental limitation is imposed on this sharpening procedure by the fact that the set of coefficients is finite in number. A point object can only be perfectly represented by a Fourier series with an infinite number of terms. The use of a finite data set for the computation of a sharpened Patterson function introduces around each peak a sequence of secondary ripples which may, by their own overlap, nullify any improvement in resolution afforded by the sharpening procedure.

The wide range of techniques which have been devised for the interpretation of Patterson functions has been described elsewhere (Buerger [1959]). A brief description of only two of these methods is given below, namely, the use of Harker sections and image-seeking methods.

Although those symmetry elements with translational components (glides and screws) of the crystal appear in the symmetry of the Patterson function as the corresponding non-translational elements (mirrors and rotation axes), it was shown by Harker that the symmetry elements of the space group of the atomic distribution were reflected in linear and planar concentrations of vector density in the Patterson function. In fact, it is possible in certain cases to determine the space group of a

compound from an analysis of the disposition of the Harker lines and planes in the Patterson function. In conjunction with a knowledge of the distribution of atoms over the equipoints in the cell, the analysis of Harker lines and sections can be useful in developing a trial structure for use as a phasing model. However, like all other Patterson techniques, its application is complicated by fortuitous overlap of vector peaks.

The image-seeking method and related superposition techniques represent a development by Buerger [1950a, 1950b, 1959] and others (Lindquist [1952], Bezjak [1953]) of the basic ideas of Wrinch [1938, 1939a, 1939b, 1950]. An essential early stage in all these methods is the identification of Patterson peaks which correspond to a single atomic interaction, or an interaction of known magnitude. This identification is often assisted by predictions of vector lengths, made from a knowledge of bond lengths or substructure configurations derived from related structures and other chemical data. Once such an identification has been made, the origin of a copy of the Patterson function is shifted to the peak position, and to positions related to it by the symmetry operations of the cell. Coincidences in peak positions in the shifted functions are then sought. By repeating this process as many times as is necessary, the atomic distribution can, in principle, be recovered. In practice, the success of the technique relies on the correct identification of the initial vector, and such identification may be precluded by peak overlap.

Notwithstanding its limitations, the Patterson synthesis provides a powerful tool for the development of an initial phasing model, particularly when there is a wide disparity in the atomic numbers of the atoms in the compound. In this case the positions of the heavy atoms, which will dominate the phases of the structure factors, can usually be found without great difficulty. The tri-iodide structures examined in

this work provide a case in point. Also, the Patterson function provides a convenient check on the validity of a model, in that the vector set derived from the model must be in agreement with the distribution of peaks in the Patterson function (see Chapter 6, Section 6 - 6).

2 - 7 The Direct Methods

In the previous section, it was stated that the Patterson function affords a means whereby a trial structure can be derived for use as a preliminary phasing model. As the Patterson function is the Fourier transform of the intensity data, it should be possible to derive a trial structure from the intensity data directly. Many attempts (Bannerjee [1933], Hughes [1949]) have been made to devise methods of an algebraic or statistical nature for the direct solution of crystal structures using only the intensity data, the unit cell dimensions and symmetry, and the chemical composition of the crystalline species. Some of these attempts have concentrated on direct solutions in crystal space for the atomic positional co-ordinates, but the most successful attempts have involved reciprocal space solutions for the phases of the structure factors. This is a rapidly developing area in the field of structure determination by diffraction methods, and so far the most progress has been made in the solution of organic structures. Currently, such structures involving as many as 100 atomic parameters have been solved in both centrosymmetric and noncentrosymmetric space groups by the routine application of direct methods of solution.

Most of these methods use as a basis the first of the criteria mentioned in Section 2 - 5. As mentioned in that Section, the fact that the electron density is everywhere real, positive and continuous in itself does not guarantee that the solution to the phase problem is a correct one. Consequently, the theoretical basis of the direct

methods includes other physically reasonable assumptions which limit the distribution of the magnitudes and phases of the structure factors. These commonly include the assumptions that the electron density distributions can be successfully approximated by the superposition of spherically symmetric atomic electron distributions, that these atomic distributions are identical, and that they are randomly distributed in the volume of the unit cell. As a first approximation, it appears that the applicability of the direct methods to a given structural problem depends upon the degree to which the structure departs from these assumptions.

Historically, the first practical application of direct methods was that of Harker and Kasper in 1948 in their work on the structure of decaborane (Harker and Kasper [1948]). Their approach involved the use of inequality relations which allowed the signs of a sufficient number of the structure factors to be determined for the structure to be solved.

Another approach was developed by Sayre [1952], who showed that the structure factors for a structure containing equally resolved atoms could be related by equations of the form

$$F(\underline{h}) = \phi(\underline{h}) \left[\sum_{\underline{h}'} (\underline{h}') (\underline{h}-\underline{h}') \right] / V$$

where $F(\underline{h})$ is the structure factor with diffraction order specified by the vector \underline{h} , $\phi(\underline{h})$ is a function of s , the length of the vector \underline{h} in reciprocal space. The same relationship was also derived at the same time by Zacharisen [1952] and Cochran [1952]. Using this relationship in conjunction with the approach of Harker and Kasper [1948] it may be shown for structure factors of large magnitude that

$$\text{sign}(\underline{h}) \text{sign}(\underline{h}') \text{sign}(\underline{h}+\underline{h}') = +1$$

where 'sign(\underline{h})' is taken to mean 'the sign of the structure factor with

diffraction order \underline{h}' . In the case where the structure factors have insufficient magnitude to ensure the validity of this relation, it is still more probable that it is true than untrue. The probability that the relationship holds was estimated or calculated by a number of workers, the best known being Hauptman and Karle [1953], Kitaigorodski [1953, 1954], Vand and Pepinsky [1953], Woolfson [1961], Cochran and Woolfson [1955], and Klug [1958]. Applications of 'Sayre's equation' together with probability calculations have been described by Woolfson [1961].

A method termed the 'symbolic addition procedure' which is based on this approach has been described by Karle and Karle [1966]. This has been successfully used for the solution of centrosymmetric structures, and makes use of statistically true relations among the normalized structure factors. The normalized structure factor is computed from the relation

$$E^2(\underline{h}) = |F(\underline{h})|^2 / (\varepsilon \sum_i f_i^2(\underline{h}))$$

where ε is an integer which assumes specified values for each class of reflection in a given space group, and the summation is carried out over the contents of the cell. As before, the f_i are the scattering factors for the atoms in the cell. The relationship used is called the Σ_2 formula by Karle and Karle, and it takes the form

$$\text{sign}(E_{\underline{h}}) \approx \text{sign}(\sum_{\underline{k}} E_{\underline{k}} E_{\underline{h}-\underline{k}})$$

where 'sign ($E_{\underline{h}}$)' means 'the sign of the normalized structure factor with diffraction order \underline{h}' . This formula has the advantage over other sign-determining equations which have been derived in that it is simple to compute and valid for all space groups. The symbolic addition procedure determines the signs of the normalized structure factors in

an iterative fashion, making use of the fact that certain structure factors (the structure invariants) can be given arbitrary signs which serve to fix the origin of the unit cell with respect to the structure. A number of large normalized structure factors are also given symbolic signs, and these are added to the structure invariants to form a basic set which is then used to find the symbolic phases of other structure factors.

If the basic set includes n symbolically signed structure factors, then in principle it is necessary to prepare 2^n Fourier maps, each one corresponding to one of the possible ways of distributing positive and negative signs among the n symbols used. However, it is often possible to reduce this number by considering relationships among the symbolic signs found during the iterative application of the Σ_2 relation.

Karle and Karle also describe a modification of this method developed for non-centric crystals which makes use of a further relation

$$\tan \phi_{\underline{h}} = \frac{(\sum_{\underline{k}} |E_{\underline{k}} E_{\underline{h}-\underline{k}}| \sin (\phi_{\underline{k}} + \phi_{\underline{h}-\underline{k}}))}{(\sum_{\underline{k}} |E_{\underline{k}} E_{\underline{h}-\underline{k}}| \cos (\phi_{\underline{k}} + \phi_{\underline{h}-\underline{k}}))}$$

where $\phi_{\underline{h}}$ is the phase angle for the reflection \underline{h} and the summation is over the contribution from all known phases. The iterative application of this relation, which has become known as the 'tangent formula', will in favourable cases allow a set of correctly phased reflection data to be built up from a small initial set of phase angles.

Direct methods have been used successfully in a number of structure determinations of both centrosymmetric and noncentrosymmetric crystals. In many cases the structure could have been solved equally well by the use of other methods, although there is a growing list of structures (particularly in the organic field) where this is not the case. The major advantage of the direct methods is that the technique lends itself to automation. Its main limitation is that the probability of success-

ful structure determination is a decreasing function of structure complexity (Woolfson [1961]). The limitations imposed on the direct methods by the substantial departure from a random arrangement of the atoms in the cell usually encountered in inorganic structures are apparently still imperfectly known.

Chapter 3 - The Crystallographic Program Suite

	page
3 - 1 Introduction	51
3 - 2 The Computer Configuration	51
3 - 3 Programming Languages	52
3 - 4 The Operating System	54
3 - 5 The Development of the Crystallographic Program Suite	55
3 - 6 The Program Suite Structure	57
3 - 7 The FILM SCALER (X0) Program	59
3 - 8 The LORENTZ/POLARIZATION CORRECTION (X1) Program	61
3 - 9 The ABSORPTION CORRECTION (X3) Program	62
3 - 10 The STRUCTURE FACTORS/LEAST SQUARES (X24) Program	64
3 - 11 The BOND LENGTHS AND ANGLES (X26) Program	72
3 - 12 The GENERAL FOURIER (X16) Program	78
3 - 13 The FOURIER PLOT (X18) Program	84
3 - 14 The LOAD DISK (X50) and CLEAN DISK (X57) programs	90
3 - 15 The Direct Methods Programs	91
3 - 15 - 1 FAME	92
3 - 15 - 2 MAGIC	92
3 - 15 - 3 LINK	93
3 - 15 - 4 SYMPL	93
3 - 16 Other programs	93

3 - 1 Introduction

A major part of this work has centred around the development of a suite of computer programs, which perform the computational tasks encountered in crystallographic structure analysis. This has been made necessary by the unusual features of the only computer installation available for this work. For this reason, a detailed description of the computer configuration, the programming languages and the operating system is given, as these have conditioned both the strategies and tactics adopted in the design of the crystallographic program suite.

3 - 2 The Computer Configuration

The computer facilities available at this University are provided by a Computer Centre which is jointly owned by the University of Tasmania and the Tasmanian Hydroelectric Commission, and is administered by the Hydro-University Computer Centre Board upon which both bodies are represented. The development of system programs is carried out on a co-operative basis by the Computer Centre staff and various members of the academic staff of the University.

The basic element of the computer configuration is an Elliott Brothers 503 general purpose digital computer, with a main store capacity of 8192 (8K) words and a core backing store capacity of 16384 (16K) words. The word length is 39 bits, and normally two single address machine code instructions are stored in each word. Each machine code instruction consists of a six bit instruction code followed by a thirteen bit code, which may be a main store address or alternatively an additional specification of the machine function to be performed. The complete repertoire of sixty-four possible instructions is implemented. The instructions which involve the manipulation of the contents of main store locations are executed in approximately nine

microseconds, while the transfer of information to and from the backing store takes approximately seventy microseconds.

Apart from the operator's console, which incorporates an input/output typewriter, the peripheral equipment includes two 1000 character/second paper tape readers, two 100 character/second paper tape punches, a 300 line/minute lineprinter and a digital incremental plotter. The normal input medium is one-inch 8-channel paper tape; seven of the eight channels are used to represent a total of 128 tape characters, and the eighth channel is used to preserve the even parity of the punched character.

Recently the basic installation was expanded by the addition of a Digital Equipment Corporation PDP8/L computer, which communicates with the Elliott 503 *via* a locally designed interface. This allows the 503 computer to make use of the PDP8/L peripherals which include four DECTape magnetic tape transports and a demountable disk file unit. Under the storage scheme adopted, each reel of half-inch magnetic tape (DECTape) has a storage capacity of 57K 39-bit words, and each of the demountable disks has a capacity of 235K words.

3 - 3 Programming Languages

Programs for the Elliott 503 are written in an Elliott implementation of the high-level programming language ALGOL. This language was defined in the ALGOL 60 Report (Naur, [1960], [1963]). The Elliott implementation, designated Elliott ALGOL F, varies in some minor respects from the language defined in that Report, and these differences have been documented in the literature (Hoare [1963]). One important facility, foreshadowed in the ALGOL 60 Report and incorporated in Elliott ALGOL F, is the ability to include sequences of machine code instructions in ALGOL text in a manner compatible with the syntactical structure of the language. Other important facilities include the

ability to segment programs and to designate whether arrays are to be established in the main store or the backing store. Elliott ALGOL F has undergone some local modification, mainly by the extension of the number of standard functions recognized by the compilers. Details of these changes are given in Appendix A.

Another programming language available on the Elliott 503 is Symbolic Assembly Code (SAC), defined in the Elliott Computing Division Publication 2.1.2 (Elliott Brothers, 1963). As its name suggests, this language allows programs to be assembled using machine code instructions, while at the same time allowing the use of user-defined mnemonic symbols as a programming aid. Programs written and punched in SAC are converted to a relocatable binary code (RLB) by the Symbolic Assembly Program, and the RLB code is then punched by this program to paper tape in a form suitable for input to the computer.

Elliott ALGOL F includes the provision for an ALGOL program to make use of one or more auxiliary RLB programs resident in store at run time for special 'behind-the-scenes' functions. For example, the output of data on the digital plotter is handled by a set of procedures inserted in the text of the ALGOL program, and these in turn communicate with an auxiliary RLB program, which performs the special functions required to achieve plotter output. The transfer of information between an ALGOL program being executed in the 503 and the magnetic media peripherals under the control of the PDP8/L is handled in a similar way. This facility allows the particular requirements of individual peripheral devices to be met efficiently without any distortion of the syntax of the primary programming language.

3 - 4 The Operating System

The locally designed 503 operating system consists of a co-operative assembly of RLB programs built around the Elliott supplied compiler, which translates ALGOL text to executable machine code. Under normal operating conditions, the operating system is held in the backing store, and the first stage in the compilation process involves transferring a fresh copy of the system to the main store. Since the advent of magnetic tape storage, a reserve copy of the operating system is held on DECTape, so that in the event of the backing store copy becoming corrupt, the system can be reloaded into the backing store in a few seconds.

The compiler is subdivided into three programs. The first of these is a highly complex recursive program which performs a transformation of the ALGOL text into an internal code, termed 'owncode'. This program also carries out a check on the syntax of the ALGOL text while making this transformation. The 'owncode' version of the ALGOL text is stored temporarily in that part of the backing store not occupied by the master copy of the operating system. When the first stage of translation is complete, the second compilation program converts the 'owncode' to machine code and lays this code down in the main store, forming links between it and the third section of the compiler. This third program provides all the necessary dynamic routines and standard functions required for the execution of the compiled program. As each stage of the compilation is completed, the program no longer required is cleared from the store.

The other elements of the operating system consist of small RLB programs, which deal with the output of error diagnostics, control the activity of plotter and punch character queues, handle the output of characters to the lineprinter, and perform other monitoring and control

functions.

3 - 5 The Development of the Crystallographic Program Suite

The development of the suite of the crystallographic programs has passed through two stages. In the first stage, the suite was designed for use with the machine configuration which existed prior to attachment of the PDP8/L with its magnetic media peripherals.

The considerations which dictated the overall design of this early suite of programs were the problem of transferring the large amounts of data encountered in crystallographic work from one program to another in a convenient and efficient manner, and the nature of the structure factor/least squares refinement program. Crystallographic calculations are very often performed in the uninterrupted sequence; structure factor calculation - least squares refinement - fourier synthesis. As the elements of this sequence involve programs of considerable size, it is not possible, at least on a machine with only 8K of main store, to combine these separate calculations into one large program and still retain sufficient room for workspace and the storage of intermediate results. The sequence must of necessity be broken into two or more programs which are run consecutively. Normally, data would be transferred from one program to the next by punching and reading paper tape. However, as the data to be transferred can be voluminous, the time consumed in the punching operation can exceed the time taken to perform the calculations. Therefore, it was decided to replace this method of transferral by the process of backing store data transfer. In this process, each program in the sequence, other than the first, receives the bulk of its data from the backing store, where it was placed in an appropriate form by the preceding program. This technique provides a very rapid means of conveying information through a chain of programs.

This technique has one restriction, namely, that as the backing store is used for the storage of data, it cannot also be used for the temporary storage of the 'owncode' generated during compilation or for the retention of a master copy of the operating system, thus making it impossible to compile any of the programs other than the first in the sequence. This restriction was circumvented by making use of the facility for precompiling Elliott ALGOL programs. By punching out a paper tape 'image' of the main store immediately after compilation, a binary tape (referred to as a *dumped* program tape) may be produced, which incorporates the compiled program plus those elements of the operating system required for its execution. In this form, a dumped program may be loaded directly into the main store of the computer without passing through the translation stage.

The structure factors/least squares program used in this early suite of programs was a modified version of a program kindly made available by the late Dr. A.D. Wadsley (C.S.I.R.O. Division of Mineral Chemistry). This program was written for the Elliott 803 computer in fixed-address machine code by P.J. Wheatley using a program developed by D.W.J. Cruickshank and D.E. Pilling as a model (cited in Wheatley [1960]). This Elliott 803 machine code program used the block-diagonal approximation for the least squares parameter refinement (Ahmed and Cruickshank [1953]). As the Elliott 803 machine employed a 5-channel paper tape code, the machine code input, output and number assembly routines were modified with the assistance of the Computer Centre staff to allow input and output using the standard 503 8-channel paper tape. Further modifications were made to allow the structure factor output to be held in the backing store for use by subsequent programs, rather than punching this information on paper tape.

The suite of programs consisting of the modified machine code

structure factors/least squares program and dumped ALGOL programs linked together by data transfers *via* the core backing store proved to be a workable system and was used for the initial refinement of the structure of NH_4I_3 (Chapter 4). However, the structure factors/least squares program was operationally inconvenient, particularly when the least squares refinement section was being used, so that when the magnetic tape and disk facilities became available a major re-organization of the program suite was undertaken.

In this second stage of development, the programs in the suite were completely rewritten in Elliott ALGOL F to take advantage of the detachable bulk storage provided by the magnetic media. At the same time, the opportunity was taken to change from block-diagonal to full-matrix least squares refinement and to make the suite compatible with a series of direct methods programs which had become available in the interim (Section 3 - 15). The overall structure and the details of the individual components of the revised program suite are described in the following sections. As an example a listing of one of the programs (the GENERAL FOURIER (X16) program) is included as part of Appendix A. This Appendix also contains some detailed programming notes concerning certain of the programs described below.

3 - 6 The Program Suite Structure

The inter-relation of the individual programs of the program suite is shown in Figure 3 - 1 in block diagram form. Also shown is the relationship of the set of direct methods programs to the crystallographic suite proper. As indicated in this figure, data is transferred among the programs STRUCTURE FACTORS/LEAST SQUARES (X24), BOND LENGTHS AND ANGLES (X26), GENERAL FOURIER (X16) and FOURIER PLOT (X18) by means of data files established on the magnetic disk. These temporary data files are set up for use by these programs by the LOAD DISK (X50) program,

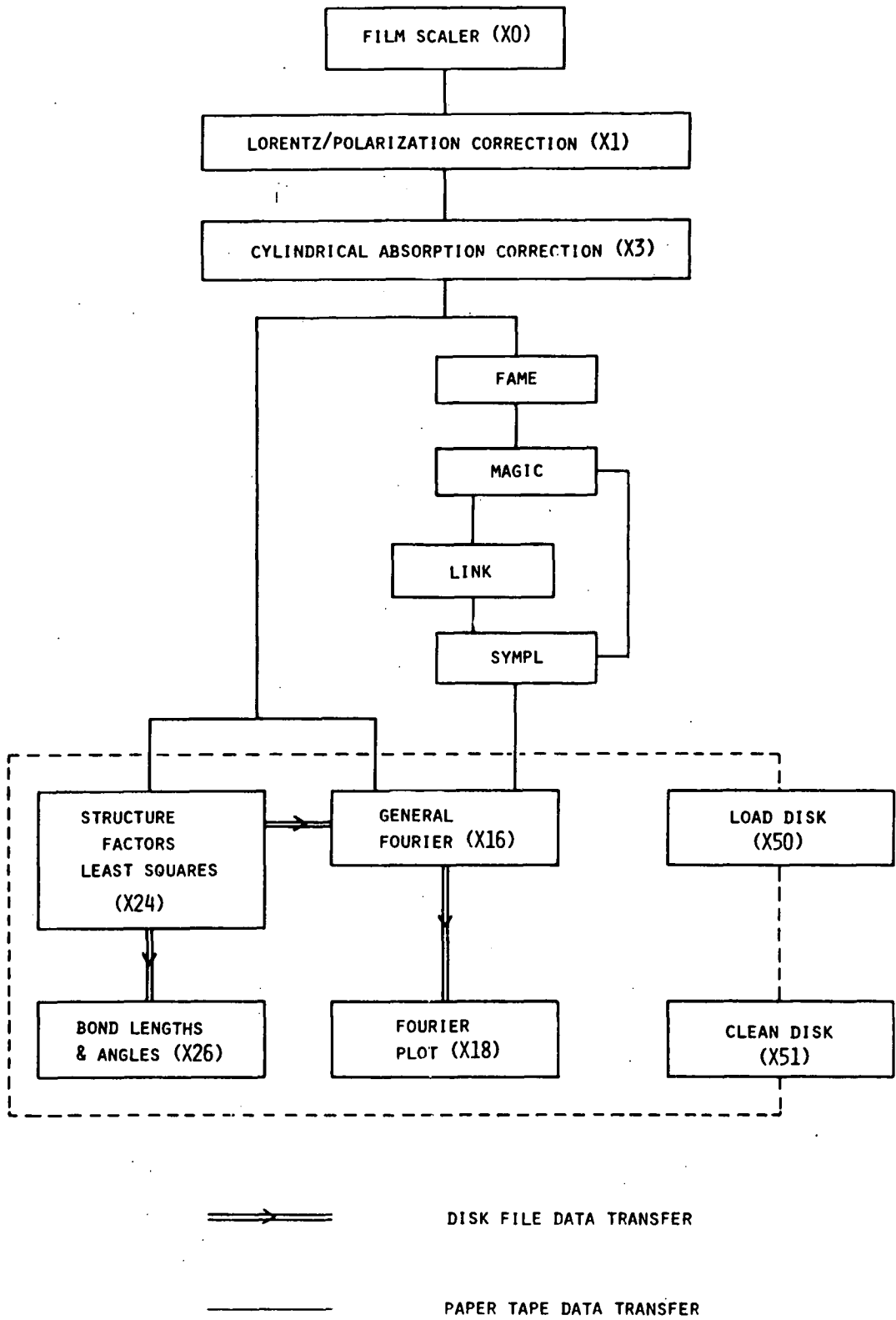


Figure 3 - 1, The crystallographic program suite structure.

which may also be used to transfer data held on magnetic tape between computer runs into selected disk files. In a similar way, the CLEAN DISK (X51) program may be used to transfer selected data from the temporary disk files to semi-permanent storage on magnetic tape before these files are expunged from the disk. For this reason, both X50 and X51 are designed to operate in a conversational mode, each program making enquiries *via* the console typewriter concerning the data file configuration required at the beginning and end of the run. Each of the programs X24, X26, X16 and X18 has its own specially identified input and output files, so that data cannot be misdirected while being transferred from one program to another. Further, a pessimistic strategy has been adopted in that all output files are cleared by the program which uses them before they are used for the storage of information for another program in the suite.

The use of these temporary disk files to convey information among the major crystallographic programs has resulted in a most efficient use of the available computer time. It has not been found necessary to use this method of data transfer for the data reduction and correction programs of the suite (X0, X3, X1).

3 - 7 The FILM SCALER (X0) Program

The multiple-film technique used to attenuate strong reflections, so that the resulting intensities fall within the linear response region of photographic films, effectively extends the range of response of the X-ray film. The silver halide in the emulsion reduces the intensity of a reflected beam as it passes through successive films in the multiple film pack, with the result that with properly judged exposures a reflection which is overexposed on the innermost film will be attenuated sufficiently to be within the linear range of one of the films beneath it. When short-wavelength X-rays are used, for example

MoK α as in this study, it is necessary to augment the attenuation produced by the emulsion by interleaving the films with sheets of metal foil.

With the multiple film technique it is necessary to calculate the attenuation factor (or film factor) k_f , by means of which the attenuated reflections can be brought to a common scale. This calculation, and the application of the factor so determined to the measured intensities is carried out by the FILM SCALER (X0) program.

The initial data for this program consists of an identifying alphanumeric string, the number of films in the multiple film pack, and the measured reflection data. This last set of data takes the form of a list, each item of which consists of the Miller indices of a reflection followed by the intensity of the reflection as measured on each film of the pack. Intensities which lie beyond the limits of the intensity scale used to measure the data are indicated by unique numerical values. The end of the list is signalled by a dummy reflection with Miller index, $h = 111$ (this end-of-list marker for reflection data is common to all programs of the crystallographic suite).

The first task executed by the program is the calculation of the film factor, k_f , as the average ratio of the intensities of reflections which have been recorded on adjacent films. In the calculation of this average, those reflections with intensities outside the range of the intensity scale on any film are disregarded. Once the film factor has been determined, the intensity of each reflection is brought to a common scale by the application of the relationship

$$I_{final} = (I_1 + k_f I_2 + k_f^2 I_3 + \dots + k_f^{n-1} I_n) / n$$

where n is the number of films in the pack. To assist in the identification of reflections which may have been inaccurately measured, the

standard deviation of this average is also calculated where there are a sufficient number of measurements to make this possible. The scaled reflection data is output to the lineprinter for visual inspection and to punched tape for use in subsequent programs.

3 - 8 The LORENTZ/POLARIZATION CORRECTION (X1) Program

Certain geometric effects must be taken into account before the raw scaled intensities generated by the previous program may be used for subsequent calculations. The most significant corrections which must be made are the polarization correction and the Lorentz correction. As only geometric considerations enter into their calculation, it is convenient to evaluate these by means of a single program. The polarization correction, p^* , arises from the reduction of the intensity of the unpolarized incident X-ray beam as a result of polarization upon reflection. This correction factor is a function of the Bragg angle, θ , only, and is given by

$$p^* = 2/(1 + \cos^2 2\theta)$$

The Lorentz correction, L^* , is concerned with the specific motion of the crystal in the camera geometry. The nature of this motion affects the time taken for the various planes to pass through the reflection condition, and the form of this correction for the Weissenberg geometry used in this study is

$$L^* = \sin \Gamma \cos^2 \nu$$

where Γ is the angle between the projections of the incident and reflected beams on the equatorial plane (normal to the rotation axis), and ν is the angle between the generator of a given layer line and the equatorial plane.

The LORENTZ/POLARIZATION CORRECTION (X1) program computes and applies

the combined correction, $(Lp)^*$, for each of a sequence of scaled reflection data collected in the equi-inclination Weissenberg geometry. The input data for the program consists of an identifying alphanumeric string, the direct unit cell constants, the wavelength of the X-radiation used for data collection, the equi-inclination setting angle, μ , for the first level, a marker indicating the axis about which the data was collected, and the scaled intensity data as generated by X0. This last consists of a sequence of h, k, l, I_{scaled} terminated by a dummy plane with $h = 111$. As each plane is read, the program computes θ , 2θ , Γ , and v from the given data, and then computes the correction factor from the relations given above. The correction is applied to the scaled intensity and the corrected data is output to the lineprinter for visual inspection and to punched paper tape for use by subsequent programs.

3 - 9 The ABSORPTION CORRECTION (X3) Program

As well as geometric effects, a correction may be necessary for the absorption of the incident and reflected beams in their passage through the crystal. The need for such a correction will depend upon the size of the crystal and the absorption coefficients of the elements present in the crystal at the wavelength in question. For this correction to be made exactly, a detailed knowledge of the crystal shape is required, and normally it is necessary to approximate the actual shape by a convex polyhedron of known geometry. As the crystals used in this study were rarely polyhedral after mounting, it was sufficient to approximate their actual shapes by cylinders of known diameter. The ABSORPTION CORRECTION (X3) program computes and applies the reciprocal transmission factor, A^* , for a cylindrical crystal bathed in a uniform beam of X-rays in the equi-inclination Weissenberg geometry.

The initial data for the program consists of an alphanumeric string which serves to identify the lineprinter output from the program, the reciprocal cell dimensions, the X-ray wavelength, the cylindrical co-ordinate ζ , the number of levels of data, an integer in the range 1 - 3 which identifies the axis about which the data was collected, and a table of reciprocal transmission factors A^* . The table has one row for each level of reflection data, and each row contains transmission factors calculated for the value of $\mu R \sec \nu$ for the level in question. Within each row there are nineteen A^* values, calculated at 5° increments in $\Gamma/2$, commencing at 0° .

Γ, ν have the same significance as in Section 3 - 8,

μ is the linear absorption coefficient, and

R is the radius of the cylinder.

The reflection data consists of a sequence of $h, k, \ell, |F|$, generated by X1 and terminated by a dummy reflection with $h = 111$. For each reflection, the program computes $\sin^2 \theta$ from the reciprocal cell constants and the wavelength, and ν from the level index and ζ . The value of $\Gamma/2$ is then determined from the relation

$$\Gamma/2 = \arcsin(\sec \nu (\sin^2 \theta - \sin^2 \nu)^{1/2})$$

The value of A^* is then computed by 2-point interpolation on the appropriate entry in the table. The value of A^* so determined is corrected in the case of upper levels by $\cos \nu$ to compensate for the larger irradiated volume. The reciprocal transmission factor is applied to $|F|^2$ and the corrected data is then output to the lineprinter for visual inspection, and to punched paper tape for use in subsequent programs.

(For the work reported here, the values of A^* were taken from TABLE 5.3.5B, *The International Tables for X-Ray Crystallographers*, Volume II, (Henry and Lonsdale [1967])).

3 - 10 The STRUCTURE FACTORS/LEAST SQUARES (X24) Program

The numerical tasks performed by crystallographic structure factors/least squares programs have been well described in the literature (Rollett [1965]), and are only briefly outlined here. Programs of this class perform two distinct but related operations. The first of these is the calculation of the structure factor F_{hkl} for each of a given set of reflections from parameters specified for a particular structural model. This calculation requires the evaluation for each reflection of the expression

$$F_{hkl} = \sum_{j=1}^n n_j f_j \sum_{\delta=1}^p \exp(-\underline{h}^T B_{j\delta} \underline{h}) \cos(2\pi \underline{h} \cdot \underline{x}_{j\delta}) \\ + i \sum_{j=1}^n n_j f_j \sum_{\delta=1}^p \exp(-\underline{h}^T B_{j\delta} \underline{h}) \sin(2\pi \underline{h} \cdot \underline{x}_{j\delta})$$

where n_j is the occupancy parameter of atom j ,

f_j is the scattering power of atom j at $(\sin\theta_{hkl})/\lambda$,

$B_{j\delta}$ is the 3 x 3 temperature factor matrix for atom j in symmetry position δ ,

$\underline{x}_{j\delta}$ is the coordinate vector for the atom j in position δ ,

\underline{h} is the reciprocal space vector hkl , and \underline{h}^T is its transpose,

n is the number of independent atoms,

p is the number of symmetry positions.

The second, and usually optional, stage is the refinement of the structural parameters by the accumulation and inversion of a normal equation matrix followed by the calculation of the corrections to be applied to the parameters. If the matrix equation to be solved is written as

$$\underline{A}\underline{X} = \underline{b}$$

where \underline{A} is the normal equation matrix,

\underline{X} is the vector of parameter corrections, and

\underline{b} is the right-hand side vector,

then the formation of an element A_{ij} of \underline{A} requires the accumulation of the sum

$$\sum^q w(\underline{h}) \frac{\delta |F(\underline{h})|}{\delta \zeta_i} \times \frac{\delta |F(\underline{h})|}{\delta \zeta_j}$$

and the formation of a b_i of \underline{b} requires the accumulation of the sum

$$\sum^q w(\underline{h}) (K F_{\text{observed}} - F_{\text{calc}}) \times \frac{\delta |F(\underline{h})|}{\delta \zeta_i}$$

where $w(\underline{h})$ is the weight of the reflection with indices hkl ,

ζ_i, ζ_j are parameters of the structural model,

K is the scale factor which relates the observed structure factors to an absolute scale,

the summation being taken over all q reflections.

The process of structure factor calculation and least squares refinement is often carried out in a cyclic fashion, the refined parameters being used for a new round of structure factor calculation and parameter refinement.

The STRUCTURE FACTORS/LEAST SQUARES (X24) program can be regarded as a greatly modified descendant of the MONLS structure factor/full matrix least squares program used by the crystallographic group of the Department of Chemistry, Monash University. The MONLS program is itself a variant of the ORFLS program of Busing and Levy (Busing and Levy [1961]). A CDC FORTRAN listing of the MONLS program was kindly made available by Dr. B. Gatehouse, (Department of Chemistry, Monash University), and from this the X24 program was developed.

The development of the X24 program passed through three major stages. In the first stage an Elliott ALGOL F program was written which followed in large measure the overall organizational pattern as well as the detailed programming of the MONLS program. Thorough checks

were made to ensure that the X24 program calculated the parameter derivatives and assembled the least squares matrix elements correctly, by comparing the relevant quantities calculated at various intermediate stages in the computation against the same quantities calculated by the MONLS program for a set of standard data. The test data consisted of 33 reflections for α -quartz, and the test calculation carried out three structure factor calculation and refinement cycles for the α -quartz model. The refinement was performed for all parameters including anisotropic temperature factors. The comparative data used in making these checks was prepared by Dr. B. Gatehouse and Mr. J.E. Davies (Department of Chemistry, Monash University), and as the checking procedure was an exhaustive one extending over several months, their co-operation is gratefully acknowledged.

Once it was established that the X24 program was functioning correctly, its development entered the second stage in which a number of major changes were made. At the level of detailed programming, the entire structure factor and parameter derivative calculation, as well as the accumulation of the least squares matrix elements, were rewritten in machine code and incorporated in the ALGOL text (c.f. Section 3 - 3). This modification was desirable in view of the time penalty incurred by array access in Elliott ALGOL F and reduced the execution time to approximately half its previous value.

At the same time, that section of the program which reproduced on the lineprinter the input data for a particular run (the 'data echo') was considerably expanded to give a complete record of the parameters of the structural model in question and the program options specified for the run. The policy of including a comprehensive data echo has been adopted with all the programs of the suite, for not only is it a desirable feature in programs of general utility which may be used by

workers other than the original author, but also it can provide, if carefully devised, a useful and to some extent self-explanatory complement to the program documentation. In the case of the X24 program, where a large amount of information must be marshalled correctly for a successful run, it gives a very useful means of checking that the users intentions have in fact been carried out.

During this reorganization, advantage was taken of the facility which enables parts or segments of an Elliott ALGOL F program to be held in the core backing store until they are required for execution. This has the effect of increasing the amount of main store available to the program, as it is now necessary to reserve only sufficient main store space to accommodate the largest program segment, the segments being brought to the main store by autonomous data transfer in the correct order under the control of the operating system. As the sections of the program concerned with data input, structure factor calculation/least squares matrix accumulation, and matrix inversion, and the output of refined parameters are required sequentially, the program was broken into three corresponding segments. The boundaries of the segmented areas were carefully chosen to equalize the sizes of the compiled segments and so gain the maximum benefit from this facility. In its final form, the three segments of X24 occupy 1024, 1042 and 1037 words of core backing store respectively.

The final stage of development was initiated by the advent of bulk magnetic storage media. The changes made in this stage were essentially twofold, the first being concerned with the efficiency of the structure factor calculation, and the second with the transfer of information to other programs of the suite. From Section 2 - 3, it can be seen that the calculation of the structure factor for a given reflection hkl requires that the value of f_{hkl} , the scattering power of each atom included

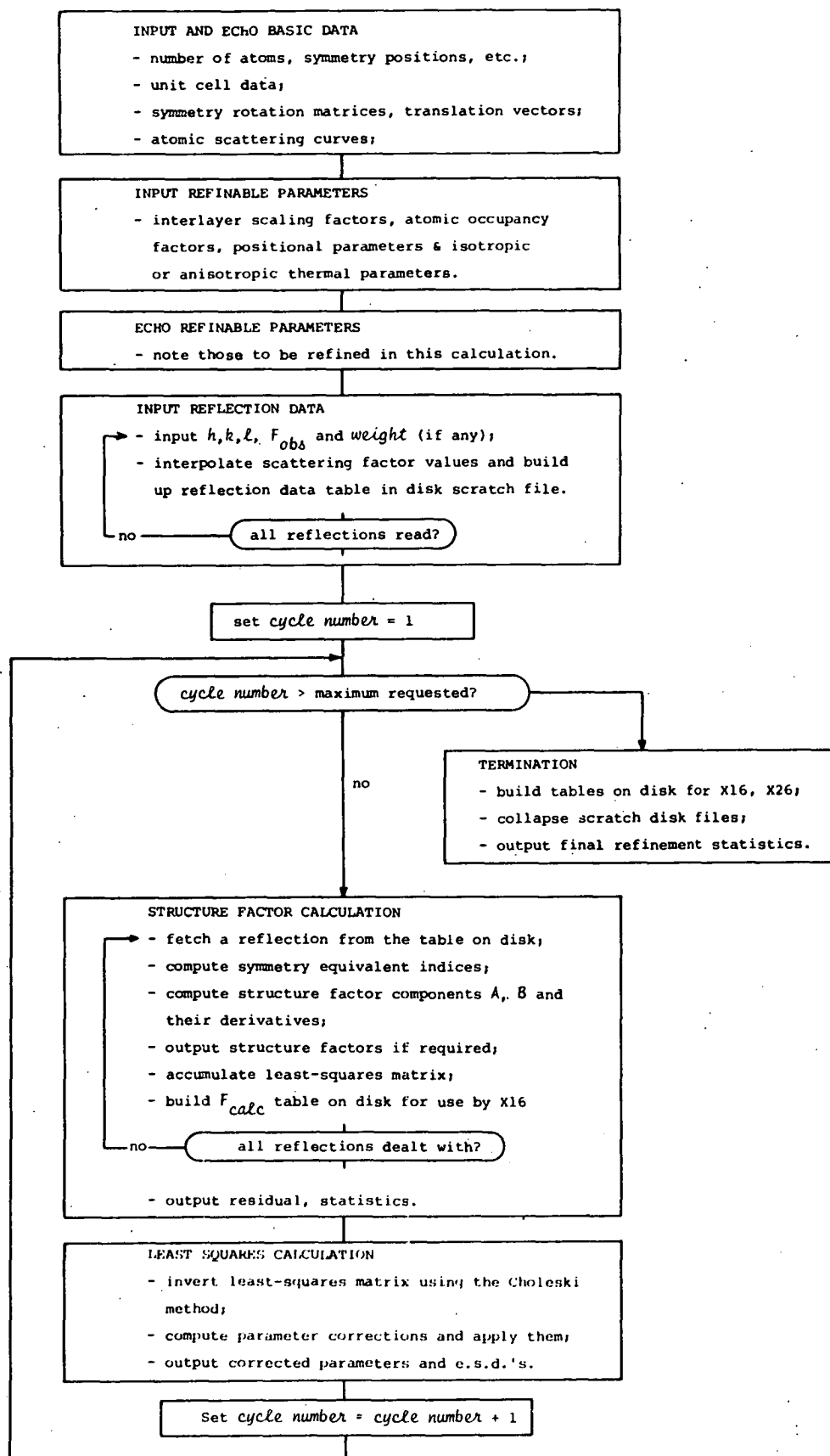


Figure 3 - 2, Generalized flow chart of the final form of the STRUCTURE FACTORS/LEAST SQUARES X24 program.

in the model at $(\sin\theta_{hkl})/\lambda$, must be determined. The determination is made in X24 (and also in the ancestral MONLS program) by two-point interpolation on the correct atomic scattering curve. The tabulated scattering curves for the atomic species present in the model are input to the program as part of its data. If the model includes n atoms and there are q reflections, then each cycle of structure factor calculation will require $n \times q$ interpolations, each of which involves the access of tabulated information held in data arrays. Further, if the duplication of stored scattering curves is to be avoided, at least one stage of indirect addressing is involved in this process to ensure that the correct scattering curve is used for each atom in the model. When more than one cycle of structure factor calculation is required, it is more efficient to calculate the interpolated values of the scattering power of each atom included in the model (together with any other pertinent information) along with the values of $h, k, l, F(\text{observed})$ for each reflection, provided that sufficient storage space is available and that it can be accessed efficiently. If these conditions can be met, the lengthy $n \times q$ interpolations need be performed only once for a given run. There was not sufficient storage available before the magnetic media peripherals were attached to the computer for this strategy to be adopted. However, with the availability of magnetic disk storage, X24 was modified to allow the list of interpolated atomic scattering factors to be built up on the disk as the reflection data is input prior to the commencement of the structure factor calculation. This change provided a 30% reduction in the time required for structure factor calculation.

The use of the disk to provide a means of conveying large volumes of information among the members of the program suite has been described in Section 3 - 6. The modifications that were necessary to allow X24 to transmit data to the GENERAL FOURIER (X16) and the BOND LENGTHS AND ANGLES (X26) programs were readily made once the change to temporary disk

```

RD13 WEISS
NUMBER OF CYCLES          3
NUMBER OF VARIABLES      17
NUMBER OF OBSERVATIONS   360
NUMBER OF F-CURVES       2
NUMBER OF ATOMS          4
NUMBER OF SYMMETRY POSITIONS 4
NUMBER OF SCALES         5
NUMBER OF ISOTROPIC ATOMS 4

AXIS OF DATA COLLECTION      B
LOWEST INDEX IS OBSERVATIONS ARE 0
WEIGHTING                     F
CENTROSYMMETRIC              SET = 1.0
                              YES

SCATTERING CURVES:

IODINE - MONASH
53.000  51.990  49.390  46.090  42.760  39.720  37.020
54.990  52.370  50.400  48.440  46.800  45.140  23.900
22.470  21.400  20.380  19.400  18.740  17.800  17.400
16.800  16.250  15.800  15.190  14.800  14.180  13.800
13.200  12.800  12.260  12.000

RUBIDIUM - MONASH
36.000  35.400  33.820  31.600  29.000  26.200  24.700
22.900  21.350  19.900  18.600  17.360  16.300  15.160
14.500  13.720  12.900  12.230  11.680  11.100  10.540
10.080  9.6400  9.2500  8.8500  8.5000  8.1000  7.8300
7.5000  7.2200  6.9900  6.7500

SYMMETRY POSITIONS:
X,      Y,      Z;
X+1/2,  -Y+1/2,  -Z+1/2;
-X,      Y+1/2,  -Z;
-X+1/2,  -Y,      Z+1/2;

RECIPROCAL CELL DATA:
A= .09187  B= .15276  C= .10559  COS(ALPHA)= .00000  COS(BETA)= .00000  COS(GAMMA)= .00000

DATA SCALES:
2.6743*
3.1288*
2.8439*
3.3904*
2.0627*

OVERALL T/FACTOR: .00000

ATOMIC PARAMETERS BEFORE REFINEMENT:

IODINE 1
FCURVE      1
OCCUPANCY   .50000
X            .15715000*
Y            .25000000
Z            .35165000*
H            3.5000*

IODINE 2
FCURVE      1
OCCUPANCY   .50000
X            .37652000*
Y            .25000000
Z            .54283000*
H            3.5000*

IODINE 3
FCURVE      1
OCCUPANCY   .50000
X            .57141000*
Y            .25000000
Z            .73506000*
H            3.5000*

RUBIDIUM
FCURVE      2
OCCUPANCY   .50000
X            .32886000*
Y            .25000000
Z            .03019000*
H            3.5000*

```

Figure 3 - 3, Photo-reduction of the X24 program data
echo - note the asterisk marking parameters
to be refined in this run.

AGREEMENT FACILITY BASED ON KARAKORUM TREATY TO BE IMPLEMENTED

4-10015S : 4-10015S 4-10015S 4-10015S

1500.00	1500.00	1500.00	1500.00
4200.61	4200.61	4200.61	4200.61
32.7990	32.7990	32.7990	32.7990

14-00000

00000000	00000000	00000000	00000000	00000000
----------	----------	----------	----------	----------

151412	911151	004166	000062	00
151413	911152	004167	000063	00

00	.400000	11/14.6	1598.85	11.9142
00	.350000	6982.00	10/3.17	15.3705

00	00000000	7542.00	1670.15	22.14
00	00000000	4248.00	1614.60	18.41

000400*	000000*	000000*	000000/	00
610-107	1000-104	000-106	000010-	00

0000000	0000000	0000000	0000000	0000000
---------	---------	---------	---------	---------

RECEIVED 1977 JAN 11

6	13962.0	2600.66	20.0593	77.
---	---------	---------	---------	-----

66 01/01/1981 01/01/1981 01/01/1981

AGREEMENT FACTORS BASED ON PARAMETERS AFTER REFINEMENT

STANDARD DEVIATION: 0.0000

SEN 13745

2.67431	- .582206	2.092198
---------	-----------	----------

3.39040	-	525799	2.86402
2.06270	-	134842	1.92276

ATOMIC WEAPONS:

100 LINE 1

4282158	110000	859148	7
0000000		0000000	1

2 301001

0000042	0000042	0000042	7
0000042	0000042	0000042	1

[illegible]

000000	000000	000000	000000
000000	000000	000000	000000

2,000.00	FURRY	2,000.00
2,000.00	SOCIETY	2,000.00

000000	000000	000000	7
000000	000000	000000	A

3 = 3 (continued) Photo-reduction of +

for the first time-

storage of the interpolated scattering data was complete. Although these latter alterations did nothing to improve the run-time efficiency of the X24 program itself, they produced a marked improvement in the efficiency and ease of operation of the program suite as a whole. It should be mentioned that throughout the development of X24, checks were made using the α -quartz test data to ensure that no numerical errors were introduced by the modifications to the structure of the program. The final structure of the X24 program is shown in Figure 3 - 2. A sample of typical output, including the comprehensive data echo, is shown in Figure 3 - 3.

3 - 11 BOND LENGTHS AND ANGLES (X26) Program

One essential component of a suite of crystallographic programs is that which calculates derived quantities of interest to the chemist from the structural parameters. The most significant of these quantities from the point of view of the chemist are the bond lengths and bond angles; the need to know certain bond lengths or angles often provides the major impetus for undertaking a particular structural determination. However, these derived quantities are also of use to the crystallographer in that they are often employed as a check on the plausibility of the structural model.

Not only must these derived quantities be computed, but some measure of their precision is also desirable. Besides the systematic errors which may be present in the data due to the effects of absorption, extinction, etc., the data will also be affected by random errors which will control the precision of the quantities derived from the structural parameters. The precision of bond lengths and angles is usually represented by the 'estimated standard deviation' (e.s.d. - cf. Rollett [1965]) and it is convenient to combine the calculation of these quantities with the computation of the derived quantities they qualify.

These numerical tasks are carried out by the BOND LENGTHS AND ANGLES (X26) program. This program receives the bulk of the information required for these calculations from the STRUCTURE FACTORS/LEAST SQUARES (X24) program, the transfer of information being accomplished by the use of one of the disk files common to the crystallographic suite. This information includes the set of positional parameters defining the asymmetric unit, the symmetry operators for the space group, the least squares matrix inverse and the residual parameter, p

$$p = \frac{\sum_{i=1}^q w_i \Delta F_i^2}{(q - n)}$$

where w_i is the weight of the i th ΔF , q is the number of observations and n is the number of parameters. A number of control parameters are also read by the program from paper tape.

As the X24 program needs only the positional parameters of the atoms in the asymmetric unit, the first operation performed by the X26 program is the generation of the entire unit cell contents from these parameters. This operation makes use of the symmetry data supplied by X24 in the form of rotation matrices and translation vectors. In the case of a centrosymmetric space group, a necessary preliminary is the augmentation of the symmetry data to produce the matrices and vectors for the inversion related general positions not needed in the structure factor calculation.

The positions of all atoms in the unit cell are then calculated using a set of ALGOL procedures devised for this purpose by Wells (Wells [1965]). The fractional co-ordinates of the atom positions so generated are then displayed on the lineprinter.

Before the calculation of the bond-lengths and angles and their associated e.s.d.'s is commenced, the least squares matrix inverse is changed to a form more suitable for e.s.d. calculation. This involves

the retention of only those elements of the inverse which refer to positional parameters and the conversion of the surviving elements to covariance, V_{ij} , form by the application of the relationship

$$V_{ij} = p \cdot b_{ij}$$

where p is the residual parameter previously defined and b_{ij} is the element of the least squares matrix inverse linking the i th and j th positional parameters.

As the calculation of all possible inter-atomic distances and 'bond' angles in the unit cell can, even in the case of structures of modest complexity, lead to very voluminous output, the process of bond length and angle calculation is constrained by the simple device of using a control parameter which places an upper limit on the lengths which will be considered as bond distances. As this constraint can be carried by the user, it does not limit the possible use of the X26 program for checking the plausibility of the model.

The design of the X26 program also takes cognizance of two other interdependent problems, namely, the possibility that the unit of chemical interest may cross the boundary between neighbouring unit cells, and that there is a possibility that identical distances and angles will be calculated repeatedly due to the presence of symmetry related groups of atoms in the volume of crystal space inspected by the X26 program. The solution to the first of these problems adopted in the design of the X26 program involves the inspection of the eight neighbouring unit cells which surround any selected origin for inter-atomic distances which satisfy the constraint imposed by the control parameter. This strategy has the consequence of producing an eight-fold increase in the possibility of the same distance or angle appearing repeatedly in the final output. To avoid this unnecessary repetition, the program is designed to build up in a disk file a list of all distances

and angles previously calculated. When a new bond distance or angle is calculated, the list is checked to see if this quantity has been calculated previously. When this is the case, a further check is made to determine whether the recurrence is fortuitous or the result of calculations involving a group of atom positions which are symmetry replicates of those which gave rise to the first occurrence in the list. If the quantity passes both tests it is output in a suitable form and the relevant data concerning it is added to the list, otherwise the quantity is rejected.

The X26 program calculates bond lengths, ℓ_{ij} , from the general relationship

$$\ell_{ij}^2 = ((\Delta xa)^2 + (\Delta yb)^2 + (\Delta zc)^2 + 2ab\Delta x\Delta y \cos \gamma + 2ac \Delta x \Delta z \cos \beta + 2bc \Delta y \Delta z \cos \alpha)^{1/2}$$

where $a, b, c, \alpha, \beta, \gamma$, are the unit cell parameters and $\Delta x, \Delta y, \Delta z$ are the differences between the fractional coordinates for atoms i and j at positions x_i, y_i, z_i and x_j, y_j, z_j .

The estimated standard deviation, σ_{ij} , for the length ℓ_{ij} is calculated from the general relationship (Stout and Jensen [1971], Rollett [1965]) which assumes correlation among the positional parameters. In matrix notation this can be written as the quadratic form:

$$\sigma_{ij}^2 = \underline{G}^T \cdot \underline{V} \cdot \underline{G}$$

where \underline{V} is a 6 x 6 symmetric matrix with elements V_{ij} taken from the transformed least squares matrix inverse for the i th and j th atoms, and \underline{G} is the six element vector of differential terms of the type:

$$G_2 = \frac{\partial \ell_{ij}}{\partial y_i} = (\Delta yb + \Delta xa \cos \gamma + \Delta zc \cos \alpha) / \ell_{ij}$$

$$G_3 = \frac{\partial \ell_{ij}}{\partial z_i} = (\Delta zc + \Delta xa \cos \beta + \Delta yb \cos \alpha) / \ell_{ij}$$

In the case of bond angles, the angle θ_{jik} subtended at the i th atom by the bonds with lengths ℓ_{ij} , ℓ_{ik} is calculated from the relationship (Stout and Jensen [1971])

$$\theta_{jik} = \cos^{-1} ((\ell_{ij}^2 + \ell_{ik}^2 - \ell_{jk}^2) / (2\ell_{ij} \ell_{ik}))$$

The estimated standard deviation, σ_θ , for the angle θ_{jik} is also calculated from a general relationship developed by Darlow [1960] which, like that for the bond length case, assumes correlation among the parameters. As before, the relationship can be written in matrix notation as a quadratic form:

$$\sigma_\theta^2 = k (\underline{G}^T \underline{V} \underline{G})$$

where the scalar term k is given by:

$$k = 1/(\ell_{ij} \ell_{ik} \sin \theta_{jik})^2$$

In this case \underline{V} is a 9×9 matrix with elements V_{ij} taken from the transformed inverse for the j, i and k th atoms. Once again, the elements of the vector \underline{G} are differential terms, but are more complex expressions than those required for the bond length case:

.....

$$G_2 = \ell_{ik} (\cos \beta_{ik} - \cos \theta_{jik} \cos \beta_{ij})$$

.....

$$G_4 = \ell_{ik} (\cos \alpha_{ik} - \cos \theta_{jik} \cos \beta_{ij}) \\ + \ell_{ij} (\cos \alpha_{ij} - \cos \theta_{jik} \cos \alpha_{ik})$$

.....

.....

$$G_9 = \ell_{ij} (\cos \gamma_{ij} - \cos \theta_{jik} \cos \gamma_{ik})$$

where $\cos \alpha_{ij}$, $\cos \beta_{ij}$, $\cos \gamma_{ij}$ and $\cos \alpha_{ik}$, $\cos \beta_{ik}$, $\cos \gamma_{ik}$ are the direction cosines of the bonds from the i th to the j th and the i th to

BOND LENGTHS

EVALUATION

AE	10.985
BE	0.5482
CE	0.4706
AEHAE	90.000
BEHBE	90.000
CEHCE	90.000

UNIT CELL PARAMETERS

BOUNDS 1 111	1.5749	25000	15153
BOUNDS 1 121	1.5749	25000	14447
BOUNDS 1 131	1.4451	25000	14447
BOUNDS 1 141	1.4451	25000	15153
BOUNDS 2 111	1.5757	25000	14444
BOUNDS 2 121	1.5757	25000	15506
BOUNDS 2 131	1.6243	25000	14550
BOUNDS 2 141	1.6243	25000	14444
BOUNDS 3 111	1.5767	25000	13494
BOUNDS 3 121	1.5767	25000	17650
BOUNDS 3 131	1.42633	25000	16506
BOUNDS 3 141	1.42633	25000	13494
BOUNDS 111	1.33074	25000	03002
BOUNDS 121	1.3374	25000	14699
BOUNDS 131	1.46926	25000	14699
BOUNDS 141	1.6926	25000	153002

BOND DISTANCES INVOLVING BOND 1 111

BOUNDS 1 111 - BOUNDS 1 121	5.7722:000718
BOUNDS 1 111 - BOUNDS 2 111	3.0157:000610
BOUNDS 1 111 - BOUNDS 2 141	4.3920:000446
BOUNDS 1 111 - BOUNDS 3 111	5.8058:000637
BOUNDS 1 111 - BOUNDS 3 121	4.0213:000665
BOUNDS 1 111 - BOUNDS 3 131	4.4663:000417
BOUNDS 1 111 - BOUNDS 111	3.5816:000869
BOUNDS 1 111 - BOUNDS 141	3.6861:000417

BOND ANGLES INVOLVING BOND 1 111

BOUNDS 1 121 - BOUNDS 1 111 - BOUNDS 2 111	56.862:015342
BOUNDS 1 121 - BOUNDS 1 111 - BOUNDS 2 141	82.049:011484
BOUNDS 1 121 - BOUNDS 1 111 - BOUNDS 3 111	58.174:008453
BOUNDS 1 121 - BOUNDS 1 111 - BOUNDS 3 121	122.572:015511
BOUNDS 1 121 - BOUNDS 1 111 - BOUNDS 3 131	47.244:007830
BOUNDS 1 121 - BOUNDS 1 111 - BOUNDS 111	38.768:013029
BOUNDS 1 121 - BOUNDS 1 111 - BOUNDS 141	96.891:013302
BOUNDS 2 111 - BOUNDS 1 111 - BOUNDS 2 141	114.071:010134
BOUNDS 2 111 - BOUNDS 1 111 - BOUNDS 3 111	1.3122:010891
BOUNDS 2 111 - BOUNDS 1 111 - BOUNDS 3 121	65.712:013864
BOUNDS 2 111 - BOUNDS 1 111 - BOUNDS 3 131	65.849:009679
BOUNDS 2 111 - BOUNDS 1 111 - BOUNDS 111	95.630:018813
BOUNDS 2 111 - BOUNDS 1 111 - BOUNDS 141	72.171:010524
BOUNDS 2 141 - BOUNDS 1 111 - BOUNDS 3 111	118.775:008236
BOUNDS 2 141 - BOUNDS 1 111 - BOUNDS 3 121	124.621:007671
BOUNDS 2 141 - BOUNDS 1 111 - BOUNDS 3 131	52.379:008001
BOUNDS 2 141 - BOUNDS 1 111 - BOUNDS 111	58.916:010282
BOUNDS 2 141 - BOUNDS 1 111 - BOUNDS 141	69.173:010580
BOUNDS 3 111 - BOUNDS 1 111 - BOUNDS 3 121	64.359:009916
BOUNDS 3 111 - BOUNDS 1 111 - BOUNDS 3 131	66.659:007545

BOUNDS 3 111 - BOUNDS 1 111 - BOUNDS 111	96.942:013153
BOUNDS 3 111 - BOUNDS 1 111 - BOUNDS 141	71.702:009805
BOUNDS 3 121 - BOUNDS 1 111 - BOUNDS 3 131	109.102:011307
BOUNDS 3 121 - BOUNDS 1 111 - BOUNDS 111	151.342:017236
BOUNDS 3 121 - BOUNDS 1 111 - BOUNDS 141	61.976:009737
BOUNDS 3 131 - BOUNDS 1 111 - BOUNDS 111	59.942:011004
BOUNDS 3 131 - BOUNDS 1 111 - BOUNDS 141	53.882:010926
BOUNDS 111 - BOUNDS 1 111 - BOUNDS 141	111.912:012631

BOND DISTANCES INVOLVING BOND 1 111

BOUNDS 1 111 - BOUNDS 1 131	5.5115:000608
BOUNDS 1 111 - BOUNDS 3 141	4.2735:000395
BOUNDS 1 111 - BOUNDS 121	3.7294:000780

BOND ANGLES INVOLVING BOND 1 111

BOUNDS 1 121 - BOUNDS 1 111 - BOUNDS 1 131	65.385:008415
BOUNDS 1 121 - BOUNDS 1 111 - BOUNDS 3 141	50.119:008496
BOUNDS 1 121 - BOUNDS 1 111 - BOUNDS 121	16.967:013539
BOUNDS 1 131 - BOUNDS 1 111 - BOUNDS 3 141	46.429:009953
BOUNDS 1 131 - BOUNDS 1 111 - BOUNDS 121	41.691:007810
BOUNDS 3 141 - BOUNDS 1 111 - BOUNDS 121	61.068:010456

BOND DISTANCES INVOLVING BOND 1 111

BOUNDS 1 111 - BOUNDS 3 121	5.6286:000688
-----------------------------	---------------

BOND DISTANCES INVOLVING BOND 1 111

BOUNDS 1 111 - BOUNDS 2 121	4.8354:008634
-----------------------------	---------------

BOND ANGLES INVOLVING BOND 1 121

BOUNDS 2 111 - BOUNDS 1 121 - BOUNDS 2 131	55.382:007039
BOUNDS 2 111 - BOUNDS 1 121 - BOUNDS 3 111	29.710:007371
BOUNDS 2 111 - BOUNDS 1 121 - BOUNDS 3 131	55.138:007346
BOUNDS 2 111 - BOUNDS 1 121 - BOUNDS 3 141	105.691:010203
BOUNDS 2 111 - BOUNDS 1 121 - BOUNDS 111	66.448:013079
BOUNDS 2 111 - BOUNDS 1 121 - BOUNDS 121	70.830:012929
BOUNDS 2 131 - BOUNDS 1 121 - BOUNDS 3 111	48.707:006722
BOUNDS 2 131 - BOUNDS 1 121 - BOUNDS 3 131	37.557:008307
BOUNDS 2 131 - BOUNDS 1 121 - BOUNDS 111	96.662:012125
BOUNDS 2 131 - BOUNDS 1 121 - BOUNDS 121	69.489:006801
BOUNDS 3 111 - BOUNDS 1 121 - BOUNDS 3 141	65.715:009790
BOUNDS 3 111 - BOUNDS 1 121 - BOUNDS 111	96.178:013313
BOUNDS 3 111 - BOUNDS 1 121 - BOUNDS 121	41.100:011047
BOUNDS 3 131 - BOUNDS 1 121 - BOUNDS 3 141	77.121:003263
BOUNDS 3 131 - BOUNDS 1 121 - BOUNDS 111	95.184:013507
BOUNDS 3 141 - BOUNDS 1 121 - BOUNDS 111	132.851:007342
BOUNDS 111 - BOUNDS 1 121 - BOUNDS 121	139.281:024708

BOND ANGLES INVOLVING BOND 1 121

BOUNDS 1 141 - BOUNDS 1 121 - BOUNDS 2 121	100.62:016317
BOUNDS 1 141 - BOUNDS 1 121 - BOUNDS 3 111	50.351:007904

Figure 3 - 4, Photo-reduction of the output from the BOND LENGTHS AND ANGLES X26 program.

the k th atom respectively.

The output of the bond lengths and angles, together with their estimated standard deviations, is arranged in the form of two lists: the first gives those bond distances from a given atom to all others which satisfy the control constraint, the second list gives the angles subtended at the given atom by the bonds included in the first list. Provision is made in these lists for the identification of atoms as members of the asymmetric unit set passed on from the X24 program, or as members of the set generated from these by the application of the space group symmetry. An example of the X26 program output is given in Figure 3 - 4.

As will be appreciated, a number of challenging organizational or 'housekeeping' problems were thrown up in the process of designing and writing the X26 program. In most cases these were solved by the 'indexing vector' technique; the program makes use of three such index vectors to ensure that the various quantities required in the course of the calculation are tied correctly to the list of atom parameters supplied from the X24 program.

3 - 12 The GENERAL FOURIER (X16) Program

The function of the GENERAL FOURIER (X16) Program is to calculate the density function

$$\rho(xyz) = (1/V) \sum_{hkl=-\infty}^{\infty} F_{hkl} \exp(2\pi i(hx + ky + lz))$$

for suitably chosen intervals of the fractional unit cell coordinates xyz . The density function may be the electron density in the case of a normal Fourier calculation, the vector density in the case of a Patterson function, or a normalized electron density distribution when E-maps are calculated (see Section 3 - 15 - 4).

In the design of a program to perform a Fourier synthesis, the overriding consideration is efficiency both in terms of execution time and program size. The time element is important, as the calculation of a 3-dimensional Fourier synthesis involves a triple summation over the reflection indices for each point xyz at which the density function is calculated. Further, the innermost of these summations requires the evaluation of trigonometric expressions, which can be a time consuming operation even on fast computers.

The question of program size is also relevant, for the larger the amount of store occupied by the program, the less there is available for the retention of the Fourier synthesis. This has the effect of limiting the fineness of the intervals into which x , y and z may be divided. Consequently, advantage must be taken of every simplification of the general density expression possible in the light of crystal symmetry and space group information to reduce the volume of computation, insofar as this does not mean an unacceptable increase in program size. In the case of 2-dimensional syntheses, where a projection of the density function is calculated and a double summation over a subset of the reflection data will suffice, the constraints of machine time and space are somewhat relaxed.

In the GENERAL FOURIER (X16) program, the now conventional Beevers-Lipson algorithm (Beevers and Lipson [1934]) has been followed. In this method the complex expression for the structure factor

$$F_{hkl} = A_{hkl} + iB_{hkl}$$

is used in conjunction with Friedel's Law

$$|F_{hkl}| = |F_{\bar{h}\bar{k}\bar{l}}|$$

to factorize the electron density expression into the form

$$\begin{aligned} \rho(xyz) = & (2/v) \sum_{h=0}^{\infty} \sum_{k=-\infty}^{\infty} \sum_{l=-\infty}^{\infty} A_{hkl} (ccc - css - scs - ssc) \\ & + \sum_{h=0}^{\infty} \sum_{k=-\infty}^{\infty} \sum_{l=-\infty}^{\infty} B_{hkl} (ccs + csc + scc - sss) \end{aligned}$$

where the summation is carried out over only half the reflections in the limiting sphere and where

$$ccc = \cos 2\pi hx \cos 2\pi ky \cos 2\pi lz,$$

and $css = \cos 2\pi hx \cos 2\pi ky \sin 2\pi lz$, etc.

The use of the product form has the advantage that, where the space group symmetry elements create relationships among the F_{hkl} , certain product terms drop out for specified index parity groups, and the summations can be readily arranged to minimize computational labour. This latter point can be more clearly seen by recasting the product expression as

$$\rho(xyz) = (2/V) \sum_h D_1(y) \cos 2\pi hx + D_2(y) \sin 2\pi hx$$

where

$$D_1(y) = \sum_k C_1 \cos 2\pi ky + C_2 \cos 2\pi ky$$

$$\text{and } D_2(y) = \sum_k C_3 \sin 2\pi ky + C_4 \sin 2\pi ky$$

where, in turn

$$C_1 = \sum_l A \cos 2\pi lz + B \sin 2\pi lz \quad (Accc + Bccs)$$

$$C_2 = \sum_l -A \sin 2\pi lz + B \cos 2\pi lz \quad (-Acss + Bcsc)$$

$$C_3 = \sum_l -A \sin 2\pi lz + B \cos 2\pi lz \quad (-Ascs + Bscc)$$

$$C_4 = \sum_l -A \cos 2\pi lz - B \sin 2\pi lz \quad (-Assc - Bssss)$$

While the indices h and k remain unchanged, the sums $C_1 - C_4$ alone need be accumulated, and only when a change in k occurs need the routine to accumulate the vectorial sums $D_1(y)$ and $D_2(y)$ be entered. Similarly,

only where a change of h occurs, either simultaneously with a change of k or otherwise, is it necessary to accumulate the elements of the array containing the section of the density function. Further, when product terms are to be skipped due to symmetry relationships, this is most conveniently done with this computational scheme by skipping the evaluation of the appropriate components of the sums $C_1 - C_4$. As implemented in X16, the Beevers-Lipson algorithm is restricted to the computation of density functions at mesh points defined by grid-lines parallel to the cell edges.

The X16 program consists of a preliminary section followed by two segmented blocks of program text which share the same area of main store core at run time. The preliminary section, apart from performing a number of initializations, handles the input and lineprinter display of the basic crystallographic information which controls the type of synthesis to be performed. This information includes data specifying the reflection data input medium, criteria specifying which reflections are to be rejected from the synthesis, data concerning the crystal system, the point group multiplicities, the particular form of the trigonometric expression required for each of the index parity groups by the space group in question, and the crystallographic axis down which the density function is to be sectioned.

The first segment encountered after the preliminary section has completed its echo of the basic data is that which prepares the reflection data for the synthesis calculation. The reflection data is read sequentially either from paper tape or from the appropriate disk file, and after the application of the rejection criteria, the indices of the surviving reflections are permuted to accord with the chosen section axis. As the efficiency of the synthesis algorithm strongly depends upon the frequency with which the indices of the reflections change as the sequence of data is processed, the reflections are sorted so that

the index which has been permuted into the first position of the new index triplet changes least rapidly and the index in the last position changes most rapidly.

After the reflection data have been sorted, the reflections are corrected for multiplicity. Following this, a code word is attached to each reflection to control the form of the trigonometric expression to be used in evaluating the contribution of each reflection to the final synthesis. The form of the codeword is determined by comparing the index parity group against the information input in the preliminary section concerning the space group in question.

The second segment of the program computes specified sections of the density function using the Beevers-Lipson algorithm described above, and displays each section on the lineprinter as each is completed. The section may also be stored on the disk for subsequent plotting by the FOURIER PLOT (X18) program. The Fourier summation is written entirely in machine code in the interests of speed and compactness. The efficiency of the implementation of this algorithm is enhanced by making use of a special routine (now incorporated as one of the standard functions of the Elliott ALGOL F language as a result of local modification) which simultaneously yields both the sine and cosine of a given argument at a single call. Further, the fact that the bit-pattern of the reflection code word indicates which of the eight trigonometric expressions are to be evaluated and accumulated in the sums $C_1 - C_4$, and also that this bit-pattern can be inspected very rapidly by the fast machine code "exclusive OR" operation, allows the innermost summation to be executed in minimum time.

In its present form, the X16 program will output the computed section on the lineprinter in such a way that the geometry of rectangular cells is reproduced. This is achieved by controlling the number of blank

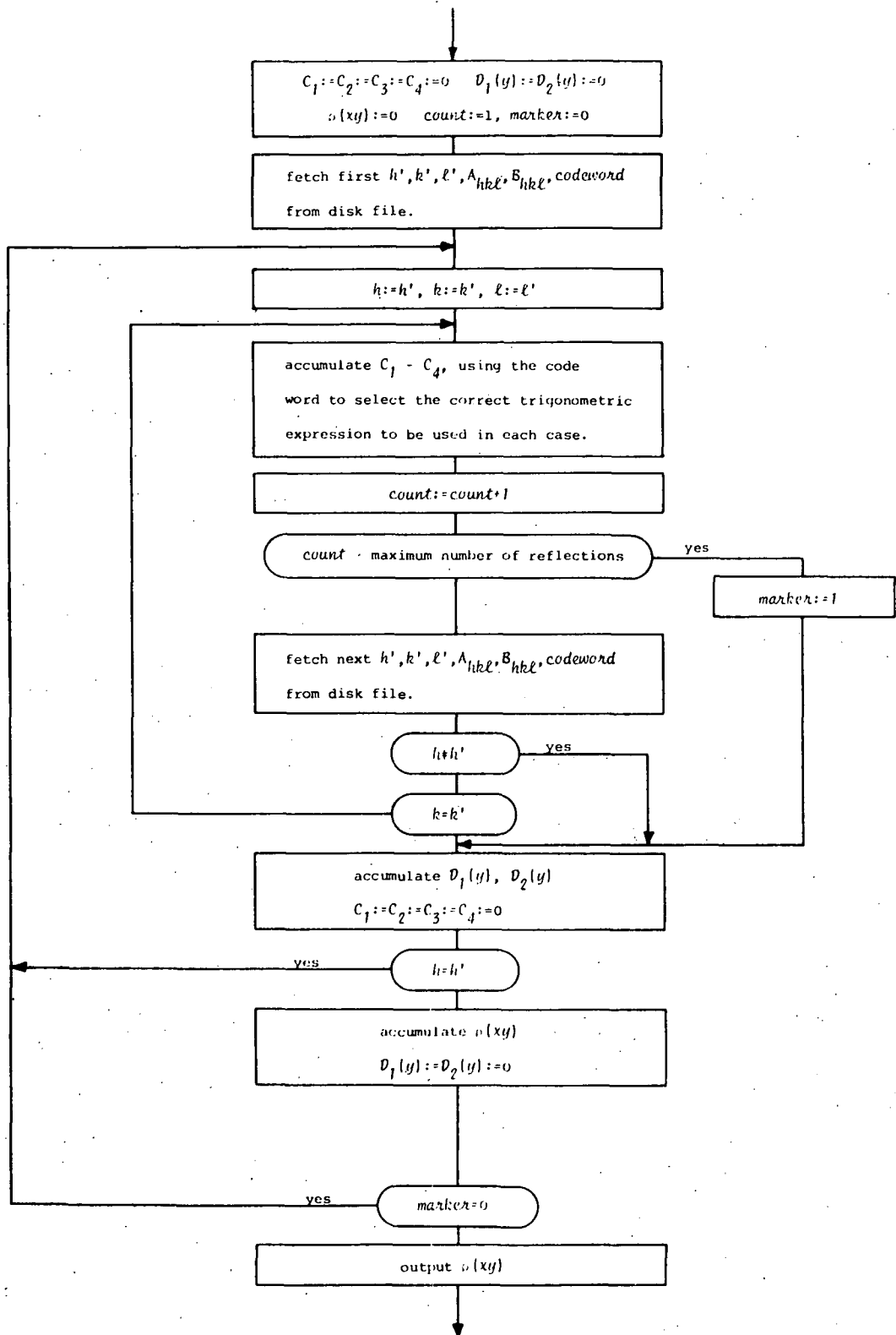


Figure 3 - 5, Generalized flow chart of the Beevers-Lipson algorithm implemented in the GENERAL FOURIER X16 program.

lines output between each line of output. The facility to approximate non-rectangular cells has not been implemented, as the contoured plot produced by the X18 program has been found to be more than adequate in these cases. Provision is made to allow the printing of the section to extend over more than one page of continuous stationery, and each page is uniquely identified in such a way that the section can be assembled readily by hand, once the output has been removed from the lineprinter. The printing of negative regions of the section may be suppressed, the numbers being replaced by the appropriate number of spaces (blanks). Overflow of the number format, which will accommodate numbers in the range -999 to 999, is signalled by the printing of a string of asterisks without disturbance to the overall format of the printed section.

With a reflection data set of the order of 500 reflections, the X16 program execution time for one section calculated at 41 x 41 grid points is approximately 55 seconds. The execution time is conditioned by the frequency of leading index changes in the reflection data list. A generalized flow chart for the program is given in Figure 3 - 5, and a specimen of the basic data echo is reproduced in Figure 3 - 6.

3 - 13 The FOURIER PLOT (X18) Program

The function of the FOURIER PLOT (X18) program is to produce contoured maps of designated sections of the density functions calculated by the X16 program. The maps, which are drawn on the digital incremental plotter, reproduce the true geometry of the unit cell section; the contour interval employed and the number of contours drawn are both under the control of the user.

The sections of the density function (Patterson, Fourier, Difference Fourier or E-map) are stored in a disk file as they are calculated by the

PATTERSON SYNTHESIS FOR K13 HYDRATE, A-AXIS PATTERSON
 REFLECTION DATA INPUT FROM PAPER TAPE
 SECTION OUTPUT ON DISK AND LINEPRINTER
 NO SUPPRESSION OF OUTPUT

SECTION ORIENTATION AND INDEX PERMUTATION
 THE (VERTICAL) X-AXIS LENGTH IS 10.15 ANGSTROM
 THE (HORIZONTAL) Y-AXIS LENGTH IS 9.892 ANGSTROM
 THE INTERAXIAL ANGLE IS 90.00 DEGREES
 THE SYNTHESIS WILL BE CALCULATED WITH SECTIONS DOWN THE ORIGINAL A-AXIS
 THE INDEX PERMUTATION IS FROM HKL TO KLM

A-COEFFICIENT TRIGONOMETRIC EXPRESSIONS

PARITY GROUP FEE	*CCC-SCS
PARITY GROUP FEO	*CCC-SCS
PARITY GROUP FUE	*CCC-SCS
PARITY GROUP FUD	*CCC-SCS
PARITY GROUP FEE	*CCC-SCS
PARITY GROUP FEO	*CCC-SCS
PARITY GROUP FUE	*CCC-SCS
PARITY GROUP FUD	*CCC-SCS

INDEX CLASS MULTIPLICITIES

INDEX CLASS 000	1
INDEX CLASS 00L	2
INDEX CLASS 0K0	2
INDEX CLASS 0KL	4
INDEX CLASS H0U	2
INDEX CLASS H0L	2
INDEX CLASS HK0	4
INDEX CLASS HKL	4

REFLECTION SELECTION

REFLECTIONS RETAINED	244
NO REFLECTIONS REJECTED	

Figure 3 - 6, Photo-reduction of the X16 program basic
 data echo.

Figure 3 - 6 (continued), Photo-reduction of the typical section
output from XI6 (see also Figure 3 - 7).

K13 HYDRATE, A-AXIS PATTERSON SECTION AT 0/20
HORIZONTAL FROM 0/20 TO 20/20. VERTICAL FROM 0/20 TO 20/20

****	661	69	-51	-137	-124	-98	-127	-94	-11	39	-11	-94	-127	-98	-124	-137	-51	69	661	****
425	174	-14	-64	-112	-109	-92	-89	-44	112	248	112	-44	-89	-92	-109	-112	-64	-14	174	425
-109	-82	-29	-55	-78	-86	-83	-52	-9	96	213	96	-9	-52	-83	-86	-78	-55	-29	-82	-109
-94	-74	-36	-22	5	-45	-41	-22	-44	-49	-32	-49	-44	-22	-41	-45	5	-22	-36	-74	-94
-139	-88	-13	131	349	167	-5	-26	-74	-95	-96	-95	-74	-26	-5	167	349	131	-13	-88	-139
-142	-109	-46	64	226	223	196	47	-65	-108	-125	-108	-65	47	196	223	226	64	-46	-109	-142
-100	-105	-80	-24	6	166	314	94	-32	-74	-101	-74	-32	94	314	166	6	-24	-80	-105	-100
-92	-99	-95	-70	-58	-1	61	9	-8	-60	-89	-60	-8	9	61	-1	-58	-70	-95	-99	-92
-130	-111	-65	-66	-78	-75	-46	36	141	49	-47	49	141	36	-46	-75	-78	-66	-65	-111	-130
-63	31	92	-7	-67	-103	-101	-14	93	79	99	79	93	-14	-101	-103	-67	-7	92	31	-63
54	232	302	66	-58	-113	-118	-49	-19	78	286	78	-19	-49	-118	-113	-58	66	302	232	54
-63	31	92	-7	-67	-103	-101	-14	93	79	99	79	93	-14	-101	-103	-67	-7	92	31	-63
-130	-111	-65	-66	-78	-75	-46	36	141	49	-47	49	141	36	-46	-75	-78	-66	-65	-111	-130
-92	-99	-95	-70	-58	-1	61	9	-8	-60	-89	-60	-8	9	61	-1	-58	-70	-95	-99	-92
-100	-105	-80	-24	6	166	314	94	-32	-74	-101	-74	-32	94	314	166	6	-24	-80	-105	-100
-142	-109	-46	64	226	223	196	47	-65	-108	-125	-108	-65	47	196	223	226	64	-46	-109	-142
-139	-88	-13	131	349	167	-5	-26	-74	-95	-96	-95	-74	-26	-5	167	349	131	-13	-88	-139
-94	-74	-36	-22	5	-45	-41	-22	-44	-49	-32	-49	-44	-22	-41	-45	5	-22	-36	-74	-94
-109	-82	-29	-55	-78	-86	-83	-52	-9	96	213	96	-9	-52	-83	-86	-78	-55	-29	-82	-109
425	174	-14	-64	-112	-109	-92	-89	-44	112	248	112	-44	-89	-92	-109	-112	-64	-14	174	425
****	661	69	-51	-137	-124	-98	-127	-94	-11	39	-11	-94	-127	-98	-124	-137	-51	69	661	****

X16 program. At the same time information is stored in another disk file concerning the mesh size, dimensional data and the section numbers of the sections in question. This latter disk file is accessed by the X18 program; and from the data stored in it, the program determines the orientation of the section on the plotter paper and its scale.

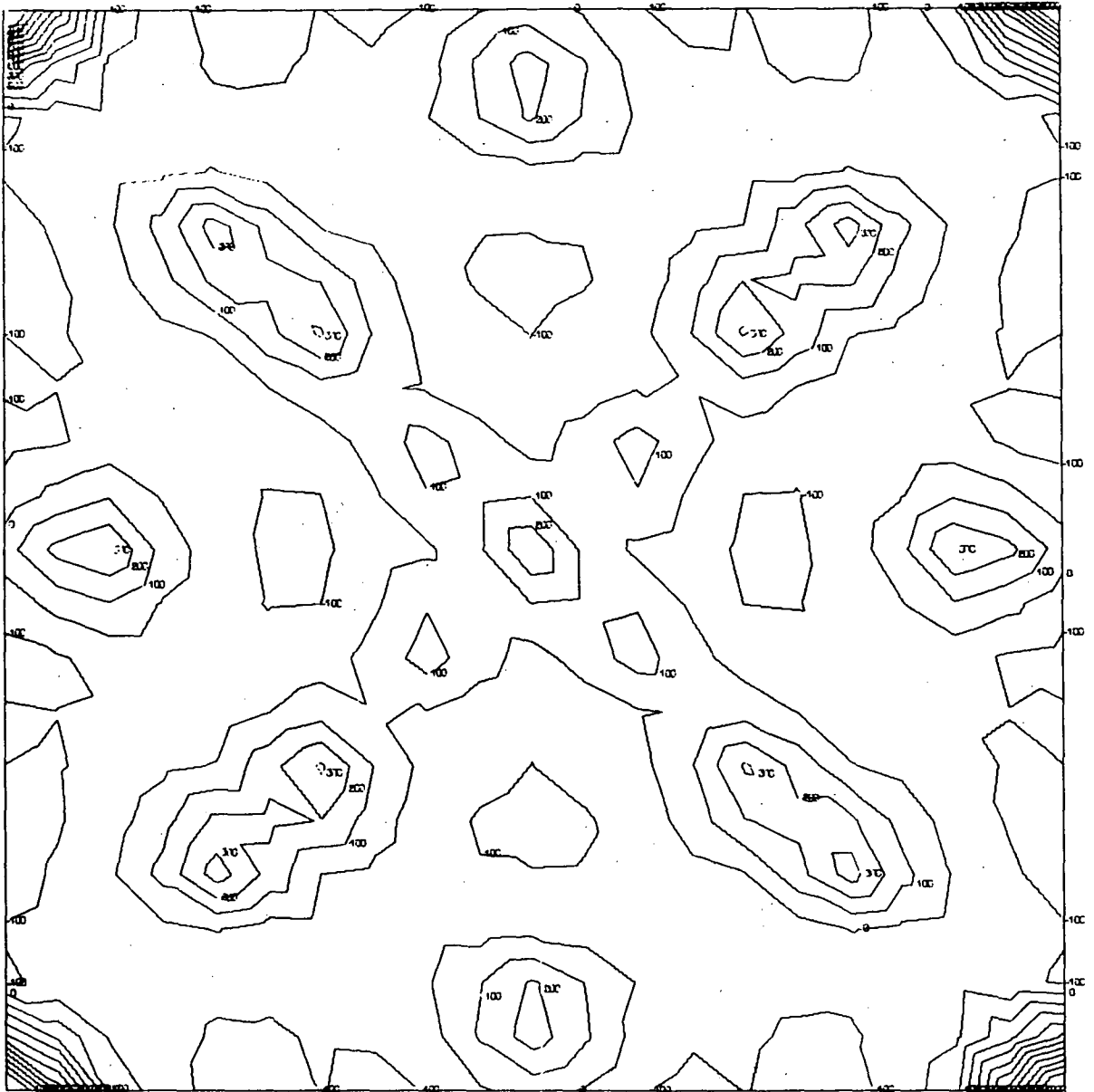
As the plotter makes use of a continuous roll of paper, in principle the contour map may be any length but cannot exceed a fixed maximum width. A length restriction is imposed by the program, so that the map of any section must fit in an area 10.5 inches wide and 14.0 inches long. Within this restriction the program adjusts the scale to give the largest possible map, if necessary the axes of the section are rotated so that the longest axis of the section runs parallel to the longest axis of the plotting area. At this stage the program also calculates the transformations which must be applied to the coordinates of the contour points to preserve the geometry of non-rectangular sections.

Once these computations have been made, the program reads from paper tape the number of the section for which a contour map has been requested. The program then searches the disk file of sections until the desired section has been found. If the section requested was not calculated by the X16 program, an appropriate message is displayed on the lineprinter. When the section has been found, the program reads from paper tape the maximum and minimum contour levels required and the contour interval to be employed.

The contour map is built up contour by contour, starting at the highest level and working down to the lowest. The co-ordinates of the contour lines for a given level are calculated by an auxiliary relocatable binary program which expresses in a compact and efficient form an algorithm developed by Hamilton and Finney [1968] from a method first presented

by Bengtsson and Nordbeck [1967])). Briefly, the contour co-ordinates are determined by linear interpolation between the mesh-points of the section, the interpolations being made in such a way that the mesh points are treated as the intersections of a triangular rather than a parallelogram mesh. Ambiguities, which arise when the function value at a mesh-point is precisely that of the contour level being developed, are removed by perturbing the function value by a small amount. This perturbation ensures that the contour line intersects an edge of the triangular mesh element rather than passing through a vertex; this in turn ensures that an unambiguous choice of the neighbouring element into which the contour line passes can be made. The routine sorts the contour coordinates into the correct order so that continuous contour lines are produced upon output. The routine is very efficient, so that the development of the contour coordinates for all levels of a complete map represents only a small fraction of the total run time of the program. Each contour line is labelled with its height upon output, and no attempt is made to smooth the contours by fitting curves through adjacent points on the contour line. The plotted contours are thus made up of straight-line segments. The unsmoothed nature of the contour lines becomes obvious when the section mesh is large, but is almost undetectable in an equidimensional section whose edges have been divided into more than thirty intervals.

As the plotter is a slow output device, the instructions to the plotter are queued so that the process of calculation is not delayed by the relatively slow speed with which these instructions are executed. As mentioned in Section 3 - 3, the operating system includes provision for queuing the output to slow peripherals, the operation of these queues being administered by an auxiliary RLB program especially designed for this purpose. The extent to which the operation of the program and the



Section No= 0 K13 HYDRATE, A-AXIS PATTERSON

Scale is 1.015 inch=1 Angstrom, contour interval= 100.0

Figure 3 - 7, Photo-reduction (approximately $\frac{1}{2}$ size) of a contoured section produced by X18. The section values contoured are those presented in Figure 3 - 6.

plotter can be decoupled by this device depends upon the amount of backing store available to hold the instruction queue. As the requirements of the X18 program are somewhat stringent in this respect, a modification of the standard system queuing program was undertaken by Mr. I.F. Jones as an exercise in interrupt programming. This modification consisted of packing the 4-bit plotter instructions 9 to a computer word. This gave an effective 9-fold increase in the size of the queue which could be maintained in the backing store. Under normal circumstances, two complete section contour maps can be held in packed form in the queue while the program is generating the plotter instructions for a third. The assistance of Mr. I.F. Jones in providing the elegant and efficient solution to this problem is gratefully acknowledged.

When the output of the contour map is complete and the boundaries of the cell have been drawn, the program labels the map with an identifying string and gives the scale and contour interval used to prepare the map. An example of a contoured section of a Patterson function plotted in 4 minutes 11 seconds by the X18 program is given in Figure 3 - 7. All the contoured sections presented in this work are photo-reductions of such plotter output, or tracings prepared from them.

3 - 14 The LOAD DISK (X50) and CLEAN DISK (X51) programs

These complementary programs serve no other purpose than to administer the disk files used by the X24, X26, X16 and X18 programs. The LOAD DISK (X50) program establishes the data files required and enquires *via* the console typewriter whether any data held temporarily on magnetic tape needs to be loaded into the files prior to the run. If this is required the transfer is executed by the X50 program which then collapses the magnetic tape copy of the file. This facility allows the sequence of program suite runs to be broken at any stage without the intermediate results being irretrievably lost.

The CLEAN DISK (X51) program restores the disk to its original condition. Before the data files on the disk are collapsed, any data which needs to be saved for a subsequent run is transferred upon request to a newly created file set up on magnetic tape.

The X50 program must be run before any of the programs X24, X26, X16 and X18 can be used. It is normally not required again unless the X51 program has been used to save data on magnetic tape. If this facility is not required, it is possible to make repeated runs of any of the members of the crystallographic suite in the appropriate order without re-establishing the data files. This flexibility of operation is a consequence of the pessimistic file strategy adopted in the development of the suite (described in Section 3 - 6). The X51 program can be run at any stage, either for the purpose of saving data or for returning the disk to its normal state for other users. If it is used for the former purpose and further runs of the suite programs are required immediately, then the files must be re-established on the disk with the X50 program.

3 - 15 The Direct Methods Programs

This is suite of four programs: FAME, MAGIC, LINK and SYMPL, designed to allow the symbolic addition method of Karle and Karle (Karle and Karle [1966]) to be applied to any centric space group of orthorhombic or lower symmetry. These programs have been translated by the author with some slight changes from FORTRAN listings made available by Dr. Y.L. Oh. These listings represent a modification of the original versions made by Dr. Y.L. Oh [1970] to allow the suite to be run on a CDC 3600 computer. The original programs were written by Dr. R.K.B. Dewar and Dr. A. Stone of the University of Chicago.

The modifications made in the translation into Elliott ALGOL F

include program optimization in the broad sense (sorting routines, etc.) as well as the incorporation of machine code inserts to allow the efficient execution of the bit-pattern manipulations required by the programs. The overall structure of the programs was not changed except where the block structure of the ALGOL language made this necessary.

As an opportunity was found in the course of this work to test in a minor way the applicability of the direct methods to the solution of inorganic structures (see Chapter 5), and because the description of the crystallographic programs brought to the point of routine use during this study would be incomplete without their mention, a very condensed outline of the functions performed by these four programs is given below.

3 - 15 - 1 FAME

The FAME program (Find All Magic E's) evaluates the scale factor and overall temperature factor required to bring a set of reflection data to an absolute scale using Wilson's method (Wilson [1942]). From this information the set of normalized structure factors E are calculated and their statistical distribution determined (see Section 2 - 7). The Σ_2 relations of the largest E -values are then examined and a number of symbolic signs for a subset of these is suggested by the program.

3 - 15 - 2 MAGIC

The MAGIC program (Multiphase Automatic Generation from Intensities in Centric crystals) performs an iterative symbolic addition procedure until the requested number of signs have received symbolic evaluation. Simultaneously, a list of probable symbol equivalences is prepared for input to LINK.

3 - 15 - 3 LINK

This program selects the origin defining symbols and assigns to them a positive value. It then examines the symbol equivalence information generated by MAGIC and reports on the number of inconsistencies which result for every possible permutation of + and - signs among the symbols remaining after the origin-defining symbols have been selected.

3 - 15 - 4 SYMPL

This program is designed to produce a set of signed Fourier coefficients suitable for the calculation of E-maps. It treats the symbolically phased data produced by MAGIC, and makes use of information concerning the absolute values of the symbols generated by LINK. The program allows for multiple processing, making possible the production of a number of sets of signed Fourier coefficients for different absolute values for the symbolic signs.

3 - 16 Other programs

In the course of this work a number of other programs were prepared to carry out numerical tasks which arose as the study progressed. In the main these were required to overcome specific difficulties and are not of general utility, consequently they are not discussed in detail here but are briefly described elsewhere (see Chapter 6, Section 6 - 5, *et seq.*) in the context of the particular problem they were designed to overcome.

Other programs of general utility, but of only peripheral relevance to this work include a program (U1212) for the refinement of powder diffraction data (Cheesman and Finney [1970]); and the one-electron VESCF-MO programs (U886, U1260) used in the Cheesman, Finney and Snook [1970] study of halogen bonding discussed in Chapter 7.

Chapter 4 - The Refinement of ammonium tri-iodide

	page
4 - 1 Introduction	95
4 - 2 The re-examination of the refinement of NH_4I_3	96
4 - 3 Comparison of the two refinements	97
4 - 4 Discussion	103

4 - 1 Introduction

The refinement of the structure of ammonium tri-iodide was undertaken with the object of improving the accuracy with which the atomic parameters of this compound are known, and also with the secondary objective of using this structural analysis as a pilot study for the other structural investigations planned for this work. In the initial investigation carried out on this compound by Mooney [1935], it was found that crystals of NH_4I_3 were unstable in the X-ray beam, and it was anticipated that $\text{KI}_3 \cdot \text{H}_2\text{O}$ would show the same behaviour in a more extreme form. The results of the refinement of the NH_4I_3 structure have been published (Cheesman and Finney [1970]). As reported in this publication (see Appendix E), six levels of diffraction data were collected in the Wiessenberg mode about the orthorhombic b -axis using Zr-filtered Mo $K \alpha$ radiation. The photographic data were collected using a Nonius Wiessenberg camera, and the reflection intensities were measured by visual estimation of spot densities recorded on multiple-film packs of four Ilford Industrial G films interleaved with 0.038 mm. tin foil. Owing to the instability of the NH_4I_3 crystals in the X-ray beam, three crystals were used for data collection. The intensity data was brought to a common scale by making use of data recorded about the a -axis of one of these crystals which was subsequently remounted and used for the collection of the $h4l$ and $h5l$ data.

The refinement was carried out using a block-diagonal program structure factors/least squares program written in machine code for the Elliott 503 computer (see Chapter 3, Section 3 - 5). When the full matrix STRUCTURE FACTORS/LEAST SQUARES (X24) program became operational, it was used to recalculate the NH_4I_3 refinement. This recalculation was carried out for two reasons: first, the X24 program allows the layer scale factors to be treated as refinable parameters (a facility not avail-

able in the block-diagonal program) and consequently it was possible to check the accuracy of the scaling of the intensity data used in the published refinement. Second, it was considered desirable to check the validity of introducing anisotropic temperature factors when using visually estimated data, as intensity data measured in this fashion is usually regarded as being insufficiently accurate to allow much significance to be attached to anisotropic temperature factors derived from such data, (Stout and Jensen [1969]).

4 - 2 The re-examination of the refinement of NH_4I

The refinement performed with the full-matrix X24 program differed from that carried out using the block-diagonal refinement in that the interlayer scaling factors were treated as refinable parameters, only isotropic temperature factors were used to specify the atomic thermal vibrations and the observed structure factors were each given unit weight in the accumulation of the least-squares sums. In the previous refinement the reflection data was weighted according to the scheme developed by Cruickshank *et alii* [1961] in which the weights are calculated from the relation

$$w = 1/(a + |F_o| + b|F_o|^2)$$

where $a = 2|F_{\min}|$ and $b = 2|F_{\max}|$. This scheme generates weights which vary parabolically with the structure factor magnitude, weak reflections receiving a larger weight than strong reflections.

The set of reflection data used included the 'unobserved' reflections, with $|F_{\text{unobs}}|$ given a value of half the magnitude of the weakest observed reflection. The atomic scattering curves were taken from the International Tables for X-Ray Crystallography VIII (Henry and Lonsdale [1965]), and were corrected for dispersion using the Mo K α correction factors taken

from the same source.

Two least squares refinement cycles were performed using the X24 program during which the interlayer scaling factors were the only parameters refined. The scaling factors were then fixed at their refined values and a further two cycles performed in which the atomic positional parameters were allowed to vary. These cycles were followed by cycles in which the isotropic temperature factors were introduced and refined. A final round of calculation was performed with all the refinable parameters free to vary, and the results of this computation were used to derive the interatomic distances and angles with the BOND LENGTHS AND ANGLES (X26) program, to compute difference Fourier sections through the atomic positions using the GENERAL FOURIER (X16) program and also to prepare the final table of $|F_{obs}|/|F_{calc}|$ presented in Table 4 - 4.

The residual, R , defined as

$$R = \Sigma(|F_o| - |F_c|)/\Sigma|F_o|$$

could not be reduced below 0.212. This should be compared with the value of $R = 0.183$ obtained in the original refinement in which anisotropic temperature factors were introduced.

4 - 3 Comparison of the Two Refinements

The refined values of the interlayer scaling factors did not change greatly during the course of the full-matrix refinement, and the final values attained by these factors differed by less than 3% from the unrefined values used in the original refinement. The two sets of scaling factors are compared in Table 4 - 1.

Table 4 - 1

Comparison of interlayer scaling factors

Level	Unrefined (block-diagonal)	Refined (Full-matrix)
0	2.075	2.0343±0.0050
1	2.058	2.07983±0.00532
2	1.433	1.39262±0.00522
3	1.383	1.35613±0.00584
4	0.871	0.86202±0.00680
5	0.927	0.93625±0.00894

The refined values of the positional parameters of the positional parameters yielded by the X24 program are also very similar to those obtained initially. The final atomic parameters from both refinements are given in Table 4 - 2. The following points should be noted: for the block-diagonal program it was necessary to specify the atomic positional parameters in Angstrom units rather than the more conventional fractional coordinates. Also, the thermal parameters could only be specified in terms of the components of the mean atomic displacement tensor, u_{ij} , whence the thermal correction in the structure factor expression takes the form (using the notation developed in the previous Chapters)

$$\exp(-2\pi^2(u_{11}h^2a^{*2} + u_{22}k^2b^{*2} + u_{33}l^2c^{*2} + 2u_{12}hka^*b^* + 2u_{13}hla^*c^* + u_{23}klb^*c^*))$$

rather than in terms of the factors B_{ij} used by the X24 program where the correction is calculated from the expression

$$\exp(-\frac{1}{2}(B_{11}h^2a^{*2} + B_{22}k^2b^{*2} + B_{33}l^2c^{*2} + 2B_{12}hka^*b^* + 2B_{13}hla^*c^* + 2B_{23}klb^*c^*))$$

Table 4 - 1

Comparison of the two refinements of NH_4I_3

(a) Fixed scale factors, anisotropic temperature factors (Cheesman and Finney [1970])

	x	z	U_{11}	U_{22}	U_{33}	U_{23}
I(1)	0.1568 ± 0.000277	0.3471 ± 0.000259	0.0376	0.0306	0.0193	-0.0116
I(2)	0.3811 ± 0.000249	0.5489 ± 0.000259	0.0343	0.0317	0.0175	0.0
I(3)	0.5784 ± 0.000277	0.7351 ± 0.000300	0.0360	0.0392	0.0258	-0.0175
N	0.8351 ± 0.00588	0.4704 ± 0.00677	0.0646	0.0614	0.0652	0.0

(b) Refined scale factors, isotropic temperature factors (this work)

	x	z	\bar{U}
I(1)	0.156466 ± 0.000068	0.346906 ± 0.000073	0.03152
I(2)	0.381316 ± 0.000068	0.548240 ± 0.000075	0.03252
I(3)	0.579543 ± 0.000069	0.734934 ± 0.000078	0.03388
N	0.833459 ± 0.000942	0.482306 ± 0.001051	0.03799

To facilitate comparison of the results of the two refinements, the positional parameters used in the block diagonal approximation have been re-calculated as fractional coordinates, and the isotropic temperature factors used in the full-matrix program have been expressed as mean atomic displacements.

An interesting comparison can be made between the estimated standard deviations calculated for the positional parameters in both cases. For the full-matrix treatment, where the residual is marginally greater than that found in the block-diagonal approximation, the e.s.d.'s are approximately one quarter as large as the corresponding block-diagonal values. Further, a comparison of the variation in e.s.d. among the positional parameters reveals the same pattern in both cases, for example, both refinements indicate that the e.s.d. of the z-parameters of I(3) is larger than the e.s.d.'s of the z-parameters of either I(1) or I(2) which are themselves very similar. The difference between the magnitude of the e.s.d.'s calculated by the two refinements has been attributed to the different weighting schemes used in each case; this effect has been noted previously by a number of workers and has been examined in detail by Dunitz and Seiler [1973].

The chemically significant interatomic distances and bond angles resulting from the two refinements have been collected together in Table 4 - 3. The greatest difference in interatomic distance is found for the iodine-nitrogen separations, the iodine-iodine separations agree to within approximately 0.01 \AA , which is reasonable in view of the high value of the residual. According to the full-matrix refinement, the tri-iodide ion is bent by 1.4° , which contrasts with the linear configuration found in the original refinement.

The question of the significance to be attached to the anisotropic parameters calculated in the initial refinement was investigated by

Table 4 - 3

Chemically significant interatomic distances and angles for NH_4I_3

(a) Block diagonal refinement (Cheesman and Finney [1970])

I(1) - I(2)	2.7912 ± 0.0039 A°
I(2) - I(3)	3.1134 ± 0.0037 ₅ A°
I(1) - I(3)	5.9046 ± 0.0038 A°
I(1) - N	3.624 ± 0.0678, 3.679 ± 0.0678 A°
I(3) - N	3.776 ± 0.0680, 3.875 ± 0.0680 A°
I(1) - I(2) - I(3)	180.00 ± 0.0022°

(b) Full-matrix (this work)

I(1) - I(2)	2.8023 ± 0.00081 A°
I(2) - I(3)	3.1147 ± 0.00079 A°
I(1) - I(3)	5.9165 ± 0.00081 A°
I(1) - N	3.6747 ± 0.0078, 3.8145 ± 0.0079 A°
I(3) - N	3.7317 ± 0.0075, 3.7089 ± 0.0037 A°
I(1) - I(2) - I(3)	178.60 ± 0.0095°

considering the change in the value of the residual, R , introduced by increasing the number of degrees of freedom of the least-squares calculation. Hamilton [1970] has published tables which allow the significance of such changes to be estimated for a given number of observational data. To make use of these tables, two quantities must be calculated. The first is the ratio of the residual found in the case where the number of degrees of freedom is restricted to that found in the case where the number is unrestricted. The second quantity required is the difference in the number of degrees of freedom obtaining in each case. For the two refinements considered here, the ratio of the residuals is 1.157 and the difference between the number of degrees of freedom is 16. From the tables it is found that for a data set of more than 500 reflections, the hypothesis that the atoms do not vibrate anisotropically can be rejected at the 0.005% confidence level. Consequently, the anisotropic temperature factors calculated in the original refinement can be regarded as significant. However, it can also be seen from the tables that for smaller data sets (i.e. less than, say, 300 reflections), the residual ratio would have to be considerably larger for anisotropic temperature factors to retain their significance.

The large value of the residual obtained in both least-squares treatments indicates that the results should be treated with caution; interatomic distances are probably not reliable to more than 0.01 Å. The layer scaling factors fall into three groups with average values of 2.056 ($h0l$ and $h1l$), 1.374 ($h2l$ and $h3l$) and 0.899 ($h4l$ and $h5l$) respectively. Each of these three groups corresponds to one of the crystals used for data collection; this demonstrates that despite the care exercised in the selection of crystals of similar size, there was a noticeable difference in the volume of the specimen irradiated by the X-ray beam among those crystals used for data collection. It is there-

fore reasonable to assume that the high value of the residual should be attributed to X-ray absorption effects rather than to specimen decomposition during exposure, although the scale factor values for the $h4l$, $h5l$ data collected from the crystal which experienced the largest total X-ray exposure indicate that at least in this case the latter phenomenon was also significant. The experience with this compound showed that to collect reliable X-ray data from tri-iodides which exhibit instability in the X-ray beam it would be necessary to refrigerate the specimen, so that the need to use more than one crystal could be eliminated. This in itself would not remove the inaccuracies introduced by absorption effects, but would at least make this problem more tractable, particularly if a careful choice of crystal shape as well as size were made.

4 - 4 Discussion

As previously concluded (Cheesman and Finney [1970]), the refinement of the NH_4I_3 structure supports the analysis originally made by Mooney [1935], and also confirms the asymmetric geometry of the I_3^- ion in this compound reported in her work. The ammonium tri-iodide structure, which is isomorphous with that of CsI_3 , has been described in Section 1 - 4 - 3; a perspective view of the unit cell contents showing the *en echelon* arrangement of the anions in planes perpendicular to the *b*-axis is given in Figure 4 - 1.

Both least-squares treatments indicate that the departure of the anion from a completely linear form is less than that found by Mooney who reported an interbond angle of $\sim 176^\circ$. The refined interbond angles are 180.0° and 178.6° for the block-diagonal and the full-matrix treatments respectively, and as the structural analyses of the rubidium and potassium tri-iodides will show, the I_3^- anion in NH_4I_3 appears to be the least bent of all the non-linear tri-iodide anions investigated so

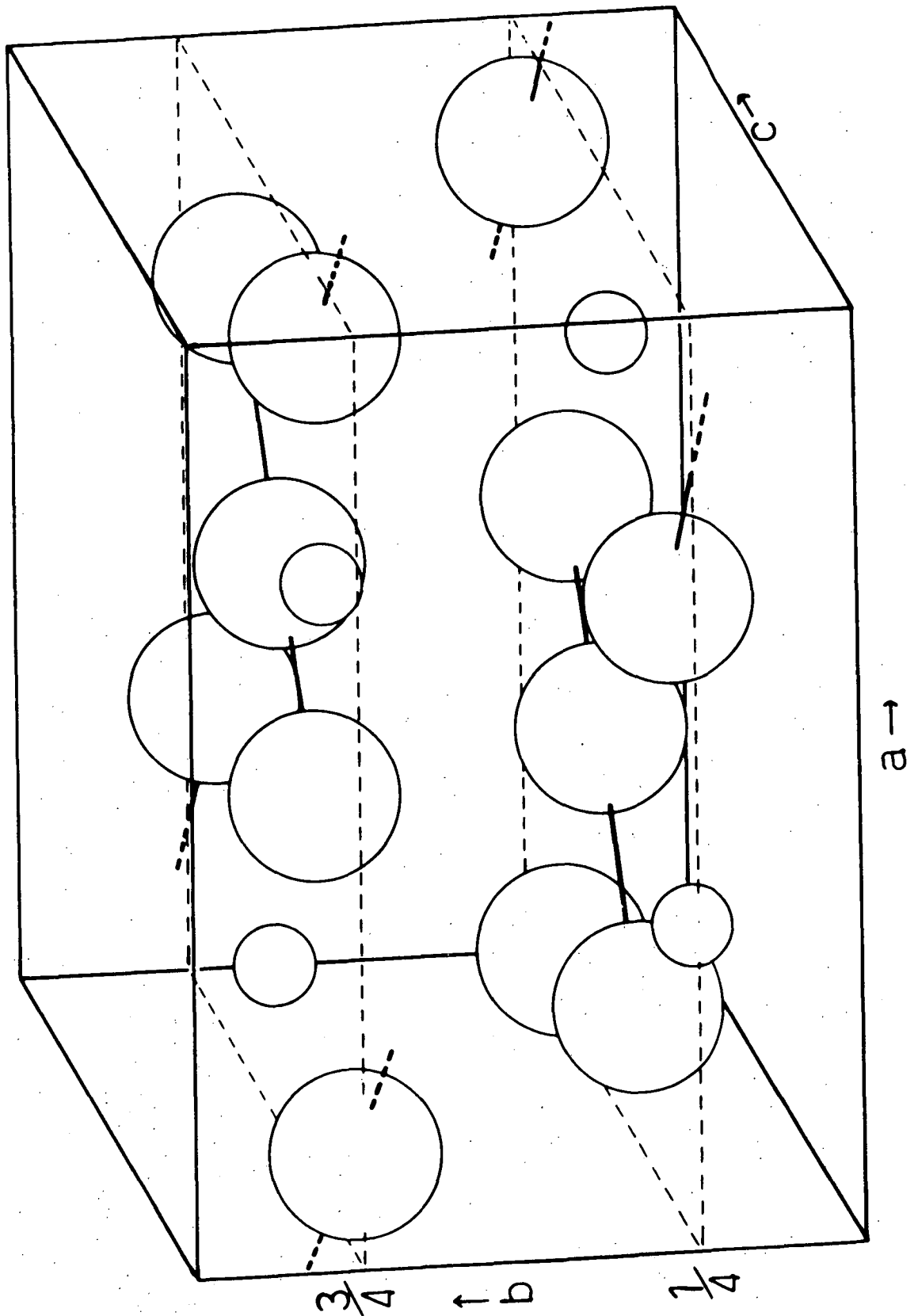


Figure 4 - 1. A perspective view of the unit cell contents of an orthorhombic tri-iodide MI_3 ($M = Cs, Rb, NH_4$). The iodine positions are represented by the larger spheres, the cation positions by the smaller spheres.

far. It may be that the non-linearity of the anion in this structure is reduced below the value it might otherwise have by cation-anion interactions.

The average iodine-nitrogen distance in ammonium tri-iodide is 3.735 \AA , with at least one separation of the order of $3.63\text{--}3.67 \text{ \AA}$, which is very similar to the iodine-nitrogen separation of 3.6307 \AA reported for ammonium iodide (Levy and Peterson [1952, 1953]). Hindered rotation of the NH_4^+ cation in the ammonium iodide lattice has been inferred from infra-red spectral evidence (Wagner and Hornig [1950], Plumb and Hornig [1953, 1955], Vedder and Hornig [1961]), and in the published account of the block-diagonal refinement the suggestion was made that hindered rotation or libration of the cation about a N-H....I axis also took place in the tri-iodide. Attempts were subsequently made to obtain infra-red evidence for such rotational motion of the ammonium cation; these were inconclusive as the characteristic absorptions of the NH_4^+ ion were completely masked by the high general absorption in spectra recorded from samples of solid NH_4I_3 mulled in paraffin oil. However Sasane, Nakamura and Kubo [1967] have reported that the nuclear quadrupole resonances assigned to one of the terminal iodine atoms of the NH_4I_3 anion behave anomalously with temperature. These resonances show an extraordinary large positive temperature coefficient compared to the normal negative temperature coefficients of the resonances assigned to the central and to the other terminal iodine. Sasane and his collaborators claim that the anomalous positive temperature coefficient observed in this case is among the largest ever reported for quadrupole resonance frequencies of halogens, and they attribute this behaviour to changes in the interaction between the terminal iodine in question and the cation. They suggest that these changes in interaction as being due to changes in the rotational behaviour of the cation with temperature.

Although the question of cation rotation or libration remains open in the presence of inconclusive infra-red spectral evidence, both the structural data and the n.q.r. results point to a measure of cation-anion interaction in this tri-iodide; for this reason NH_4I_3 should be regarded as standing a little apart from the alkali metal tri-iodides.

TABLE 4 - 4

PART 1

F(OBS), F(CALC) FOR AMMONIUM TRI-IODIDE
(UNOBSERVED REFLECTIONS MARKED *)

H	K	L	F _O	K*F _C	H	K	L	F _O	K*F _C
H= 0, K= 0					4	0	5	-35	-49*
0	0	2	-355	-299	4	0	6	-38	-24*
0	0	4	308	374	4	0	7	-256	-194
0	0	6	-119	-63	4	0	8	150	92
0	0	8	41	54*	4	0	9	293	237
H= 1, K= 0					4	0	10	451	384
1	0	2	360	353	H= 5, K= 0				
1	0	3	411	475	5	0	1	-519	-590
1	0	4	-856	-848	5	0	2	-313	-261
1	0	5	247	183	5	0	3	-130	-68
1	0	6	-300	-394	5	0	4	466	451
1	0	7	-580	-567	5	0	5	-170	-190
1	0	8	41	6*	5	0	6	400	503
1	0	9	44	99*	5	0	7	235	225
1	0	10	47	21*	5	0	8	-260	-264
1	0	11	-226	-227	5	0	9	116	70
1	0	12	-152	-129	5	0	10	174	144
H= 2, K= 0					5	0	11	282	238
2	0	0	181	136	H= 6, K= 0				
2	0	1	-217	-160	6	0	0	-32	-100*
2	0	2	-303	-282	6	0	1	400	373
2	0	3	-1103	-1183	6	0	2	288	256
2	0	4	469	456	6	0	3	356	330
2	0	5	318	366	6	0	4	-695	-680
2	0	6	-331	-374	6	0	5	359	269
2	0	7	-713	-711	6	0	6	594	579
2	0	8	102	78	6	0	7	275	254
2	0	9	-141	-125	6	0	8	-130	-82
2	0	10	-48	-3*	6	0	9	169	155
2	0	11	51	125*	H= 7, K= 0				
H= 3, K= 0					7	0	1	-89	-62
3	0	1	103	68	7	0	2	363	404
3	0	2	-159	-54	7	0	3	470	532
3	0	3	-825	-772	7	0	4	221	202
3	0	4	-683	-677	7	0	5	-141	-168
3	0	5	33	81*	7	0	6	43	103*
3	0	6	-199	-139	7	0	7	-131	-122
3	0	7	480	446	7	0	8	270	295
3	0	8	-348	-307	7	0	9	-174	-100
3	0	9	-45	-17*	H= 8, K= 0				
3	0	10	153	140	8	0	0	38	99*
3	0	11	52	28*	8	0	1	-584	-561
H= 4, K= 0					8	0	2	390	510
4	0	0	-1530	-1410	8	0	3	283	252
4	0	1	943	916	8	0	4	-41	-92*
4	0	2	-201	-129	8	0	5	129	203
4	0	3	-492	-473	8	0	6	45	71*
4	0	4	-152	-118	8	0	7	47	100*
					8	0	8	-114	-235
					8	0	9	-180	-170

TABLE 4 - 4

PART 2

F(0BS), F(CALC) FOR AMMONIUM TRI-IOIDE
(UNOBSERVED REFLECTIONS MARKED *)

H	K	L	FO	K*FC	H	K	L	FO	K*FC
H= 9, K= 0					2	1	3	-205	-220
9	0	1	412	460	2	1	4	196	206
9	0	2	42	32*	2	1	5	144	99
9	0	3	-43	-43*	2	1	6	-154	-134
9	0	4	-44	-110*	2	1	7	-94	-60
9	0	5	46	23*	2	1	8	-419	-471
9	0	6	-314	-269	2	1	9	168	182
H= 10, K= 0					2	1	10	117	96
10	0	0	-44	-86*	2	1	11	-177	-110
10	0	1	-264	-246	2	1	12	-125	-247
10	0	2	45	92*	2	1	13	57	14*
10	0	3	45	65*	H= 3, K= 1				
10	0	4	279	256	3	1	1	562	534
10	0	5	-428	-474	3	1	2	-811	-850
10	0	6	-114	-228	3	1	3	464	350
H= 11, K= 0					3	1	4	-43	-2
11	0	1	-47	-43*	3	1	5	-130	-188
11	0	3	-108	-131	3	1	6	-145	-52
11	0	4	49	10*	3	1	7	157	133
11	0	5	51	53*	3	1	8	-433	-459
H= 12, K= 0					3	1	9	-335	-409
12	0	0	150	164	3	1	10	48	27*
12	0	3	51	14*	3	1	11	-52	-4*
12	0	5	-184	-218	3	1	12	119	146
H= 0, K= 1					3	1	13	-232	-138
0	1	3	-376	-315	H= 4, K= 1				
0	1	5	1462	1513	4	1	0	-137	-81
0	1	7	-160	-164	4	1	1	-106	-77
0	1	9	44	79*	4	1	3	-127	-106
0	1	11	51	38*	4	1	4	-791	-707
0	1	13	-57	-46*	4	1	5	-855	-920
H= 1, K= 1					4	1	6	473	512
1	1	3	-228	-235	4	1	7	-51	-63
1	1	4	79	15	4	1	8	-253	-199
1	1	5	-89	-87	4	1	9	-46	-34*
1	1	6	416	425	4	1	10	-121	-76
1	1	7	215	253	4	1	11	-52	-40*
1	1	8	153	156	4	1	12	-55	-18*
1	1	9	-391	-444	4	1	13	117	59
1	1	10	132	156	H= 5, K= 1				
1	1	11	-115	-116	5	1	1	-524	-603
1	1	12	-114	-233	5	1	3	560	431
1	1	13	-57	-6*	5	1	4	-304	-278
H= 2, K= 1					5	1	5	-137	-141
2	1	0	-572	-510	5	1	6	-442	-477
2	1	1	669	668	5	1	7	-78	-64
2	1	2	1543	1465	5	1	8	89	58
					5	1	9	177	185
					5	1	10	-114	-137
					5	1	11	111	225
					5	1	12	178	116

TABLE 4 - 4

PART 3

F(OBS), F(CALC) FOR AMMONIUM TRI-IODIDE
(UNOBSERVED REFLECTIONS MARKED *)

H	K	L	FO	K*FC	H	K	L	FO	K*FC
5	1	13	-168	-115	9	1	5	214	129
	H= 6,	K= 1			9	1	6	497	262
6	1	0	-398	-373	9	1	7	-99	-59
6	1	1	-798	-912	9	1	8	-103	-27
6	1	2	-338	-381	9	1	9	-54	-12*
6	1	3	279	222	9	1	10	56	7*
6	1	4	-298	-315	9	1	11	-103	-146
6	1	5	-110	-77	9	1	12	62	37*
6	1	6	242	227	9	1	13	91	77
6	1	7	44	31*		H= 10,	K= 1		
6	1	8	244	170	10	1	0	677	621
6	1	9	-293	-298	10	1	1	352	323
6	1	10	142	115	10	1	2	-126	-95
6	1	11	118	191	10	1	3	129	74
6	1	12	141	115	10	1	4	198	199
6	1	13	-85	-13	10	1	5	-136	-63
	H= 7,	K= 1			10	1	6	-172	-136
7	1	1	-251	-239	10	1	9	177	130
7	1	2	344	378	10	1	10	-158	-201
7	1	3	-538	-496	10	1	11	-98	-95
7	1	4	135	99		H= 11,	K= 1		
7	1	5	129	38	11	1	2	-47	-53*
7	1	6	-149	-122	11	1	3	272	304
7	1	7	264	187	11	1	4	-156	-89
7	1	8	337	399	11	1	5	51	57*
7	1	9	102	114	11	1	6	52	24*
7	1	10	-150	-127	11	1	9	58	45*
7	1	11	56	41*	11	1	10	60	52*
7	1	12	-59	-14*	11	1	11	-125	-82
7	1	13	194	126		H= 12,	K= 1		
	H= 8,	K= 1			12	1	0	253	285
8	1	0	-222	-199	12	1	1	50	9*
8	1	1	-144	-132	12	1	2	-50	-26*
8	1	2	-191	-212	12	1	3	-279	-324
8	1	3	529	480	12	1	4	-73	-22
8	1	4	372	452	12	1	5	168	99
8	1	5	183	113	12	1	6	55	40*
8	1	6	-696	-362		H= 13,	K= 1		
8	1	7	228	305	13	1	1	-53	-32*
8	1	8	43	125	13	1	2	106	91
8	1	9	-52	0*	13	1	3	-76	-55
8	1	10	132	129	13	1	4	-189	-266
8	1	11	57	17*	13	1	6	-162	-107
8	1	12	60	4*	13	1	7	59	44*
8	1	13	-125	-65		H= 14,	K= 1		
	H= 9,	K= 1			14	1	0	-192	-319
9	1	1	280	263	14	1	3	-160	-147
9	1	2	-118	-106					
9	1	3	-148	-165					
9	1	4	304	406					

TABLE 4 - 4

PART 4

F(OBS), F(CALC) FOR AMMONIUM TRI-IODIDE
(UNOBSERVED REFLECTIONS MARKED *)

H	K	L	FO	K*FC	H	K	L	FO	K*FC
H= 1, K= 1					4	2	2	110	76
1	1	3	-119	-118	4	2	3	288	286
H= 0, K= 2					4	2	4	91	71
0	2	2	168	178	4	2	5	35	30*
0	2	4	-255	-220	4	2	6	38	15*
0	2	6	97	39	4	2	7	172	120
0	2	7	38	0*	4	2	8	-123	-58
0	2	8	-41	-33*	4	2	9	-186	-149
0	2	10	250	364	4	2	10	-128	-242
H= 1, K= 2					4	2	11	182	117
1	2	1	-85	-192	H= 5, K= 2				
1	2	2	-886	-206	5	2	1	282	357
1	2	2	-216	-206	5	2	2	167	160
1	2	3	-271	-284	5	2	3	32	41*
1	2	4	417	509	5	2	4	-326	-277
1	2	5	-177	-113	5	2	5	187	117
1	2	6	276	242	5	2	6	-351	-313
1	2	7	436	352	5	2	7	-245	-140
1	2	8	-41	-5*	5	2	8	128	165
1	2	9	-44	-62*	5	2	9	-117	-44
1	2	10	-48	-13*	5	2	10	-160	-91
1	2	11	127	142	5	2	11	-114	-151
H= 2, K= 2					H= 6, K= 2				
2	2	1	147	95	6	2	0	32	62*
2	2	2	184	162	6	2	1	-221	-229
2	2	3	656	705	6	2	2	-177	-155
2	2	4	-405	-277	6	2	3	-221	-204
2	2	5	-279	-223	6	2	4	399	422
2	2	6	227	230	6	2	5	-239	-167
2	2	7	344	442	6	2	6	-458	-361
2	2	8	-42	-49*	6	2	7	-185	-159
2	2	9	142	79	6	2	8	113	51
2	2	11	-125	-79	6	2	9	-83	-98
H= 3, K= 2					6	2	10	73	13
3	2	1	-22	-35*	6	2	11	109	55
3	2	2	25	32*	H= 7, K= 2				
3	2	3	386	468	7	2	1	36	38*
3	2	4	428	412	7	2	2	-235	-251
3	2	5	-47	-48	7	2	3	-300	-330
3	2	6	36	86*	7	2	4	-183	-126
3	2	7	-390	-278	7	2	5	142	104
3	2	8	106	192	7	2	6	-106	-65
3	2	9	45	11*	7	2	7	129	77
3	2	10	-119	-68	7	2	8	-271	-186
3	2	11	-52	-17*	7	2	9	101	62
H= 4, K= 2					H= 8, K= 2				
4	2	0	760	839	8	2	0	-76	-63
4	2	1	-368	-548	8	2	1	293	349
					8	2	2	-298	-317
					8	2	3	-170	-156

TABLE 4 - 4

PART 5

F(UBS), F(CALC) FOR AMMONIUM TRI-IODIDE
(UNOBSERVED REFLECTIONS MARKED *)

H	K	L	F0	K*F0	H	K	L	F0	K*F0
8	2	4	83	57	0	3	7	107	87
8	2	5	-162	-128	0	3	9	-44	-43*
8	2	6	-91	-44	0	3	11	-51	-22*
8	2	7	-67	-62	0	3	13	57	26*
8	2	8	211	148					
8	2	9	81	108					
	H= 9,	K= 2				H= 1,	K= 3		
9	2	1	-241	-287	1	3	2	-452	-407
9	2	2	-42	-21*	1	3	3	150	113
9	2	3	43	28*	1	3	4	-27	-7*
9	2	4	44	69*	1	3	5	44	42
9	2	5	-91	-14	1	3	6	-277	-225
9	2	6	252	169	1	3	7	-208	-138
9	2	7	-70	-59	1	3	8	-154	-85
9	2	8	-127	-101	1	3	9	162	243
9	2	9	203	147	1	3	10	-96	-86
					1	3	11	72	64
					1	3	12	103	130
	H= 10,	K= 2				H= 2,	K= 3		
10	2	1	153	154	2	3	1	-283	-324
10	2	2	-63	-58	2	3	2	-728	-718
10	2	3	-46	-41*	2	3	3	142	112
10	2	4	-175	-161	2	3	4	-170	-105
10	2	5	281	298	2	3	5	-64	-50
10	2	6	187	144	2	3	6	132	74
10	2	8	54	25*	2	3	7	39	32*
					2	3	8	218	256
	H= 11,	K= 2			2	3	9	-142	-99
11	2	1	47	27*	2	3	10	-48	-53*
11	2	2	202	228	2	3	11	51	61*
11	2	3	118	83	2	3	12	219	138
11	2	4	-49	-6*					
11	2	5	-51	-33*		H= 3,	K= 3		
11	2	6	148	78	3	3	1	-290	-266
11	2	7	54	8*	3	3	2	439	429
11	2	8	137	91	3	3	3	-254	-179
					3	3	4	-73	-1
	H= 12,	K= 2			3	3	5	148	99
12	2	1	-50	-22*	3	3	6	89	26
12	2	2	214	219	3	3	7	-79	-72
12	2	3	-51	-9*	3	3	8	271	250
12	2	4	-52	-4*	3	3	9	110	225
12	2	5	169	138	3	3	10	-49	-15*
12	2	8	-117	-102	3	3	11	52	3*
	H= 13,	K= 2				H= 4,	K= 3		
13	2	1	129	146	4	3	0	25	33*
					4	3	1	25	38*
	H= 14,	K= 2			4	3	2	-242	-216
14	2	5	-166	-160	4	3	3	102	56
					4	3	4	376	370
	H= 0,	K= 3			4	3	5	470	491
0	3	3	225	154	4	3	6	-203	-276
0	3	5	-769	-795	4	3	7	41	35*

TABLE 4 - 4

PART 6

FLORES, FICALCO FOR AMMONIUM TRI-iodide
(UNOBSERVED REFLECTIONS MARKED *)

H	K	L	FO	K*FC	H	K	L	FO	K*FC
4	3	8	151	108					
4	3	9	47	18*		H= 9,	K= 3		
4	3	10	50	43*	9	3	1	-117	-143
4	3	11	53	23*	9	3	2	42	58*
					9	3	3	61	90
	H= 5,	K= 3			9	3	4	-208	-222
5	3	1	285	318	9	3	5	-65	-71
5	3	2	142	120	9	3	6	-179	-145
5	3	3	-232	-225	9	3	7	100	32
5	3	4	212	149		H= 10,	K= 3		
5	3	5	90	77	10	3	0	-258	-339
5	3	6	252	258	10	3	1	-125	-177
5	3	7	42	36*	10	3	2	45	51*
5	3	8	-45	-32*	10	3	3	-46	-41*
5	3	9	-166	-103	10	3	4	-115	-109
5	3	10	102	76	10	3	5	48	35*
5	3	11	-152	-125	10	3	6	100	74
						H= 11,	K= 3		
	H= 6,	K= 3			11	3	3	-97	-168
6	3	0	203	196	11	3	4	99	49
6	3	1	369	481	11	3	7	172	147
6	3	2	200	202		H= 12,	K= 3		
6	3	3	-110	-118	12	3	3	126	180
6	3	4	214	169	12	3	7	114	127
6	3	5	55	40		H= 0,	K= 4		
6	3	6	-185	-124	0	4	4	81	94
6	3	7	-44	-16*	0	4	6	-34	-18*
6	3	8	-147	-94	0	4	8	41	15*
6	3	9	197	164	0	4	10	-152	-176
6	3	10	-128	-64		H= 1,	K= 4		
6	3	11	-174	-107	1	4	3	113	127
					1	4	4	-186	-227
	H= 7,	K= 3			1	4	5	31	52*
7	3	1	123	125	1	4	6	-109	-112
7	3	2	-192	-203	1	4	7	-120	-165
7	3	3	249	267	1	4	8	41	3*
7	3	4	-55	-53		H= 2,	K= 4		
7	3	5	-41	-21*	2	4	2	-52	-67
7	3	6	106	67	2	4	3	-316	-312
7	3	7	-171	-104	2	4	4	103	126
7	3	8	-297	-220	2	4	5	77	101
7	3	9	-102	-63	2	4	6	-86	-107
					2	4	7	-164	-208
	H= 8,	K= 3			2	4	8	42	23*
8	3	0	121	110		H= 3,	K= 4		
8	3	1	54	71	3	4	1	18	11*
8	3	2	124	115	3	4	2	-22	-14*
8	3	3	-235	-260					
8	3	4	-264	-245					
8	3	5	-43	-62*					
8	3	6	203	199					
8	3	7	-178	-168					

TABLE 4 - 4

PART 7

F(OBS), F(CALC) FOR AMMONIUM TRI-IOIDE
(UNOBSERVED REFLECTIONS MARKED *)

H	K	L	FO	K*FC	H	K	L	FO	K*FC
3	4	3	-200	-214	8	4	4	-42	-26*
3	4	4	-162	-187	8	4	5	87	62
3	4	5	33	21*	8	4	6	46	21*
3	4	6	-36	-41*	8	4	7	48	30*
3	4	7	112	131					
3	4	8	-60	-91					
	H= 4,	K= 4				H= 9,	K= 4		
4	4	0	-342	-370	9	4	1	235	136
4	4	1	220	243	9	4	2	42	10*
4	4	2	-52	-33	9	4	3	-86	-14
4	4	3	-129	-128	9	4	4	-45	-34*
4	4	4	-32	-31*	9	4	5	46	7*
4	4	5	-35	-15*	9	4	6	-118	-81
4	4	6	-38	-8*	9	4	7	50	29*
4	4	7	-41	-56*					
4	4	8	44	28*		H= 10,	K= 4		
	H= 5,	K= 4			10	4	0	-44	-26*
5	4	1	-171	-160	10	4	1	-109	-73
5	4	2	-84	-74	10	4	2	45	28*
5	4	3	-45	-18	10	4	3	46	19*
5	4	4	128	129	10	4	4	116	78
5	4	5	-37	-54*	10	4	5	-132	-144
5	4	6	125	147	10	4	6	-76	-70
5	4	7	60	66	10	4	7	74	4
5	4	8	-45	-60*					
	H= 6,	K= 4				H= 11,	K= 4		
6	4	0	-32	-29*	11	4	2	-180	-110
6	4	1	136	105					
6	4	2	90	69		H= 12,	K= 4		
6	4	3	110	95	12	4	0	50	50*
6	4	4	-180	-198	12	4	1	50	11*
6	4	5	95	78	12	4	2	-91	-107
6	4	6	155	171					
6	4	7	62	76		H= 13,	K= 4		
6	4	8	-47	-24*	13	4	1	-131	-72
	H= 7,	K= 4							
7	4	1	-35	-17*		H= 0,	K= 5		
7	4	2	136	118	0	5	3	-13	-68*
7	4	3	168	156	0	5	5	337	376
7	4	4	111	59	0	5	7	-38	-41*
7	4	5	-83	-49	0	5	9	45	20*
7	4	6	44	31*					
7	4	7	-46	-38*		H= 1,	K= 5		
7	4	8	119	90	1	5	3	-16	-50*
	H= 8,	K= 4			1	5	4	25	3*
8	4	0	38	30*	1	5	5	-30	-19*
8	4	1	-211	-164	1	5	6	97	107
8	4	2	222	149	1	5	7	76	67
8	4	3	99	73	1	5	8	59	43
					1	5	9	-110	-120
						H= 2,	K= 5		
					2	5	3	-41	-51
					2	5	4	26	49*
					2	5	5	31	22*

TABLE 4 - 4

FLOBS), F(CALC) FOR AMMONIUM TRI-iodide
(UNOBSERVED REFLECTIONS MARKED *)

PART 8

H	K	L	F()	K*FC
2	5	6	-35	-38*
2	5	7	-39	-15*
2	5	8	-119	-125
2	5	9	46	49*

H = 3, K = 5

3	5	2	-122	-197
3	5	3	84	83
3	5	4	29	2*
3	5	5	-65	-47
3	5	6	-36	-12*
3	5	7	40	34*
3	5	8	-122	-124
3	5	9	-113	-111

H= 4, K= 5

4	5	0	-21	-11*
4	5	1	-22	-17*
4	5	2	78	101
4	5	3	-28	-27*
4	5	4	-159	-174
4	5	5	-207	-236
4	5	6	119	134
4	5	7	-41	-17*

H= 5. K= 5

5	5	1	-156	-151
5	5	2	-71	-56
5	5	3	89	106
5	5	4	-107	-72
5	5	5	-37	-37*
5	5	6	-125	-126
5	5	7	-42	-19*

H = 6, K = 5

6	5	0	-153	-93
6	5	1	-77	-228
6	5	2	-114	-97
6	5	3	34	55*
6	5	4	-911	-82
6	5	5	-39	-17*
6	5	6	83	61
6	5	7	44	7*

$$H = 7, \quad K = 5$$

7	5	1	-86	-59
7	5	2	135	99
7	5	3	-159	-129
7	5	4	39	25*
7	5	5	41	10*
7	5	6	-44	-33*
7	5	7	46	52*

H	K	L	F0	K*FC
	H=	8,	K=	5
8	5	0	-94	-55
8	5	1	-55	-34
8	5	2	-79	-55
8	5	3	162	127
8	5	4	133	120
8	5	5	44	31*
8	5	6	-130	-99
8	5	7	97	84

$H = 9, K = 5$

9	5	1	118	70
9	5	2	-42	-29*
9	5	3	-43	-45*
9	5	4	155	110
9	5	5	47	35*
9	5	6	97	73

$$H = 10, \quad K = 5$$

10	5	0	236	167
10	5	1	127	88
10	5	2	-45	-25*
10	5	3	46	21*
10	5	3	46	21
10	5	4	95	54

$$H = 11, \quad K = 5$$

11	5	1	48	28*
11	5	2	-48	-15*
11	5	3	121	85

H= 12, K= 5

12	5	0	124	80
12	5	2	-51	-7*
12	5	3	-128	-90

H= 14, K= 5

Chapter 5 - The Solution of the Structure of Rubidium Tri-iodide

	page
5 - 1 Introduction	116
5 - 2 Experimental Details	117
5 - 3 Structure Determination and Refinement	118
5 - 4 Discussion	123

5 - 1 Introduction

Rubidium tri-iodide was first reported in 1892 by Wells and Wheeler [1892] in a paper describing the properties of a number of rubidium and potassium trihalides. In this study the macroscopic crystallography of the trihalides they prepared was described in some detail, and RbI_3 was assigned by Wells and Wheeler to the orthorhombic system, being in their view isomorphous with CsI_3 .

Subsequent investigations of rubidium tri-iodide were carried out in the context of phase studies of the binary system RbI-I_2 and the ternary systems RbI-I_2 -solvent where the solvent was water, benzene or toluene. The binary system was examined by Fialkov [1935] and also by Briggs and Patterson [1932]; Fialkov found no evidence for the existence of RbI_3 in this system whereas Briggs and Patterson did, quoting an incongruent melting point (188°C) for the compound. The ternary system $\text{RbI-I}_2\text{-H}_2\text{O}$ was studied at 25°C by Foote and Chalker [1911] and a very thorough polythermal investigation of the same system was made by Briggs *et alii* [1941]. The tri-iodide was found to be the only stable polyiodide species in this system.

Apart from the initial description of the macroscopic crystallography given by Wells and Wheeler, no other crystallographic examination of this compound appears to have been made; in the literature it has been generally assumed on the basis of isomorphism that rubidium tri-iodide is isostructural with caesium tri-iodide. As this reasonable assumption was without experimental proof, and as information regarding the geometry of the tri-iodide ion in the rubidium tri-iodide lattice would be of value in reaching a better understanding of the postulated relationship between anion stability, geometry and electrostatic environment, an X-ray crystallographic determination of the structure of this compound was undertaken.

5 - 2 Experimental Details

Crystals of rubidium tri-iodide suitable for X-ray structural determination were prepared by the slow evaporation of a solution of BDH laboratory grade rubidium iodide and resublimed iodine in water. Reference was made to Briggs phase diagram (Briggs *et alii* [1941]) in preparing this solution to ensure that the crystallization path adopted upon evaporation led to a product free of solid iodine and the parent iodide. The solution was prepared by weighing to give a composition of 44 w.% I_2 , 35 w.% RbI and 21 w.% H_2O . This solution was slowly evaporated over sulphuric acid in a desiccator. As RbI_3 has the tendency, remarked upon by Wells and Wheeler, of forming magnificent tabular crystals some centimeters on a side, the solution was frequently agitated as crystallization proceeded to ensure the development of a significant population of small crystals. The crystallization was terminated as soon as a sufficiently large number of small crystals had grown, and the product was separated from mother liquor by rapid suction filtration on a sintered glass disk. A suitable crystal with dimension less than 0.2 millimeter was taken directly from the disk and sealed in a previously dried Lindeman glass tube. Crystals mounted in this way were stable both in and out of the X-ray beam, unlike both NH_4I_3 (see Section 4 - 1) and $KI_3 \cdot H_2O$ (see Section 6 - 2).

The cell dimensions were determined from single crystal oscillation and Weissenberg photographs using single films (the radius of the cylindrical film holder having been previously calibrated using the powder lines from an annealed silver wire specimen). The orthorhombic cell dimensions so determined were $a = 10.885 \text{ \AA}$, $b = 6.54_6 \text{ \AA}$ and $c = 9.470 \text{ \AA}$, and the systematic absences observed corresponded to those for the orthorhombic space groups $Pnma$, $Pnm2_1$ (the axial labelling corresponds to that for $Pnma$ in the standard orientation adopted by the

International Tables for X-ray Crystallography). The density of the compound was determined by pycnometry using iodine saturated paraffin oil as the working fluid to be 4.574 gm/cc. giving a calculated value of 4 stoichiometric units/unit cell. (A full survey of the experimental difficulties attending the determination of the density of the compounds examined in this work is given in Section 6 - 2, and the experimental data are presented in Appendix B).

Five levels of data about the *b*-axis were collected photographically using Zr-filtered MoK α radiation and a Nonius Weissenberg camera. All photographs used for intensity measurements were made with multiple-film packs of four Ilford Industrial Type G films interleaved with 0.038 millimeter tin foil. The intensities of 278 independent reflections were measured by visual estimation against a calibrated strip and the interfilm scaling factors were determined using the FILM SCALER (XO) program. The average value for these factors was 2.08 with a range of ± 0.02 about this mean.

5 - 3 Structure Determination and Refinement

The raw intensity data was corrected for geometric effects using the LORENTZ/POLARIZATION CORRECTION (X1) program, but in view of the small size of the crystal used for data collection, no absorption correction was applied.

As the information gathered at this stage (cell dimensions, space group, number of stoichiometric units/cell) taken together with the reported isomorphism of RbI₃ with CsI₃ lent support to the hypothesis that these compounds are isostructural, it was considered that an attempt to solve the structure of RbI₃ by direct methods would provide a useful measure of the applicability of this approach to structures of this type. In the event of the direct methods failing to produce a

useful phasing model, it was planned to fall back upon the standard techniques for extracting a phasing model from the Patterson synthesis. This, however, proved to be unnecessary.

The calculation of the normalized structure factors (E) from the scaled and corrected intensity data was performed by the FAME program, and the magnitude distribution of the E -values so calculated is compared to the theoretical distributions for centric and acentric structures in Table 5 - 1.

Table 5 - 1

E -statistics for RbI_3 computed by FAME

Quantity	Rubidium tri-iodide	Theoretical (centric)	Theoretical (acentric)
average $ E $	0.809	0.798	0.886
average $ E-1 $	0.955	0.968	0.736
% $ E > 1.0$	33.00	32.00	37.00
% $ E > 2.0$	4.68	5.00	1.80
% $ E > 3.0$	0.33	0.30	0.01

The E -statistics for RbI_3 presented in Table 5 - 1 have been computed after rescaling the normalized structure factors to give an average E^2 value of 1.0 as required by theory (Karle and Karle [1966]). These results indicate very strongly that RbI_3 has a centric distribution of normalized structure factor magnitudes, which implies that the correct space group is $Pnma$ rather than the noncentrosymmetric $Pnm2_1$.

As mentioned previously, the FAME program also calculates the Σ_2 relationships among the E 's and assigns symbolic signs to a small number of reflections on the basis of a figure of merit which takes into account the magnitude of the normalized structure factor and the number of Σ_2 relationships entered into by the reflection in question. The seven reflections given symbolic signs by FAME are presented in Table 5 - 2,

together with the information used by the program when assigning symbolic signs.

Table 5 - 2

Symbolic Sign assignments made by FAME

Reflection Indices	Parity Group	E	Number of relations	Symbol assigned
2 5 2	eeo	2.07	37	a
8 6 1	eeo	1.87	20	b
6 3 1	eeo	2.90	34	c
9 2 1	oeo	2.26	23	d
3 5 2	ooe	1.93	31	e
11 1 3	ooo	1.69	44	f
6 4 4	eee	1.65	15	g

A total of 107 of the largest E 's, including those listed in Table 5 - 2, were given as input to the MAGIC program which built up a pyramid of symbolically phased reflections by iteration over the set of Σ_2 relations and symbolic signs. All of the reflections input were eventually assigned symbolic signs (either as +/-, single symbols or symbol products) in four iterations. In the first cycle only those sign indications which had a probability value greater than 0.9, and for which there were no contrary indications, were accepted as being correct. In subsequent cycles the latter criterion was relaxed so that a sign indication was accepted if the ratio of indications *for* the sign in question to those *against* was greater than 5 : 1 and there were no more than two such contrary indications. The growth of the pyramid of symbolically phased reflections during the cycles of the MAGIC program is shown in Table 5 - 3.

Table 5 - 3

Summary of the results of the MAGIC program

Cycle Number	Total number of Symbolically Phased Reflections	probability level	maximum Number of allowed contrary indications
0	7	-	-
1	30	0.9	0
2	68	0.9	2
3	99	0.9	2
4	107	0.88	2

The entry in Table 5 - 3 for cycle 0 refers to the seven reflections assigned symbolic signs by the FAME program. Note that for cycle 4 the probability threshold for acceptance of a sign indication was automatically decreased by the program to allow the phase pyramid to propagate further. MAGIC also determined 442 equivalence relationships among the 107 symbolic signs, these relationships taking the form of simple equations among symbol products. This set of relationships formed the input to the LINK program which defined the origin by assigning positive values to the symbols a , c and e . The remaining symbols b , d , f and g were each given positive and negative values in turn by LINK, and each of the 2^4 possible combinations of signs so generated was checked against the list of 442 equivalence relationships established by MAGIC for contradictions. The list of sign combinations ranked according to the number of inconsistencies discovered by LINK is given in Table 5 - 4.

The first combination listed in Table 5 - 4 was taken to be the correct one, and together with the 107 symbolically phased E's generated by MAGIC it formed the input to the SYMPL program which evaluated the symbolic sign of each reflection in terms of this assignment of signs to

Table 5 - 4

Summary of the results of the LINK program

Sign Combination	Number of Contradictions
<i>a b c d e f g</i>	
+ + + + + - -	15
+ + + - + + -	29
+ + + - + - +	29
+ + + + + + -	30
+ - + + + + +	30
+ + + - + + -	30
+ - + + + + +	30
+ + + + + - +	31
+ - + - + - +	31
+ - + + + - +	31
+ - + - + + +	32
+ - + - + + -	32
+ + + - + + +	32
+ + + + + + +	32
+ - + + + - -	33
+ - + - + - -	33

give a set of algebraically signed E 's. An E -map was computed using the appropriate input option of the GENERAL FOURIER (X16) program with this data. The map contained 16 well-defined peaks with their maxima localized in planes at $y=\frac{1}{4}$, and $y=\frac{3}{4}$ in positions closely similar to those of the Cs and I positions in CsI_3 . The $y=\frac{1}{4}$ section of the E -map is reproduced in Figure 5 - 1 with the final atomic positions superimposed. A structure factor calculation with scale factor refinement using the atomic positions derived from the E -map yielded a residual of 0.24. Examination of the signs of the calculated structure factors revealed that only 15 of the signs predicted by the direct methods program were incorrect, the majority of these arising from sign indications accepted at the lowered probability threshold during the fourth cycle of MAGIC.

Subsequent full matrix least squares refinement proceeded normally to give a final residual of 0.094. Anisotropic temperature factors were not employed as it was considered that there was insufficient visually estimated data to justify their introduction. (See Chapter 4, Section 4 - 3). The final refined parameters are given in Table 5 - 5 and the final $y=\frac{1}{4}$ Fourier section is shown in Figure 5 - 2. The estimated standard deviations given in Table 5 - 5 and those calculated by the refinement program using a weighting scheme in which each reflection is given unit weight, and they probably represent underestimates of the true uncertainties in the atomic coordinates.

5 - 4 Discussion

In Table 5 - 6 the chemically significant interatomic distances and angles are presented. The values of these quantities, and the relative arrangement of the atoms in the cell demonstrate that RbI_3 is isostructural with both CsI_3 and NH_4I_3 . There are, however, some important differences in detail among these three compounds.

Table 5 - 5

Refined fractional coordinates and isotropic temperature
factors for RbI_3

Atom	x	y	z	B
I (1)	0.157485 ± 0.000077	0.25	0.351526 ± 0.000090	3.92368 ± 0.0228
I (2)	0.377570 ± 0.000077	0.25	0.544937 ± 0.000090	3.93383 ± 0.0228
I (3)	0.573667 ± 0.000082	0.25	0.734940 ± 0.000093	4.23894 ± 0.0238
Rb	0.330737 ± 0.000124	0.25	0.030017 ± 0.000148	4.48735 ± 0.0333

Table 5 - 6

Chemically significant interatomic distances and angles for RbI_3

I(1) - I(2)	3.0157 ± 0.000718	Å°
-------------	-------------------	----

I(2) - I(3)	2.7918 ± 0.000633	Å°
-------------	-------------------	----

I(1) - I(3)	5.8058 ± 0.000637	Å°
-------------	-------------------	----

I.....I	3.9101, 4.835	Å°
---------	---------------	----

I.....Rb	3.7585	Å°
----------	--------	----

I(1) - I(2) - I(3)	177.221 ± 0.015°
--------------------	------------------

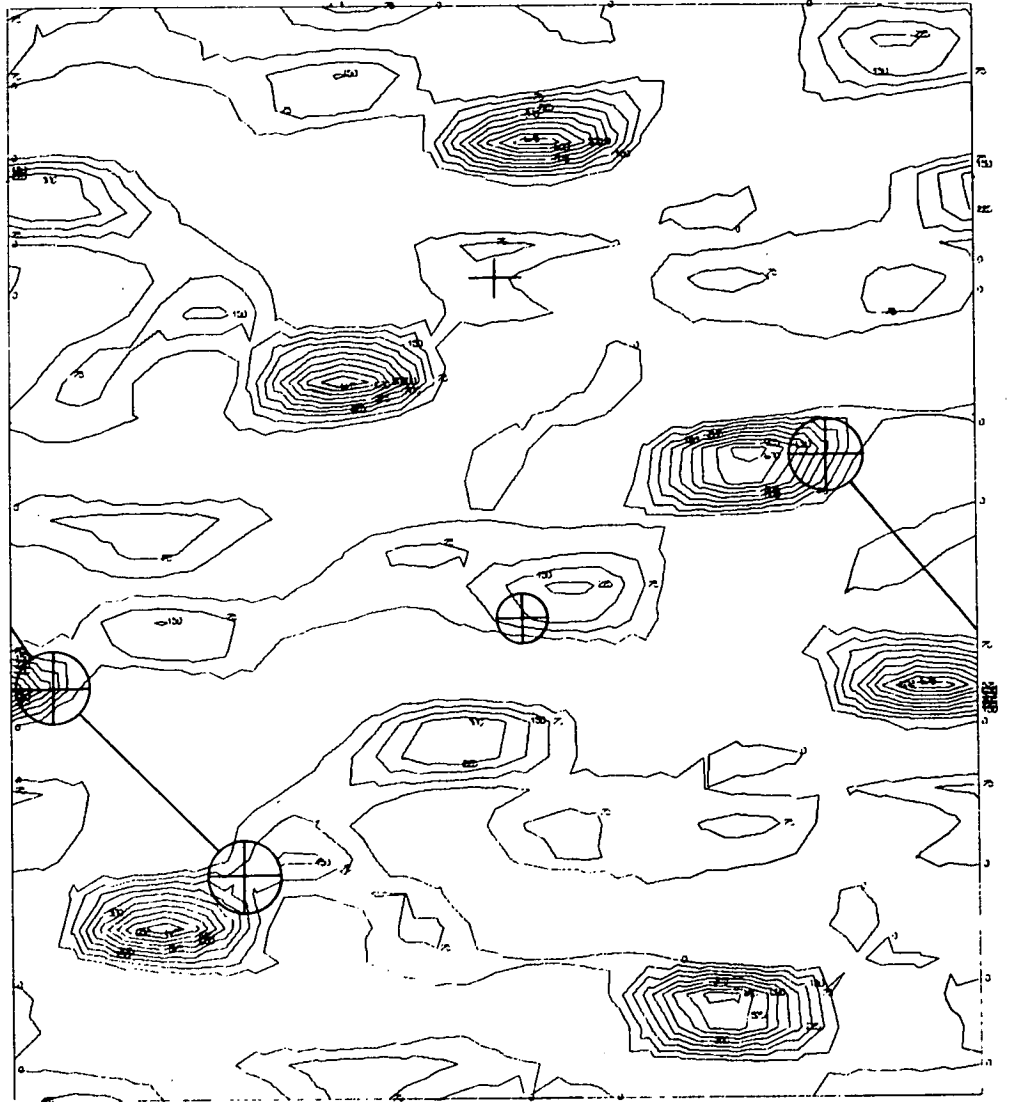
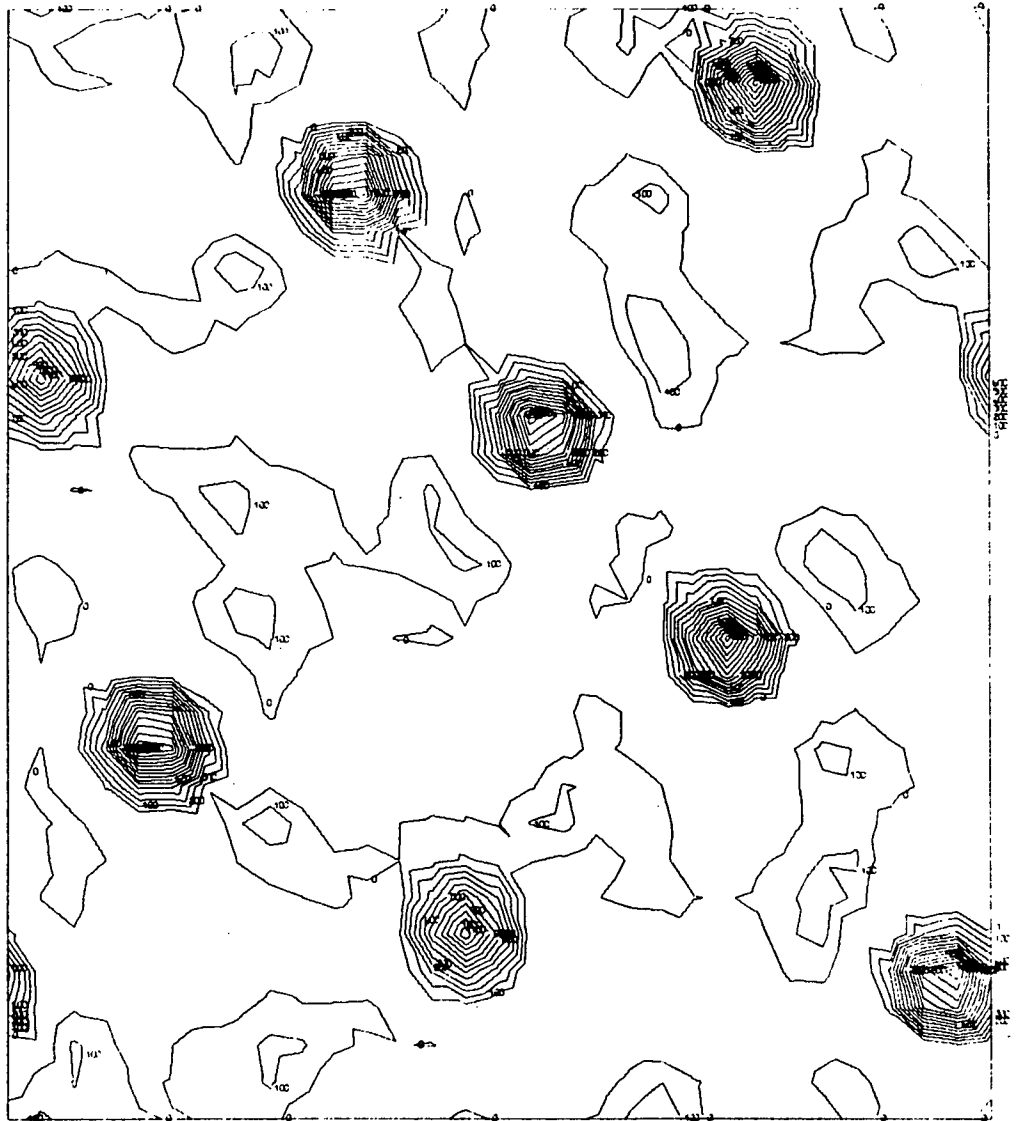


Figure 5 - 1, Photoreduction (approximately $\frac{1}{4}$ size) of the compound RbI_3 E-map at $y = \frac{1}{4}$. The final atomic positions have been superimposed. Note that the conventional cell origin is shown at the point marked +.

The shortest distance between an iodine atom and the rubidium cation is 3.758 \AA , which is larger than the separation of 3.655 \AA between the cation and anion in RbI (Davey [1923]); in this respect RbI_3 resembles CsI_3 . It is also similar in that in both compounds the anion is bent, but the departure from linearity is greater for RbI_3 (2.6°) than for CsI_3 (2.0°) or for NH_4I_3 (1.4°). Differences are seen, however, when the lengths of the bonds in the anions are compared. In RbI_3 the long anion bond is shorter than the corresponding bond in NH_4I_3 (3.1147 \AA) and in CsI_3 (3.0420 \AA), being only 3.0157 \AA in length. A similar difference, although not so marked, is observed for the short anion bond; in this case the bond lengths are 2.8023 \AA , 2.840 \AA and 2.7918 \AA respectively for NH_4I_3 , CsI_3 and RbI_3 . Thus, RbI_3 does not fall neatly between the CsI_3 and NH_4I_3 anion configurations; this raised the possibility that NH_4I_3 may be regarded as being somewhat of an extreme case, and that the anionic geometry of RbI_3 might well represent an intermediate configuration between that found in CsI_3 and that of $\text{KI}_3 \cdot \text{H}_2\text{O}$. This conjecture provided an added motive for undertaking the structural determination of potassium triiodide monohydrate.

The observed and calculated structure factors for both observed and unobserved reflections are presented in Table 5 - 7. The unobserved reflections were arbitrarily assigned a structure factor magnitude half that of the weakest F_{obs} .

The solution of this structure by the direct methods provided an interesting test of the applicability of this technique to inorganic compounds possessing non-random relationships among the atomic coordinates. The concentration of scattering matter in two planes at $y = \frac{1}{4}$ represents a serious departure from the assumption of a random distribution of atoms within the cell upon which the theory of the direct methods of structure solution is based (see Section 2 - 7).



Section No. 4 RbI₃

Scale is 1.006 inch 1 Angstrom, contour interval 100.0

Figure 5 - 2, Photoreduction of the final RbI₃ fourier synthesis section at $y=4$. The contours are drawn at arbitrary intervals corresponding to differences of approximately $0.03e/A^\circ$.

Thus the application of the direct methods to RbI_3 using the FAME-MAGIC-LINK-SYMPLE suite of programs described in Chapter 3 (Section 3 - 15) can be viewed as a test case in which there is one systematic relationship between the coordinates of all atoms. The presence of this relationship has not hampered the ability of the direct methods to give a good phasing model in this instance, even to the extent of making it possible to distinguish between iodine and rubidium positions in the E -map. It is possible that the success of the technique in this case was due to the extended nature of the iodine electronic cloud, and that the method would fail for an analogous structure containing atoms with a sharper electron density profile.

TABLE 5 - 7

F[OBS], F[ALC] FOR RUBIDIUM TRI-IODIDE
(UNOBSERVED REFLECTIONS MARKED *)

PART 1

H	K	L	FO	K*FC	H	K	L	FO	K*FC
H= 0, K= 0					H= 6, K= 0				
0	0	6	56	27*	6	0	0	196	174
0	0	8	68	80*	6	0	1	248	275
0	0	10	-200	-265	6	0	2	346	323
H= 1, K= 0					6	0	3	175	148
1	0	1	83	66	6	0	4	-280	-284
1	0	2	131	145	6	0	5	225	202
1	0	3	229	206	6	0	6	345	298
1	0	4	-538	-621	6	0	7	124	111
1	0	5	100	113	H= 7, K= 0				
1	0	6	-398	-388	7	0	1	-50	-55
1	0	7	-292	-299	7	0	2	191	186
1	0	8	-64	-96*	7	0	3	242	275
1	0	9	69	46*	7	0	5	-58	-75
H= 2, K= 0					H= 8, K= 0				
2	0	1	-62	-58	8	0	0	-63	-55*
2	0	2	-358	-364	8	0	1	-248	-251
2	0	4	282	232	8	0	2	282	264
2	0	5	387	323	8	0	3	98	94
2	0	6	-258	-237	8	0	4	-83	-90
2	0	7	-281	-253	8	0	5	158	155
2	0	8	60	36*	H= 9, K= 0				
H= 3, K= 0					9	0	1	297	316
3	0	1	292	287	9	0	2	57	6*
3	0	2	-23	-15*	9	0	3	52	52*
3	0	3	-331	-333	9	0	4	-47	-64*
3	0	4	-348	-368	9	0	5	44	24*
3	0	5	82	85	H= 10, K= 0				
3	0	6	-73	-72	10	0	0	-138	-144
3	0	7	239	243	10	0	1	-124	-132
3	0	8	-135	-156	10	0	2	63	38*
H= 4, K= 0					10	0	3	58	2*
4	0	1	504	570	10	0	4	53	67*
4	0	2	-288	-247	10	0	5	-278	-263
4	0	3	-380	-351	H= 11, K= 0				
4	0	4	-119	-95	11	0	1	-93	-90
4	0	5	-111	-109	11	0	2	-94	-148
4	0	6	-38	-65*	H= 12, K= 0				
4	0	7	-185	-198	12	0	0	99	88
H= 5, K= 0					12	0	1	-70	-11*
5	0	1	-504	-457	12	0	2	-71	-101
5	0	2	-75	-85	H= 13, K= 0				
5	0	3	-103	-123	13	0	1	-74	-97
5	0	4	357	328	H= 0, K= 1				
5	0	5	-171	-142	0	1	3	-411	-449
5	0	6	441	406					
5	0	7	84	61					

TABLE 5 - 7
F[OBS], F[ALC] FOR RUBIDIUM TRI-IODIDE
(UNOBSERVED REFLECTIONS MARKED *)

PART 2

H	K	L	F0	K*FC	H	K	L	F0	K*FC
0	1	7	-176	-163	5	1	5	-32	-21*
0	1	9	-71	-37*	5	1	6	-237	-208
0	1	11	-59	-12*	5	1	7	-42	-26*
					5	1	8	47	56*
					5	1	9	54	54*
	H= 1,	K= 1				H= 6,	K= 1		
1	1	1	271	324	6	1	0	-333	-328
1	1	2	697	664	6	1	2	-178	-176
1	1	3	-310	-343	6	1	3	36	43*
1	1	4	124	100	6	1	4	-245	-261
1	1	5	-146	-163	6	1	5	-110	-101
1	1	6	339	328	6	1	6	166	135
1	1	7	155	160	6	1	7	-39	-30*
1	1	8	145	147	6	1	8	93	68
1	1	9	-202	-186	6	1	9	-199	-199
1	1	10	136	135					
	H= 2,	K= 1				H= 7,	K= 1		
2	1	2	1187	1270	7	1	2	262	279
2	1	3	-136	-105	7	1	3	-395	-403
2	1	4	354	348	7	1	4	158	144
2	1	5	131	147	7	1	6	-36	-31*
2	1	6	47	12*	7	1	7	91	98
2	1	7	-53	-4*					
2	1	8	-271	-277		H= 8,	K= 1		
2	1	9	143	147	8	1	0	-63	-33*
	H= 3,	K= 1			8	1	2	52	30*
3	1	1	408	388	8	1	3	373	369
3	1	2	-795	-728	8	1	4	315	304
3	1	3	293	271	8	1	5	87	83
3	1	4	-233	-212	8	1	6	-158	-140
3	1	5	-118	-99	8	1	7	237	220
3	1	6	-185	-136		H= 9,	K= 1		
3	1	7	97	100	9	1	1	185	204
3	1	8	-399	-371	9	1	2	-102	-134
3	1	9	-226	-188	9	1	3	-52	-40*
	H= 4,	K= 1			9	1	4	154	157
4	1	0	-328	-351		H= 10,	K= 1		
4	1	1	74	25	10	1	0	262	296
4	1	2	98	99	10	1	1	124	115
4	1	3	-27	-41*	10	1	2	-109	-109
4	1	4	-607	-640		H= 11,	K= 1		
4	1	5	-564	-496	11	1	1	94	88
4	1	6	288	271	11	1	2	-68	-26*
4	1	7	-82	-58	11	1	3	174	181
4	1	8	-51	-72*		H= 12,	K= 1		
4	1	9	58	13*	12	1	0	121	155
	H= 5,	K= 1			12	1	1	-70	-32*
5	1	1	-366	-301	12	1	2	-71	-49*
5	1	2	-87	-66	12	1	3	-184	-170
5	1	3	363	390					
5	1	4	-139	-101					

TABLE 5 - 7
F(OBS), F(CALC) FOR RUBIDIUM TRI-IODIDE
(UNOBSERVED REFLECTIONS MARKED *)

PART 3

H	K	L	F0	K*FC	H	K	L	F0	K*FC
H= 14, K= 1					H= 5, K= 2				
14	1	0	-110	-102	5	2	1	460	449
H= 0, K= 2					5	2	2	76	85
0	2	4	-398	-363	5	2	3	103	122
0	2	6	-57	-27*	5	2	4	-365	-328
0	2	8	-69	-80*	5	2	5	150	142
0	2	10	240	271	5	2	6	-409	-410
H= 1, K= 2					5	2	7	-85	-62
1	2	3	-229	-203	H= 6, K= 2				
1	2	5	-112	-112	6	2	0	-150	-174
1	2	6	339	387	6	2	1	-272	-273
1	2	7	278	301	6	2	2	-324	-318
1	2	8	84	95	6	2	3	-162	-149
1	2	9	-70	-46*	6	2	4	280	287
1	2	10	70	26*	6	2	5	-197	-204
H= 2, K= 2					6	2	6	-314	-301
2	2	2	422	341	6	2	7	-108	-113
2	2	4	-254	-229	H= 7, K= 2				
2	2	5	-282	-319	7	2	1	52	54*
2	2	6	215	237	7	2	2	-181	-188
2	2	7	251	257	7	2	3	-250	-278
2	2	8	-61	-36*	7	2	4	-39	-6*
2	2	9	67	50*	7	2	5	83	76
2	2	10	-70	-13*	7	2	6	38	20*
H= 3, K= 2					H= 8, K= 2				
3	2	1	-293	-265	8	2	0	63	53*
3	2	2	27	16*	8	2	1	230	253
3	2	3	353	333	8	2	2	-297	-267
3	2	4	367	364	8	2	3	-99	-94
3	2	5	-38	-83*	8	2	4	84	89
3	2	6	43	74*	8	2	5	-138	-158
3	2	7	-265	-246	8	2	6	-40	-44*
3	2	8	150	158	H= 9, K= 2				
3	2	9	-63	-12*	9	2	1	-313	-320
3	2	10	-68	-50*	9	2	2	-58	-6*
H= 4, K= 2					9	2	3	-53	-52*
4	2	1	-483	-553	9	2	4	49	66*
4	2	2	261	239	9	2	5	-45	-24*
4	2	3	386	344	9	2	6	135	133
4	2	4	104	93	H= 10, K= 2				
4	2	5	112	109	10	2	1	140	133
4	2	6	40	65*	10	2	2	-64	-39*
4	2	7	204	199	10	2	3	-59	-2*
4	2	8	-52	-24*	10	2	4	-54	-69*
4	2	9	-58	-76*	10	2	5	278	268
4	2	10	-142	-160	H= 11, K= 2				
					11	2	1	94	91

TABLE 5 - 7
FIBERS, [FICALG] FOR RUBIDIUM TRI-iodide
(UNOBSERVED REFLECTIONS MARKED *)

PART 4

H	K	L	FO	K*FC	H	K	L	FO	K*FC
12	2	H = 12, K = 2	0	-64	12	2	0	181	18*
0	0	H = 0, K = 3	7	110	5	3	7	45	22*
0	0	H = 0, K = 3	9	71	5	3	8	168	18*
0	0	H = 0, K = 3	125	29*	5	3	9	36	18*
1	1	H = 1, K = 3	3	274	5	3	0	255	255
1	1	H = 1, K = 3	5	113	5	3	1	480	480
1	1	H = 1, K = 3	6	-236	6	3	2	140	140
1	1	H = 1, K = 3	7	-110	6	3	3	153	153
1	1	H = 1, K = 3	8	-85	6	3	4	500	500
1	1	H = 1, K = 3	9	129	6	3	5	234	234
1	1	H = 1, K = 3	10	-98	6	3	6	255	255
2	2	H = 2, K = 3	1	-363	6	3	7	207	207
2	2	H = 2, K = 3	3	75	6	3	8	161	161
2	2	H = 2, K = 3	4	-255	6	3	9	142	142
2	2	H = 2, K = 3	5	-105	6	3	10	-47	-56*
2	2	H = 2, K = 3	6	-49	6	3	11	24*	24*
2	2	H = 2, K = 3	7	55	6	3	12	-108	-108
2	2	H = 2, K = 3	8	212	6	3	13	76	76
2	2	H = 2, K = 3	9	-113	6	3	14	207	207
2	2	H = 2, K = 3	10	-118	6	3	15	140	140
3	3	H = 3, K = 3	1	-276	6	3	16	255	255
3	3	H = 3, K = 3	2	620	6	3	17	168	168
3	3	H = 3, K = 3	3	-242	6	3	18	181	181
3	3	H = 3, K = 3	4	163	6	3	19	36	36
3	3	H = 3, K = 3	5	84	6	3	20	255	255
3	3	H = 3, K = 3	6	106	6	3	21	140	140
3	3	H = 3, K = 3	7	-81	6	3	22	168	168
3	3	H = 3, K = 3	8	279	6	3	23	181	181
3	3	H = 3, K = 3	9	148	6	3	24	36	36
3	3	H = 3, K = 3	10	152	6	3	25	255	255
4	4	H = 4, K = 3	0	226	6	3	26	140	140
4	4	H = 4, K = 3	2	-70	6	3	27	168	168
4	4	H = 4, K = 3	3	33	6	3	28	181	181
4	4	H = 4, K = 3	4	537	6	3	29	36	36
4	4	H = 4, K = 3	5	420	6	3	30	255	255
4	4	H = 4, K = 3	6	-221	6	3	31	140	140
4	4	H = 4, K = 3	7	47	6	3	32	168	168
4	4	H = 4, K = 3	8	53	6	3	33	181	181
4	4	H = 4, K = 3	9	-60	6	3	34	36	36
5	5	H = 5, K = 3	1	248	6	3	35	255	255
5	5	H = 5, K = 3	2	63	6	3	36	140	140
5	5	H = 5, K = 3	3	-272	6	3	37	168	168
5	5	H = 5, K = 3	4	86	6	3	38	181	181
5	5	H = 5, K = 3	5	234	6	3	39	36	36
5	5	H = 5, K = 3	6	-300	6	3	40	255	255
5	5	H = 5, K = 3	7	52	6	3	41	140	140
5	5	H = 5, K = 3	8	83	6	3	42	168	168
5	5	H = 5, K = 3	9	110	6	3	43	181	181
5	5	H = 5, K = 3	10	111	6	3	44	36	36
5	5	H = 5, K = 3	11	112	6	3	45	255	255
5	5	H = 5, K = 3	12	113	6	3	46	140	140
5	5	H = 5, K = 3	13	114	6	3	47	168	168
5	5	H = 5, K = 3	14	115	6	3	48	181	181
5	5	H = 5, K = 3	15	116	6	3	49	36	36
5	5	H = 5, K = 3	16	117	6	3	50	255	255
5	5	H = 5, K = 3	17	118	6	3	51	140	140
5	5	H = 5, K = 3	18	119	6	3	52	168	168
5	5	H = 5, K = 3	19	120	6	3	53	181	181
5	5	H = 5, K = 3	20	121	6	3	54	36	36
5	5	H = 5, K = 3	21	122	6	3	55	255	255
5	5	H = 5, K = 3	22	123	6	3	56	140	140
5	5	H = 5, K = 3	23	124	6	3	57	168	168
5	5	H = 5, K = 3	24	125	6	3	58	181	181
5	5	H = 5, K = 3	25	126	6	3	59	36	36
5	5	H = 5, K = 3	26	127	6	3	60	255	255
5	5	H = 5, K = 3	27	128	6	3	61	140	140
5	5	H = 5, K = 3	28	129	6	3	62	168	168
5	5	H = 5, K = 3	29	130	6	3	63	181	181
5	5	H = 5, K = 3	30	131	6	3	64	36	36
5	5	H = 5, K = 3	31	132	6	3	65	255	255
5	5	H = 5, K = 3	32	133	6	3	66	140	140
5	5	H = 5, K = 3	33	134	6	3	67	168	168
5	5	H = 5, K = 3	34	135	6	3	68	181	181
5	5	H = 5, K = 3	35	136	6	3	69	36	36
5	5	H = 5, K = 3	36	137	6	3	70	255	255
5	5	H = 5, K = 3	37	138	6	3	71	140	140
5	5	H = 5, K = 3	38	139	6	3	72	168	168
5	5	H = 5, K = 3	39	140	6	3	73	181	181
5	5	H = 5, K = 3	40	141	6	3	74	36	36
5	5	H = 5, K = 3	41	142	6	3	75	255	255
5	5	H = 5, K = 3	42	143	6	3	76	140	140
5	5	H = 5, K = 3	43	144	6	3	77	168	168
5	5	H = 5, K = 3	44	145	6	3	78	181	181
5	5	H = 5, K = 3	45	146	6	3	79	36	36
5	5	H = 5, K = 3	46	147	6	3	80	255	255
5	5	H = 5, K = 3	47	148	6	3	81	140	140
5	5	H = 5, K = 3	48	149	6	3	82	168	168
5	5	H = 5, K = 3	49	150	6	3	83	181	181
5	5	H = 5, K = 3	50	151	6	3	84	36	36
5	5	H = 5, K = 3	51	152	6	3	85	255	255
5	5	H = 5, K = 3	52	153	6	3	86	140	140
5	5	H = 5, K = 3	53	154	6	3	87	168	168
5	5	H = 5, K = 3	54	155	6	3	88	181	181
5	5	H = 5, K = 3	55	156	6	3	89	36	36
5	5	H = 5, K = 3	56	157	6	3	90	255	255
5	5	H = 5, K = 3	57	158	6	3	91	140	140
5	5	H = 5, K = 3	58	159	6	3	92	168	168
5	5	H = 5, K = 3	59	160	6	3	93	181	181
5	5	H = 5, K = 3	60	161	6	3	94	36	36
5	5	H = 5, K = 3	61	162	6	3	95	255	255
5	5	H = 5, K = 3	62	163	6	3	96	140	140
5	5	H = 5, K = 3	63	164	6	3	97	168	168
5	5	H = 5, K = 3	64	165	6	3	98	181	181
5	5	H = 5, K = 3	65	166	6	3	99	36	36
5	5	H = 5, K = 3	66	167	6	3	100	255	255

TABLE 5 - 7
F(OBS), F(CALC) FOR RUBIDIUM TRI-IODIDE
(UNOBSERVED REFLECTIONS MARKED *)

PART 5

H	K	L	F _O	K*F _C	H	K	L	F _O	K*F _C
H= 12, K= 3					H= 5, K= 4				
12	3	0	-63	-126*	5	4	1	-177	-205
12	3	1	69	26*	5	4	2	-41	-42*
12	3	2	71	40*	5	4	3	-39	-56*
12	3	3	146	138	5	4	4	149	154
H= 0, K= 4					5	4	5	-54	-66
0	4	4	144	160	5	4	6	236	195
0	4	6	60	14*	5	4	7	62	30
0	4	8	70	38*	H= 6, K= 4				
0	4	10	-140	-133	6	4	0	67	80
H= 1, K= 4					6	4	1	106	127
1	4	3	89	94	6	4	2	161	144
1	4	4	-280	-274	6	4	3	88	71
1	4	5	49	52*	6	4	4	-139	-138
1	4	6	-184	-182	6	4	5	80	97
1	4	7	-144	-144	6	4	6	173	144
1	4	8	-67	-44*	H= 7, K= 4				
1	4	9	70	22*	7	4	1	-55	-24*
1	4	10	-70	-12*	7	4	2	92	91
H= 2, K= 4					7	4	3	141	134
2	4	2	-118	-146	H= 8, K= 4				
2	4	3	-274	-277	8	4	0	-66	-22*
2	4	4	106	105	8	4	1	-125	-121
2	4	5	118	145	8	4	2	141	129
2	4	6	-117	-111	H= 9, K= 4				
2	4	7	-141	-125	9	4	1	155	153
2	4	8	63	17*	H= 10, K= 4				
2	4	9	-68	-27*	10	4	0	-71	-71*
H= 3, K= 4									
3	4	1	97	111					
3	4	2	-35	-8*					
3	4	3	-152	-156					
3	4	4	-161	-168					
3	4	5	42	37*					
3	4	6	-48	-37*					
3	4	7	116	118					
3	4	8	-88	-76					
H= 4, K= 4									
4	4	0	-375	-406					
4	4	1	252	248					
4	4	2	-101	-109					
4	4	3	-155	-154					
4	4	4	-67	-42					
4	4	5	-40	-51*					
4	4	6	-45	-31*					
4	4	7	-119	-93					

Chapter 6 - The Solution of the Structure of $\text{KI}_3 \cdot \text{H}_2\text{O}$.

	page
6 - 1 Introduction	136
6 - 2 Preparation of Single Crystals	141
6 - 3 Determination of Density	149
6 - 4 Low-Temperature Data Collection	151
6 - 5 Unit Cell Determination and the Indexing of Reflections	166
6 - 6 Structural Determination	172
6 - 7 Discussion	188

6 - 1 Introduction

In 1877 G.S. Johnson published the first account of the preparation and characterisation of potassium tri-iodide. In view of the controversy which subsequently arose concerning the existence of this compound, it is worthwhile reproducing his account of its preparation:

"I have succeeded in preparing the potassium tri-iodide in crystals by dissolving iodine to saturation in an aqueous or alcoholic solution of potassium iodide and evaporating slowly over sulphuric acid. The crystals first deposited were dark coloured cubes, which proved to be potassium iodide coloured by a little free iodine; but, after some days, lustrous dark blue prismatic crystals, sometimes two inches long, were deposited, which had the composition required by KI_3 ."

Johnson based his formulation of this compound as the tri-iodide on analyses of the crystalline material performed by three different methods. He noted that for the analytical method he judged to be most reliable the percentage of iodine and potassium did not sum to exactly 100%. He attributed this deficiency to the presence of adventitious moisture, but as the compound was subsequently shown to be a monohydrate, the discrepancy can most probably be attributed to an incorrect formulation rather than to incorrect analyses. It is interesting to note that Johnson's volumetric determinations of the iodine content of his solid gave an average figure of 58.97 w.%, compared with a theoretical value of 60.46 w.% for KI_3 and 57.97 w.% for $KI_3 \cdot H_2O$ respectively. As these analyses were performed on partially dried material, a relative increase in the iodine value due to some loss of water of crystallization is to be expected. Johnson also determined the melting point to be 45°C, and the specific gravity to be 3.498 gm/cm³ at 15°C by the Archimedean technique employing the mother liquor as the displaced fluid.

The tri-iodide was probably also prepared by Berthelot in 1880, but as he found that the product had the same heat of solution as a stoichiometric mixture of iodine and potassium iodide, he concluded that potassium tri-iodide was not a distinct chemical species. In 1892 Wells, Wheeler and Penfield, in a survey of the known alkali metal polyiodides, reported the preparation of potassium tri-iodide and gave its melting point as 38°C. They also studied the macroscopic crystallography of this compound, describing it as forming massive monoclinic crystals which had a monoclinic angle of 86.79°. They also noted the propensity of this compound to develop twinned forms.

For the next forty years the chemical status of potassium tri-iodide was in doubt. The phase system $\text{KI} - \text{I}_2 - \text{C}_6\text{H}_6$ was studied by Abegg and Hamburger [1906], who reported the formation of KI_3 as a solid species in this system. They also studied the binary system $\text{KI} - \text{I}_2$; unfortunately, they misinterpreted their experimental data and derived an incomplete phase diagram for this system which they believed supported their conclusion regarding the existence of a potassium polyiodide. On the other hand, Parsons and Corliss [1910] examined the system $\text{KI} - \text{I}_2$ - aqueous alcohol while Parsons and Whittemore [1911] studied the $\text{KI} - \text{I}_2 - \text{H}_2\text{O}$ system, and both groups came to the conclusion that there was no evidence for the existence of a potassium tri-iodide. This result was in direct conflict with the findings of Foote and Chalker [1908] who had also investigated the $\text{KI} - \text{I}_2 - \text{H}_2\text{O}$ system and found evidence not only for KI_3 but also a higher polyiodide which they formulated as KI_7 . The situation was further complicated by the work of Kremann and Schoulz [1912] who re-examined the binary $\text{KI} - \text{I}_2$ system, made the same error as Abegg and Hamburger and as a consequence supported their findings in favour of an anhydrous polyiodide. It remained for Briggs and Giegler [1930] to re-determine an accurate phase diagram for the binary system and demonstrate that it showed no evidence for compound formation.

The first X-ray examination of potassium tri-iodide was carried out during this period by Duane and Clark (Duane and Clark [1922, 1923], Clark and Duane [1923a, 1923b]). This work, commenced in 1922, represents one of the pioneering application of the then novel technique of structural analysis by X-ray diffraction (Duane, together with Hunt, established in 1915 the existence of the short-wavelength limit to the X-ray spectrum predicted from quantum theory (Duane and Hunt [1915])). Their study of potassium tri-iodide was preceded by an examination of the structure of potassium iodide, and their first publication (Duane and Clark [1923]) concerning KI_3 also reports work in progress on the structure of the related tri-iodide, CsI_3 . Notwithstanding the weight of evidence against the existence of potassium tri-iodide accumulated from the phase studies mentioned above, Duane and Clark apparently had no difficulty in preparing crystals of the compound using Johnson's method. Initially they described potassium tri-iodide as having cubic symmetry, but in subsequent publications (Duane and Clark [1923], Clark and Duane [1923]) they correct this and confirm the observation of Wells, Wheeler and Penfield that the compound forms crystals which possess monoclinic symmetry. They concluded that this compound had essentially the same body-centred structure as potassium iodide with the extra iodine atoms accommodated on the body diagonal of the cell. Only one cell dimension of 4.68 \AA was reported.

The structural studies carried out by Duane and Clark employed a technique in which certain diffraction maxima from a crystal were interpreted as being produced by characteristic fluorescent X-radiation generated by the elements contained in the compound undergoing Bragg reflection from the lattice planes. This method of interpretation was presented in some detail in a later paper by Clark [1924], in which it was claimed that the correct identification of these 'characteristic reflections' allowed the positions of atoms to be located within the unit

cell. The structural analysis of potassium and caesium iodide, potassium and caesium tri-iodide and caesium dibromiodide were advanced as examples of the successful application of this technique. In the case of the tri-iodides, the iodine atoms were located by their K-series 'characteristic reflections'. The validity of this approach was severely criticised by both Wyckoff [1924] and Ewald and Herman [1926]. It was also attacked by Bozorth and Pauling [1925] who showed in some detail that the results of its application in the case of CsI_3 were completely incorrect.

In 1930 the available evidence concerning the nature of the tri-iodide ion in solution and the probable existence of potassium tri-iodide was reviewed by Grinell-Jones [1930]. His conclusion was that, on the balance of the evidence, potassium tri-iodide existed as a solid compound at temperatures below 25°C . This was immediately challenged by Bancroft and his collaborators who published in the following year a paper entitled '*The hypothetical potassium polyiodides*' (Bancroft, Scherer and Gould [1931]), in which the case for the non-existence of potassium tri-iodide was vigorously advanced in an acerbic and idiosyncratic style unusual in scientific writing of that period. In this paper considerable emphasis was laid on the negative results of both the ternary phase studies of Parsons and his co-workers [1910, 1911] and the more recent examination of the binary system $\text{KI} - \text{I}_2$ carried out by Briggs and Giegle [1930]. Bancroft and his collaborators prepared solid material according to the method of Johnson and Wells, Wheeler and Penfield and reported deficiencies in the analyses similar to those noted by Johnson. They also presented some X-ray powder data collected by Southworth [1931] from the powdered solid and commented that this did not show any diffraction lines other than those attributable to KI. The X-ray work of Duane and Clark was dismissed with an invidious comparison to the practices of the billiard-sharp in 'The Mikado' (Gilbert [1885]). Their conclusion

was that the material examined in all previous studies of solid potassium tri-iodide was in fact potassium iodide contaminated with iodine.

In the same year, Grace submitted a thesis which embodied the results of his examination of the ternary system $KI - I_2 - H_2O$ at $25^\circ C$ (Grace [1931]). Using an elegant method of complete analysis for iodine, iodide and water he was able to demonstrate the existence of potassium tri-iodide as a monohydrated species at this temperature. He also showed that the higher polyiodide reported by Foote and Chalker [1911], potassium hepta-iodide, was also present at this temperature as a solid monohydrate. The significance of his work, apart from the light it shed on the perplexing results of previous studies, was that it focussed attention on the role of solvation in the field of polyhalide chemistry - a possibility which apparently had not been seriously entertained by any of his predecessors in the field. His findings were substantiated by a more elaborate polythermal study of the same system by Briggs *et alii* [1940], which showed that there were in fact two stable hydrated tri-iodide species present in the system, $KI_3 \cdot H_2O$ and $KI_3 \cdot 2H_2O$. The dihydrate can evidently adopt two polymorphic forms, α - $KI_3 \cdot 2H_2O$ and β - $KI_3 \cdot 2H_2O$; the α -form changing to the β -form below $1^\circ C$, and the β -form melting incongruently at $12^\circ C$ to give the monohydrate, potassium iodide and invariant solution.

Although the existence of potassium tri-iodide monohydrate as a solid species was firmly established as a result of these ternary phase studies and considerable impetus was given to the search for other solvated polyiodides (Briggs *et alii* [1930], Cheesman *et alii* [1940], Cheesman and Nunn [1964]), no further X-ray work appears to have been performed with this compound. $KI_3 \cdot H_2O$ is the first species encountered in traversing the alkali metal tri-iodide series from caesium to lithium in which the presence of the water molecule in the structure is necessary

for a crystalline solid to form. For this reason, in view of the major objective of this work, it was considered worthwhile to perform a structural analysis of this compound despite the formidable difficulties presented by its instability.

The potassium compound was chosen in preference to the hydrated ammonium tri-iodide for a number of reasons. It was hoped that a study of a hydrated tri-iodide would give some insight into the stabilizing role performed by the solvate molecule in such structures. As the refinement of the unsolvated ammonium tri-iodide reported in Chapter 4 gave some evidence that interactions other than purely electrostatic ones between the anion and the cation in this compound might play a part in stabilizing the structure, it seemed reasonable to examine a hydrated tri-iodide in which such interactions would be absent. In making this decision, the higher melting point of potassium tri-iodide monohydrate (30°C) as compared to that of the hydrated ammonium tri-iodide (7°C) also carried some weight. Finally, there is the possibility that $\text{NH}_4\text{I}_3 \cdot 3\text{H}_2\text{O}$ is not strictly analogous to $\text{KI}_3 \cdot \text{H}_2\text{O}$, but should be regarded as the analogue of $\text{KI}_3 \cdot 2\text{H}_2\text{O}$, for both $\text{NH}_4\text{I}_3 \cdot 3\text{H}_2\text{O}$ and $\text{KI}_3 \cdot 2\text{H}_2\text{O}$ melt incongruently at low temperatures to give unsolvated and partially solvated tri-iodides respectively.

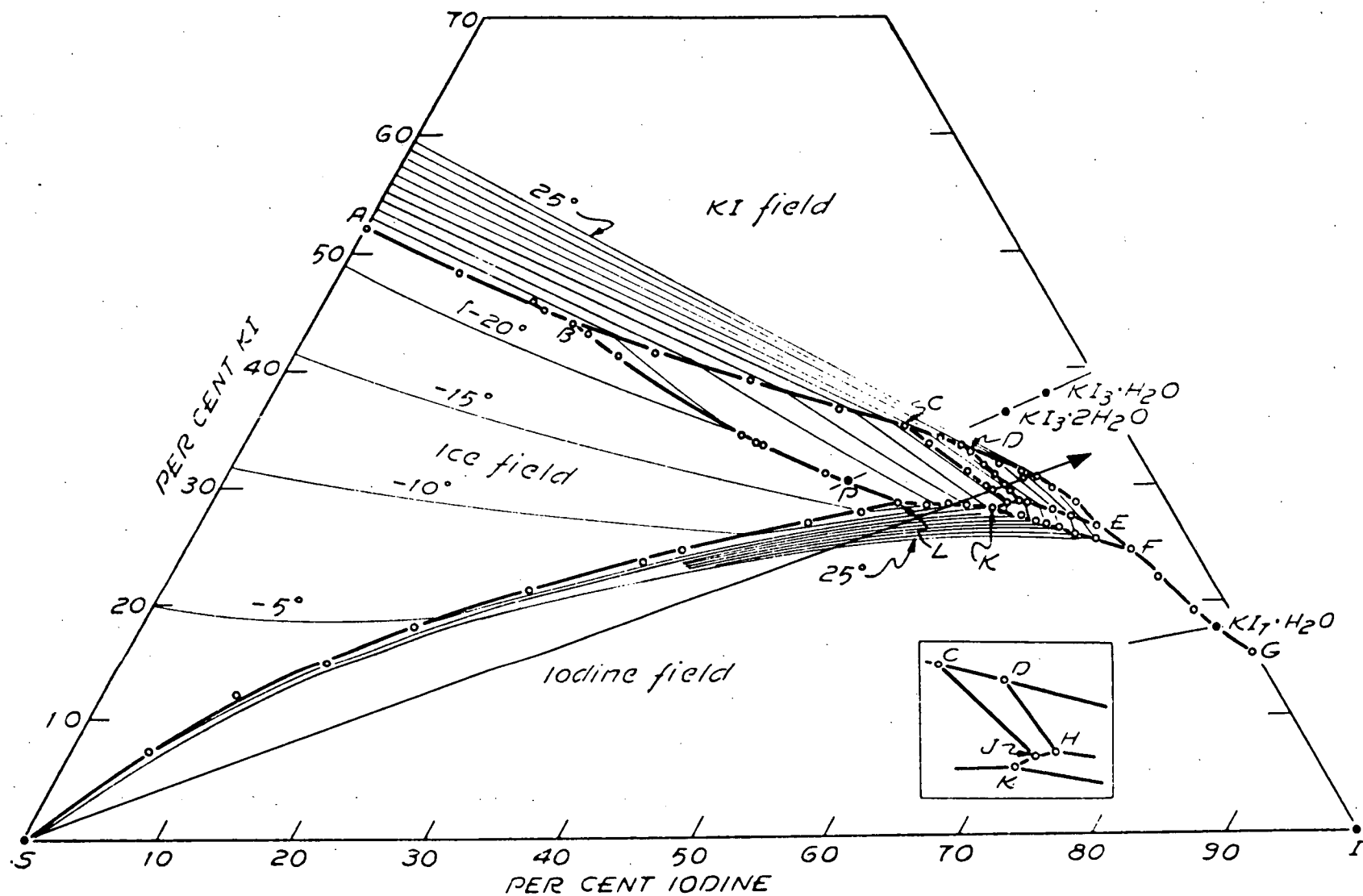
6 - 2 Preparation of Single Crystals

A number of techniques for the preparation of single crystals of $\text{KI}_3 \cdot \text{H}_2\text{O}$ were explored, but of these only two produced material suitable for X-ray analysis after considerable trial-and-error development. As in the previous structural studies reported here, analytic grade solid reagents were used to prepare the compounds for study. In all cases solid $\text{KI}_3 \cdot \text{H}_2\text{O}$ was crystallized from a solution consisting of 60% I_2 , 31% KI and 9% H_2O , as the previously mentioned polythermal phase study of Briggs *et alii* [1940] shows that a solution of this particular compo-

sition will yield a solid consisting only of the monohydrate upon loss of water. In Figure 6 - 1 the ternary diagram at 20°C is reproduced from their data, and superimposed on it is shown the crystallization path taken upon the removal of water from a solution of this composition. The first promising technique for the preparation of single crystals suitable for X-ray work involved the *in situ* growth of crystals within a sealed capillary; this technique was eventually superseded by one in which a dry crystal was transferred to a capillary attached to a drying vessel.

For the *in situ* growth technique a bulk supply of approximately 40 grams of $\text{KI}_3 \cdot \text{H}_2\text{O}$ was prepared by the dehydration of the appropriate solution over sulphuric acid. A portion of the wet solid so produced was gradually warmed until a concentrated solution of the tri-iodide, dissolved in its own water of crystallization and adherent moisture, was obtained. Extreme care was required at this stage to ensure that the temperature did not rise above 30°C at which point iodine vapour was lost from the solution. The warm solution was then sucked by capillary action into thin-walled Pyrex capillary tubes, which were immediately sealed at both ends in a small flame. The capillaries used were approximately 40 mm. long, 0.7 mm. in internal diameter and had a wall thickness of the order of 0.02 mm. When sealed the tri-iodide solution occupied between 15 to 20 mm. of the total length at one end of the tube. As soon as the seals had cooled to room temperature, the capillary tube was immersed in ice-water for about 30 seconds to initiate crystallization and then removed and maintained at approximately 15°C for some 25 minutes. At the end of this period, the capillary was placed in a larger tube, with the end containing the solution plus crystals uppermost and the lower end resting on a pad of glass wool. Supported in this position the tube was centrifuged for five minutes to separate the crystals from the mother liquor. As the

Figure 6 - 1. The polythermal projection diagram for the system $\text{KI} - \text{I}_2 - \text{H}_2\text{O}$ taken from Briggs, Clark, Ballard and Sassman [1940]. The initial composition of the mixture from which $\text{KI}_3 \cdot \text{H}_2\text{O}$ was crystallized is shown as the point in the region labelled DEH lying on the line running to 100% H_2O apex of the triangle. At this position it projects between the 15°C and 20°C isothermals. Removal of water from the mixture would be represented by the movement of the point along the line away from the H_2O apex. $\text{KI}_3 \cdot \text{H}_2\text{O}$ crystallization is initiated when the point passes through the equilibrium surface in the neighbourhood of the 20°C isotherm.



mother liquor at this concentration does not readily wet glass, the separation is a clean one, tri-iodide crystals of varying degrees of perfection remain adhering to the walls of the capillary in the region previously occupied by the solution and the surplus liquor settles at the other end of the tube under the influence of the applied centrifugal acceleration.

As it was impossible to obtain a single crystal which was simultaneously free from secondary crystallite growth and in such a position within the tube that it could be oriented on the goniometer so that neither the incident nor the diffracted X-ray beam was impeded by neighbouring crystals, this technique was eventually abandoned in favour of that described below. However, the technique did provide crystals with which some preliminary work was undertaken.

The preparation of a single crystal for diffraction by the transfer technique commenced with the crystallization of some 15 grams of $\text{KI}_3 \cdot \text{H}_2\text{O}$ by slow dehydration of the appropriate solution in a desiccator over concentrated sulphuric acid. If the solution is left undisturbed under these conditions, large tabular crystals several centimeters in length invariably form; (see Plate 6 - 1 and also the Frontispiece); to avoid this the crystallization dish was agitated daily, with the result that a large number of small crystals were formed. The dehydration process was not allowed to go to completion, but was arrested when about 60% of the water had been removed. The crystals were then freed from the bulk of the mother liquor by gentle suction on a sintered glass disk, and were then transferred, while still damp, to the apparatus shown in Plate 6 - 2.

This apparatus was designed to enable dry crystals of the tri-iodide to be introduced into a dry capillary without absorption of adventitious moisture. It consisted of a glass bulb of approximately 500 millilitres

Plate 6 - 1. Two views of a large single crystal of $\text{KI}_3 \cdot \text{H}_2\text{O}$.
The dimensions of this specimen were approximately
3.0 cm x 1.5 cm x 0.5 cm.

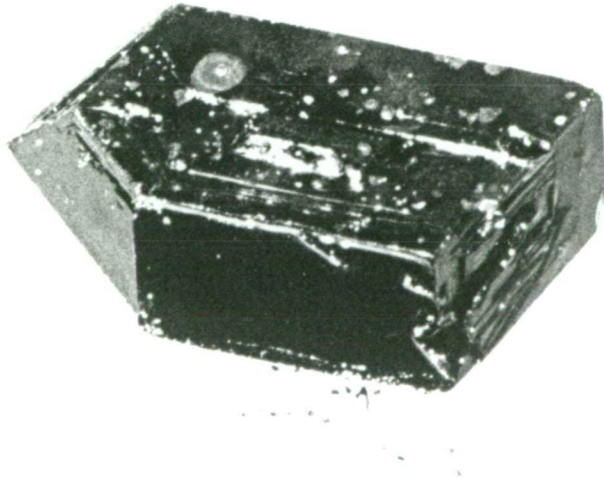
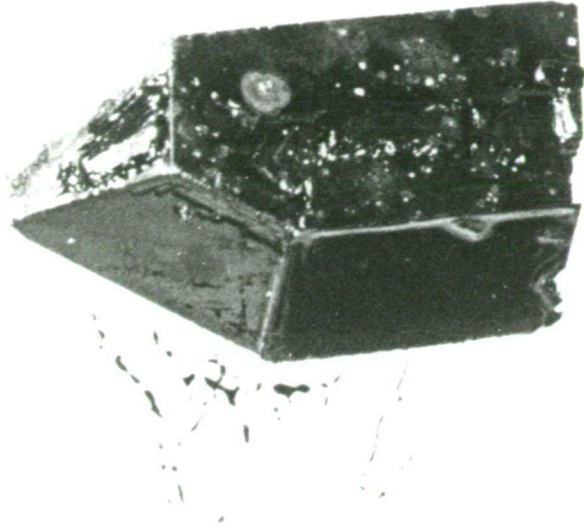
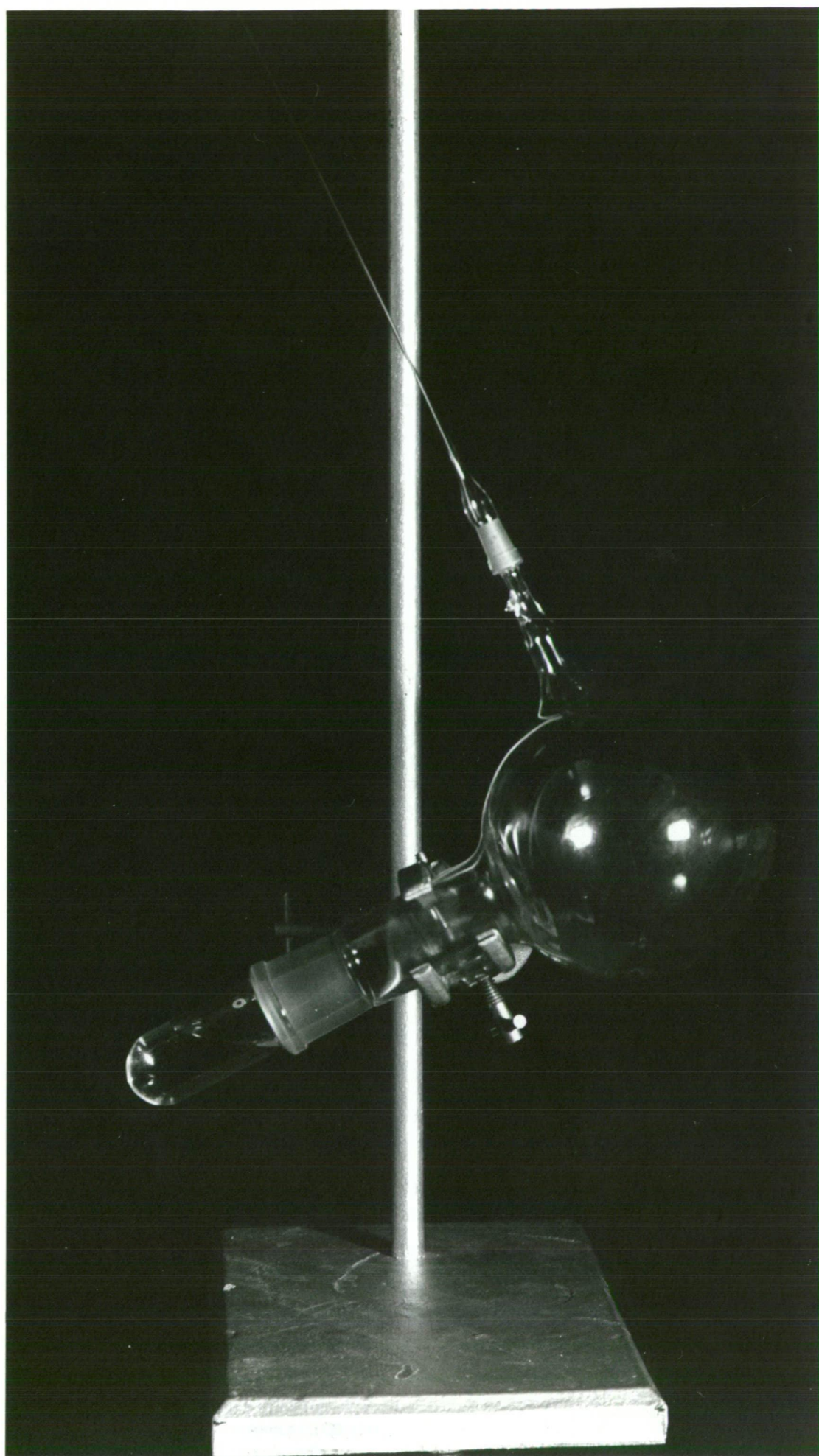


Plate 6 - 2. The apparatus used for the transfer of $\text{KI}_3 \cdot \text{H}_2\text{O}$ single crystals. The capillary tube is visible leading towards the top left corner of the photograph.



capacity; a 'Quickfit' B29 ground glass joint allowed a sidearm containing a drying agent to communicate with the volume of the bulb. Similarly, a thin-walled glass capillary was attached to the bulb with a B7 joint.

In this apparatus the remaining water was absorbed by sulphuric acid held in the sidearm. The acid was partially diluted to specific gravity 1.42 so that the water was removed very gradually from the mass of crystals. Periodically the crystals were agitated to overcome their tendency to stick together as the water was removed, by smartly tapping the wall of the bulb in their vicinity with a metal rod. The dehydration process was followed by visual inspection of the crystals with a hand lens through the wall of the bulb. After about eight days all visible signs of surface moisture had vanished, and on or about the fourteenth day evidence of decomposition in the form of white encrustations on the crystal surfaces could be seen. Consequently, it was judged that ten to twelve days were sufficient to produce a loose mass of dry crystals by this process, and after that time the sidearm containing sulphuric acid was replaced with a blank stopper.

A crystal of a size suitable for X-ray analysis was then introduced into the capillary. This was accomplished by manipulation of the whole apparatus accompanied by gentle tapping of the bulb wall so that only the selected crystal entered the capillary. Once the crystal was satisfactorily positioned within the tube, the capillary was sealed off with a small flame and the seals inspected under the microscope for potential leaks. With care and the use of a considerable length of capillary tubing, a number of crystals could be transferred and sealed into tubes from the one parent batch of dry crystals. Crystals sealed into tubes in this way could be kept indefinitely at room temperature, although for safety a practice was made of keeping a supply of mounted

crystals under refrigeration.

6 - 3 Determination of Density

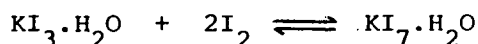
The determination of the density of the solid tri-iodides poses some interesting practical problems as a consequence of the instability of this family of compounds, and in particular the extreme deliquescence of the polyiodides of small cations. These difficulties were met with in their most severe form in the case of potassium tri-iodide, and although the technique finally adopted for the determinations of densities is described with reference to this compound, the same method was also used for the other density determinations reported in this work. The experimental data and results are set out in Appendix B.

Crystals of $\text{KI}_3 \cdot \text{H}_2\text{O}$ were reported by Johnson to have a specific gravity of 3.489. This value was the mean of three determinations made at 15°C by the Archimedean method using the mother liquor as the displaced liquid; at this temperature the correction for the volume occupied by one gram of water will only marginally affect the fourth significant figure, so that little error is introduced by regarding this value as the density of $\text{KI}_3 \cdot \text{H}_2\text{O}$ in gm/cm^3 units. In view of the difficulty of obtaining a dry crystal of $\text{KI}_3 \cdot \text{H}_2\text{O}$ in the first instance, and of maintaining such a crystal free of moisture for any period of time in the open laboratory, it was considered necessary to redetermine the density by another technique. The pycnometric method was chosen, and an inert working liquid which would not react with or dissolve the tri-iodide was sought.

The aqueous mother liquor in equilibrium with crystalline $\text{KI}_3 \cdot \text{H}_2\text{O}$ at a given temperature was considered as a possible working fluid but was rejected for the following reasons. The steepness of the $\text{KI}_3 \cdot \text{H}_2\text{O}$ solubility surface as determined by Briggs *et alii* implies that temperature control to better than 0.02°C would be required during a pycnometric

determination if any degree of precision was to be obtained. Further, the mother liquor is a very hygroscopic, corrosive black liquid which does not readily wet glass; not only is it a difficult material to handle in the laboratory but it also has the disadvantage that it has a high density (approximately 3 gm/cc depending upon composition) and consequently would not differ greatly from the density expected for the material being determined.

The choice of working liquid was thus essentially limited to those non-polar liquids in which ionic solids are not soluble. As iodine is soluble in most non-polar liquids, any tendency for the tri-iodide to decompose by losing iodine to the working liquid must be prevented by pre-saturating the chosen liquid with iodine. It is desirable that the solubility of iodine in the chosen non-polar liquid be as small as possible, as there is a small but nonetheless finite probability of conversion of some of the tri-iodide to solid hepta-iodide by abstraction of iodine from the working fluid. The polythermal phase study referred to above shows that in the aqueous system the two hydrated polyiodides can coexist in equilibrium with a liquid phase rich in iodine. As the equilibrium constant for the reaction:



is apparently not known, it is not possible to estimate the uncertainty such interconversion might introduce into a pycnometric determination when using a working liquid rich in dissolved iodine. In the absence of this information an attempt was made to use a working fluid which could be pre-saturated at a very low iodine concentration. A small quantity of fluorinated kerosene ('perfluorokerosene') was available, and as the saturated iodine concentration at 20°C was determined to be only 0.0005 mole%, a pycnometric determination of the density of $\text{KI}_3 \cdot \text{H}_2\text{O}$ was undertaken using this liquid as the working fluid. Unfortunately,

this attempt was unsuccessful, as it was impossible to dislodge small air bubbles which became attached to the crystal surfaces when they were immersed in the liquid. Even when the pressure over the liquid was reduced with a vacuum pump and the container vigorously shaken, some air bubbles remained firmly attached to the crystal surfaces. The density of $\text{KI}_3 \cdot \text{H}_2\text{O}$ determined by this method was 3.306 gm/cm^3 .

Eventually iodine saturated paraffin oil was used as the working fluid for the pycnometric density determinations. The saturated iodine concentration of paraffin oil at 20°C was determined to be 0.0092 mole%, approximately eighteen times greater than that of perfluorokerosene, so that the probability of inaccuracy due to the formation of hepta-iodide is correspondingly greater. However, this liquid did not allow air bubbles to form on the surface of the crystalline solid to the extent observed with perfluorokerosene. Air bubbles which did form could be readily dislodged by agitation under reduced pressure. The density of $\text{KI}_3 \cdot \text{H}_2\text{O}$ determined by this method was 3.606 gm/cm^3 , compared with the value of 3.498 gm/cm^3 determined by Johnson. As will be shown subsequently from the crystallographic data (see Section 6 - 5), the theoretical density for this compound is 3.330 gm/cm^3 ; the results of both the pycnometric determination using paraffin oil and Johnson's Archimedean determination are consistent with the formation of small amounts of the hepta-iodide, the latter determination not surprisingly being the most seriously affected.

6 - 4 Low-Temperature Data Collection

The diffraction data were collected with zirconium filtered molybdenum radiation. This radiation was chosen to minimize absorption effects, the mass absorption coefficient of $\text{KI}_3 \cdot \text{H}_2\text{O}$ at the $\text{Mo K}\alpha$ wavelength of 0.71069 \AA (Henry and Lonsdale [1965]) being $35.49 \text{ cm}^2 \text{ gm}^{-1}$ compared with a value of $299.49 \text{ cm}^2 \text{ gm}^{-1}$ for $\text{Cu K}\alpha$ radiation. All the

data were collected by the photographic method; a 'Nonius' weissenberg camera being used for the major part of the work, and a 'Nonius' precession camera for some exploratory photography.

Some preliminary photographs were taken using specimens prepared by the *in situ* growth technique. It was observed that the crystals rapidly decomposed when exposed to the X-ray beam at room temperature. In the case of a large plate-like crystal, which had a cross-section comparable to the diameter of the collimated beam, the phenomenon of decomposition during irradiation was demonstrated dramatically. The specimen was mounted on the precession camera with the plate normal to the beam; after about 1½ hours exposure only those parts of the crystal which had not been in the beam remained intact, and these defined a ragged hole in the centre of the plate where decomposition had taken place. Such behaviour was not entirely unexpected, as ammonium tri-iodide crystals were observed to decompose slowly in the X-ray beam (see Section 4 - 1), and potassium tri-iodide is considerably less stable than its ammonium analogue. As a result of these preliminary experiments, all further attempts to collect data from this compound were carried out at reduced temperatures.

An attempt was made to secure an oscillation photograph using the 'Nonius' low-temperature attachment for the weissenberg camera. This consists of a vacuum-jacketed tube through which a stream of cold gas (usually N_2) can be directed at the crystal. The tube is supported in the layer-line screen, and the supports for this insulated tube also carry a coil of resistance wire with which the screen and adjacent film cassette can be warmed to control ice formation. It was found that when the camera was used with this attachment, in the oscillation mode it was necessary to partially withdraw the screen to allow more than one layer line to record on the film. Under these operating conditions the

heat output from the coil was not sufficient to keep the camera free of ice. In particular, the build-up of ice in the vicinity of the goniometer head was so severe that one specimen was lost when the enclosing capillary broke under the load of ice accumulated in the course of a four hour exposure. Even in the weissenberg mode it was discovered that, if the layer line screen was to be kept free of ice, the appropriate combination of cold gas flow rate and heat output from the heating coil did not allow the crystal to be kept below -15°C . At this temperature, specimen decomposition was still evident. At lower temperatures, the slit in the layer-line screen choked with ice which eventually fouled the motion of the film cassette. It appeared that this low-temperature attachment could not achieve the required reduction in temperature in the humid conditions prevailing in this laboratory. For this reason an alternative cooling device was constructed.

A number of devices and attachments to provide refrigeration of a crystal on the weissenberg camera have been described in the literature (Post [1964]), but few of these appear to eliminate the problems associated with operation in a humid atmosphere. The design of the apparatus developed for this case sprang from the assumption that if the refrigerant gas could be restricted to the immediate vicinity of the crystal, so that it came in contact with as little of the camera as possible, the problems arising from the accumulation of ice could be reduced or eliminated. To this end the goniometer head and specimen were enclosed in a demountable cylindrical metal chamber with large X-ray transparent windows. These windows were made from X-ray film base from which the emulsion had been stripped. The chamber was designed to fit the camera in place of the beam-stop assembly; it therefore carried its own beam-catcher attached to the inner wall. An aperture was cut in the opposite wall to accommodate the collimator; this aperture was backed with a strip of spongy

foam plastic in which a slit was cut so that it could act as a seal around the nose of the collimator (this can be seen in Plate 6 - 4).

The cold gas was conducted to and from the chamber by a pair of co-axial metal tubes. The outermost of these was machined so that it not only made a good friction fit inside the end of the chamber, but could also be held in position by the layer-line screen clamping ring on the camera. The inner tube, which brought the gas into the chamber, carried an adjustable mounting for a thermistor. The thermistor was used to monitor the temperature of the chamber; by means of the adjustable mounting, its position could be arranged so that its sensitive element was as close as possible to the crystal but clear of the beam and the volume swept out by the oscillating capillary.

The cylindrical shape of the cold chamber demanded good circulation of the refrigerant gas for efficient cooling of the specimen and its enclosing capillary. This was found to be best achieved by ensuring that the gas stream entered the chamber with a reasonable velocity. The refrigerant gas was therefore generated by atomizing liquid nitrogen; by this method a rapidly moving stream of cold gas could be supplied to the chamber at a reasonable rate of consumption of liquid nitrogen. It had the further advantage of obviating the need for a high pressure supply of cold gas.

The liquid nitrogen was forced from a 25 litre storage dewar with compressed air from the laboratory supply line, and was fed to the atomizer through a 0.375 inch brass delivery pipe. The pressure of the liquid nitrogen delivered to the atomizing nozzle was determined by the pumping pressure which could safely be applied to the storage dewar. The dewars used were specified by their manufacturers to have a maximum safe internal pressure limit of 20 pounds/square inch, so the laboratory compressed air supply was limited to a maximum pressure of 15 pounds/

square inch to give a margin of safety on the manufacturer's limit.

With the liquid nitrogen pressure at the atomizing nozzle so determined, a number of experiments was performed to determine a nozzle design which would best produce a stream of liquid nitrogen droplets small enough to be rapidly vapourized. In its final form, the nozzle consisted of a 0.028 inch thick copper plate perforated by six 0.04 inch diameter holes, the plate being soldered to the end of the delivery pipe. Five of the six holes were drilled at the vertices of a pentagon having a circumscribed circle of radius 0.12 inches, the sixth hole being drilled at the centre. This nozzle produced a stream of droplets just visible to the naked eye; at room temperature the stream of droplets was completely vapourized at a distance of 1.5 - 2.0 inches from the nozzle, producing a gas stream moving at approximately 10 feet/second.

At this point in the development of the cooling attachment it was realized that the circulation of refrigerant gas could be improved by making use of the fast-moving stream in the vicinity of the nozzle to drive a venturi pump which could extract used gas from the chamber. Discussions with the Department of Civil Engineering of this University revealed that a venturi of an appropriate size had been designed by Dr. P. Doe of that Department for operation with gas stream velocities in the 5 - 15 feet/second range. Dr. Doe kindly made available a 3-section brass reverse mould, and this mould was used to make a venturi as an epoxy resin casting with the designed internal profile. After cleaning up the casting on a lathe, the venturi had an overall length of 12.7 cm. and a diameter of 3.8 cm.

The atomizing nozzle and the venturi were held in the correct axial relationship centrally within a 4.0 inch diameter tube, made from a length of heavy-duty polyvinyl chloride water conduit. It was found

Figure 6 - 2. General relationship of the components of the crystal refrigeration system.

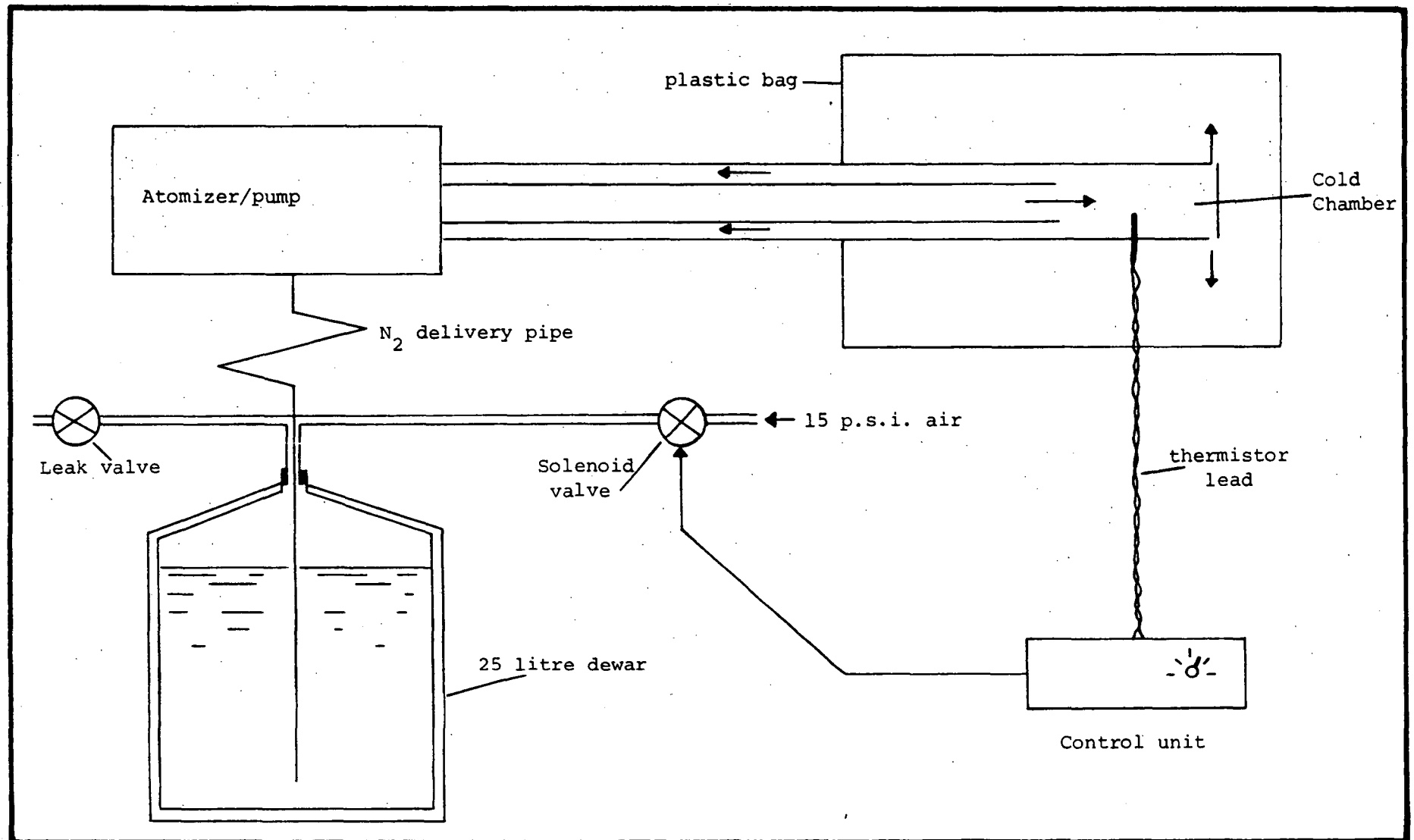


Figure 6 - 3 Sectional drawing (to scale) of the atomizer/pump assembly; points noted are:

- A - Outer case (wood).
- B - Vermiculite insulation.
- C - Liquid nitrogen delivery pipe.
- D - Threaded coupling for liquid nitrogen supply.
- E - PVC inner chamber.
- F - Atomizing nozzle.
- G - Venturi.
- H - Inner flexible trunk delivering cold gas to the cold chamber assembly.
- I - Outer flexible trunk returning used gas to the atomizer/pump assembly.

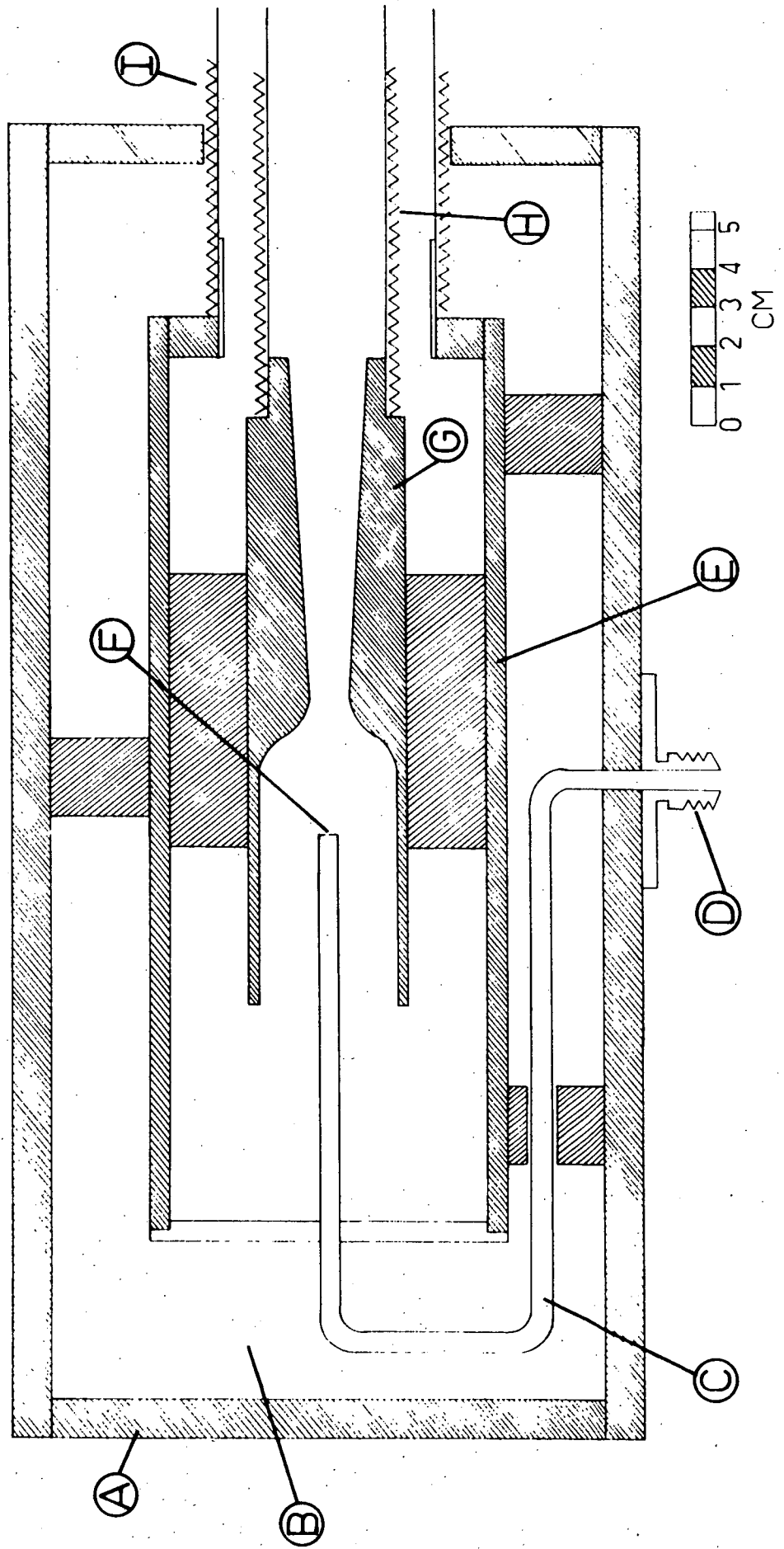


Figure 6 - 4 Sectional drawing (to scale) of cold chamber assembly; points noted are:

- A - Sealing ring in the wall of the plastic bag.
- B - Outer coupling for the outer flexible trunk which returns used gas to the atomizer/pump assembly.
- C - Inner coupling for the inner flexible trunk which supplies cold gas to the cold chamber assembly.
- D - Wall of the plastic bag.
- E - Cold gas inlet tube.
- F - Thermistor lead tube.
- G - Layer-line clamping ring.
- H - Used gas return tube.
- I - Cylindrical film cassette.
- J - Thermistor.
- K - Beam catcher.
- L - Goniometer head mounting boss.
- M - Camera body.
- N - Cold chamber with X-ray transparent windows mounted on a cylindrical frame.
- P - Seal for X-ray beam collimator.

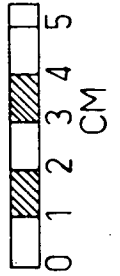
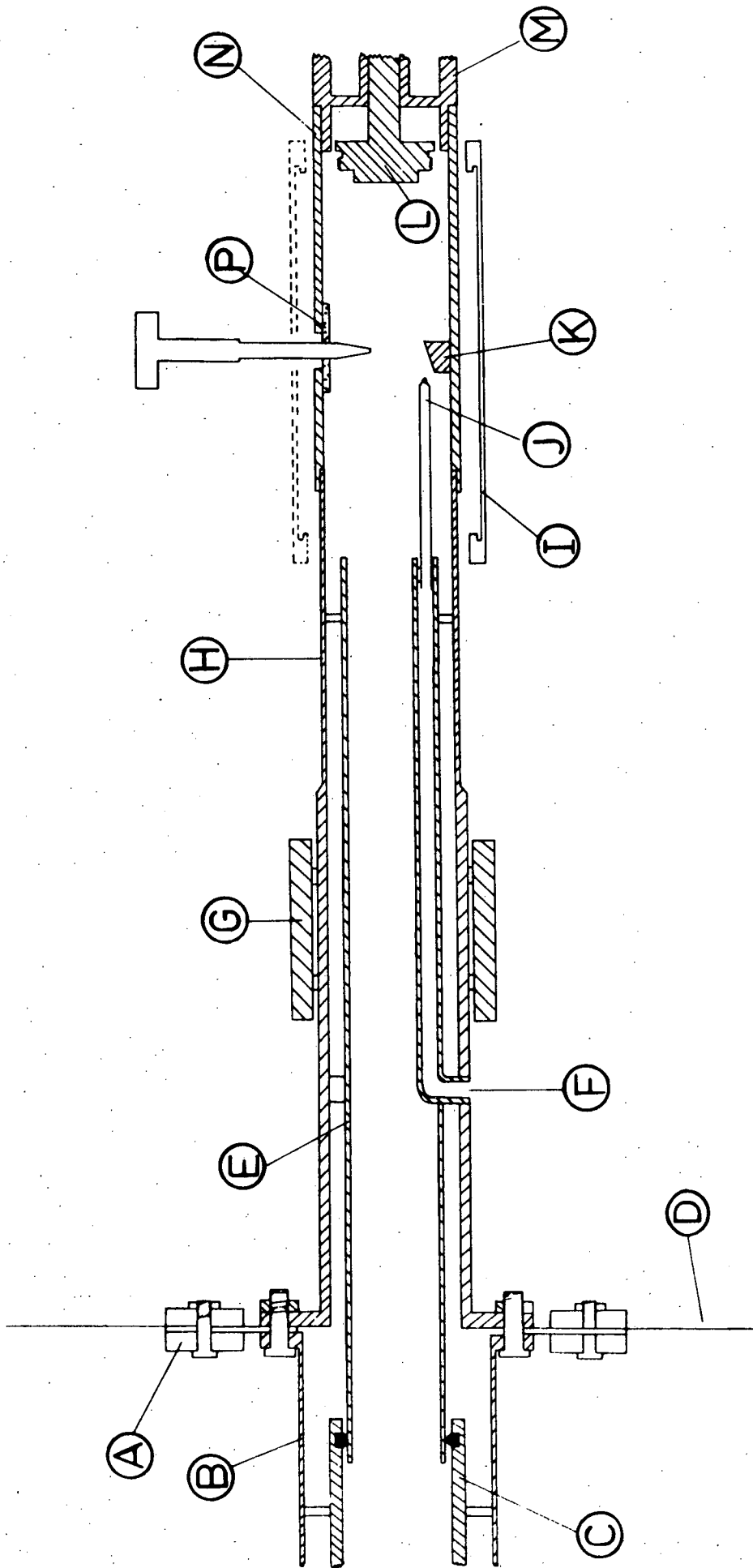
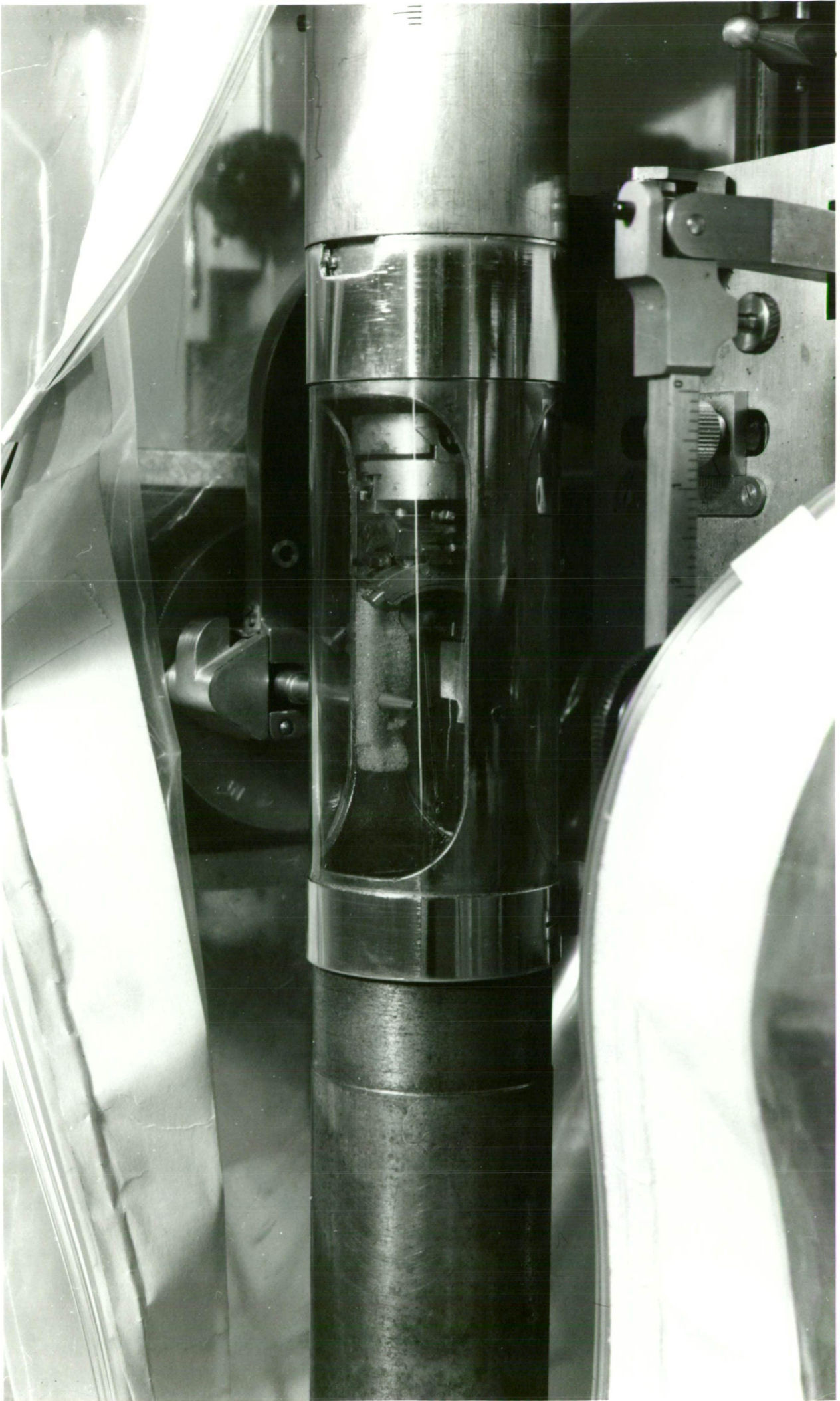


Plate 6 - 3. The crystal refrigeration system in operation;
the specimen temperature was -50°C .



Plate 6 - 4. A close-up view of the cold chamber mounted
on the weissenberg camera.



that the venturi functioned most efficiently when its constriction was 1.75 inches from the front face of the atomizing nozzle. In this position gas returning from the chamber was entrained by the venturi and returned to the chamber mixed with freshly evaporated nitrogen. The mixed gas stream emerging from the venturi was conducted to the inlet tube of the cold chamber through a length of flexible trunking. This trunking consisted of a plastic film supported on a spring steel spiral. A coaxially mounted length of trunking of larger diameter returned the used gas from the cold chamber to the atomizer nozzle-venturi pump assembly. This latter unit was insulated by supporting it in a wooden box filled with vermiculite. The relationship of the various parts of the refrigeration system is shown in Figure 6 - 2, scale diagrams of the atomizer/pump and the cold chamber are presented in Figures 6 - 3 and 6 - 4.

In this form, the refrigeration unit met the requirements of good gas circulation in a low pressure, partially closed apparatus. This design had the added advantage that the cold gas stream proceeding to the camera was insulated from the warm room air by the stream of used gas returning to the atomizer-pump. Temperature control was achieved by using the thermistor to control a solenoid valve in the compressed air line which pressurized the storage dewar; a rise in temperature in the cold chamber caused the valve to open, resulting in liquid nitrogen being forced through the atomizer. The refrigeration system could reach and maintain temperatures in the -90°C to -100°C range. However, the operating point was set at -50°C because, at lower temperatures, the oscillation drive bearings of the camera began to seize. An attempt was made to reduce this tendency to seizure by breaking the conduction path from the goniometer head to the rest of the instrument by inserting a 'teflon' spacer between the head and the oscillation drive shaft. Unfortunately, this did not greatly improve

the low-temperature performance of the system, but merely prolonged the period before the onset of bearing seizure at temperatures below -50°C .

At the chosen operating temperature, the temperature excursion was fairly large (typically $\pm 2^{\circ}\text{C}$), a consequence of the on/off nature of the control of the liquid nitrogen flow. It is probable that a smaller temperature excursion about the operating point could have been achieved if a means of proportional control of the liquid nitrogen supply had been available. The operating temperature was normally reached some 15 minutes after the system was assembled and the control system activated. The average rate of liquid nitrogen consumption, once a steady state had been reached, was 2.5 litres/hour, with some variation depending upon ambient temperature. This compares favourably with the consumption rates of other refrigeration systems using liquid nitrogen that have been described (Post [1964]). A full 25-litre storage dewar could be relied upon to provide an uninterrupted 9 hour exposure.

With this method of refrigeration, it was possible to secure a diffraction record from crystals of $\text{KI}_3 \cdot \text{H}_2\text{O}$. However, the first exposures taken with this system exhibited considerable patchiness due to the absorption of the diffracted beams by a thin film of frost which formed on the windows of the cold chamber. The final refinement involved placing the entire weissenberg camera in a specially made plastic bag. Access to the interior of the bag for changing the film cassette was afforded by a large opening along the top surface which was held closed during operation by a plastic press-seal. When the refrigeration system was operating, the bag was inflated with dry nitrogen escaping from leaks in the cooling system (i.e. around the nose of the collimator) and kept the camera completely free of ice. The system in

operation is shown in Plate 6 - 3, and Plate 6 - 4 gives a view of the cold chamber in position on the camera.

It was hoped that the diffraction data could be collected in the weissenberg mode, and to this end the cold chamber was fitted with a pair of cylindrical sleeves which together acted as a layer line screen. However, it was found that the average lifetime of a crystal small enough to minimize absorption effects had a lifetime of the order of only 70 hours at -50° under Mo K α irradiation. As this period was too short to allow complete alignment and the collection of a full set of multiple-film weissenberg data from one crystal, it was necessary to turn to the oscillation method for the collection of data suitable for intensity measurement.

6 - 5 Unit Cell Determination and the Indexing of Reflections

The difficulties experienced with the X-ray photography of this compound were only partially overcome by the development of the cooling device described in the previous section, and the collection of data was effectively limited to a set of oscillation photographs and a number of weissenberg exposures. As the oscillation data was collected with multiple film packs interleaved with tin foil using overlapping oscillation ranges, and as the same rod-like crystal was employed for this series of exposures, these photographs were suitable for intensity measurement assuming that the reflections could be indexed. The weissenberg photographs were secured using larger crystals, and were seriously affected by absorption; consequently these exposures could not be used for intensity measurements although they provided useful information about the geometry of the reciprocal cell. As a new crystal was usually required for each set of weissenberg exposures, it was highly probable that these photographs would include examples of more than one orientation of the crystal in the X-ray beam.

The main stages in the process of identifying the unit cell and determining its size prior to indexing the oscillation data are briefly set out below; a more detailed account is presented in Appendix C.

A study of the weissenberg photographs revealed that the crystals had in fact been mounted in one or other of two different orientations. Reconstruction of the reciprocal lattice by plotting the reflection positions on the film with respect to polar coordinates (Buerger [1962]) showed that in one orientation the lattice appeared to have monoclinic symmetry with direct cell elements of $a = 4.64 \text{ \AA}$, $b = 10.152 \text{ \AA}$, $c = 8.84 \text{ \AA}$ and $\beta = 92^\circ$ (Orientation I). Note that the a -dimension for this cell corresponds closely with the only cell dimension reported by Duane and Clark (4.68 \AA). A similar reconstruction of the lattice from data collected in the other orientation (Orientation II) gave a direct cell with triclinic elements. These apparently conflicting interpretations could be reconciled by the assumption that Orientation II corresponded to an oscillation about an axis which caused the hkl ($k=l$) reflections referred to the monoclinic cell of Orientation I to form the zero layer of Orientation II.

When the data from both orientations were brought together and referred to the monoclinic cell, the only systematic absence observed was for reflections in the $h0l$ plane. In this reciprocal plane the reflections were absent when $h+l$ was an odd number. As this does not correspond to an allowed absence pattern for a monoclinic space group in the second setting, it was necessary to transform the cell to give a primitive lattice in which $h0l$ reflections were absent when l is odd. The transformed cell had direct space cell dimensions of $a = 4.868 \text{ \AA}$, $b = 10.152 \text{ \AA}$, $c = 9.852 \text{ \AA}$ and $\beta = 116.2^\circ$, with the symmetry of space groups Pc or $P2/c$. The unit cell thus has a volume of 436.67 \AA^3 , for

a cell of this volume both density values yield approximately two for the number of molecules of $\text{KI}_3 \cdot \text{H}_2\text{O}$ contained within one cell. The theoretical density for $Z = 2$ is 3.330 gm/cm^3 ; the density found with perfluorokerosene as the working fluid (3.306 gm/cm^3) although lowered by the presence of attached air bubbles, is marginally closer to the theoretical value than that determined with paraffin oil as the working fluid (3.606 gm/cm^3). As previously mentioned the high value found in the latter determination is most likely explained by the formation of hepta-iodide by absorption of iodine from the iodine-saturated working fluid.

Once the unit cell constants had been determined, in principle the reflections could be indexed and their intensities measured. In practice, this task was complicated by the possibility of fortuitous coincidence of spots within a layer line, and also by the fact that the oscillation data had been collected in Orientation II, which corresponded to oscillation about an axis inclined to the axial directions of the final unit cell.

The possibility of spot coincidence in the oscillation technique can be a considerable limitation, particularly if the oscillation angle is badly chosen. In fact, this limitation provided one of the motives for the development of moving-film methods of photographic data collection. The probability of coincidence rises with increasing diffraction angle, as the lunes of reflection encounter an increasing number of reciprocal lattice points which differ only slightly in the length of their reciprocal vector as the diffraction angle becomes larger. If the lunes are broad, at high diffraction angles the fortuitous coincidence of reflections may be so severe as to preclude indexing altogether, particularly when the data is gathered with short wavelength X-rays. Fortunately, at least from this point of view, in the case of $\text{KI}_3 \cdot \text{H}_2\text{O}$ the diffraction fell off quite rapidly with increasing diffraction angle

even at low temperature. At -50°C there was no useful data beyond about $\theta = 55^{\circ}$, and although this meant that the difficulties introduced by spot coincidence were much reduced, it also curtailed the data available for measurement.

With these circumstances it was found from experiment that an oscillation angle of 8° could be used without creating difficulties from the overlap of reflections from that part of the reciprocal lattice sampled by the lune of reflection. Consequently the data was collected using a constant oscillation angle of 8° , arranged so as to give a 3° overlap with the preceding oscillation, each successive multiple-film exposure thus captured data from a fresh 5° lune of reciprocal space. Twenty consecutive oscillation photographs spanning 200° around the oscillation axis were secured in this manner from the same crystal before decomposition became evident.

The relationship of the lunes swept out by the sphere of reflection to the axial directions of the lattice in Orientation II was established by reference to the weissenberg data collected in the same orientation. Once this had been done, the indexing of the reflections was carried out by a variant of the classical procedure (Bernal [1926]). The positions of spots along a layer line were calculated for a given oscillation range from the known geometry of the Orientation II cell by a computer program especially written for this purpose. This program (U446) also produced an enlarged scale diagram of the oscillation photograph on the digital plotter. On this diagram the reflection positions were marked and labelled with their indices referred to the final monoclinic cell. An example of one of these diagrams is reproduced in Figure 6 - 5.

The lengthy process of identifying each reflection was considerably assisted by the use of these diagrams and overlays prepared from them, and also by the existence of the weissenberg data taken in Orientation I.

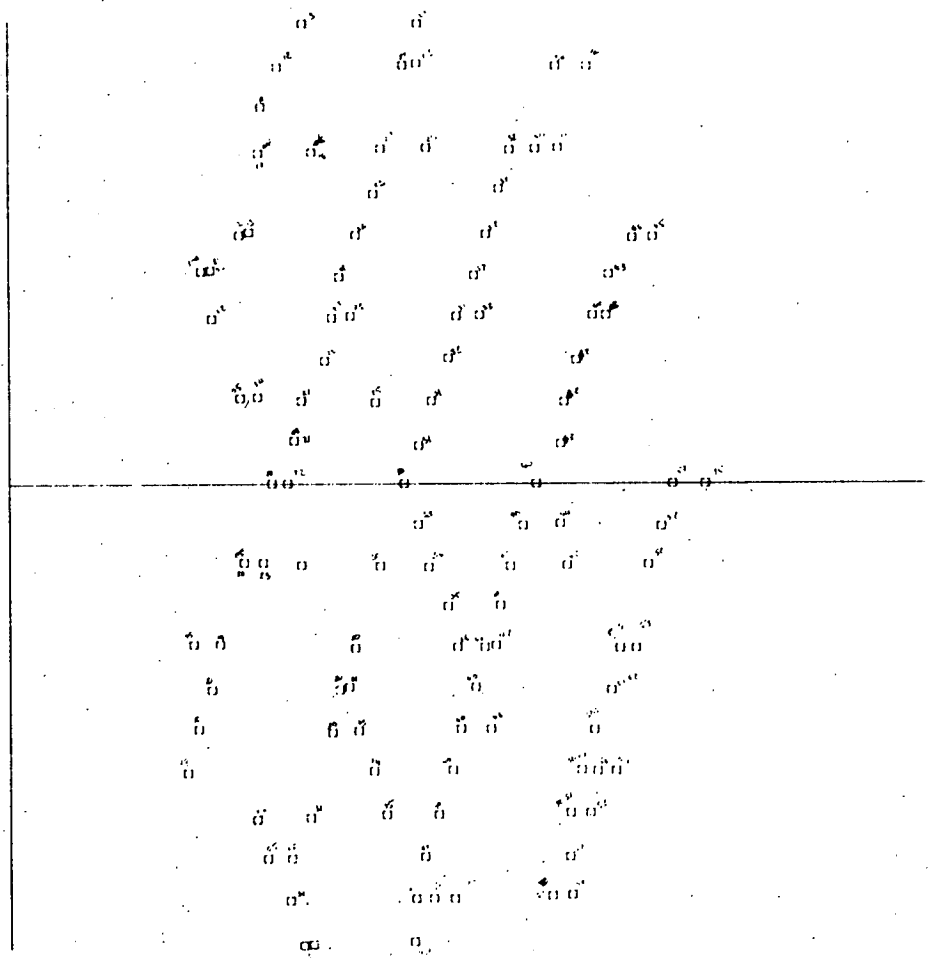


Figure 6 - 5. Photoreduction of one of the computer generated charts used to assist in the indexing of the Orientation II photographs. Note the oblique alignment of the spot positions corresponding to the 4.868 \AA a -axis spacing. The horizontal line marks the zero layer line locus, while the vertical line marks the centre of the beam stop shadow.

When a question arose concerning the correct index to be given to a reflection (due to poor spatial resolution), the question could usually be resolved by comparing the intensities of the spots with the contending indices on the weissenberg film with intensity recorded on the oscillation photograph. Although this method is only semi-quantitative, due to the different sizes of the crystals involved in the two sets of photographs, it did enable most ambiguities to be resolved. For this reason, the intensity measurements were confined to reflections corresponding to reciprocal points contained in the $0kl$, $1kl$ and $2kl$ levels of the final monoclinic cell for which weissenberg data was available. Although reflections from other levels were measurable, it was judged wise to proceed with a small set of reflections whose indices could be relied upon rather than to employ an extended data set which could include a significant proportion of misindexed reflections.

In the region where the diffraction record was strong enough to warrant measurement, about 350 reciprocal points on these three levels fell within the lunes of reflection (in the region where the diffraction record was strong enough to warrant measurement). Of these 24 could not be given an unambiguous index and a further 74 were either too faint to be measured ('unobserved reflections') or fell into regions of the film shadowed by the structure of the cold chamber. Thus a total of 253 reflections were measured by visual comparison against a calibrated strip.

The four-film data was brought to a common scale by the FILM SCALER (X0) program; the average interfilm scaling factor was 2.035 with a variation of $\pm 0.07_1$ about this mean. As the crystal closely approximated a rod of diameter 0.25 mm oscillated about the cylinder axis, a cylindrical absorption correction was applied to the raw data using the ABSORPTION CORRECTION (X3) program. Because the data had been collected in the oscillation mode, it was necessary to write a special program to

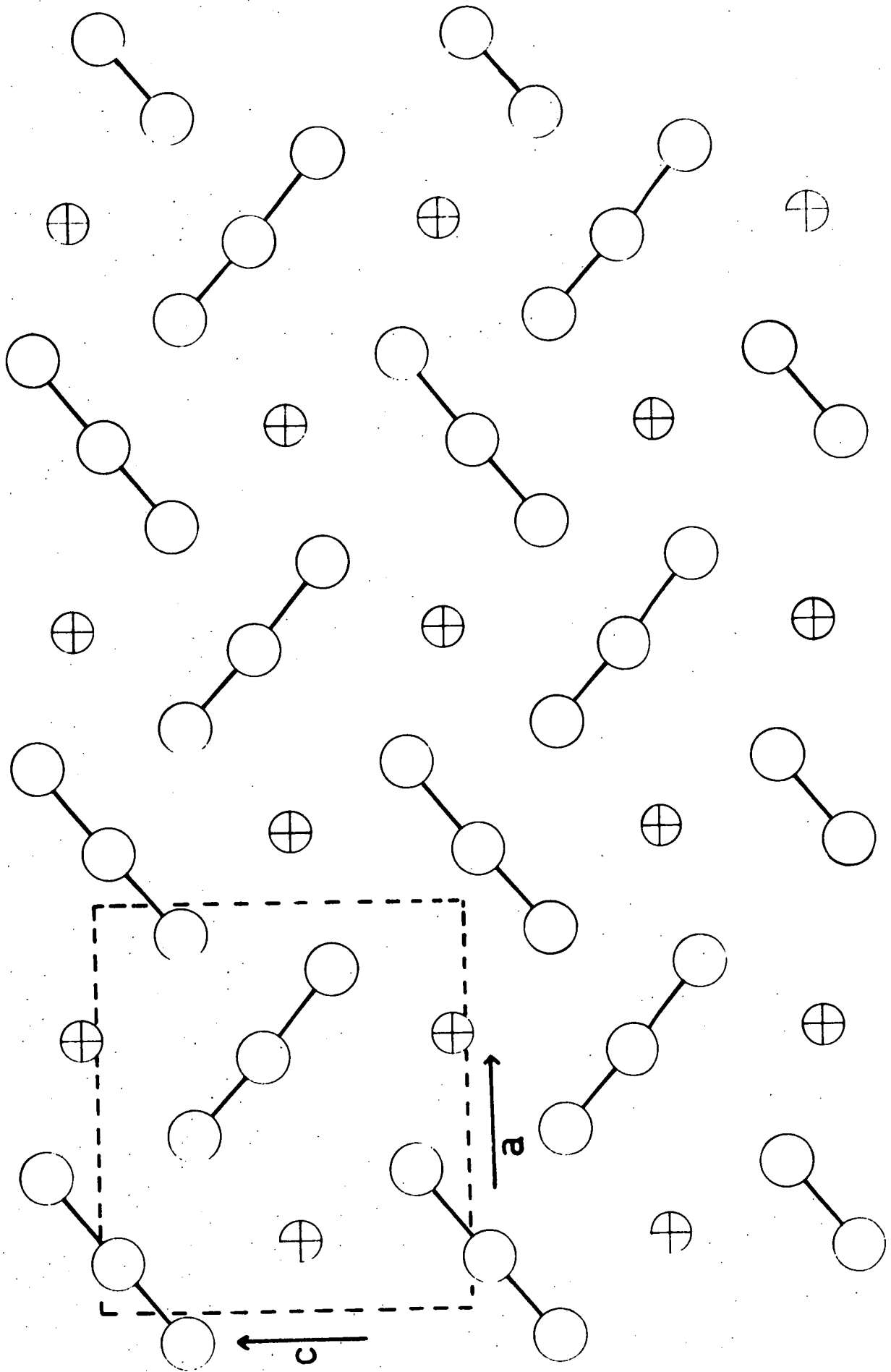
apply the Lorentz/polarization correction required by the geometry of this method of data collection.

6 - 6 Structural Determination

The collection, indexing and measurement of the low-temperature oscillation data was a lengthy process. While it was being carried forward, an investigation was made into the distributions of vector density which might be expected in the Patterson function from given structural features of models for the $\text{KI}_3 \cdot \text{H}_2\text{O}$ structure which took into account the information already to hand (unit cell parameters, number of molecules/cell, space group(s)). As will appear, this preparatory work was well spent, for when the Patterson function finally became available, it was readily solved in the light of the theoretical considerations set out below.

In the isostructural tri-iodides NH_4I_3 , RbI_3 and CsI_3 the cations and the I_3^- anions are arranged in layers perpendicular to the *b*-axis of the orthorhombic cell. Although the separation between the layers shows some slight dependence on cation size, it can be taken to have an average value of 3.34 Å. This structural motif is known to be shared by the trihalides CsBr_3 (Brenemann and Willett [1969]), CsI_2Br (Carpenter [1966]), CsIBr_2 (Davies and Nunn [1969]), RbIClBr (Shugam, Agre and Oboznenko [1967]), NH_4BrICl (Migchelsen and Vos [1967]) and presumably also NH_4Br_3 (Brenemann and Willett [1967]), all of which crystallize in orthorhombic cells with *Pnma* symmetry and with comparable unit cell dimensions. In all cases there are four formula units within the unit cell. With the exception of ammonium tri-bromide (for which no structural data has yet been reported), the geometrical arrangement of cations and trihalide anions within the layers in all these compounds is identical (see Figure 6 - 6).

Figure 6 - 6. The *en echelon* arrangement of I_3^- units in the layered orthorhombic tri-iodides.



It was noted that the *bc* face of the monoclinic unit cell of $\text{KI}_3 \cdot \text{H}_2\text{O}$ was a rectangle with similar dimensions ($10.152 \text{ \AA} \times 9.852 \text{ \AA}$) to the *ac* face of the orthorhombic unit cell of RbI_3 ($10.885 \text{ \AA} \times 9.470 \text{ \AA}$). This similarity, taken together with the ubiquity of layered trihalide structures raised the possibility that $\text{KI}_3 \cdot \text{H}_2\text{O}$ might also possess a layered structure, with the layers lying parallel to the *bc* plane. A point against this hypothesis was the observation that the perpendicular distance between opposite *bc* faces of the monoclinic cell was 4.366 \AA , which is considerably greater than the average interlayer spacing of 3.34 \AA observed in the orthorhombic trihalides. The need to accommodate a water molecule between the layers could be advanced as a possible explanation for the increased spacing in $\text{KI}_3 \cdot \text{H}_2\text{O}$, if in fact the structure of this compound was based on the layer motif. The alternative hypothesis, namely that this distance represented twice the interlayer spacing in potassium tri-iodide, could not be entertained as not only would an interlayer spacing of 2.183 \AA imply that the cell contained four formula units (giving the compound a theoretical density of 6.66 gm cm^{-3}), but also that iodine atoms in adjacent layers would be much too close together.

The choice of space group also has a considerable influence on the development of a layered model for the structure of $\text{KI}_3 \cdot \text{H}_2\text{O}$. The general and special positions available in space group *P2/c* are given in Table 6 - 1.

The ten non-hydrogen atoms can be distributed over the equipoints of the cell in two ways: four iodine atoms can be placed in the four-fold general position and the remaining iodine, potassium and oxygen atoms are then distributed over two-fold special positions, or all the I, K, and O atoms are placed in special positions. For the model to exhibit layering similar to that found in the orthorhombic tri-halides,

Table 6 - 1

General and Special Positions in Space Group $P2/c$

Number of positions, Wyckoff notation, and point symmetry			Coordinates of equivalent positions	
4	g	1	$x, y, z;$	$\bar{x}, \bar{y}, \bar{z}; \bar{x}, y, \frac{1}{2}-z; x, \bar{y}, \frac{1}{2} + z.$
2	f	2	$\frac{1}{2}, y, \frac{1}{2};$	$\frac{1}{2}, \bar{y}, \frac{3}{4}.$
2	e	2	$0, y, \frac{1}{2};$	$0, \bar{y}, \frac{3}{4}.$
2	d	$\bar{1}$	$\frac{1}{2}, 0, 0;$	$\frac{1}{2}, 0, \frac{1}{2}.$
2	c	$\bar{1}$	$0, \frac{1}{2}, 0;$	$0, \frac{1}{2}, \frac{1}{2}.$
2	b	$\bar{1}$	$\frac{1}{2}, \frac{1}{2}, 0;$	$\frac{1}{2}, \frac{1}{2}, \frac{1}{2}.$
2	a	$\bar{1}$	$0, 0, 0;$	$0, 0, \frac{1}{2}.$

the x-coordinate of all the atoms (with the possible exception of the water oxygen atoms) must be the same. In the case where the four-fold general position is used it is possible to develop a structural model which has I_3^- units arranged in layers. For example, if the following combination is used:

Iodine 1 in position $2e$ with coordinates $0, y_1, \frac{1}{2}$

Iodine 2 in position $4g$ with coordinates $0, y_2, z_2$

with a suitable choice for the values of the unspecialized coordinates the structural model will consist of layers of I_3^- units at $x = 0, 1$ with the long axes of the anions parallel to the z-direction of the cell. If $y_1 = y_2$ the tri-iodide units will be symmetric and linear, but if $y_1 \neq y_2$ then the units retain their symmetrical bonds but become bent (see Figure 6 - 7a,b).

If all atoms occupy special positions, a layered structure with discrete I_3^- units can also be developed by placing iodine atoms as follows:

Iodine 1 in $2e$ with coordinates $0, y_1, \frac{1}{2}$

Iodine 2 in $2e$ with coordinates $0, y_2, \frac{1}{2}$

Iodine 3 in $2e$ with coordinates $0, y_3, \frac{1}{2}$ ($y_1 \neq y_2 \neq y_3$).

Again, the structural model consists of parallel tri-iodide units arranged in layers at $x = 0, 1$, but in this case the long axes of the anions lie parallel to the y-direction of the cell. In this case the I_3^- unit can be made to have symmetric or asymmetric bonds by the appropriate choice of y_1, y_2 and y_3 but it cannot be bent (see Figure 6 - 7c). A related model with the same characteristics can be generated with the plane of tri-iodide anions at $x = \frac{1}{2}$ by using the special position $2f$ rather than $2a$.

It is not possible to develop reasonable structural models consisting of layered arrays of bonded tri-atomic units using the special positions

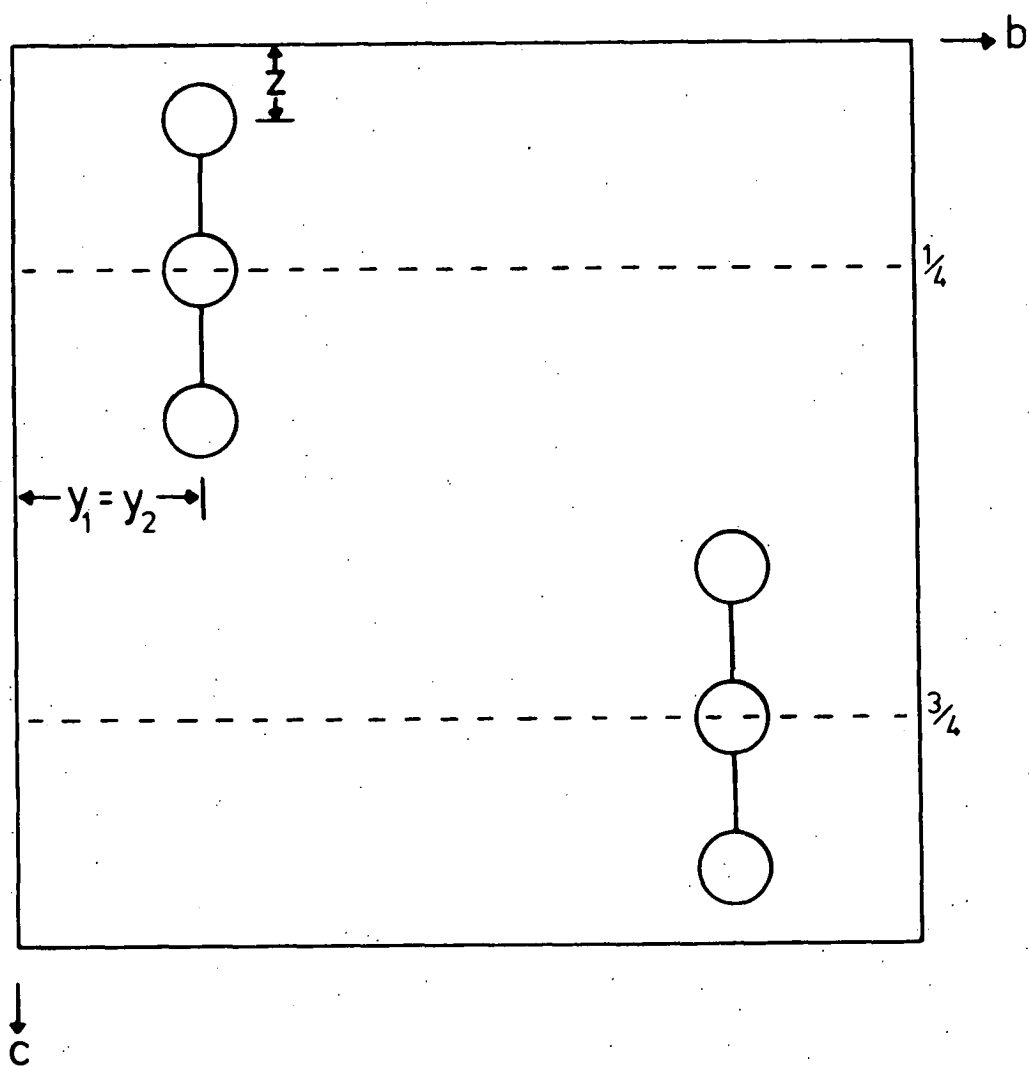


Figure 6 - 7a. A layered structure in $P2/c$ of linear, symmetric I_3^- groups.

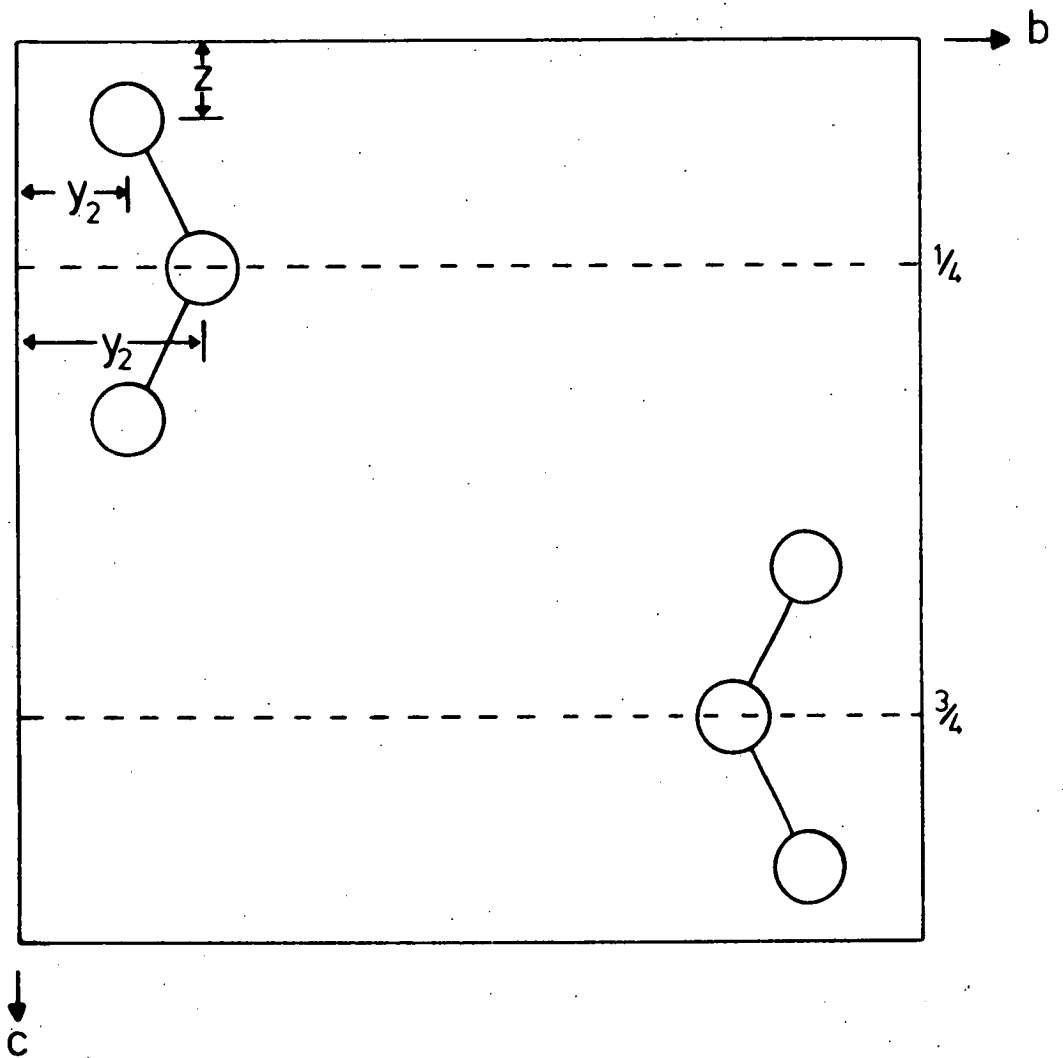


Figure 6 - 7b. As in Figure 6 - 7a, but with bent, symmetric I_3^- groups.

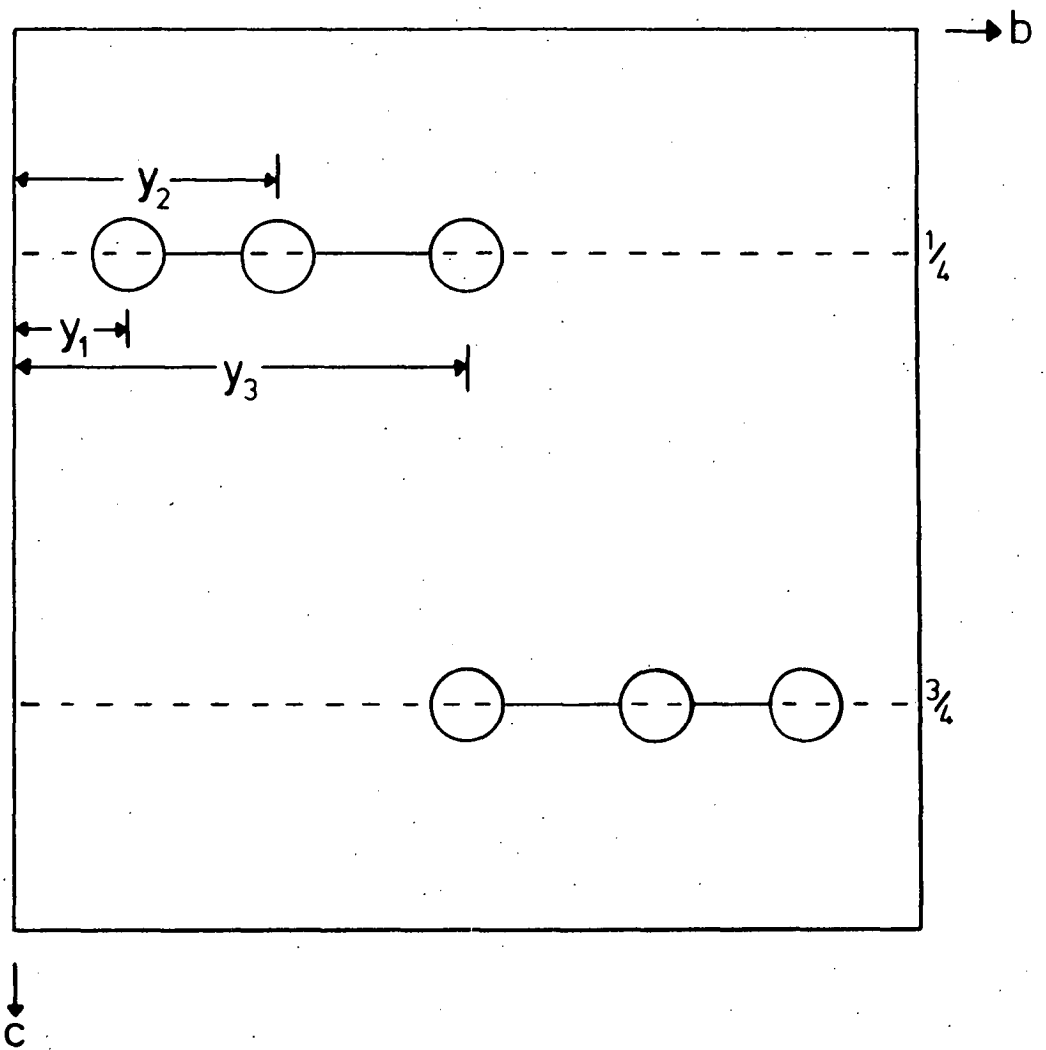


Figure 6 - 7c. As in Figure 6 - 7a, but with linear, asymmetric I_3^- groups.

2a, 2b, 2c and 2d, in which all coordinates are specialized, in combination with either 2e or 2f.

In the two cases where a layered arrangement of I_3^- anions could be generated, it was not possible to reproduce the *en echelon* arrangement of the anions within the layer which is a characteristic structural feature of the orthorhombic trihalide. In particular it was not possible to propose a plausible position for the potassium atom in those models developed using only the special positions of space group $P2/c$.

As shown in Table 6 - 2, there are no special positions in the related non-centrosymmetric space group Pc .

Table 6 - 2

Symmetry positions in Space Group Pc

Number of positions, Wyckoff notation, and point symmetry			Coordinates of equivalent positions
---	--	--	-------------------------------------

2	a	1	$x, y, z; \bar{x}, \bar{y}, \frac{1}{2} + z.$
---	---	---	---

In this space group it is possible to generate a number of model structures which show both layering of the I_3^- ions and the *en echelon* arrangement of the anions within the layers. It is also possible to propose not unreasonable cation positions in some of these model structures.

These preliminary considerations suggested that if $KI_3 \cdot H_2O$ followed the structural pattern of the orthorhombic tri-halides in which discrete, approximately linear but asymmetric I_3^- units are arranged *en echelon* in layers characterised by mutually orthogonal repeat translations of approximately 10 \AA and 9.5 \AA , then there was a high probability that the correct choice of space group was the noncentrosymmetric group Pc .

The Patterson function was calculated from the reflection data after

the absorption and Lorentz/polarization corrections had been applied, with sections taken down the a -axis. The major concentration of vector density occurred in the Oyz plane, with a linear concentration in that plane at $0, y, \frac{1}{2}$ (Figure 6 - 8). There were no other significant concentrations of vector density in the volume of the Patterson function, in particular the xOz plane did not contain any peaks comparable to those present in the plane at Oyz .

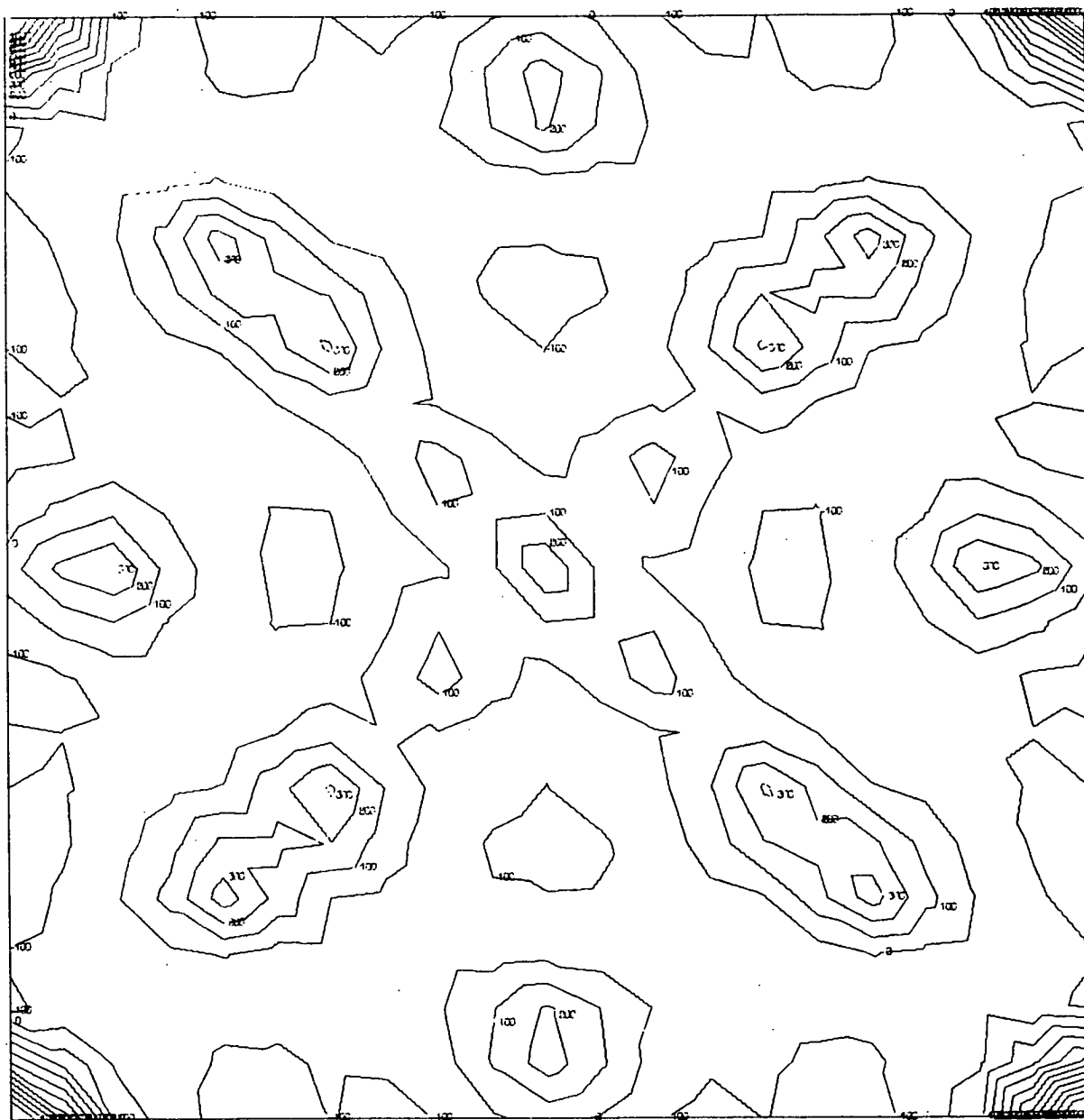
The C -glide operation common to both space groups will generate Harker peaks in the line at $0, y, \frac{1}{2}$. If the space group is centrosymmetric and the general positions are occupied, Harker peaks will also be present in the xOz plane due to vectors between atoms in positions of the type x, y, z and $-x, y, \frac{1}{2}-z$. The absence of any concentration of vector density which could be interpreted as Harker peaks due to atoms in such positions led to the conclusion that either the space group was Pc or that the atoms were confined to the $2e/2f$ special positions of $P2/c$. Further, the absence of any large peaks in the volume of the cell confirmed the original supposition that at least the iodine atoms were localized in planes parallel to the bc face of the unit cell.

The prominent non-Harker peaks present in the Oyz plane of the Patterson function could not be interpreted on the assumption that the iodine atoms were present in the $2e/2f$ special positions of $P2/c$. If this were the case, peaks would be expected in the $Oy0$ line due to vectors between non-symmetry related iodine atoms making up the I_3^- unit, for example, using the previous notation:

TABLE 6 - 3

Predicted I - I Vector Positions

Interaction	Vector Position
Iodine 1 and Iodine 2	$0, y_1 - y_2, 0$
Iodine 1 and Iodine 3	$0, y_1 - y_3, 0$
Iodine 2 and Iodine 3	$0, y_2 - y_3, 0$



Section No= 0 K I3 HYDRATE, A-AXIS PATTERSON

Scale is 1.015 inch=1 Angstrom, contour interval= 100.0

Figure 6 - 8. The Harker section of the $KI_3 \cdot H_2O$ Patterson function.

Depending upon the difference between the two I - I bond lengths, the peaks due to I(1) - I(2) and I(2) and I(3) could overlap to a considerable degree or coalesce in the case of a symmetric anion. However, no peaks were present on the $0y0$ line, the closest peak of any significance being at $0, \frac{1}{2}, 1/10$.

The alternative hypothesis, that the non-Harker peaks in the Oyz plane correspond to interactions between iodine atoms in the general positions of space group Pc was then examined. The peak at position $0, 0.2125, 0.2050$ is 2.955 \AA° from the origin. This distance falls within the range ($2.92 - 3.11 \text{ \AA}^\circ$) expected for the bond lengths of the tri-iodide ion. This peak was therefore taken to be the result of interactions between the central and terminal iodine atoms of the I_3^- unit.

Turning to the Harker peaks present along the $Oy\frac{1}{2}$ line, the peak at $0, 0.0875, 0.5$ allowed the determination of the y -parameter of one of the iodine atoms to be determined as $y = 0.0437_5$. In this space group the choice of the remaining co-ordinates for the first atom is arbitrary. If only this atom was used to phase the structure factor data for a Fourier calculation, the resulting electron density map would contain peaks for both the true structure and its mirror image. The use of two atoms to phase the structure factor data will normally remove this spurious symmetry; fortunately, in this case a second atom position can be calculated from the known length and direction of the iodine-iodine bond already determined from the non-Harker peak at $0, 0.2125, 0.2050$.

A structure factor calculation was performed with iodine atoms in the following positions:

Iodine 1	0,0000, 0.0437 ₅ , 0.0000;
Iodine 2	0.0000, 0.2563, 0.2050.

After refinement of the interlayer scaling factors, the residual stood at 0.402 and the third iodine position was easily found in the zero x -axis section of the Fourier calculated from these data.

A new structure factors calculation using the three iodine positions brought the residual to 0.345. In the zero section of the Fourier calculated from these data the relative arrangement of the tri-iodide groups could be clearly seen. As had been postulated, the I_3^- units were arranged *en echelon* in the plane, one anion lying with its long axis approximately parallel to the diagonal of the bc unit cell face, and the other with its long axis at right angles to it.

It was expected on the basis of the anion-cation arrangement found in the orthorhombic trihalides, that the potassium atom would be located approximately in the centre of the quadrilateral formed by four neighbouring I_3^- ions. It was not possible to identify with confidence any peak in this vicinity as that due to the unphased cation, because with the residual at 0.345 the Fourier background was considerable. A difference Fourier calculated from the same data showed a region of positive density at this position, indicating a corresponding deficiency of electron density in the model structure. However, this positive region extended in the x -direction out of the plane of the I_3^- groups, and it did not possess any local maximum which could be identified as the unphased potassium atom.

Another round of structure factor calculations was performed, followed by a least squares refinement of the positional parameters of the iodine atoms; this refinement reduced the residual to 0.279. The ΔF synthesis performed with this data showed a clear concentration of difference density at the centre of the I_3^- quadrilateral, but with its maximum displaced out of the plane at $x = -0.15$.

The potassium position was further refined by Fourier methods, making use of the 19-point least squares procedure for locating the coordinates

of Fourier peak maxima (Dawson [1961])). By repeated application of this procedure, the residual was reduced in stages to a value of 0.231; beyond this point no further progress could be made by Fourier methods.

The location of the water molecule oxygen atom presented some difficulties. In this structure, the oxygen atom makes a maximum contribution of only 8% to the total scattering from the crystal, and at this level of refinement series-termination effects in the Fourier produced ripples about the iodine positions which were comparable with the expected height of the unphased oxygen peak. From a consideration of the space available in the model structure developed so far, it became clear that the water molecule could only be accommodated within a specified volume; in any other position in the cell the interatomic distance between the oxygen and its neighbours was too small. This volume was the parallelepiped located between adjacent tri-iodide layers and defined by corresponding I_3^- quadrilaterals separated by the a -axis translation. A search of this volume in the ΔF synthesis yielded a number of maxima, but all of these gave potassium-oxygen distances of the order of 2.5 \AA , which is considerably shorter than the short hydrate K - O distance of 2.79 \AA reported by Christ *et alii* [1953]. These maxima are most probably due to imperfect cancellation of the series-termination ripples in the difference Fourier.

The oxygen position was eventually located by a similar technique to that used to locate a trial position for the potassium atom. A structure factors/least squares refinement calculation was performed in which the positional and isotropic temperature factors of the iodine and potassium atoms were refined, reducing the residual to 0.152. The ΔF synthesis calculated from these data was less confused than previous syntheses, but even so only showed a region of positive $\Delta\rho$ without a clearly defined maximum in the volume in which the oxygen peak was expected. However, by making use of one of the options incorporated in

the GENERAL FOURIER (X16) program, a ΔF synthesis was calculated in which the coefficients were weighted, the weights, w , being calculated by the formula (Stout and Jensen [1969])

$$w = |F_{calc}|^4 / (|F_{calc}|^4 + |F_{obs}|^4)$$

In this synthesis a positive peak was located in the specified volume with its maximum between sections at $x = 0.40$ and $x = 0.45$. This peak was well separated from all other peaks of comparable height by regions of low relief, and these comparable peaks all lay outside the volume which must accommodate the water molecule. The coordinates of the peak maximum were determined by the Dawson procedure and a structure factors calculation performed which included the oxygen atom at this position. After this calculation the residual stood at 0.129.

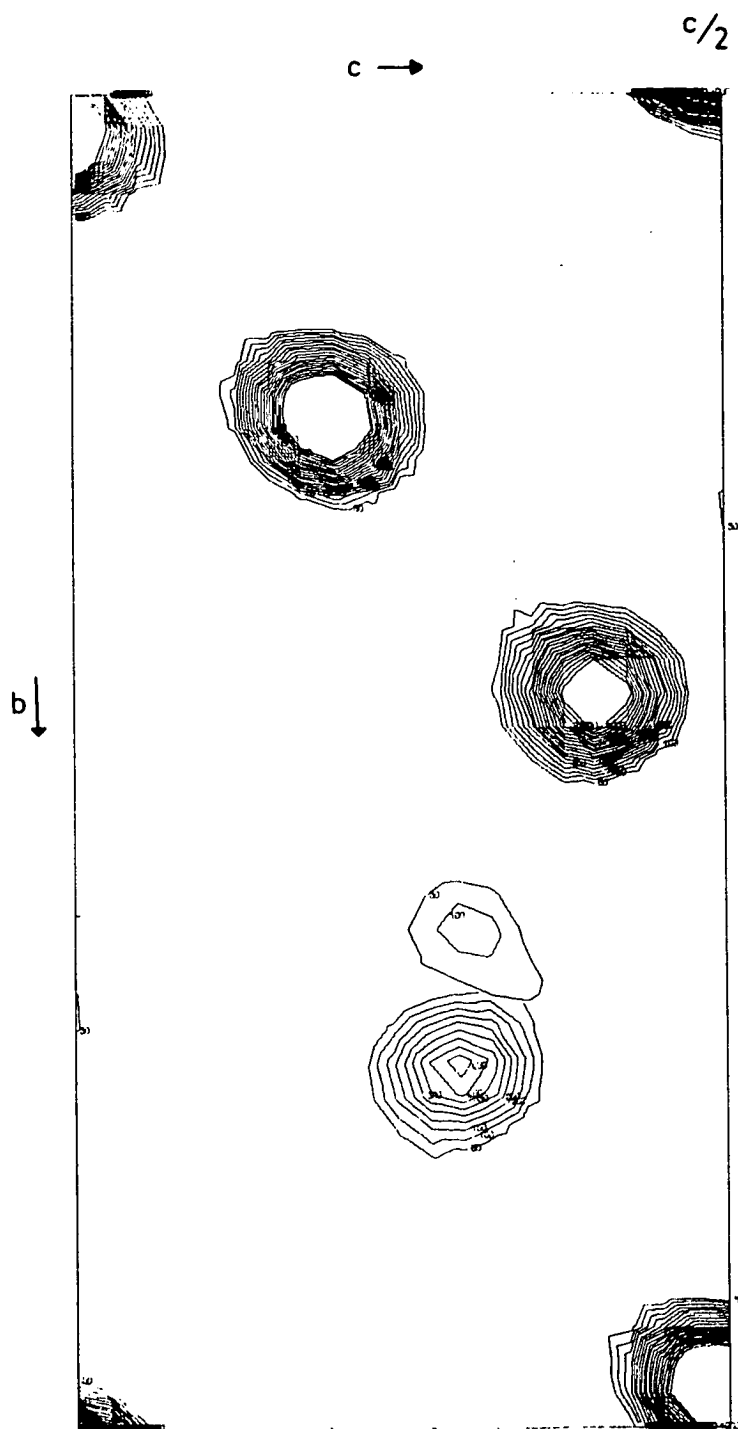
The oxygen position was refined by Fourier methods, as it was found that any attempt to refine the positional parameters by least squares resulted in oscillating corrections being calculated in successive cycles. Consequently, the final positional parameters for this atom are estimates derived from the analysis of the electron density and weighted difference syntheses. Similarly, the isotropic temperature factor for this atom was estimated by trial-and-error guided by the form of the difference density at the oxygen position in the weighted difference density function. Although the parameters for this atom must be treated with caution, it is located in the appropriate volume of the cell at a reasonable distance from the nearest potassium atom.

In Table 6 - 4 the final positional and thermal parameters determined from the least squares refinement in which all atomic parameters other than those for oxygen were refined are presented. Although the weighted difference synthesis gave some evidence that the thermal

vibrations of the iodine atoms are not perfectly represented by isotropic temperature factors (the $\Delta\rho$ peaks comparable to the unphased oxygen peak occupy positions in the synthesis consistent with this interpretation), it was judged that the small size of the visually estimated data set did not justify the introduction of meaningful anisotropic temperature factors (see Section 4 - 3). The final residual attained with the parameters given in Table 6 - 4, including the 'unobserved' reflections, was 0.11. The observed and calculated structure factors for both observed and unobserved reflections are presented in Table 6 - 6. A number of equivalent $0kl$ reflections have been included to give an indication of the quality of the measured data. A projection of the final Fourier is shown in Figure 6 - 9, and in Figure 6 - 10 a projection of the cell contents is also shown.

6 - 7 Discussion

The chemically significant interatomic distances and angles for $KI_3 \cdot H_2O$ as determined from this structural analysis are presented in Table 6 - 5. As the account of the structural determination has already indicated, crystalline $KI_3 \cdot H_2O$ contains slightly bent asymmetric I_3^- ions arranged in layers parallel to the bc face of the monoclinic cell. The average separation of the layers is 4.366 \AA ; this is greater than the interlayer spacing of 3.34 \AA found in the unsolvated orthorhombic tri-iodides but is similar to the spacing (4.3 \AA) between the layers of I_5^- anions in $(CH_3)_4NI_5$ (see Section 1 - 4 - 7). Not only does $KI_3 \cdot H_2O$ share this feature of a layered structure with the orthorhombic trihalides, but it also preserves the *en echelon* arrangement of anions within the layer common to these compounds. However, unlike CsI_3 , RbI_3 and NH_4I_3 , the cation in potassium tri-iodide is displaced out of the plane of the anionic groups, and is closely associated with a water molecule accommodated between the anion layers.



Section No:- 26 KIO₃ MONOHYDRATE

Scale is 1.379 inch:-1 Angstrom, contour interval- 50.00

Figure 6 - 9. The final Fourier synthesis - the iodine peaks have not been contoured to their full height, and all peaks have been projected onto the plane of the I_3^- unit. The contour interval is approximately $0.04e/A^3$.

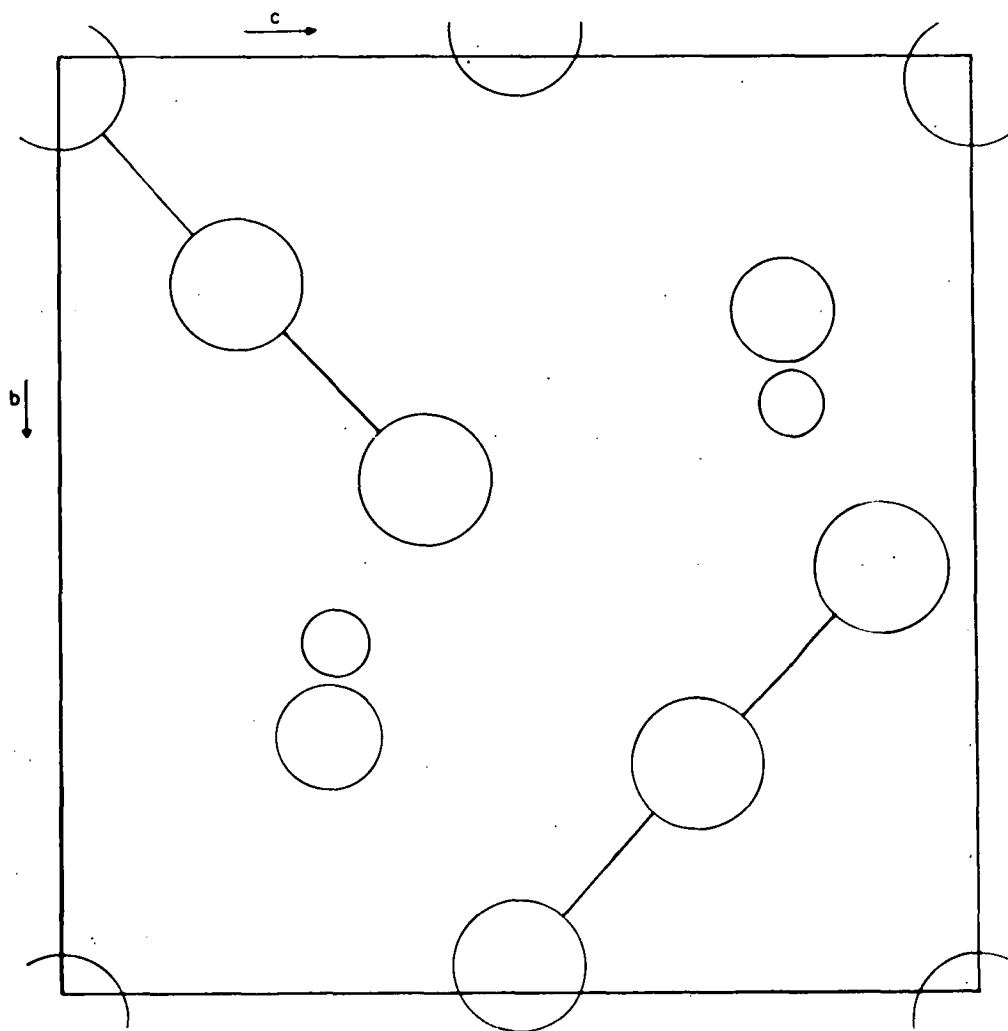


Figure 6 - 10. The unit cell contents of $\text{KI}_3 \cdot \text{H}_2\text{O}$ projected onto the I_3^- plane. The largest circles represent iodine atoms, the smallest circles represent the water oxygen atoms and the intermediate circles the potassium cations. Note the *en echelon* arrangement of the I_3^- groups.

The noncentrosymmetry of the $\text{KI}_3 \cdot \text{H}_2\text{O}$ cell arises because the *en echelon* arrangement of asymmetric I_3^- ions in a plane is not in itself a centrosymmetric structural motif, and the monoclinic cell contains only one such layer. Centrosymmetry is achieved in the orthorhombic trihalides based on this motif by the incorporation of two centrically related layers within the one cell; in potassium tri-iodide the anionic layers are related only by the *a*-translation of the monoclinic cell.

Although potassium tri-iodide crystallizes as a hydrate and possesses a unit cell symmetry different from that of both the unsolvated caesium and rubidium tri-iodides, the values found for the I_3^- bond lengths and interbond angle in the potassium compound appear to substantiate the view foreshadowed in Sections 4 - 4 and 5 - 4 that there is a discernible trend in anion geometry in passing from CsI_3 through RbI_3 to $\text{KI}_3 \cdot \text{H}_2\text{O}$, and that NH_4I_3 stands a little apart from this trend. A detailed comparison of the configuration of the I_3^- ion in the simple tri-iodides will be undertaken in Chapter 7; it is sufficient here to note the trend in the length of the longer iodine-iodine bond from a value of 3.040 Å in CsI_3 , 3.016 Å in RbI_3 to 2.895 Å in $\text{KI}_3 \cdot \text{H}_2\text{O}$. These lengths should be compared with the value of 3.112 Å found for the long I_3^- bond of NH_4I_3 . The interbond angles show a similar trend: for the alkali metal tri-iodides the departure of the anion from a completely linear geometry is 2.0°, 2.6° and 4.65° for caesium, rubidium and potassium respectively. Again, these angles should be compared with the value of 1.4° found in the NH_4I_3 case.

Of all the atomic positions determined for this structure, the greatest uncertainty is associated with that of the oxygen atom. The two shortest potassium-oxygen distances calculated from this position are given in Table 6 - 5; as the positional parameters of the oxygen atom were not refined by the least-squares process, the estimated standard deviations for these separations presented in that Table must

Table 6 - 4

Fractional positional parameters and isotropic temperature factors for

 $\text{KI}_3 \cdot \text{H}_2\text{O}$ at -50°C

Atm.	x	y	z	B
I(1)	0.000000	0.030293±0.000102	0.000000	1.2385±0.0255
I(2)	0.013647±0.000779	0.241151±0.000118	0.200493±0.000200	1.3372±0.0222
I(3)	0.075988±0.000589	0.448081±0.000119	0.398137±0.000170	1.8741±0.0288
K	0.847523±0.001889	0.730817±0.000389	0.272830±0.000490	1.8953±0.0317
O	0.4218	0.6228	0.3825	3.0

be regarded as underestimates. This comes about because the error calculation performed by the BOND LENGTHS AND ANGLES (X26) program will only, for these particular interatomic distances, include contributions from the least-squares matrix inverse due to uncertainties in the position of the potassium atom. It is estimated that the e.s.d.'s should be multiplied by three or four to obtain a measure of the reliability of these K-O separations. Even so, the calculated potassium-oxygen distances, namely 2.744 and 2.885 Å, are not unreasonable, as K-O distances in the range 2.74 - 3.02 Å are commonly reported for structures containing hydrated K^+ ions (Brown and Weiss [1969, 1970]).

The only other hydrated polyhalide which has been the subject of a full structural analysis is $KICl_4 \cdot H_2O$ (Mooney [1937]; Elema, de Boer and Vos [1963]). Unlike the trihalides, this compound does not develop a layer structure; however, the relationship between the potassium cation and its neighbouring water molecules in $KICl_4 \cdot H_2O$ is very similar to that in $KI_3 \cdot H_2O$. In particular, the two short K-O distances in the tetrachloro-iodate (2.74, 2.79 Å) compare reasonably well with those found in the tri-iodide. The water molecule in the tri-iodide structure is evidently forced to occupy the interlayer region, as the quadrilateral, defined by four adjacent I_3^- ions, which accommodates the cation at its centre in CsI_3 , RbI_3 and NH_4I_3 is too small to allow both the cation and its associated water molecule to occupy this space together, and at the same time remain in the anionic plane. The presence of the water molecule between the I_3^- layers accounts for the larger interlayer spacing in $KI_3 \cdot H_2O$, and undoubtedly also has an influence on the stability of this compound. The nature of this influence will be explored in further detail in Chapter 7, Section 7 - 4; however it should be noted that one of the objectives of this study was the investigation of the role performed by the water molecule in this structure. The evidence suggests that this role is primarily one of cation hydration,

Table 6 - 5

Chemically significant interatomic distances and angles for
 $\text{KI}_3 \cdot \text{H}_2\text{O}$ at -50°C

I(1) - I(2)	$2.8951 \pm 0.0021 \text{ \AA}$
I(2) - I(3)	2.7901 ± 0.0023
I(1) - I(3)	5.6805 ± 0.0016
I(1)...I(2)	4.0617 ± 0.0024
I(3)...I(2)	4.4423 ± 0.0033
I.....K	3.4281 ± 0.0036
I.....O	3.4323 ± 0.0023
K.....O	$2.7440 \pm 0.0113, 2.8855 \pm 0.0119$
I(1) - I(2) - I(3)	$175.35 \pm 0.0637^\circ$
O - K - O*	$119.87 \pm 0.174^\circ$

and this conclusion is supported by comparison with other crystalline monohydrates known to contain water molecules coordinated about the cation.

In a recent paper Ferraris and Franchini-Angela [1972] have developed a general classification of water molecules in crystalline hydrates. This classification takes into account the geometry of the water molecule and its environment and is based on a survey of more than forty crystalline hydrates studied by the neutron diffraction technique; it represents an extension of an earlier system of classification advanced by Chidambaram, Sequeira and Sikka [1964]. The water molecule in $\text{KI}_3 \cdot \text{H}_2\text{O}$ (and perhaps also that in $\text{KICl}_4 \cdot \text{H}_2\text{O}$) evidently falls into Class 2, Type A of the Ferraris and Franchini-Angela classification. In this Class each water molecule of the hydrate coordinates two cations, and these are located in the lone-pair orbital directions of the water molecule; the Type A subgroup of this class includes only those hydrates in which both cations are monovalent. The cation- H_2O -cation angle (ϵ) for the fifteen hydrates placed in this subgroup by Ferraris and Franchini-Angela ranges from 79° to 135° . In most of these hydrates the cation is sodium for which the 'tetrahedral' angle ϵ ranges from 81° - 111° , with an average value of 93° . It would appear that the ranges for K^+ and Li^+ substantially overlap that of sodium with average values for ϵ above and below the Na^+ value respectively. The ϵ value of 119° calculated from the atomic positions in $\text{KI}_3 \cdot \text{H}_2\text{O}$ is therefore well within the expected range for coordinated water in this environment.

The structural analysis of $\text{KI}_3 \cdot \text{H}_2\text{O}$ has revealed that this compound is structurally related to the unsolvated monovalent tri-iodides, sharing with them a major structural motif in the arrangement of I_3^- ions within anionic layers; the major point of difference being the incorporation of

the water molecule coordinated to the cation between these layers.

It is worthwhile considering the bearing these findings have upon the possible structures of the known hydrated potassium polyiodides.

Without a body of structural analyses for a number of hepta-iodides to be used as a basis for comparison, it is difficult to advance any preferred models for the structure of $\text{KI}_7 \cdot \text{H}_2\text{O}$; however, the situation is a little better in the case of potassium tri-iodide hydrate. If the structural features of $\text{KI}_3 \cdot \text{H}_2\text{O}$ persist in $\text{KI}_3 \cdot 2\text{H}_2\text{O}$, it is possible to develop in broad outline a structural model which can account for the presence of the α - and β -modifications of this compound found by Briggs *et alii* [1940]. If the two water molecules are accommodated between the anionic layers as in $\text{KI}_3 \cdot \text{H}_2\text{O}$, it is probable that the interlayer spacing in $\text{KI}_3 \cdot 2\text{H}_2\text{O}$ is even greater than that of the monohydrate. At large interlayer spacings different arrangements of the anionic layers relative to one another would be distinguished by smaller energy differences than would prevail when the layers are close together and interactions between them correspondingly greater. This smoothing out of the energy differences between alternative arrangements of the I_3^- layers is presumably responsible for the existence near room temperature of two crystalline modifications of $(\text{C}_2\text{H}_5)_4\text{NI}_3$, as the interlayer spacing in this compound is of the order of 7 Å. The presence of disorder in $(\text{CH}_3)_4\text{NI}_3$ (Migchelsen and Vos [1967]) can probably be ascribed to the same cause. Potassium tri-iodide dihydrate therefore probably has a structure consisting of I_3^- anions arranged in layers in the familiar *en echelon* pattern, with the K^+ ion at or near the position it occupies in $\text{KI}_3 \cdot \text{H}_2\text{O}$. The two water molecules would occupy the interlayer space giving the compound a large interlayer spacing and consequently a rather open structure. The two modifications of the dihydrate probably crystallize in the same crystal system, their structures differing in the relative arrangement of the anionic layers.

TABLE 6 - 6

PART 1

F(OBS), F(CALC) FOR POTASSIUM TRI-IODIDE MONOHYDRATE
(UNOBSERVED REFLECTIONS MARKED *)

H	K	L	F0	K*FC	H	K	L	F0	K*FC
H= 0, K= 0					0	4	-4	425	469
0	0	2	200	294	0	4	-3	315	280
0	0	4	627	563	0	4	-2	196	168
0	0	6	459	440	0	4	-1	650	665
H= 0, K= 1					0	4	0	894	847
0	1	-1	456	407	0	4	1	708	665
0	1	0	45	27*	0	4	2	215	168
0	1	1	505	407	0	4	3	287	280
0	1	2	601	577	0	4	4	431	469
0	1	3	252	292	0	4	5	45	103*
0	1	4	702	701	0	4	6	325	288
0	1	5	574	541	0	4	8	45	46*
0	1	6	524	532	H= 0, K= 5				
0	1	7	239	228	0	5	-5	803	794
0	1	8	258	231	0	5	-4	216	176
0	1	9	241	250	0	5	-3	142	218
H= 0, K= 2					0	5	-2	235	189
0	2	-3	324	250	0	5	-1	452	479
0	2	-2	1060	1134	0	5	0	321	295
0	2	-1	484	364	0	5	1	471	479
0	2	0	241	188	0	5	2	206	189
0	2	1	439	364	0	5	3	176	218
0	2	2	997	1134	0	5	4	186	176
0	2	3	341	250	0	5	6	246	206
0	2	4	183	163	0	5	7	45	56*
0	2	5	45	21*	0	5	8	45	84*
0	2	6	156	108	H= 0, K= 6				
0	2	7	209	136	0	6	-6	221	252
0	2	8	464	481	0	6	-4	228	276
H= 0, K= 3					0	6	-3	388	383
0	3	-7	501	544	0	6	-2	434	403
0	3	-6	323	340	0	6	-1	572	570
0	3	-5	45	64*	0	6	0	364	353
0	3	-4	539	463	0	6	1	586	570
0	3	-3	770	747	0	6	2	442	403
0	3	-2	351	321	0	6	3	403	383
0	3	-1	145	193	0	6	4	293	276
0	3	0	45	152*	0	6	5	45	81*
0	3	1	179	193	0	6	6	256	252
0	3	2	398	321	0	6	7	222	231
0	3	4	511	463	H= 0, K= 7				
0	3	5	45	64*	0	7	-3	628	622
0	3	6	346	340	0	7	-2	251	268
0	3	7	550	544	0	7	-1	45	75*
0	3	8	187	194	0	7	1	45	75*
H= 0, K= 4					0	7	2	301	268
0	4	-6	236	288	0	7	3	590	622
0	4	-5	45	103*	0	7	4	45	55*
					0	7	6	45	94*
					0	7	7	400	450

TABLE 6 - 6

PART 2

F[OBS], F[ALC] FOR POTASSIUM TRI-IODIDE MONOHYDRATE
(UNOBSERVED REFLECTIONS MARKED *)

H	K	L	FO	K*FC	H	K	L	FO	K*FC
					1	2	-4	194	234
	H= 0,	K= 8			1	2	-3	173	262
0	8	-3	248	270	1	2	-2	969	908
0	8	-2	371	394	1	2	-1	307	402
0	8	-1	412	401	1	2	1	465	476
0	8	0	106	98	1	2	2	1161	1150
0	8	1	425	401	1	2	3	343	293
0	8	2	384	394	1	2	4	175	121
0	8	3	342	270	1	2	5	96	32
0	8	4	222	249	1	2	7	116	101
0	8	5	45	66*	1	2	8	364	382
0	8	8	217	209					
	H= 0,	K= 9				H= 1,	K= 3		
0	9	-1	312	328	1	3	-5	110	127
0	9	0	220	223	1	3	-4	493	549
0	9	1	314	328	1	3	-3	996	1022
0	9	3	45	88*	1	3	-2	480	454
0	9	4	271	271	1	3	0	248	154
0	9	5	389	395	1	3	3	592	581
	H= 0,	K= 10			1	3	4	351	417
0	10	-1	192	258	1	3	5	225	153
0	10	0	384	440	1	3	6	330	316
0	10	1	234	258	1	3	7	423	501
0	10	2	104	82	1	3	8	217	216
0	10	4	204	220					
	H= 0,	K= 11				H= 1,	K= 4		
0	11	2	205	204	1	4	-3	243	182
	H= 1,	K= 0			1	4	-2	92	36
1	0	0	228	304	1	4	-1	665	634
1	0	10	355	392	1	4	0	801	863
	H= 1,	K= 1			1	4	1	671	580
1	1	-7	257	268	1	4	2	85	149
1	1	-6	503	490	1	4	4	552	491
1	1	-4	769	759	1	4	5	182	165
1	1	-3	353	333	1	4	6	295	288
1	1	-2	686	712	1	4	8	45	88*
1	1	-1	650	616	1	4	9	198	212
1	1	0	267	247	1	4	10	210	241
1	1	2	305	276					
1	1	3	120	145		H= 1,	K= 5		
1	1	4	591	529	1	5	-2	170	182
1	1	5	410	430	1	5	-1	675	704
1	1	6	503	503	1	5	0	262	283
1	1	7	163	170	1	5	1	294	299
1	1	8	226	272	1	5	3	221	139
1	1	9	268	248	1	5	4	158	177
	H= 1,	K= 2			1	5	5	693	645
1	2	-6	95	69	1	5	6	166	173
					1	5	7	45	118*
					1	5	8	45	49*
					1	5	9	321	300
						H= 1,	K= 6		
					1	6	-2	405	410

TABLE 6 - 6

PART 3

F(ORS), F(CALC) FOR POTASSIUM TRI-IODIDE MONOHYDRATE
(UNOBSERVED REFLECTIONS MARKED *)

H	K	L	FO	K*FC	H	K	L	FO	K*FC
1	6	-1	467	407	2	1	0	224	247
1	6	0	289	317	2	1	1	293	264
1	6	1	629	629	2	1	2	45	93*
1	6	2	366	360	2	1	7	110	79
1	6	3	478	395	2	1	8	240	195
1	6	4	391	319	2	1	9	225	161
1	6	5	104	141					
1	6	6	277	263		H= 2,	K= 2		
1	6	7	132	109	2	2	-2	435	453
1	6	8	198	166	2	2	-1	178	183
					2	2	0	243	264
	H= 1,	K= 7			2	2	1	249	306
1	7	-1	112	76	2	2	2	625	704
1	7	0	190	169	2	2	3	122	200
1	7	1	271	213	2	2	4	143	117
1	7	2	249	269	2	2	5	86	94
1	7	3	483	476	2	2	6	298	234
1	7	4	118	55	2	2	7	45	51*
1	7	5	214	170	2	2	8	287	234
1	7	6	130	114	2	2	9	45	76*
1	7	7	393	431					
						H= 2,	K= 3		
	H= 1,	K= 8			2	3	-1	45	60*
1	8	-1	397	410	2	3	1	323	360
1	8	0	169	121	2	3	2	204	120
1	8	1	327	356	2	3	4	210	203
1	8	2	393	440	2	3	5	98	107
1	8	3	402	345	2	3	6	237	211
1	8	4	178	212	2	3	7	366	303
1	8	5	132	84	2	3	8	179	168
1	8	6	194	188	2	3	9	45	41*
	H= 1,	K= 9				H= 2,	K= 4		
1	9	-1	356	382	2	4	0	424	455
1	9	1	283	288	2	4	1	330	357
1	9	2	128	126	2	4	2	169	155
1	9	3	130	107	2	4	3	336	341
1	9	4	232	238	2	4	4	516	369
1	9	5	342	363	2	4	5	145	133
					2	4	6	221	183
	H= 1,	K= 10			2	4	7	45	51*
1	10	0	372	419	2	4	8	45	79*
1	10	1	234	269					
1	10	5	190	263		H= 2,	K= 5		
					2	5	1	169	184
	H= 2,	K= 0			2	5	2	94	80
2	0	4	542	546	2	5	3	45	23*
2	0	6	190	180	2	5	4	204	125
2	0	8	45	32*	2	5	5	435	377
2	0	10	342	238	2	5	6	116	101
					2	5	7	124	114
	H= 2,	K= 1			2	5	8	45	38*
2	1	-2	514	535	2	5	9	199	204
2	1	-1	494	542					

TABLE 6 - 6

PART 4

F(OBS), F(CALC) FOR POTASSIUM TRI-IODIDE MONOHYDRATE
(UNOBSERVED REFLECTIONS MARKED *)

H	K	L	F0	K*FC	H	K	L	F0	K*FC
H= 2, K= 6									
2	6	1	379	434					
2	6	2	230	215					
2	6	3	334	252					
2	6	4	270	232					
2	6	6	245	170					
2	6	7	45	44*					
H= 2, K= 7									
2	7	1	157	235					
2	7	2	157	223					
2	7	3	312	286					
2	7	4	45	71*					
2	7	5	45	106*					
2	7	6	128	75					
2	7	7	302	272					
H= 2, K= 8									
2	8	3	211	280					
2	8	4	45	76*					

Chapter 7 - Discussion

	page
7 - 1 Introduction	202
7 - 2 Covalent Interactions	202
7 - 2 - 1 The symmetric I_3^- case	204
7 - 2 - 2 The asymmetric I_3^- case	206
7 - 3 The Crystal Field Approach	209
7 - 4 The Infrared/Raman data	223
7 - 5 The Potassium Tri-iodide case	228
7 - 6 Extension to other polyiodides	231
7 - 6 - 1 The anion-anion interaction	232
7 - 6 - 2 The solvate-anion interactions	236
7 - 6 - 3 The cation-solvate interaction	245
7 - 6 - 4 Solvate-solvate and mixed interactions	251
7 - 7 Summary	252

7 - 1 Introduction

In Chapter 1 of this work mention was made of the various bonding models advanced to describe trihalide bonding, the theories developed to account for the apparent sensitivity of the tri-iodide ion to its crystalline environment, and the eventual coalescence of these ideas in the crystal field/molecular orbital studies pioneered by Nunn [1964] and Brown and Nunn [1966] and subsequently extended by Migchelsen and Vos [1967]. In that Chapter the comment was also made that the relative arrangement of I_3^- ions in CsI_3 and NH_4I_3 was reminiscent of the arrangement of iodine molecules in crystalline iodine. These points will now be re-examined in some detail in the light of the structural data accumulated in the course of this study, paying particular attention to their relevance to the hydrated tri-iodide $KI_3 \cdot H_2O$. A necessary part of this examination is an evaluation of the applicability of crystal field theory to the tri-iodide case, in view of the criticisms which have been directed at this theory in the field of transition metal chemistry. In the discussion which follows considerable reference will be made to the structural data for the tri-iodides which is summarized in Section 4 of Chapter 1, and to the new data presented in Chapters 4, 5 and 6.

7 - 2 Covalent interactions

The straightforward application of crystal field theory has been shown to be inadequate in the field of transition metal chemistry, as it takes no account of the partially covalent nature of the interactions between the central metal and its surrounding ligands. Another inadequacy is that crystal field theory treats the ligand atoms as point charges and not as extended electronic systems of a size and complexity comparable with the central metal (Cotton and Wilkinson [1972]). The

tri-iodide anion is made up of atoms with very extended electron clouds, and in a tri-iodide such as CsI_3 the electronic system of the cation is of comparable size. It might be expected as a consequence that the crystal field approach would provide an even more inadequate basis for a theoretical understanding of the bond-length variation and stability of tri-iodide anions than it does for explaining metal-ligand interactions in transition metal complexes, and that the true explanation of the observed variation in geometry and stability of I_3^- ions is to be sought in covalent interactions between the extended electronic clouds of the anion and the cation.

It should be noted at the outset that in the case of transition metal complexes the crystal field usually employed is a *local* one, involving only point charges at the ligand sites, whereas the crystal field considered in the tri-iodide case is a lattice field generated by appropriate point charges placed at all the atomic sites in the crystal. In the latter case the field is more properly termed a crystal field, and in the theoretical studies already mentioned (Nunn [1964], Brown and Nunn [1966], Migchelsen and Vos [1967]) it was necessary to resort to special numerical techniques (i.e. Ewald's method for lattice sums (Ewald [1921])) for its evaluation. None the less, as the nearest neighbour charges make a significant contribution to the final value of the crystal field, it may prove necessary to give some attention to the possibility that mechanisms other than simple electrostatic interactions may be responsible for the observed variations in bond length among tri-iodide ions.

This hypothesis can be tested by considering the case of the two crystalline modifications of tetraethylammonium tri-iodide ($\text{C}_4\text{H}_{10}\text{N}^+\text{I}_3^-$, Chapter 1, Section 1 - 4 - 3). As alkyl groups are substituted for the ammonium hydrogen atoms there will be little delocalization of positive charge

over the hydrocarbon chains, and the cation in these compounds will be a good approximation to a point positive charge. In this case we cannot expect significant covalent cation-anion interactions, yet modification II of $(C_2H_5)_4NI_3$ contains two crystallographically distinct asymmetric tri-iodide ions of different geometry. Even so, the same compound presents certain difficulties for the crystal field approach, as modification I of $(C_2H_5)_4NI_3$ contains two distinct symmetric tri-iodide ions which have significantly different bond lengths.

7 - 2 - 1 The symmetric I_3^- case

The crystal field-variable electronegativity self-consistent field (CF-VESCF) molecular orbital calculations of Migchelsen and Vos [1967] indicate that these anions experience a symmetric crystal field, and it is known from model calculations performed by Wiebenga and Kracht [1969] that the bond order and hence the bond distance is not affected by symmetric fields. Runsink *et alii* [1972] suggest that the only remaining mechanism which can be invoked to explain the bond-length variation in this case is covalent anion-anion interaction between neighbouring I_3^- ions. Although the distances involved are large ($> 4.0 \text{ \AA}$), it can be seen from Figure 7 - 1, in which the 5p-sigma overlap integral calculated for Slater-type iodine 5p orbitals (see Appendix D) is plotted as a function of internuclear separation, that even at 5.0 \AA there is some overlap between the $5p_z$ orbitals.

If this mechanism does in fact account for the variation of the bond lengths of the symmetric anions in $(C_2H_5)_4NI_3 - I$, then the bond lengths should show some dependence on the value of the overlap integral at the anion-anion separation in question. In Table 7 - 1 the value of $S_{5p\sigma}$ at this separation is given together with the I_3^- bond length, the overlap integral values being taken from the same calculation used to prepare Figure 7 - 1. The Table includes a zero value for $S_{5p\sigma}$ between I_3^- ions

Table 7 - 1

Sp_o overlap integral for anion-anion separations
in tri-iodides with symmetrical I₃⁻ ions

Compound	Bond Length (A°)	Anion-Anion Separation (A°)	Overlap integral S _{5pσ}
(C ₂ H ₅) ₄ NI ₃ -IB*	2.943	4.14 ^a	0.0408
(C ₂ H ₅) ₄ NI ₃ -IA	2.928	4.72 ^a	0.0136
(C ₆ H ₅) ₄ AsI ₃	2.920	>5.0 ^b	0.0

* Two independent ions

^a Migchelson and Vos [1967]

^b Mooney-Slater [1958]

in tetraphenylarsonium tri-iodide, as the symmetric anions in this compound are well separated and may be regarded as being completely isolated from each other. The data presented in Table 7 - 1 are plotted in Figure 7 - 2 and it can be seen that the relationship between the bond length and anion-anion $5p\sigma$ overlap integral is linear. The data is too sparse for this to be more than indicative of the form of the relationship; confirmation must await either structural analysis of more tri-iodides containing symmetrical I_3^- ions in the *en echelon* arrangement, or information from some other independent line of evidence.

Although the possibility of covalent cation-anion interactions in the tetraethylammonium tri-iodides can be reasonably discounted, there is the possibility that anion-anion interactions are responsible not only for the bond-length variation among the symmetric anions for which crystal field effects cannot be responsible, but also for the variation observed among the asymmetric I_3^- ions.

7 - 2 - 2 The asymmetric I_3^- case

Modification II of $(C_2H_5)_4NI_3$, and the tri-iodides of caesium, rubidium, potassium and the ammonium ion all possess the *en echelon* arrangement of asymmetric I_3^- ions which makes it possible for the bonding p -orbital of the terminal atom of one anion to overlap the non-bonding p -orbital of the central atom of the other. In each case one anion is asymmetrically disposed between the two lying perpendicular to it, so that one terminal atom is closer to the central atom of the neighbouring anion than is the terminal atom at the other end of the ion (see Figure 7 - 3). In modification I of $(C_2H_5)_4NI_3$ the symmetric anions are symmetrically disposed between their neighbours.

If anion-anion interaction is the sole agent responsible for modify-

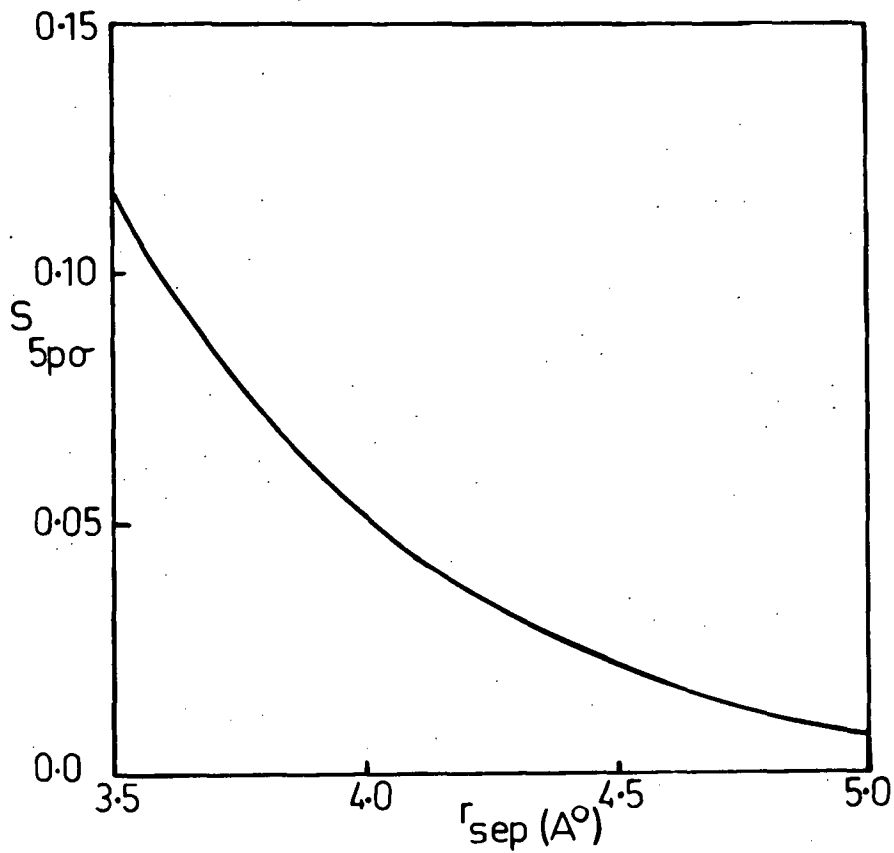


Figure 7 - 1. The $5p\sigma$ overlap integral as a function of internuclear separation $> 3.5 \text{ \AA}$.

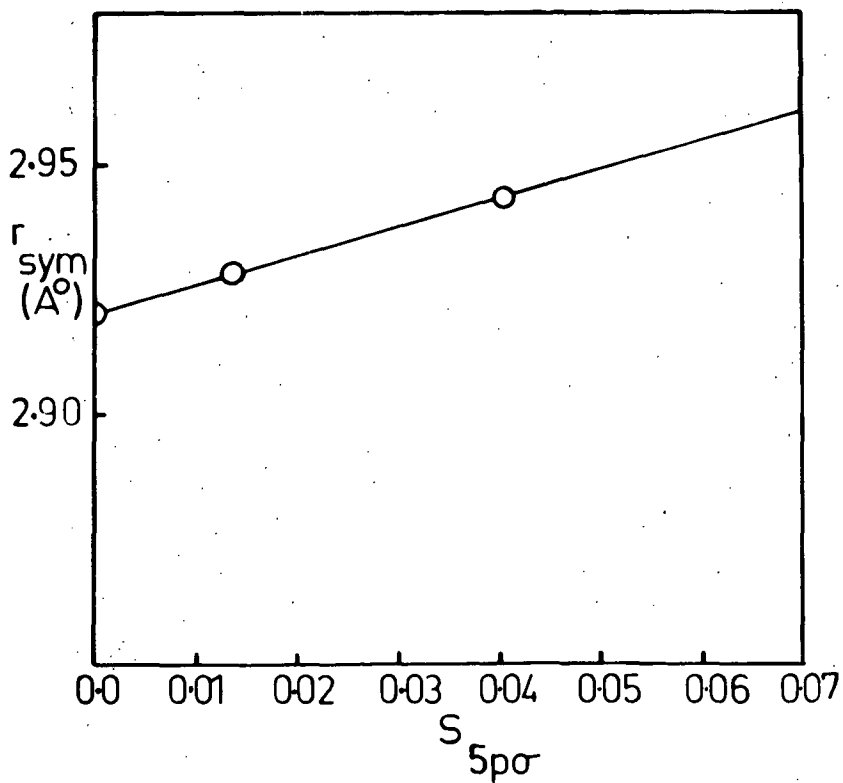


Figure 7 - 2. Bond length in symmetrical I_3^- as a function of $5p\sigma$ overlap.

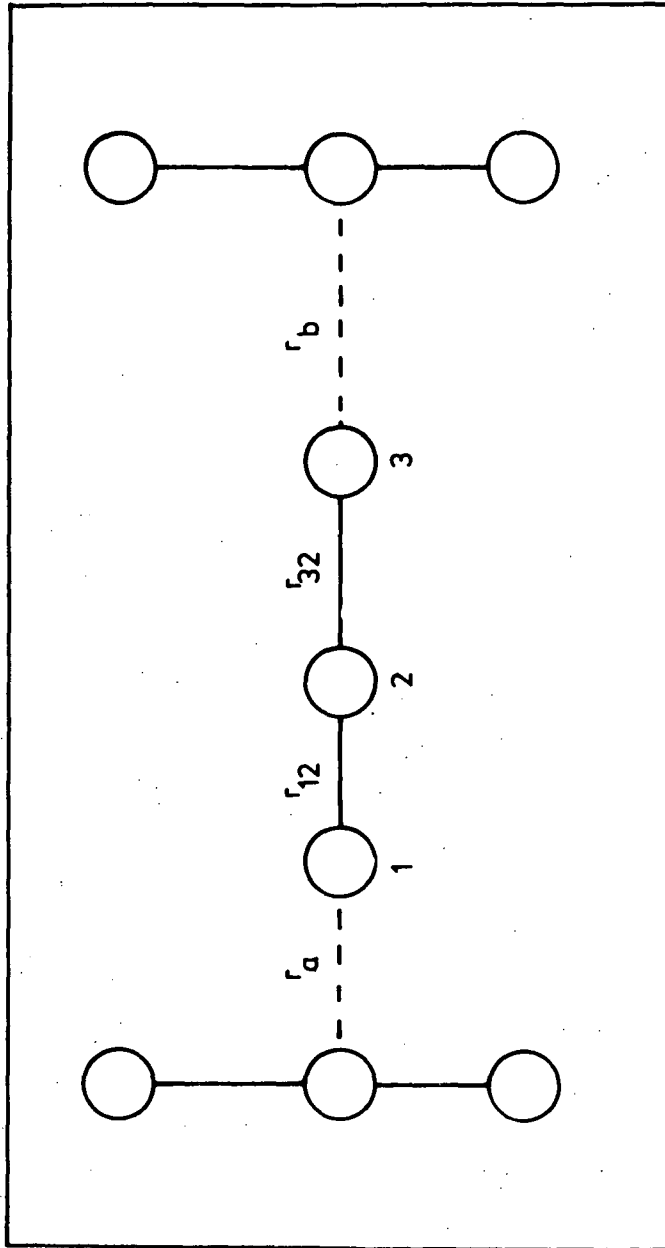


Figure 7 - 3. Typical relative arrangement of asymmetric I_3^- ions.

ing the length of the I-I bond, and if the functional relationship between bond length and p-orbital overlap is that suggested by the $r_{\text{sym}}/S_{5p\sigma}$ plot presented in Figure 7 - 2, then it might be expected that the longest bond of the asymmetric ion should be that linking the terminal atom which makes the closest approach to the central atom of the neighbouring anion. The inter-iodine distances for the relevant structures are given in Table 7 - 2, and these show that, in fact, in all cases precisely the opposite situation prevails.

This does not prove that anion-anion interactions do not occur between the I_3^- ions in those compounds which possess asymmetric anions, but it does show that some further agency operates in determining the observed bond-length variation, and further that this agency over-rides the effect of the anion-anion interaction to produce a resultant modification which is opposite in sense to that which would be generated by anion-anion overlap.

If it can be shown that the crystal field effects will produce bond-length changes of the right kind, and in particular if it can be demonstrated that the forces involved are of the right order of magnitude, then on the basis of the test case fortunately presented by modification II of $(\text{C}_2\text{H}_5)_4\text{NI}_3$, in which the cation is a good approximation to a point charge, the principle of Occam's Razor (Occam [1495]) will allow the hypothesis that cation-anion interaction is the responsible agency to be ruled out of consideration.

7 - 3 The Crystal Field Approach

The Migchelsen and Vos results for the CF-VESCF calculations performed for modification II of $(\text{C}_2\text{H}_5)_4\text{NI}_3$ and CsI_3 are presented in Table 7 - 3; the bond lengths for the asymmetric I_3^- ions of these compounds are given together with the potentials developed at the terminal

Table 7 - 2

Inter-iodine distances for structures containing
asymmetric I_3^- ions

(The atomic numbering is that of Figure 7-5)

Compound	$r_{12} (A^\circ)$	$I_1 \cdots I_2^+ (A^\circ)$	$r_{32} (A^\circ)$	$I_3 \cdots I_2$	Reference
$(C_2H_5)_4NI_3^-$ -IIA*	2.892	4.100	2.981	5.237	Migchelson and Vos [1967]
$(C_2H_5)_4NI_3^-$ -IIB	2.912	4.240	2.961	4.483	Migchelson and Vos [1967]
CsI_3	2.842	4.029	3.040	4.575	Runsink <i>et alii</i> [1972]
RbI_3	2.792	3.910	3.016	4.835	This work
NH_4I_3	2.802	3.880	3.112	4.842	This work
$KI_3 \cdot H_2O$	2.790	4.062	2.895	4.442	This work

* Two independent ions.

† $I \cdots I$ represents the shortest distance between a terminal iodine and the central iodine (I_2) of the nearest neighbouring anion.

Table 7 - 3

CF-VESCF results for asymmetric I_3^- ions

T. Migchelson and A. Vos [1967]

(The atomic numbering is that of Figure 7 - 5)

Compound	r_{12} (Å)	r_{32} (Å)	$V_1 - V_2$ (volts)	$V_3 - V_2$ (volts)
$(C_2H_5)_4NI_3^-$ -IIA*	2.892	2.981	0.022	0.379
$(C_2H_5)_4NI_3^-$ -IIB	2.912	2.961	0.072	0.174
CsI_3	2.830	3.040	-0.236	1.030

* Two independent ions

atoms with respect to the central atom by the self-consistent crystal field. In Figure 7 - 4 the bond lengths are plotted against these potential differences, and although the scatter of points about the least-squares line fitted to these data is considerable, there are some grounds for presuming that there is a systematic relationship between these quantities. Surprisingly, the underlying relationship appears to be linear; at first sight this is an unexpected result, as some nonlinearity due to interaction between the two I_3^- bonds might have been anticipated. However, this interaction has already been accounted for in the VESCF calculation performed to determine the charge distribution over the anion prior to carrying out the Ewald summation for the crystal field.

Before this possible systematic relationship can be investigated further, it is convenient to devise a parameter which expresses the asymmetry of the field over the anion in a manner which allows a more direct comparison of field asymmetries to be made than is possible by a consideration of the potential differences given in Table 7 - 3. Also, the examination of the symmetric anions carried out in the previous Section showed that anion-anion interactions were responsible for significant changes in the bond length of these ions. There is no *a priori* reason why such interactions may not also operate between asymmetric ions, and this effect should be taken into consideration when treating the effect of an asymmetric crystal field upon the triiodide bond lengths.

For this purpose the *crystal field asymmetry parameter*, α , is defined as follows in terms of the potential differences between the central and terminal iodine atoms. In the case of symmetric I_3^- ions the potentials developed by the crystal field between each terminal atom and the central atom are identical. Using the atomic numbering

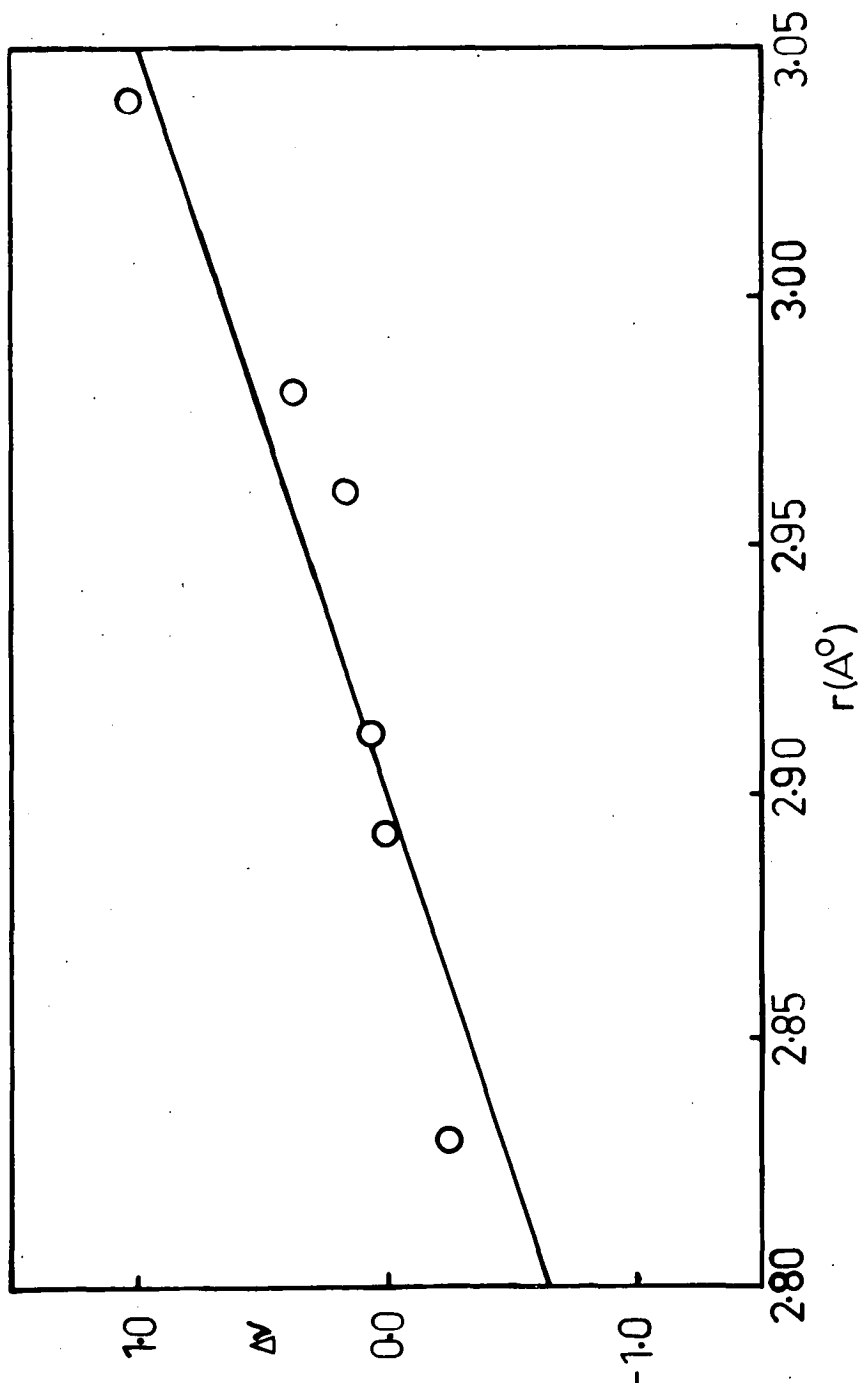


Figure 7 - 4. Potential difference between the terminal and central iodines as function of bond length.

given in Figure 7 - 5, this can be written

$$V_1 - V_2 = \Delta V_{12} = \Delta V_{32} = V_3 - V_2$$

For asymmetric anions an average potential difference, $\Delta V'$, is defined as the difference between the mean potential at the terminal iodines and the central iodine,

$$\Delta V' = \frac{1}{2} (V_1 + V_3) - V_2$$

In the symmetric case, as $V_1 = V_3$, it follows that

$$\Delta V' = \Delta V_{12} = \Delta V_{32}.$$

The asymmetry parameters for the potential differences between the terminal atoms and the central atom could be expressed in terms of the ratios

$$\alpha'_{12} = \Delta V_{12} / \Delta V'$$

and $\alpha'_{32} = \Delta V_{32} / \Delta V'$,

in which case, for asymmetric fields $\alpha'_{12} = \alpha'_{32} = 1.0$ and for asymmetric fields $\alpha'_{12} \neq \alpha'_{32} \neq 1.0$. As however it is more convenient if a symmetric crystal field is regarded as having asymmetry parameters of zero, a more workable set of parameters is defined by the relations

$$\alpha_{12} = \alpha'_{12} - 1 = (\Delta V_{12} / \Delta V') - 1$$

$$\alpha_{32} = \alpha'_{32} - 1 = (\Delta V_{32} / \Delta V') - 1$$

in which case, for a symmetric field $\alpha_{12} = \alpha_{32} = 0$, and for an asymmetric field $\alpha_{12} = -\alpha_{32} \neq 0.0$. Table 7 - 4 represents the data of Table 7 - 3 expressed in this form.

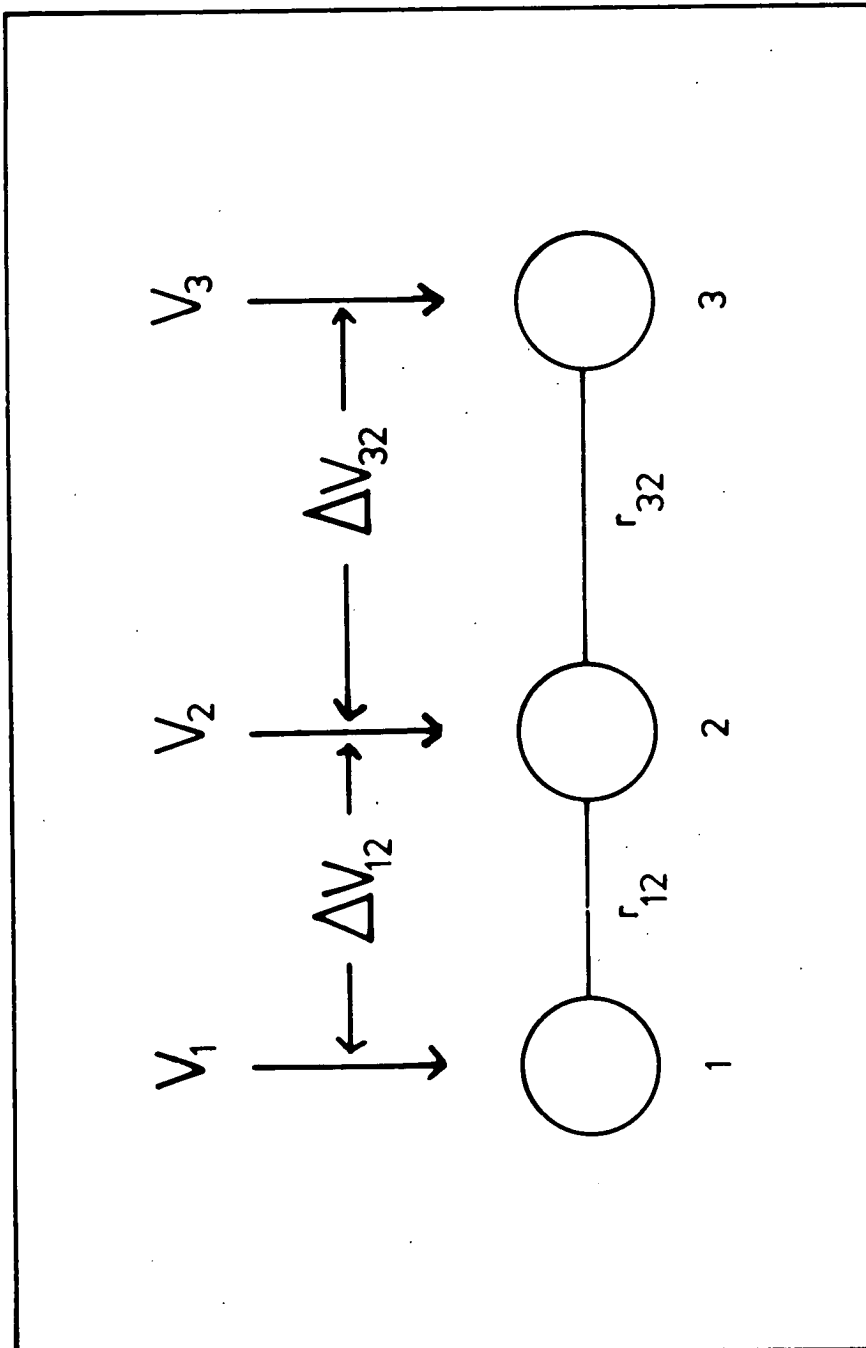


Figure 7 - 5. The bond and atom labels used in Section 7 - 3.

Table 7-4

Asymmetry parameters for three asymmetric I_3^- ions

(The atomic numbering is that of Figure 7-5)

Compound	$r_{12}(\text{\AA})$	$r_{32}(\text{\AA})$	ΔV_{12}	ΔV_{32}	ΔV^1	α_{12}	α_{32}
$(\text{C}_2\text{H}_5)_4\text{NI}_3^- \text{IIA}^*$	2.892	2.981	0.022	0.379	0.200_5	-0.890	0.890
$(\text{C}_2\text{H}_5)_4\text{NI}_3^- \text{IIB}$	2.912	2.961	0.072	0.174	0.123	-0.415	0.415
CsI_3	2.830	3.040	-0.236	1.030	0.379	-1.594	1.594

* Two independent ions

Turning now to the anion-anion effect; the linear relationship displayed in Figure 7 - 2 may be expressed by the equation

$$r_{aa} = r_{eq} + 0.5619 S$$

where r_{aa} is the bond length after extension by anion-anion interaction, r_{eq} is the bond length of the 'isolated' anion in $(C_6H_5)_4AsI_3$ and S is the value of the $5p\sigma$ iodine-iodine overlap integral at the anion separation in question. In conjunction with the data for asymmetric anion-anion separations given in Table 7 - 2, the theoretical geometries for these three anions due to anion-anion interactions alone may be calculated; the results of these calculations are given in Table 7 - 5. Assuming that the crystal field effect accounts for the difference, Δr , between the observed bond lengths and the theoretical bond lengths resulting from anion-anion interaction, and further that the relationship between bond length change and field asymmetry is approximately linear, as is suggested by Figure 7 - 4, then a plot of Δr against α should be a straight line. The available values of Δr and α are collected in Table 7 - 6 and the plot is presented in Figure 7 - 6. From this Figure it can be seen that the bond length change exhibits a linear dependence upon the field asymmetry parameter. The linearity of the dependence is remarkable in view of the approximations involved in the CF-VESCF calculations from which the interatomic potentials have been derived. Not only is the form of the relationship as anticipated, but also the bond length changes are of the right kind in that large changes are associated with large $|\alpha|$.

It is thus possible to form a general equation for the tri-iodide bond length in the *en echelon* environment which incorporates both the anion-anion effect and the field asymmetry effect, namely

$$r = r_{eq} + \Delta r = r_{eq} + 0.5619 S \pm 0.0666 |\alpha|;$$

Table 7-5

Theoretical asymmetric I_3^- geometries due to
anion-anion interaction

(The atomic numbering is that of Figure 7-5)

Compound	$r_{12} (A^\circ)$	$r_{32} (A^\circ)$
$(C_2H_5)_4NI_3^-$ -IIA *	2.945	2.923
$(C_2H_5)_4NI_3^-$ -IIB	2.939	2.932
CsI_3	2.948	2.930

* Two independent ions

Table 7-6

Bond Length differences and asymmetry parameters

Compound	$r_{12}(\text{\AA})^\dagger$	α_{12}	$\Delta r_{32}(\text{\AA})$	α_{32}
$(\text{C}_2\text{H}_5)_4\text{NI}_3\text{-IIA}^*$	-0.053	-0.890	0.058	0.890
$(\text{C}_2\text{H}_5)_4\text{NI}_3\text{-IIB}$	-0.027	-0.415	0.029	0.415
CsI_3	-0.106	-1.594	0.110	1.594

$^\dagger \Delta r_{12} = r_{12}(\text{observed}) - r_{12}(\text{theoretical})$

* Two distinct anions

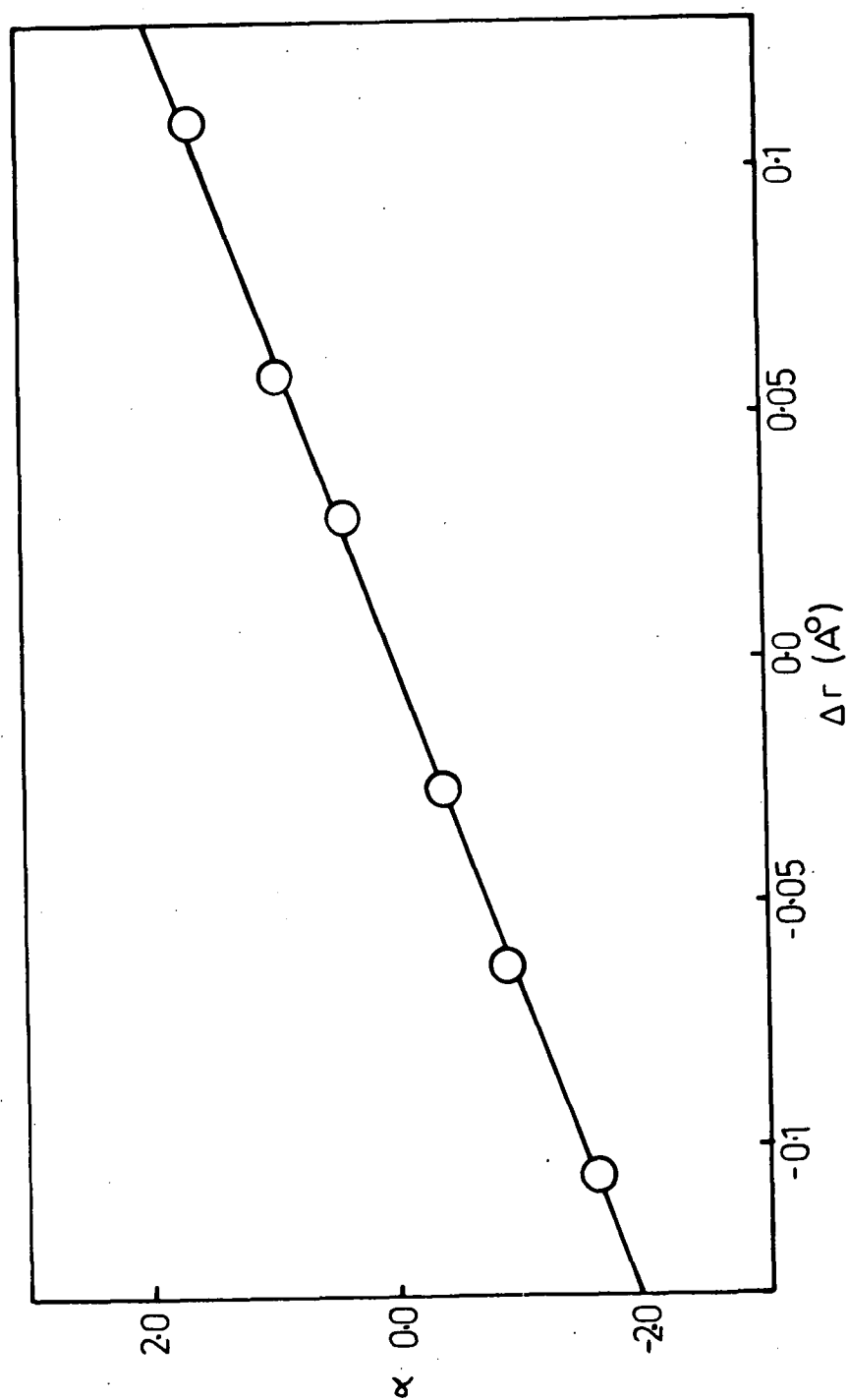


Figure 7 - 6. The relationship between field asymmetry parameter (α) and (Δr) the difference between the observed and theoretical bond lengths.

this equation has two solutions for the asymmetric field case, and only one for the symmetric field case when α vanishes. It should be noted that nothing can be predicted about the validity of this relationship for I_3^- environments other than the *en echelon* arrangement found in the tri-iodides discussed here.

This analysis would suggest that in this situation the tri-iodide bonds behave as if they followed Hooke's Law, the geometry of the 'isolated' ion being deformed by an amount which is linearly dependent upon the deforming forces. The Hooke's Law behaviour of interatomic bonds is an assumption more usually encountered in the context of the analysis of molecular vibrations. In this case it should be emphasised that the analysis of the bond length changes has not been carried out in terms of deforming forces, but rather in terms of quantities (S , α) which themselves seem to be linearly related to these forces. The presence of two force constants in the general equation derived above is explained if the forces have quantitatively different dependence on S and α .

A model of the I_3^- ion in which the bonds obey Hooke's Law suggests that Δr_{12} , Δr_{32} , the differences between the observed tri-iodide bond lengths and that found in the 'isolated' anion, may be used as coordinates which would determine the position of the anion in a two-dimensional strain domain. Such a map would provide a fresh perspective on the question of the relationships among the tri-iodides under discussion. In Figure 7 - 7 the values of Δr_{12} , Δr_{32} for $(C_6H_5)_4AsI_3$, $(C_2H_5)_4NI_3$, CSI_3 , RbI_3 , NH_4I_3 and $KI_3 \cdot H_2O$ have been used to prepare such a map. Detailed consideration of this diagram will be made below, but some points may be mentioned here; the anion in RbI_3 is strained to an extent intermediate between that of the $KI_3 \cdot H_2O$ anion and that of NH_4I_3 , similarly, CSI_3 falls between the most strained $(C_2H_5)_4NI_3$ anion

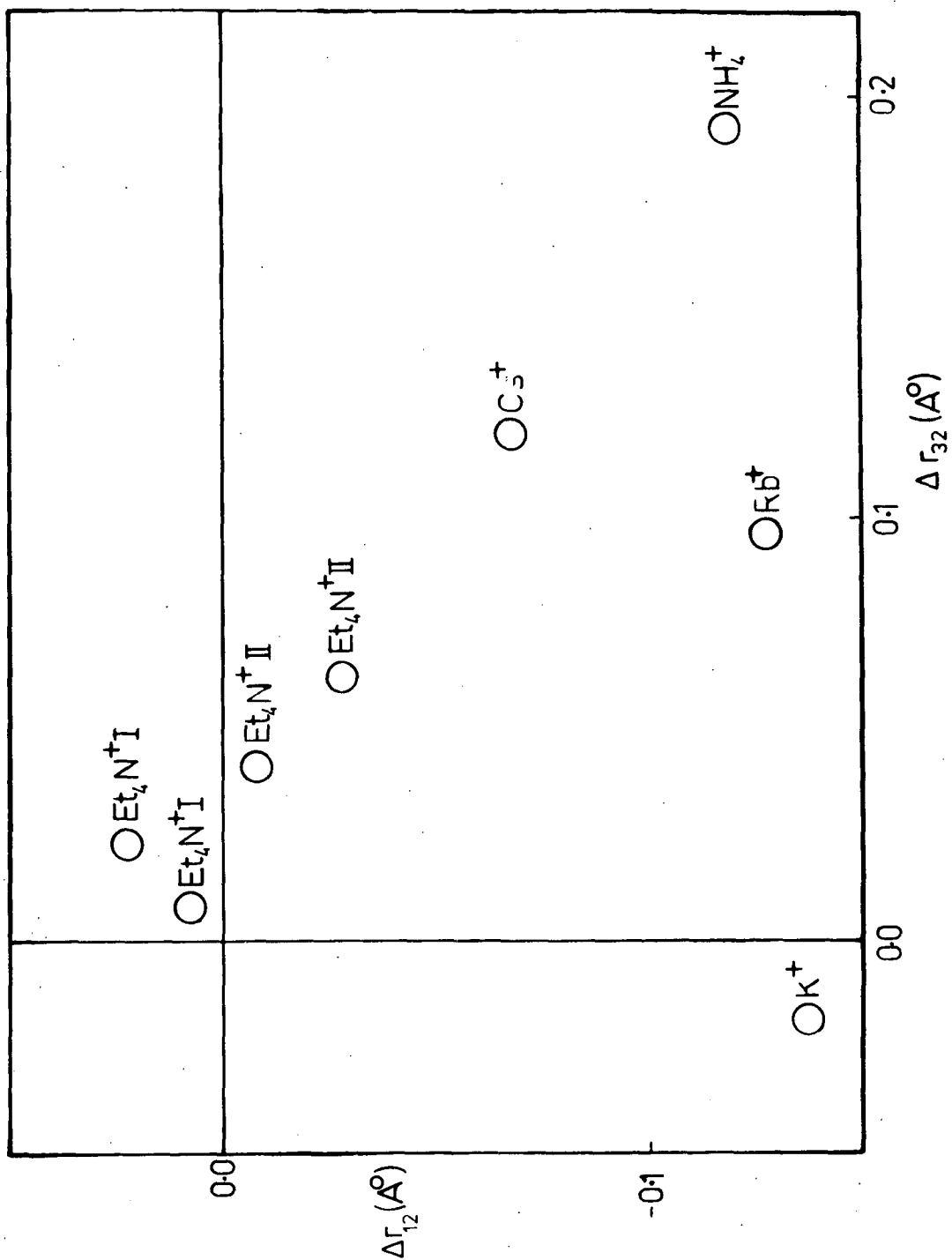


Figure 7 - 7. The positions of the tri-iodides in the strain domain as mapped by Δr_{12} , Δr_{23} . The position of the tri-iodide $(\text{C}_6\text{H}_5)\text{AsI}_3$ is represented by the point 0,0.

and NH_4I_3 . Also, if distance from the point representing $(\text{C}_6\text{H}_5)_4\text{AsI}_3$ can be roughly correlated with stability, the point for $\text{KI}_3 \cdot \text{H}_2\text{O}$ would be expected to be more remote from this point than that for the more stable ammonium tri-iodide.

The analysis presented here is suggestive, but it rests upon a very small number of cases. Before it can be seriously used as an aid to interpretation and understanding it should be supported by more data. In this connection, it is unlikely that further crystallographic work will do more than extend the number of known symmetrical I_3^- ions, as the lighter alkali polyiodides probably contain anionic groups which are more complex than the simple tri-iodides (see Section 1 - 1), and the substituted ammonium tri-iodides are unlikely to contain asymmetric ions unless they crystallize in more than one modification (like $(\text{C}_2\text{H}_5)_4\text{NI}_3$). Further, the foregoing analysis gives no indication of the magnitude of the forces arising from the anion-anion and field asymmetry effects, and this question is not likely to be answered solely by the accumulation of structural data.

Fortunately, an independent body of evidence can be found in the infrared/Raman spectral data for this family of compounds. This provides some confirmation for the analysis presented here and also allows the order of magnitude question to be investigated.

7 - 4 The infrared/Raman data

The Hooke's Law behaviour of the tri-iodide ion can be investigated by making use of the infrared/Raman spectral data for these compounds. The atomic vibrations which give rise to resonant absorptions in the infrared region of the spectrum or to Raman shifts of the wavelength of incident radiation are normally treated by considering the atomic system to be a linked set of harmonic oscillators in which the restoring

forces are assumed to obey Hooke's Law. In the simplest treatment an analysis of the normal vibration modes derived from the spectra allows a determination to be made of the values of the force constants defining the Hooke's Law behaviour of the bonds linking the vibrating atoms.

In the I_3^- case, if the appropriate force constants were available it would be possible to determine the magnitude of the forces required to distort the 'isolated' anion into the geometries found from the structural analyses of $(C_2H_5)_4NI_3$, CsI_3 , RbI , NH_4I_3 and $KI_3 \cdot H_2O$. If these forces turn out to be of the same order of magnitude as those operating as a result of, say, the field asymmetry effect, then the analysis presented in the previous section would be well substantiated. A further check would be provided by the linear relationship between deforming force, f , and the bond length change Δr . By using the deforming forces, f_{12} and f_{32} , calculated from the infrared/Raman force constants to prepare a map similar to Figure 7 - 7, the same relative arrangement of points should be reproduced with the only difference being one of scale.

The infrared and Raman spectra of a large number of trihalide compounds have recently been redetermined by Gabes and Gerding [1972]. In their work they indicate that force constant calculations based upon their observations are to be published, but these had not appeared in the literature at the time of writing. As a result, it was necessary to perform a force constant calculation for the I_3^- ion. Unfortunately, Gabes and Gerding did not include $(C_6H_5)_4AsI_3$ in their study, so that the force constants could not be calculated for the 'isolated' symmetrical anion. However, the spectra of $(C_2H_5)_4NI_3$ and $(C_4H_9)_4NI_3$ were recorded, so the calculation could be made for compounds which contain symmetric or near-symmetric anions.

The symmetric I_3^- anion exhibits $D_{\infty h}$ symmetry and consequently has one Raman active vibration mode (ν_1 , symmetric stretching mode) and two infrared active modes (ν_2 , doubly degenerate bending mode and ν_3 , the asymmetric stretching mode). The force constants defining the bond stretch are given in this case by the equations (Maki and Forneris [1967])

$$4\pi^2 c^2 \nu_1^2 = \lambda_1 = (k + k_{12})\mu$$

$$4\pi^2 c^2 \nu_3^2 = \lambda_3 = 3(k - k_{12})\mu$$

where c is the velocity of light, μ is the reciprocal atomic mass of the iodine atom, k is the stretching force constant and k_{12} is the constant defining the interaction of the bond length changes. This last constant is positive if the lengthening of one bond is accompanied by the shortening of the other and negative if the extension of one bond causes the extension of the other. From these formulae and the absorption frequencies observed for the two substituted ammonium tri-iodides the two force constants were calculated to be

$$k = 0.575 \text{ millidyne/\AA}^\circ$$

$$k_{12} = 0.325 \text{ millidyne/\AA}^\circ$$

These values compare well with those reported in the literature for other trihalide species (ICl_2^- , IBr_2^- , I_2Br^- , etc. - see Appendix D, Table D - 3). Using these values and an interactive procedure, the forces required to deform a symmetric anion with bond lengths of 2.920 \AA° into the observed configurations were calculated. (Details of both calculations are given in Appendix D). The calculated deforming forces are given in Table 7 - 7 for each anion configuration so treated.

Taking the I_3^- ion $(\text{C}_2\text{H}_5)_4\text{HI}_3$ - IIA as the anion least affected by anion-anion interaction, the force acting on a terminal iodine due to the

Table 7 - 7

Forces required to distort the 'isolated' I_3^- ion
into the observed geometrical configurations

Compound	$r_{12} (A^\circ)$	$r_{32} (A^\circ)$	$f_{12} (\text{millidyne})^\dagger$	$f_{32} (\text{millidyne})$
$(C_2H_5)_4NI_3-IA^*$	2.928	2.928	0.00476	0.00476
$(C_2H_5)_4NI_3-IB$	2.943	2.943	0.01343	0.01343
$(C_2H_5)_4NI_3-IIA$	2.892	2.981	-0.01660	0.03504
$(C_2H_5)_4NI_3-IIB$	2.912	2.961	-0.00781	0.02356
CsI_3	2.840	3.042	-0.04614	0.07019
RbI_3	2.791	3.016	-0.07422	0.05505
NH_4I_3	2.805	3.112	-0.06641	0.11023
$KI_3 \cdot H_2O$	2.790	2.895	-0.07813	-0.01074

[†] Note that positive forces correspond to bond extensions,
negative forces to bond contractions.

* Two independent ions.

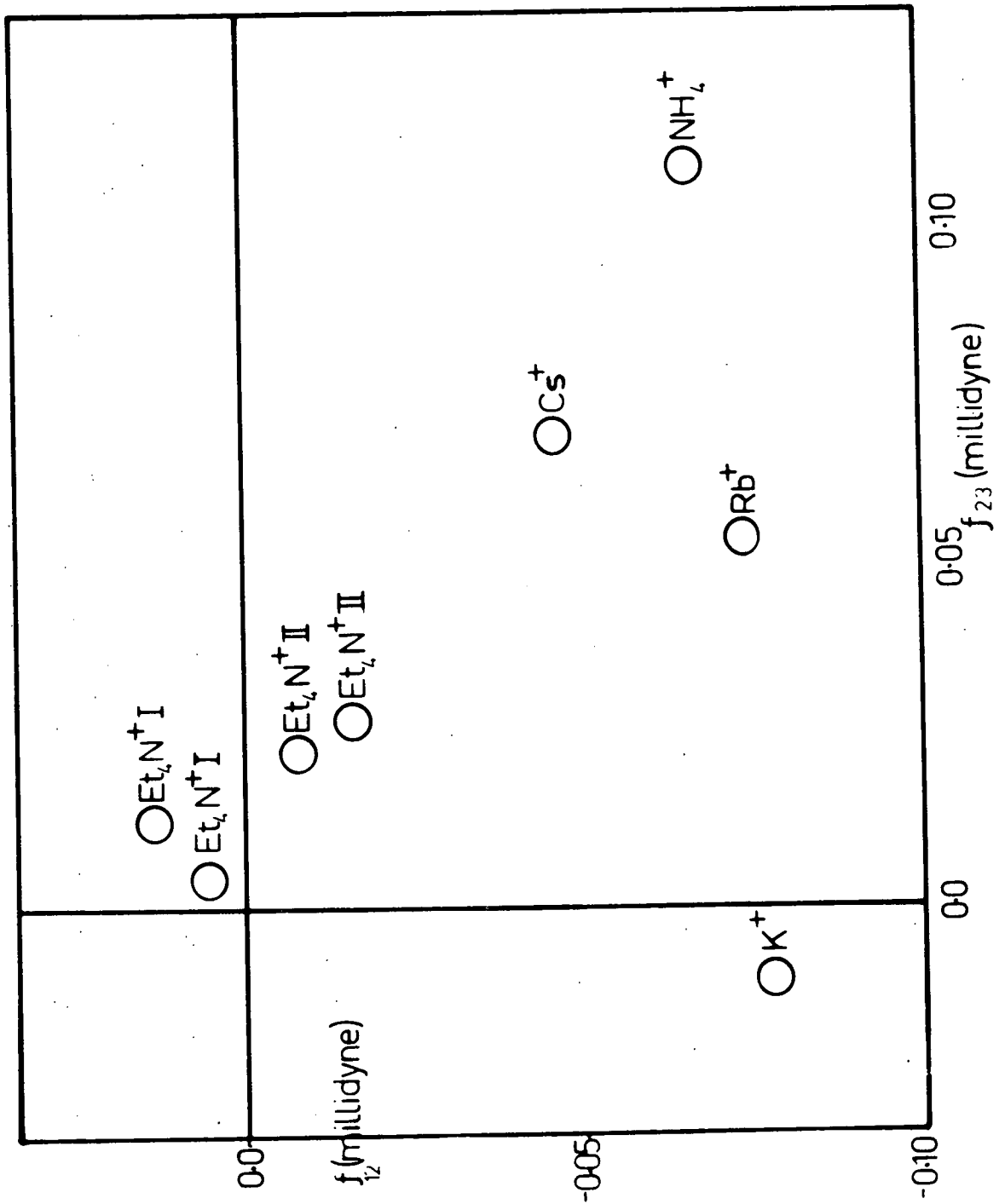


Figure 7 - 8. The positions of the tri-iodides as mapped by the distorting forces.

asymmetric crystal field can be calculated approximately from the equation

$$\delta = (Q \times \Delta V \times 1.602 \times 10^{-12})/r \text{ dynes}$$

where Q is the charge in units of electronic charge on the atom in question. For this ion Q_3 is calculated by Migchelsen and Vos to be -0.54, so that

$$\begin{aligned} \delta_{32} &= (Q_3 \times \Delta V_{32} \times 1.602 \times 10^{-12})/r_{32} \\ &= -0.54 \times 0.379 \times 1.602 \times 10^{-12} / 2.981 \times 10^{-8} \\ &= -0.109 \times 10^{-4} \text{ dynes} \\ &= -0.0109 \text{ millidynes.} \end{aligned}$$

Neglecting the difference in sign, which is a consequence of the difference in definition of contracting and extending forces, this is of the same order of magnitude as the distorting force calculated from the force constants ($\delta_{23} = 0.03504$ millidyne) for this bond length change. Thus the hypothesis that the tri-iodide bond length changes are due in part to the effect of the asymmetric crystal field perturbing the anionic electron configuration is supported by the infrared/Raman evidence. Finally, in Figure 7 - 8 the diagram produced by plotting δ_{12} against δ_{32} for each anion is presented; the similarity of the arrangement of points to that of Figure 7 - 7 is immediately obvious. It now remains to discuss the significance of these conclusions for the $\text{KI}_3 \cdot \text{H}_2\text{O}$ case.

7 - 5 The Potassium Tri-iodide case

The foregoing analysis allows the asymmetry of the electrostatic field at the anion site to be identified with some confidence as a major influence governing the stability of the I_3^- ion in the tri-iodide

lattice. Increasing field asymmetry is accompanied by a movement of the central iodine towards one end of the I_3^- unit so that geometrically the anion more closely approximates an iodine molecule with an iodide ion in close association. This trend is accompanied by a decrease in the stability of the compound (C_6 , Chapter 1, Section 1 - 2.). As well as this destabilizing influence, attention has been drawn to the stabilizing effect of interactions between neighbouring I_3^- anions. The overlap of p -orbitals on the terminal atoms of an anion with those on the central atoms of neighbouring anions - made possible by the *en echelon* arrangement - is evidently accompanied by an extension of both I_3^- bonds and makes possible electron delocalization over the entire anionic layer. One manifestation of this electron delocalization is the two-dimensional semiconduction of layered polyiodides reported by Kawai, Kiriya and Uhida [1965]. For a given tri-iodide, with a structure based upon the layered *en echelon* motif, the stability of the compound and the geometry of its anions will depend upon the balance struck between these stabilizing and destabilizing interactions.

In the case of $KI_3 \cdot H_2O$ it is to be expected that the gradient of the crystal field over the anion site will not have the same character as that calculated for the simple unsolvated tri-iodides. In this compound the cation is displaced out of the anionic plane, and the planes themselves are further apart. Also, the water molecule in the interlayer space will itself be polarized by its environment and as a result will make its own contribution to the electrostatic field experienced by the anion. This expectation is supported by the position of the point corresponding to potassium tri-iodide in Figure 7 - 7; in $KI_3 \cdot H_2O$ one of the I_3^- bond lengths is not very different from the value of 2.92 \AA assumed for the 'isolated' anion, and the

other is markedly shorter. In this respect the $\text{KI}_3 \cdot \text{H}_2\text{O}$ geometry differs from that of the other simple tri-iodides for which data is available, in that all other anions show at least one bond with a length greater than 2.92 \AA . It should also be noted that anion-anion interaction in the anionic layers of potassium tri-iodide will be of considerable significance as the average anion separation is smaller for this structure than for all the other known simple tri-iodides.

Taking the distance of a point from the origin of Figure 7 - 7 (or Figure 7 - 8) as a measure of the total strain exhibited by the anion represented by that point, and making the assumption that this distance may be used as a rough measure of stability, it appears that $\text{KI}_3 \cdot \text{H}_2\text{O}$ should be more stable than both NH_4I_3 and RbI_3 . That this conclusion is at variance with the chemical evidence may point to a failure in the correlation of anion geometry and stability. On the other hand, it is more likely that it indicates that the instability of solid $\text{KI}_3 \cdot \text{H}_2\text{O}$ is due not so much to the electrostatic stresses acting on the anion but rather to the location of the coordinated water molecule in the relatively open interlayer space. Potassium tri-iodide should perhaps be best regarded as a stable tri-iodide but an unstable hydrate.

The large interlayer spacing of $\text{KI}_3 \cdot \text{H}_2\text{O}$ would allow water molecules to move within, and eventually be lost from the interlayer volume, as a consequence of increasing thermal motion accompanying a rise in temperature. The low incongruent melting point of this compound can then be seen as a reflection of the low tolerance of the structure to any gross disturbance of the cation-solvate substructure. The marked tendency of crystals of $\text{KI}_3 \cdot \text{H}_2\text{O}$ to deliquesce in the open can be explained on the same grounds. Atmospheric water molecules would have

little difficulty in penetrating the structure through the interlayer space to reach the cation site. As the potassium cation is thought to retain four water molecules in its coordination sheath when in solution (Kavanau [1964]), and because these could not all be accommodated at the cation site without disrupting the anionic layer, increasing cation solvation is accompanied by dissolution of the crystal.

The structure adopted by solid $KI_3 \cdot H_2O$ is one in which the destabilizing influence of the crystal field is minimized by an increase in the spacing of the anionic layers made necessary by the need to accommodate the cation solvate molecule in the structure. Coordination between the solvate molecule and the cation displaces the latter out of the plane of the anionic layer; this has the effect of allowing the anions to draw closer together with the result that the destabilizing influence of anion-anion interaction is enhanced. The overall stability of the solid is primarily controlled by the vulnerability of the cation-solvate substructure to the gain or loss of solvate molecules.

7 - 6 Extension to other Polyiodides

The interpretation of the relationship between the structure and stability of crystalline potassium tri-iodide presented above can be extended to other polyiodides, whether solvated or not, and in principle should also be applicable to all polyhalides. Indeed, it should be of general validity for all those compounds which include molecular groups within which the bonding is sufficiently weak for it to be disrupted by electrostatic forces of the same order of magnitude as average crystal fields; the polyhalide family being convenient exemplars of this class. In the most general terms, the crystalline

structure of such compounds will be those in which the charged species are arranged in space so that the disruptive effects of the crystal field are minimized, and any cooperative interactions among the components of the compound which stabilize the weakly bonded entity are maximized. Among the polyiodides the following possible stabilizing interactions may be identified: the anion-anion interactions already mentioned, anion-solvate interactions of the charge transfer type, cation-solvate and solvate-solvate interactions leading to the development of substructures contributing to the overall stability, and combinations of these major types.

7 - 6 - 1 The anion-anion interaction

The ubiquity of the *en echelon* arrangement of the I_3^- anions in the simple tri-iodides and related trihalides suggests that the contribution made to the overall stability by anion-anion interactions is very significant. This structural motif is obviously related to the molecular arrangement found in the crystalline solid halogens. Unlike fluorine, which exhibits polymorphism in the solid state (Jordan, Streib and Lipscomb [1964], Meyer, Barrett and Greer [1968]), iodine (Townes and Dailey [1952]), bromine (Kitaigorodskii, Khotsyanova and Struchkov [1953]) and chlorine (Collin [1952, 1956]) all crystallize in isomorphous lattices with the symmetry of space group $Cmca$. The halogen molecules lie in planes normal to the a -axis and the arrangement of the molecules is that shown in Figure 7 - 9. Townes and Dailey first remarked that in iodine the relative orientation of the molecules and the fact that nearest neighbours in the plane are closer than the sum of their van der Waals radii could be taken as evidence of intermolecular bonding within the plane. Bersohn [1962] used a simplified Bloch orbital approach to investigate the intermolecular bonding in crystalline iodine and showed that $5p$ -electron interactions between

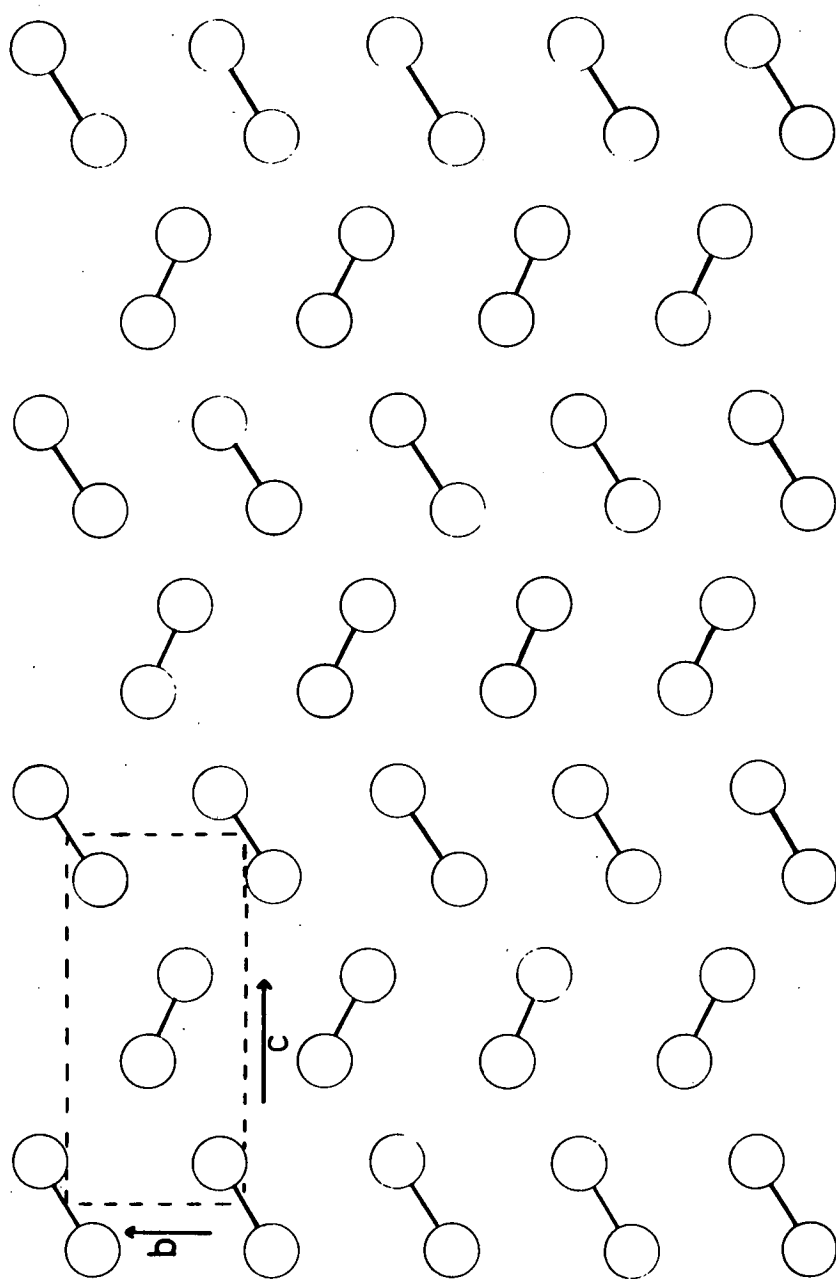


Figure 7 - 9; The arrangement of I_2 molecules within the layered structure of solid iodine. The unit cell translations are indicated.

neighbouring iodine molecules in the plane could account for the lattice energy, conductivity, nuclear quadrupole coupling and the electronic spectrum of the solid. Rosenberg [1964] used Bersohn's model but revised the treatment; his estimates of the same physical properties also supported the hypothesis that intermolecular bonding involving 5p-electron delocalization is present in crystalline iodine. Although similar theoretical investigations do not appear to have been carried out for bromine, Yamasaki [1962], Hillier and Rice [1967], Nyberg [1968] and Suzuki, Yokoyami and Ito [1969] have studied chlorine; and the results of these investigations similarly confirm that intermolecular bonding is also significant in solid chlorine and accounts for some 5 - 25% of the total lattice energy. As a result of their study, Hillier and Rice conclude that charge delocalization is important in determining the cohesive energy of molecular crystals for which there is a non-vanishing overlap between molecules.

In Figure 7 - 10 the characteristic *en echelon* arrangement of the tri-iodide layers has been drawn to the same scale as Figure 7 - 9. The geometric similarities between these two arrangements, taken together with the arguments presented in Section 7 - 2 lead to the conclusion that anion-anion interaction involving the delocalization of 5p-electrons over the anionic network not only contributes to the stability of the tri-iodides in the solid state, but that in the absence of over-riding effects due to the presence of solvate molecules in the lattice, this interaction should be regarded as the dominant influence shaping the crystal chemistry of these compounds. Where the final crystal structure is not controlled by solvate-solvate, cation-solvate or anion-solvate interactions, the components of the compound arrange themselves to achieve the maximum anion-anion interaction consistent with the minimization of the electrostatic field asymmetry at the anion sites.

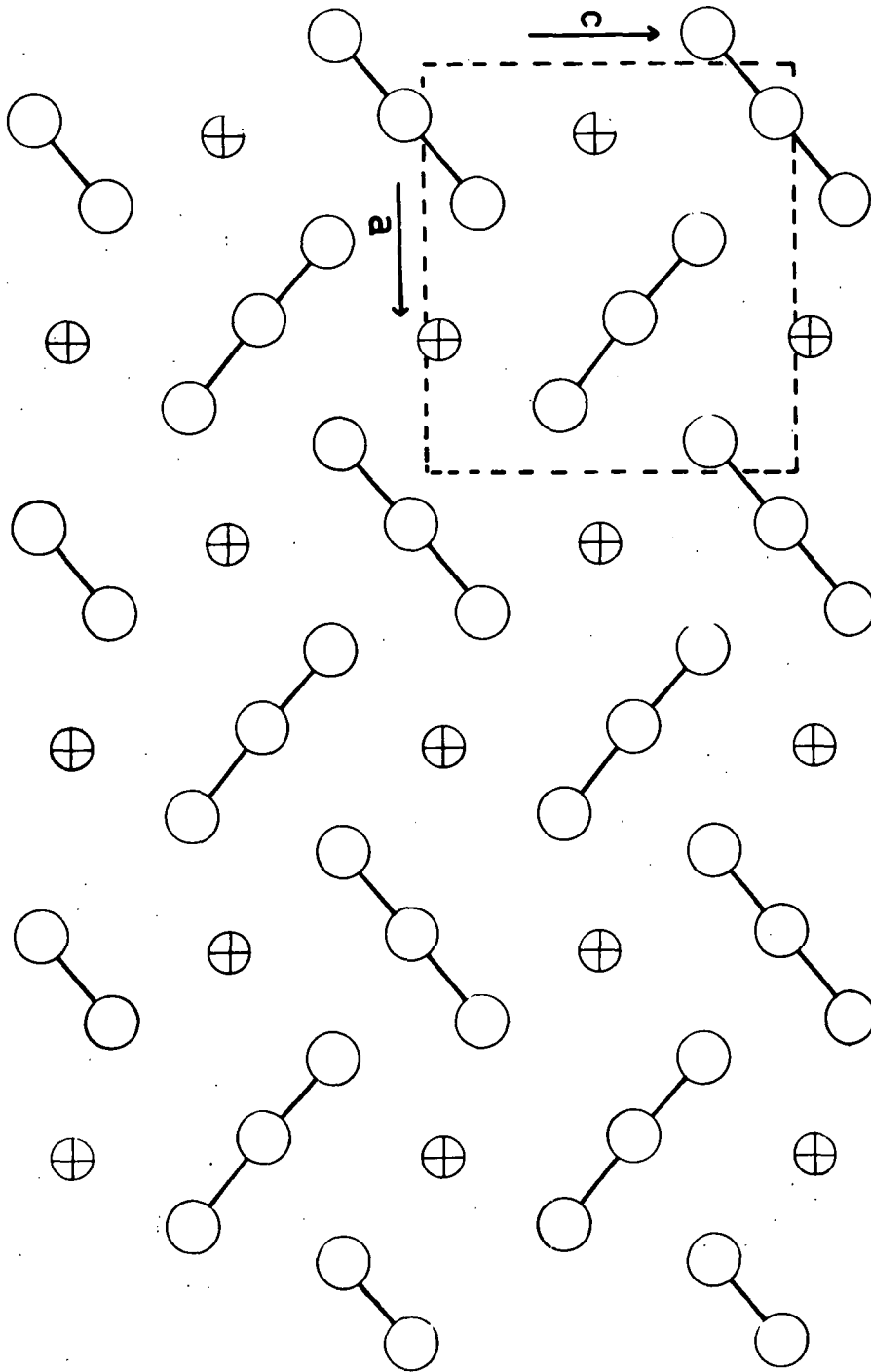


Figure 7 - 10; The arrangement of I_3^- ions within the layered structure of an orthorhombic tri-iodide.

It is highly probable that this principle holds true for the higher polyiodides as well. The anionic arrangement within the layers of $(\text{CH}_3)_4\text{NI}_5$ is shown in Figure 7 - 11 to the same scale as Figures 7 - 9, - 10. In this case interactions between anions would involve overlap between p -orbitals on the iodine at the apex of the V-shaped anion and those on terminal atoms of the neighbouring anions. The structural data for even higher polyiodides is sparse, but when the available data is compared against this background, the impression is that the anions are arranged in two- or three-dimensional networks in which the number of p -orbital overlaps between neighbouring anions is large.

Useful experimental evidence of the magnitude of the anion-anion interaction might be obtained from measurements of the diamagnetic anisotropy of polyiodide single crystals. Tri-iodides and penta-iodides, in which the anions are arranged in layers, should show differences between the magnetic susceptibilities measured with the field normal to and parallel with the anionic plane if significant electron delocalization occurs among the anions.

7 - 6 - 2 The solvate-anion interactions

As well as the contribution to lattice stability arising from electron delocalization among overlapping anions, it is necessary to consider the related mechanism in which delocalizing interactions are presumed to occur between anions and neutral solvate molecules. Like the anion-anion interactions, the question of solvate-anion interactions can be approached by making use of the halogen molecule case as a model. A large family of addition compounds in which halogen or interhalogen molecules and organic molecules crystallize together as definite species is known. The structural chemistry of these halogen addition compounds has been extensively investigated by Hassel and his co-workers, and a

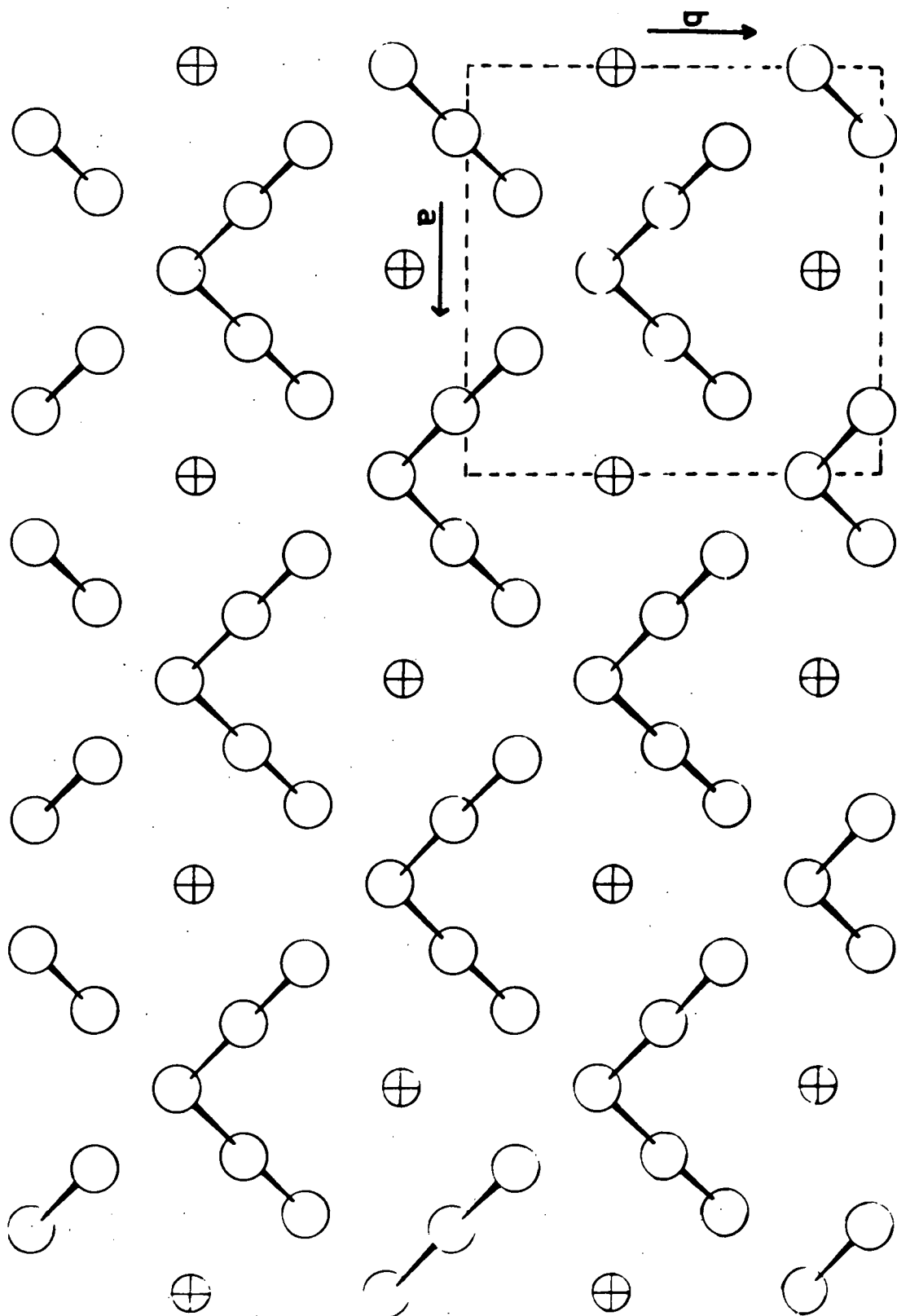


Figure 7 - 11; The arrangement of I_5^- ions within the layered structure of $(CH_3)_4NI_3$.

representative group of the compounds for which structural data is available have been collected together in Table 7 - 8. As a group, these compounds are characterised by low stability; melting accompanied by decomposition commonly taking place below 0°C. These compounds are not clathrates, as there is no structural evidence for the development of 'cages' within the lattice, and they possess definite simple stoichiometries. The reported structural data shows that the common feature of this family of compounds is the close association of a halogen and an organic molecule to form either a paired group or a chain in which the two molecules alternate. An example of the latter type is afforded by the isomorphous addition compounds of benzene with chlorine or bromine. In both benzene.Cl₂ and benzene.Br₂ alternating chains of benzene and halogen molecules run through the structure with the halogen molecule lying on the six-fold axis of the benzene ring. In these two compounds, as well as in the other mentioned in Table 7 - 8, the halogen-halogen bond is slightly longer than that found in the free molecule (Hassel and Rømming [1967]). The organic molecules which form these addition compounds are aromatic hydrocarbons, ethers, ketones, amines and alcohols. It is significant that with the exception of the alcohols, the organic molecules known to solvate polyiodides are drawn from the same classes (cf. Table 1 - 2).

It is also of significance that two compounds which were first thought to be halogen addition compounds were subsequently shown by structural analysis to be polyhalides. The first of these, piperazinium di-dichloroiodide, C₄H₁₄N₂(ICl₂)₂, (Rømming [1958]) contains linear asymmetric ICl₂⁻ ions arranged in chains with pairs of anions alternating with piperazine molecules. As already mentioned in Section 1 - 4 - 12, it is possible that compounds of this type contain the cation H₃O⁺; in this case there is no structural evidence for associating the protons with the organic component of the structure. The compound is prepared

TABLE 7 - 8

Halogen addition compounds

<u>Compound</u>	<u>Reference</u>
2(methyl alcohol).Br ₂	Groth and Hassel [1964]
acetone.Br ₂	Hassel and Strømme [1959c]
1,4-dioxane.ICl	Hassel and Hvorslef [1956]
1,4-dioxane.Br ₂	Hassel and Hvorslef [1954]
1,4-dioxane.Cl ₂	Hassel and Strømme [1959a]
1,4-dithiane.2I ₂	Chao and McCulloch [1960]
dibenzylsulphide.I ₂	Rømning [1960]
1,4-diselenane.2I ₂	Chao and McCulloch [1961]
tetrahydroselenophene.I ₂	Hope and McCulloch [1964]
benzene.Br ₂	Hassel and Strømme [1958]
benzene.Cl ₂	Hassel and Strømme [1959b]
pyridine.ICl	Hassel and Rømning [1957]
4-picoline.I ₂	Hassel [1957]
trimethylamine.I ₂	Strømme [1959]
trimethylamine.ICl	Hassel and Hope [1960]
hexamethylenetetramine.2Br ₂	Eia and Hassel [1956]

from aqueous solution and in the absence of any analytical data, the possibility that the organic molecule is not the cation cannot be ruled out; this possibility will be considered in further detail below. The situation is much clearer in the case of the compound originally formulated as pyridine. 2I_2 (Hassel and Hope [1961]). The structural analysis of this species showed that it should be more properly be formulated as the hepta-iodide of the dipyridine iodonium cation: $[(\text{C}_5\text{H}_5\text{N})_2\text{I}^+] \text{I}_7^-$. The hepta-iodide anion is built up of a loose association of I_3^- and I_2 groups, as in $(\text{C}_2\text{H}_5)_4\text{NI}_7$ (Havinga and Wiebenga [1955]). This compound is of interest in that it is a high polyiodide of a complex iodonium cation, and also because it gives additional dimensional information about the hepta-iodide anion. The fact that a structural analysis was required to place this compound among the polyiodides points to the similarity in general physical and chemical properties between the halogen addition compounds and certain of the solvated polyiodides.

The resemblance between these two groups is perhaps most striking for the well characterised benzene solvated polyiodides. This group includes $2\text{CsI}_9 \cdot 3\text{benzene}$, $\text{RbI}_9 \cdot 2\text{benzene}$, $\text{RbI}_7 \cdot 2(\text{benzene})$ and $\text{KI}_9 \cdot 3(\text{benzene})$; two other benzene solvated potassium polyiodides are listed in Table 1 - 2, but the evidence for their existence is less convincing (Grace [1933]). The role of the benzene molecule may be nothing more than the passive one of providing a means of increasing the spacing between anionic layers with a consequent reduction in the electrostatic field asymmetry at the anion sites. However, if these compounds can be related to the benzene addition compounds of bromine and chlorine, as seems probable, then the benzene molecules would play a more active part in stabilizing the lattice through solvate-anion interactions. It does not appear likely that the structure of $\text{C}_6\text{H}_5\text{ICl}_2$ (Archer and Schalkwyk [1953]) - in which the benzene molecule is bonded to the central iodine

of the linear ICl_2 group - can be used as a model for the benzene solvated polyiodides. Therefore, by analogy with the known structures of the addition compounds, it is expected that these compounds would have structures based on a motif in which I_3^- units and iodine molecules alternate with benzene molecules, the latter lying with the plane of the ring normal to the long axes of the halogen groups so that interactions between the aromatic π -system and the extended p -orbitals of the iodine atoms would be maximized. Structures with a strong resemblance to ferricinium tri-iodide (Bernstein and Herbstein [1968] - C₆. Section 1 - 4 - 5) could reasonably be anticipated. Plausible structures based on this model which account for the relative increase in benzene solvation encountered in passing from the ennea-iodide of caesium to that of potassium can be developed; despite the expected experimental difficulties, a structural investigation of this series of compounds would be very useful.

Snook [1967] has presented some spectral data which may be indicative of solvate-anion interactions in polyiodides. As part of a study of the polyiodides of calcium he prepared a number of doubly solvated calcium hexa-iodides and measured the infrared transmission and the UV/visible reflectance spectra of three of these, namely $\text{CaI}_6 \cdot 6\text{H}_2\text{O} \cdot 6(\text{succinimide})$, $\text{CaI}_6 \cdot 4\text{H}_2\text{O} \cdot 6(\text{benzamide})$, $\text{CaI}_6 \cdot 4\text{H}_2\text{O} \cdot 4(\text{diethyl-oxalate})$. In the infrared spectra marked changes in the intensity of the organic solvate absorptions were noted, together with damping of the characteristic carbonyl absorptions and splitting of others. It is an open question whether these changes should be attributed to the presence of anion-solvate or solvate-solvate (hydrogen bonding?) interactions. In the UV/visible reflectance spectra (measured over the range 200 - 1000 $\text{m}\mu$), the characteristic tri-iodide absorptions at 360 - 370 $\text{m}\mu$ and 280 - 290 $\text{m}\mu$ were observed, together with weaker absorptions at higher wavelengths; these weaker absorptions occurred at

different wavelengths in each of the three compounds, and in each case were relatively broad. The three organic solvates were also examined over the same wavelength range and showed no absorption maxima from 1000 μ to 270 μ . Below 270 μ the absorption increases due to the carbonyl peak at 200 μ .

Similar high wavelength absorptions were observed by Robin [1956] in the spectra of benzamide solvated alkali metal tri-iodides. Robin regarded the solvate molecules as providing an inert host lattice for the anions and cations, and attributed the absorptions in the 720 - 450 μ region to exciton coupling of transitions between the elements of the anionic chains presumed to exist in these compounds. In the case of the doubly solvated calcium polyiodides, this explanation requires that there be significant anionic interaction within the structure. The absence of quasi-metallic lustre and the strong pleochroism associated with any significant degree of interaction between polyiodide anions would seem to indicate that such interactions do not take place in these compounds. Even so, if interanionic transitions are responsible, the fact that the spectra are different for different organic solvates remains a problem. Only two explanations appear possible: either the observed changes are due to different geometrical arrangements of the anions with respect to one another occasioned by differences in the inert organic framework in each case, or these spectral differences reflect differing degrees of solvate-anion interaction. Once again, structural investigation of this series of compounds would do much to settle this question.

The possibility of solvate-anion interactions also emerges from a consideration of the role of the solvate molecules in the solvated hydrogen polyiodides, although here the interpretation is more complicated by the questions that have already been raised regarding the true

nature of the cation in this group of compounds. A number of hydrogen polyiodides with different solvate molecules are known, and representative compounds are listed in Table 1 - 2. The conventional formulation of these compounds implies that the cation is H^+ ; which, given the rarity of the isolated cationic proton in the solid state, is most unlikely. A number of authors (Rømming [1958], Reddy, Knox and Robin [1964], Baenziger, Buckles and Simpson [1967], and Herbstein and Kapon [1972]) when discussing the structures of solvated hydrogen polyhalides have suggested that the organic molecule is protonated and should be regarded as the cation; if this is generally true of this class of compounds, the possibility of solvate-anion interactions in the sense used here can be dismissed as far as the hydrogen polyiodides are concerned.

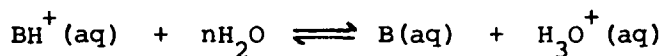
However, as the hydrogen polyhalides have all been prepared by crystallization from aqueous acid media, the hypothesis that the cation is the oxonium ion must be considered, particularly as the analytic discrepancy introduced by an additional water molecule in these high molecular weight compounds is sufficiently small for it to be masked by normal experimental error. Further, most of the hydrogen polyiodides were prepared and analysed at a time when it was not generally recognized that the hydrogen ion is normally linked to a water molecule to form H_3O^+ . Consequently, no special attempt was made to determine the presence of water in these compounds; where H_2O was analytically determined, it was assumed to be present as water of crystallization. Some support for the hypothesis that the cation in these compounds is the oxonium ion is afforded by the existence of the well-characterised hydrogen polyiodide, $HI\cdot 4H_2O$ (Caglioti [1929]). It is difficult to entertain the view that this compound does not incorporate the H_3O^+ cation; in all probability the correct formulation is $[H_3O^+][I_4^-]\cdot 3H_2O$. For the case of the hydrogen polyiodides which can be crystallized from aqueous HI with organic molecules in the lattice, the question to be answered is: at the point of crystallization, does the proton transfer

from the oxonium ion to the organic species, or does H_3O^+ enter the lattice? Taking $\text{HI}_3 \cdot 4(\text{C}_6\text{H}_5\text{CN})$ (Martin [1932]) as a case in point: is the cation in this compound H_3O^+ or the benzonitrilium ion, $\text{C}_6\text{H}_5\text{CNH}^+$? Stabilizing interactions between the I_3^- anion and the benzonitrile molecules in the lattice can only be a possibility if the cation is the oxonium ion.

The outcome of any competition between water and benzonitrile molecules for the proton may be predicted from the value of the equilibrium constant for the reaction



Perrin [1965] uses the analogous general form



to define the dissociation constant, K_a , for an organic base, B, in aqueous solution. Unfortunately, benzonitrile is not included in his compilation of pK_a values for over 3,800 organic bases, and a survey of subsequent literature has not revealed any report of its experimental determination. Estimating the pK_a of $\text{C}_6\text{H}_5\text{CH}$ to be approximately -5.3 and performing an order-of-magnitude calculation (Appendix D, Sections D-4 and D-5), the ratio $[\text{H}_3\text{O}^+] : [\text{C}_6\text{H}_5\text{CNH}^+]$ at the crystallization point is determined to be about $10^6 : 1$; it is therefore concluded that the benzonitrile molecules in this hydrogen polyiodide are not cationic.

Similar calculations for those molecules which are reported to form solvated hydrogen polyiodides and for which the pK_a data is available indicate that the oxonium ion is most probably the cation in $\text{HI}_3 \cdot (\text{benzamide})$ and $\text{HI} \cdot (\text{antipyrine})$, while the organic molecule is probably the cation in those polyiodides containing nicotine, phenacetin, triphenin and the related quasi-alkaloids. Similarly, the piperazine and tetra-*p*-anisthylethylene molecules are probably correctly regarded as the cations of the dichloroiodates studied by Rømming [1958] and

Baenziger, Buckles and Simpson [1967] respectively. It is therefore possible to classify the hydrogen polyiodides into two groups. The first group encompasses those which possess an organic cation and may be regarded as analogues of the well-known group of tetra-alkyl ammonium polyiodides. The second group includes those hydrogen polyiodides which crystallize with H_3O^+ in the lattice. The members of the latter group may be considered as the end-members of the appropriate series of solvated alkali metal polyiodides. Just as $[\text{H}_3\text{O}^+][\text{ICl}_4^-].3\text{H}_2\text{O}$ can be regarded as the end-member of the series of hydrated tetrachloroiodates listed in Table 7 - 9, so in the same way $[\text{H}_3\text{O}^+][\text{I}_3^-].3(\text{C}_6\text{H}_5\text{CN})$ can be regarded as the end-member of a similar series of benzonitrile solvated polyiodides. In Table 7 - 9 the four series of solvated polyiodides of alkali metal cations have been set out for comparison; ammonium species are also shown. As well as the two attested oxonium forms, two postulated proposed solvated oxonium tri-iodides are included. The hydrated oxonium tri-iodide has not been reported, but a comparison of the relative stabilities of the ICl_4^- and the I_3^- ions gives some grounds for expecting its eventual synthesis (although, it must be admitted, its anticipated stability would be low). Similarly, the diethyloxalate solvated oxonium tri-iodide has not been reported, but like the benzamide and diethyloxalate lithium polyiodides, it appears that no serious attempt at synthesis has been made. The completion of these solvated series presents an interesting research problem in itself.

With the exception of the hydrated polyiodides, in which the evidence points to cation hydration, the possibility of solvate-anion interactions making a contribution to the overall stability of the members of the three remaining series cannot be overlooked.

7 - 6 - 3 The cation-solvate interaction

The question of cation-solvate interactions and its implications with regard to the stability of hydrated polyiodides has already been

Table 7 - 9

Oxonium polyiodides as the end-numbers of
series of solvated alkali metal polyiodides

Compound	Reference(s)
Hydrated tetrachloroiodates	
$[\text{H}_3\text{O}^+][\text{ICl}_4^-] \cdot 3\text{H}_2\text{O}$	Caglioti [1929]
$\text{LiICl}_4 \cdot 4\text{H}_2\text{O}$	Wells, Wheeler and Penfield [1892b]
$\text{NaICl}_4 \cdot 2\text{H}_2\text{O}$	Rae [1918], de Celis and Moles [1932]
$\text{KICl}_4 \cdot \text{H}_2\text{O}$	Filhol [1839a-d]
$\text{NH}_4\text{ICl}_4 \cdot 3\text{H}_2\text{O}$	Caglioti and Centola [1933]
Benzonitrile Solvated tri-iodides	
$[\text{H}_3\text{O}^+][\text{I}_3^-] \cdot 4(\text{benzonitrile})$	Martin [1937]
$\text{LiI}_3 \cdot 4(\text{benzonitrile})$	"
$\text{NaI}_3 \cdot 2(\text{benzonitrile})$	"
$\text{KI}_3 \cdot 2(\text{benzonitrile})$	"
Benzamide Solvated tri-iodides	
$[\text{H}_3\text{O}^+][\text{I}_3^-] \cdot 2(\text{benzamide})$	Robin [1964]
$\text{NaI}_3 \cdot 3(\text{benzamide})$	"
$\text{KI}_3 \cdot 3(\text{benzamide})$	"
$\text{RbI}_3 \cdot 3(\text{benzamide})$	"
$\text{CsI}_3 \cdot 3(\text{benzamide})$	"

Table 7 - 9 (contd)

Compound	Reference(s)
Diethyloxalate solvated tri-iodides	
$[\text{H}_3\text{O}^+][\text{I}_3^-].n(\text{diethyloxalate})?$	-
$\text{NaI}_5.4(\text{diethyloxalate})$	Skrabal and Flach [1919]
$\text{KI}_3.2(\text{diethyloxalate})$	"
$\text{RbI}_3.2(\text{diethyloxalate})$	"
$\text{CsI}_3.2(\text{diethyloxalate})$	"
$\text{NH}_4\text{I}_3.2(\text{diethyloxalate})$	"
Hydrated tri-iodides	
$[\text{H}_3\text{O}^+][\text{I}_3^-].n\text{H}_2\text{O}?$	-
$\text{Li}_2\text{I}_8.4\text{H}_2\text{O}$	Cheesman and Nunn [1964]
$\text{NaI}_3.\text{NaI}_5.4\text{H}_2\text{O}$	Cheesman, Duncan and Harris [1940]
$\text{NaI}.\text{NaI}_3.6\text{H}_2\text{O}$	"
$\text{KI}_3.\text{H}_2\text{O}$	Johnson [1877], Grace [1931]
$\alpha, \beta\text{-KI}_3.2\text{H}_2\text{O}$	Briggs <i>et alii</i> [1940]
$\text{NH}_4\text{I}_3.3\text{H}_2\text{O}$	Briggs, Ballard <i>et alii</i> [1940]

discussed in Section 7 - 4. It remains to survey the known hydrated polyiodides in the light of the interpretation given in that Section, namely, that the stability of the compound may be conditioned by the strength of the cation-solvate substructure as much as by the intrinsic strength of the intra and interanionic bonding.

The hydrated polyiodide $\text{LiI}_4 \cdot 4\text{H}_2\text{O}$ (Nunn [1964], Cheesman and Nunn [1964]), found in a phase study of the ternary system $\text{LiI} - \text{I}_2 - \text{H}_2\text{O}$ at 0°C , has already been mentioned (cf. Chapter 1, Section 1 - 1). In his thesis, Nunn made the point that in view of its diamagnetism, this compound should be formulated as $[\text{Li} \cdot 4\text{H}_2\text{O}]_2\text{I}_8$, analogous to the dimeric caesium polyiodide Cs_2I_8 . Although examples of lithium ions in a tetrahedral oxygen environment are known, $\text{LiOH} \cdot \text{H}_2\text{O}$ being one example, the usual configuration in hydrates is for the cation to be octahedrally surrounded by six water molecules, the octahedra sharing faces to give an overall stoichiometry of $\text{LiR} \cdot 3\text{H}_2\text{O}$ ($\text{R} = \text{Cl}, \text{Br}, \text{I}, \text{ClO}_3, \text{ClO}_4, \text{MnO}_4, \text{NO}_3$, etc. - Wells [1962]). A structural model for $[\text{Li} \cdot 4\text{H}_2\text{O}]_2\text{I}_8$ can be developed in which the Li^+ ion preserves its sixfold coordination and which gives the correct $\text{Li}:\text{H}_2\text{O}$ ratio by allowing the octahedra to share two opposite edges rather than two opposite faces. The structure would then consist of chains of linked octahedra enclosing the lithium ions, interlocking with either I_8^{2-} ions or $\text{I}_3^- \cdot \text{I}_5^-$ ion pairs. A similar structure in which tetrahedrally coordinated lithium ions substitute for the caesium ions in the Cs_2I_8 structure seems equally probable. This latter structure would be vulnerable to attack by adventitious water, by means of which the cation could achieve its more usual sixfold coordination.

In view of the uncertainty surrounding the correct formulation of the hydrated sodium polyiodides it is perhaps premature to advance any predictions concerning their probable structures. However, if the

empirical formulae given by Cheesman, Duncan and Harris [1940] can be relied upon, and further, assuming that $\text{NaI}_2 \cdot 3\text{H}_2\text{O}$ and $\text{NaI}_4 \cdot 2\text{H}_2\text{O}$ should be written as the double salts $\text{NaI} \cdot \text{NaI}_3 \cdot 6\text{H}_2\text{O}$ and $\text{Na}_2\text{I}_8 \cdot 4\text{H}_2\text{O}$, plausible structural models can be derived. Radius ratio calculations predict that sodium should normally be coordinated by six water molecules, and hydrates exhibiting octahedral coordination of sodium are known (for example: $\text{Na}_2\text{SO}_4 \cdot 10\text{H}_2\text{O}$, $\text{Na}_2\text{B}_4\text{O}_7 \cdot 10\text{H}_2\text{O}$ and the hydrates of NaOH). The correct $\text{Na}:\text{H}_2\text{O}$ ratio for $\text{NaI} \cdot \text{NaI}_3 \cdot 6\text{H}_2\text{O}$ could be achieved by the face-sharing of these hydration octahedra, leading to the formation of cation-hydrate chains similar to those found in the hydrated lithium halides. The chains of linked octahedra and the two anions could be arranged in a similar fashion to the packing of the cation, the N-methylacetamide molecules and the I^- and I_3^- anions in $\text{K}_2\text{I}_4 \cdot 6(\text{CH}_3\text{CONHCH}_3)$ (Cf. Section 1 - 4 - 10). In this arrangement, rows of alternating iodide and tri-iodide ions lie parallel to a linear structure built up from the K^+ ions and the organic molecules. This hypothetical structure for $\text{Na}_2\text{I}_4 \cdot 6\text{H}_2\text{O}$, like that of the potassium compound, would be dominated by the 3-fold symmetry of the cation-solvate substructure and might reasonably be expected to exhibit hexagonal or trigonal symmetry. The $\text{Na}:\text{H}_2\text{O}$ ratio for $\text{Na}_2\text{I}_8 \cdot 4\text{H}_2\text{O}$ cannot be easily satisfied by any model which preserves an octahedral arrangement of six water molecules about the sodium ion, as the high degree of octahedron sharing dictated by this ratio leads to somewhat implausible layered or framework cation-solvate substructures which impose severe constraints on the space available for the anion(s). It is more probable that the cation coordination is reduced below six, and the structure of $\text{NaBr} \cdot 2\text{H}_2\text{O}$ (Culot, Piret and van Marsche [1962]) may provide a model for this case, as sodium iodide also exists as a dihydrate. In the sodium bromide dihydrate structure each sodium atom is surrounded by a distorted tetrahedral arrangement of water molecules, and it is possible

to envisage a structure for $\text{Na}_2\text{I}_8 \cdot 4\text{H}_2\text{O}$ analogous to that of Cs_2I_8 , with tetrahedrally hydrated Na^+ substituting for Cs^+ . Of these two hypothetical sodium polyiodide structures, it is expected that the latter would be the more stable.

For the polyiodides of the alkaline earth metals the situation is even less clear. Snook [1967] found evidence in a phase study of the system $\text{CaI}_2 - \text{I}_2 - \text{H}_2\text{O}$ for the existence at 0°C of a highly hydrated polyiodide, which he formulated as $\text{CaI}_8 \cdot 10\text{H}_2\text{O}$. He also found some slender evidence for a lower polyiodide which he tentatively identified as $\text{CaI}_4 \cdot 6\text{H}_2\text{O}$. Thomas [1973] indicates that work in progress on the related system $\text{SrI}_2 - \text{I}_2 - \text{H}_2\text{O}$ at 0°C has yielded evidence for a high polyiodide, $\text{SrI}_n \cdot 7\text{H}_2\text{O}$ ($n = 12-14$), and also for a low polyiodide provisionally formulated as $\text{SrI}_4 \cdot 7\text{H}_2\text{O}$ (see also Meyer [1902]). Some early work on the system $\text{BaI}_2 - \text{I}_2 - \text{H}_2\text{O}$ by Rivett and Packer [1927] gave no evidence for the formation of barium polyiodides. The systems $\text{BeI}_2 - \text{I}_2 - \text{H}_2\text{O}$ and $\text{MgI}_2 - \text{I}_2 - \text{H}_2\text{O}$ do not appear to have been studied.

Calcium chloride, bromide and iodide, strontium chloride, bromide and iodide and barium iodide are all known to crystallize as isomorphous hexahydrates. In $\text{SrCl}_2 \cdot 6\text{H}_2\text{O}$ each strontium atom is coordinated by nine water molecules, six shared with adjacent polyhedra and three unshared. The six shared molecules lie at the vertices of a trigonal prism, while the remaining three occupy equatorial positions close to the centers of the prism faces. The sharing of the six coordinated water molecules between polyhedra leads to the development of an infinite one-dimensional cation-water substructure (Jensen [1940]). If this structural motif is common to the isomorphous hexahydrates, it may provide a model for the structures of the calcium and strontium polyiodides. A structural model based on this motif and bearing a strong resemblance to that suggested for $\text{Na}_2\text{I}_4 \cdot 6\text{H}_2\text{O}$ can be developed for $\text{CaI}_4 \cdot 6\text{H}_2\text{O}$. Once again a hexagonal or trigonal symmetry would be expected. Possibly $\text{SrI}_4 \cdot 7\text{H}_2\text{O}$

could have a similar structure; if so, the extra water molecule would be incorporated within the structure as lattice water (it is interesting to note that Thomas has found that the strontium iodide hydrate stable at 0°C is $\text{SrI}_2 \cdot 7\text{H}_2\text{O}$ rather than $\text{SrI}_2 \cdot 6\text{H}_2\text{O}$). The higher polyiodides of calcium and strontium are not sufficiently well characterised at this stage for any useful predictions concerning their probable structures to be made, although the reported high hydration numbers suggest that they include both coordinated and lattice water.

A re-examination of the $\text{BaI}_2 - \text{I}_2 - \text{H}_2\text{O}$ system at low temperature would seem to be warranted, as the polyiodide $\text{BaI}_4 \cdot n\text{H}_2\text{O}$ ($n = 6 - 8$) appears to be a distinct possibility. A survey of the systems $\text{BeI}_2 - \text{I}_2 - \text{H}_2\text{O}$ and $\text{MgI}_2 - \text{I}_2 - \text{H}_2\text{O}$ could also be profitable. Low temperature X-ray structural analyses of the characterised alkaline earth metal polyiodides would also do much to elucidate the role of cation solvation in this family of compounds.

7 - 6 - 4 Solvate-solvate and mixed interactions

The arrangement of benzamide molecules in $[\text{H}_3\text{O}^+][\text{I}_3^-] \cdot 2\text{C}_6\text{H}_5\text{CONH}_2$ ($\text{HI}_3 \cdot 2(\text{benzamide})$ - Reddy, Knox and Robin [1963]) is very similar to that in crystalline benzamide itself. In crystalline benzamide the molecules are dimerized through hydrogen bonding of the amide groups and hydrogen bonds are also formed between dimer pairs in the stacking direction (Penfield and White [1959]). This similarity suggests that hydrogen bonds also exist in the polyiodide, and taken together with the unusual arrangement of I_3^- units in two parallel chains located in channels formed by dimerized benzamide molecules, gives rise to the strong impression that the anion-anion interaction (which leads to the common *en echelon*, or at least rectilinear arrangements of I_3^- ions) has been overridden by stronger interactions between the solvate molecules, and these are responsible for the final architecture of the

structure. It is expected that the diethyloxalate solvated polyiodides would show the same feature, and perhaps also those solvated by succinimide and benzonitrile.

The discussion of stabilizing interactions has been carried forward by concentrating attention on each such possible interaction in turn; however, it should be pointed out that the proposed interactions are not necessarily mutually exclusive. For example, the doubly solvated calcium polyiodides with general formula $\text{CaI}_6 \cdot x\text{H}_2\text{O} \cdot y$ (organic solvate) mentioned in Section 7 - 4 - 2, almost certainly involve cation hydration, probably involve solvate-solvate and solvate-anion interactions and could also include a measure of anion-anion interaction, all acting in concert to stabilize the structure. Similarly the polar N-methylacetamide molecules in $\text{K}_2\text{I}_4 \cdot 3(\text{N-methylacetamide})$ appear to be so oriented that both cation-solvate and solvate-anion interactions are possible; the arrangement is very reminiscent of the cation-solvate-anion disposition in the NaBr and KI di-acetamide structures studied by Roux and Boeyens [1969a, 1969b, respectively].

7 - 7 Summary

The structural basis for the belief that the tri-iodide ion displays its sensitivity to its crystalline environment by changes in its geometry has been augmented by the refinement of the structure of NH_4I_3 and the solution of the structures of RbI_3 and $\text{KI}_3 \cdot \text{H}_2\text{O}$. The interactions at work between the molecular and ionic components of the simple tri-iodides in the crystalline state have been examined and their relationship to both structure and stability have been investigated.

It has been shown that the major destabilizing influence is the crystal field asymmetry at the anion site, so that to a first-order

approximation the I_3^- anion responds to any such asymmetry by changes in the lengths of the iodine-iodine bonds, and that in the unsolvated tri-iodide these changes can be correlated with stability. The bond length changes can be adequately described in terms of a simple Hooke's Law model, which leads to a view of the tri-iodide anion as a 'strain gauge' of molecular dimensions by means of which the nature of certain crystalline environments may be evaluated. Such an interpretation has also led to an appreciation of the significance of cooperative electronic interaction among tri-iodide anions, both as a stabilizing influence and also as a major determinant of tri-iodide structure. This has given a rationale to the similarities often noted between the packing of I_2 molecules in crystalline iodine and the arrangement of anions in unsolvated tri-iodides and higher polyiodides.

The finding that the role of the water molecule in the $KI_3 \cdot H_2O$ structure is primarily one of cation solvation, and that the anionic arrangement preserves the common structural motif of the unsolvated alkali metal tri-iodides has suggested a fresh interpretation of the considerable range in stability of solvated polyiodides. It has been argued here that the stability of solvated polyiodides may be a reflection not only of crystal field asymmetry, but also of the strength of stabilizing interactions between solvate molecules and the ionic species in the structure, or interactions between the solvate molecules themselves.

Unfortunately, the body of structural data available for solvated polyiodides is small, and a critical evaluation of this interpretation is hampered by the absence of data for a series of compounds involving, say, the same solvate and a variety of cations, or the same cation and a variety of solvate molecules. A number of areas have already been indicated where structural analyses might be undertaken with profit;

the doubly solvated calcium hexa-iodides would probably present the least practical difficulties and at the same time provide the first structural data for a polyiodide of a divalent cation. A structural analysis of the series of benzene solvated alkali metal ennea-iodides would be more demanding, but would also be useful in establishing the status of the solvate-anion interactions postulated for this family of compounds. Finally, a neutron diffraction study for the location of hydrogen positions in a solvated hydrogen polyiodide could settle the interesting question of the nature of the cation in these compounds. The benzamide compound, which has already been the subject of an X-ray structural examination, presents itself as a possible candidate.

Two areas requiring further work can be indicated as far as the unsolvated polyiodides are concerned. First, the structure of a number of the high polyiodide anions is known from only one structural analysis, and more X-ray analyses will be required before comparative studies of their response to their crystalline environment can be undertaken. Second, more theoretical studies of the solid polyiodides would be desirable; in particular, Bloch orbital treatments similar to those already applied to the crystalline halogens or less complex MO treatments which take into account molecular clusters or polymeric systems could provide further insight into the role and magnitude of the anion-anion interactions.

Finally, the polybromides and the polychlorides (Wise [1971]), as well as the heteropolyhalogen anions, still await a thorough systematic structural and theoretical investigation.

The inter-iodine distances found in the structural analyses reported in this thesis are reliable to 0.01 Å° (*c.f.* ROLLETT [1965], page 115), which is sufficient to support the analysis of bond-length variation presented in Chapter 7.

Bibliography

Bibliography

- ABEGG & HAMBURGER, [1906], Z. anorg. Chem., 50, p.403.
- AHMED & CRUICKSHANK, [1953], Acta Cryst., 6, p.765.
- ALBERT, MILLS & ROYER, [1947], J. Chem. Soc., p.1452.
- ALGOL, 503 [1969], "503 ALGOL Manual", reprinted (with permission) by the University of Tasmania Photographic and Printing Service, University of Tasmania, Hobart, Tas.
- ALGOL F, [1972], "Algol F Reference Manual", Hydro-University Computing Centre publication, University of Tasmania, Hobart, Tas.
- APPELMAN, [1960], U.S. Atomic Energy Commission UCRL-9025 (Chem. Abstracts, 54, 16998).
- ARCHER & SCHALKWYK, [1953], Acta Cryst., 6, p.88.
- van ARKEL & de BOER, [1928], Recueil Trav. chim., 47, p.593.
- AUMERAS & RICCI, [1939], Société chim. Bulletin Memoires, 5th series, Volume 6.
- BAENZIGER, BUCKLES & SIMPSON, [1967], J.A.C.S., 89, p.3405.
- BALLHAUSEN, [1962], "Introduction to Ligand Field Theory", p.174 McGraw-Hill, New York.
- BANCROFT, SCHERER & GOULD, [1931], J. Phys. Chem., 35, p.764.
- BANERJEE, [1933], Proc. Roy. Soc. (Lond), A141, p.188.
- BAUDRIMONT, [1860], Comptes rendus, 51, p.827.
- BEEVERS & LIPSON, [1934], Phil. Mag. (7) 17, p.855.
- BENGTTSSON & NORDBECK, [1967], B.I.T., 4, p.87.
- BERNAL, [1926], Proc. Roy. Soc. (Lond), A113, p.117.
- BERNSTEIN & HERBSTEIN, [1968], Acta Cryst. B24, p.1640.
- BERSOHN, [1962], J. Chem. Phys., 36, p.3445.
- BERTHELOT, [1880],
- BEZJAK, [1953], Acta Cryst., 6, p.748.
- BOZORTH & PAULING, [1925], J.A.C.S., 47, p.1561.
- BRAGG, [1912], Proc. Camb. Phil. Soc. November 1912.

- BRENEMAN & WILLETT, [1967], *Acta Cryst.*, 23, p.334.
- BRIGGS & GEIGLE, [1930], *J. Phys. Chem.*, 34, p.2250.
- BRIGGS & PATTERSON, [1932], *J. Phys. Chem.*, 36, p.2621.
- BRIGGS & BALLARD, [1940], *J. Phys. Chem.*, 44, p.322.
- BRIGGS, BALLARD, ALRICH & WIKSO, [1940], *J. Phys. Chem.*, 44, p.325.
- BRIGGS, CLACK, BALLARD & SASSAMAN, [1940], *J. Phys. Chem.*, 44, p.350.
- BRIGGS, GEIGLE & EATON, [1941], *J. Phys. Chem.*, 45, p.595.
- BRIGGS, CONRAD, GREGG & REED, [1941], *J. Phys. Chem.*, 45, p.614.
- BROEKEMA, HAVINGS & WIEBENGA, [1957], *Acta Cryst.*, 10, p.596.
- BROWN & NUNN, [1966], *Aust. J. Chem.*, 19, p.1567.
- BROWN & WEISS, [1969], "Bond Index to the Determinations of Inorganic Crystal Structures", McMaster University, Hamilton, Ontario.
- BROWN & WEISS, [1970], "Bond Index to the Determinations of Inorganic Crystal Structures", McMaster University, Hamilton, Ontario.
- BUERGER, [1950a], *Acta Cryst.*, 3, p.87.
- BUERGER, [1950b], *Acta Cryst.*, 3, p.243.
- BUERGER, [1959], "Vector Space", John Wiley & Sons Inc., New York.
- BUERGER, [1962], "X-Ray Crystallography", John Wiley & Sons Inc., New York.
- BUSING & LEVY, [1961], "Computing Methods and the Phase Problem", Pergamon, Oxford, U.K.
- CAGLIOTI, [1929], *Atti Acad. naz. Lincei, Rend. Classe Sci. fis. mat. nat.*, 9, p.563 (*Chem. Abstracts*, 23, 4633).
- CAGLIOTI & CENTOLA, [1933], *Gazzetta*, 63, p.907.
- CARPENTER, [1966], *Acta Cryst.*, 20, p.330.
- de CELIS & MOLES, [1932], *Anales real Soc. espan. Fis. Quím.*, 30, (Chem. Abstracts, 26, 5508).
- CHAO & McCULLOCH, [1960], *Acta Cryst.*, 13, p.727.
- CHAO & McCULLOCH, [1961], *Acta Cryst.*, 14, p.940.
- CHEESMAN, DUNCAN & HARRIS, [1940], *J. Chem. Soc.*, p.837.
- CHEESMAN & NUNN, [1964], *J. Chem. Soc.*, p.2265.

- CHEESMAN, FINNEY & SNOOK, [1970], Theoret. chim. Acta, 16, p.33.
- CHEESMAN & FINNEY, [1970], J. App. Cryst., 3, p.399.
- CHEESMAN & FINNEY, [1970], Acta Cryst., 1326, p.904.
- CHIDAMBARAM, SEQUIRA & SIKKA, [1964], J. Chem. Phys., 41, p.3616.
- CHRIST, CLARK & EVANS, [1953], J. Chem. Phys., 21, p.1114.
- CLARK & DUANE, [1923a], J. Opt. Soc. Amer., 7, p.472.
- CLARK & DUANE, [1923b], Proc. Nat. Acad. Sci. Washington, 9, p.126.
- CLARK, [1924], J.A.C.S., 46, p.1924.
- COCHRAN, [1952], Acta Cryst., 5, p.65.
- COCHRAN & WOOLFSON, [1955], Acta Cryst., 8, p.1.
- COLLIN, [1952], Acta Cryst., 5, p.431.
- COLLIN, [1956], Acta Cryst., 9, p.537.
- COTTON & WILKINSON, [1972], "Advanced Inorganic Chemistry", p.555
3rd edition, Interscience, New York.
- CREMER & DUNCAN, [1931a], J. Chem. Soc., p.1857.
- CREMER & DUNCAN, [1931b], J. Chem. Soc., p.2243.
- CREMER & DUNCAN, [1932], J. Chem. Soc., p.2031.
- CREMER & DUNCAN, [1933], J. Chem. Soc., p.181.
- CRUICKSHANK, PILLING, BUJOSA, LOVELL & TRUTER, [1961], Intern. Tracts.
Computer Sci. Technol. Appl. (edited by PEPINSKY, ROBERTSON &
SPEAKMAN), 4, p.32.
- CULOT, PIRET & van MARSCHE, [1962], Bull. Soc. France Min. Crist.,
85, p.282.
- DARLOW, [1960], Acta Cryst., 13, p.683.
- DAVEY, [1923], Phys. Rev., 21, p.143.
- DAVIES & GWYNNE, [1952], J.A.C.S., 74, p.2748.
- DAVIES & NUNN, [1969], Chem. Comm., p.1734.
- DAWSON & GOODSON, [1904], J. Chem. Soc., 85, p.796.
- DAWSON, [1961], Acta Cryst., 14, p.999.
- DOSSIOS & WEITH, [1869], Z. fur. Chem., 5, p.380.
- DUANE & HUNT, [1915], Phys. Rev., 6

- DUANE & CLARK, [1922], Phys. Rev., 20, p.85.
- DUANE & CLARK, [1923], Phys. Rev., 21, p.380.
- DUNITZ & SEILER, [1973], Acta Cryst., B29, p.589.
- EIA & HASSEL, [1956], Acta Chem. Scand., 10, p.139.
- ELEMA, de BOER & VOS, [1963], Acta Cryst., 16, p.243.
- ELLIOTT BROTHERS, [1963] - see ALGOL, 503.
- EMERY & PALKIN, [1916] - J.A.C.S., 38, p.2166.
- EMERY, [1926], J.A.C.S., 38, p.140.
- EPHRAIM, [1917], Berichte, 50, p.1069.
- EVANS & LO, [1966a], J. Chem. Phys., 44, p.3368.
- EVANS & LO, [1966b], J. Chem. Phys., 44, p.4356.
- EWALD, [1921a], Ann. Phys., 64, p.253.
- EWALD, [1921b], Zeit. fur Kryst., 56, p.129.
- EWALD & HERMANN, [1926], Strukterbericht, p.287.
- FERRARIS & FRANCHINI-ANGELA, [1972], Acta Cryst., B28, p.3572.
- FIALKOV, [1935], Acta physicochem USSR, 3, p.711.
- FILHOL, [1839a], J. Pharmacol., 25, p.431.
- FILHOL, [1839b], J. prakt. Chem., 18, p.457.
- FILHOL, [1839c], J. Pharmacol., 25, p.506.
- FILHOL, [1839d], J. prakt. Chem., 18, p.460.
- FLEXSER, HAMMETT & DINGWALL, [1935], J.A.C.S., 57, p.2103.
- FOOTE & CHALKER, [1911], J.A.C.S., 33, p.1933.
- FOOTE & BRADLEY, [1933], J. Phys. Chem., 37, p.21.
- FOOTE & FLEISCHER, [1940], J. Phys. Chem., 44, p.633.
- GABES & GERDING, [1972], J. Mol. Structure, 14, p.267.
- GARRIDO, [1951], Bull. Soc. Franc mineral et crist., 84, p.397.
- GAY-LUSSAC, [1814], Ann. Chimie, 91, p.72.
- GILBERT, [1885], "The Mikado", Chappel & Co., London.
- GILLESPIE & MORTON, [1971], Quart. Rev., 25, p.553.
- GMELIN, [1933], "Handbuch der anorganische Chemie", 8th edition, Vol. 8, Verlag Chemie, Berlin.

- GOLDFARB, MELE & GUTSTEIN, [1955], J.A.C.S., 77, p.6194.
- GRACE, [1931], Ph.D. Thesis, University of London.
- GRACE, [1933], J. Phys. Chem., 37, p.347.
- GRINELL-JONES, [1930], J. Phys. Chem., 34, p.673.
- GROTH & HASSEL, [1964], Acta Chem. Scand., 18, p.402.
- HACH & RUNDLE, [1951], J.A.C.S., 73, p.4321.
- HAMILTON, [1965], Acta Cryst., 18, p.502.
- HAMILTON & FINNEY, [1967], "MG15, procedure contour", H.U.C.C. Procedure Library Manual.
- HARKER & KASPAR, [1948], Acta Cryst., 1, p.70.
- HARRIS, [1932], J. Chem. Soc., p.1694.
- HARTREE, [1927], Proc. Camb. Phil. Soc., 24, p.89.
- HARTREE, [1957], "The Calculation of Atomic Structures", J. Wiley & Sons, New York.
- HASSEL & HVOSLEF, [1954], Acta Chem. Scand., 8, p.873.
- HASSEL & HVOSLEF, [1956], Acta Chem. Scand., 10, p.138.
- HASSEL & RØMMING, [1957], Acta Chem. Scand., 11, p.696.
- HASSEL, [1957], Proc. Chem. Soc., p.250.
- HASSEL & STRØMME, [1958], Acta Chem. Scand., 12, p.1146.
- HASSEL & STRØMME, [1959a], Acta Chem. Scand., 13, p.275.
- HASSEL & STRØMME, [1959b], Acta Chem. Scand., 13, p.1775.
- HASSEL & STRØMME, [1959c], Acta Chem. Scand., 13, p.1781.
- HASSEL & HOPE, [1960], Acta Chem. Scand., 14, p.391.
- HASSEL & HOPE, [1961], Acta Chem. Scand., 15, p.407.
- HASSEL, RØMMING & TUFTE, [1961], Acta Chem. Scand., 15, p.967.
- HASSEL & RØMMING, [1967], Acta Chem. Scand., 21, p.2659.
- HAUPTMANN & KARLE, [1953], "The Solution of the Phase Problem - The Centrosymmetric Crystal", A.C.A. Monograph No. 5, Polycrystal Book Service, New York.
- HAVINGA, BOSWIJK & WIEBENGA, [1924], Acta Cryst., 7, p.487.
- HAVINGA & WIEBENGA, [1955], Koninkl. Nederl. Akad. van Wetenschappen, B58, p.412.

- HAVINGA, [1957], Thesis, University of Gronigen, The Netherlands.
- HAVINGA & WIEBENGA, [1959], *Rec. Trav. Chim.*, 78, p.724.
- HENRY & LONSDALE, [1965], "International Tables for X-Ray Crystallography", The Kynoch Press, Birmingham, U.K.
- HERBSTEIN & KAPON, [1972], *Nature (Phys. Sci.)*, 239, p.153.
- HILLIER & RICE, [1967], *J. Chem. Phys.*, 46, p.3881.
- HOARE, [1963], *Computer Journal*, 5, p.345.
- HOPE & McCULLOCH, [1964], *Acta Cryst.*, 17, p.712.
- HOSEMAN & BAGCHI, [1953], *Acta Cryst.*, 6, p.318.
- HUBARD, [1942], *J. Phys. Chem.*, p.227.
- HUGHES, [1949], *Acta Cryst.*, 2, p.37.
- JAKOWKIN, [1894], *Zeit. physik Chem.*, 13, p.539.
- JAKOWKIN, [1895], *Zeit. physik Chem.*, 18, p.585.
- JAKOWKIN, [1896], *Zeit. physik Chem.*, 20, p.19.
- JAMES, [1948], "The Crystalline State", Volume II, Bell & Sons, London.
- JAMES, HACH, FRENCH & RUNDLE, [1955], *Acta Cryst.*, 8, p.814.
- JENSEN, [1940], *K. danske vidensk. Selsk. Skr., Nat.-fys Medd.*, 17, No. 9.
- JOHANSEN, [1965], "ALGOL programs for MO Calculations", Chemical Laboratory IV Internal Publication, University of Copenhagen.
- JOHNSON, [1877], *J. Chem. Soc.*, 31, p.249.
- JOHNSON, [1878], *J. Chem. Soc.*, 32, p.397.
- JORDAN, STREIB & LIPSCOMB, [1964], *J. Phys. Chem.*, 41, p.760.
- JORGENSEN, [1856a], *J. prakt. Chem.*, 2, p.347.
- JORGENSEN, [1856b], *J. prakt. Chem.*, 3, p.145.
- KARLE & KARLE, [1966], *Acta Cryst.*, 21, p.849.
- KAVANAU, [1964], "Water and Solute-water Interactions", Holden-Day, San Francisco.
- KAWAI, KIRIYAMA & UHIDA, [1965], *Bull. Chem. Soc. (Japan)*, 38, p.799.
- KIMBALL, [1940], *J. Chem. Phys.*, 8, p.188.
- KITAIGORODSKI, [1953], *Zhur. eksp. teor. Fiz.*, 24, p.747.

- KITAIGORODSKI, [1954], Travaux de l'Institut de Crystallographie (Communication au III^e Congres International de Crystallographie), Moscow, USSR Academy of Sciences.
- KITAIGORODSKI, KHOTSYANOVA & STRUCHKOV, [1953], Zhur. Fiz. Kim., 27, p.780.
- KLUG, [1958], Acta Cryst., 11, p.575.
- KREMANN & SCHOUZL, [1912], Monatsch., 33, p.1087.
- LANGMAIR & WRINCH, [1938], Nature, 142, p.58.
- von LAUE, FRIEDRICH & KNIPPING, [1912], Sitz. ber. Bayer Akadamie d. Wiss, June 1912.
- LEMAIR & LUCAS, [1951], J.A.C.S., 73, p.5198.
- LEVY & PETERSON, [1952], Phys. Rev., 86, p.766.
- LEVY & PETERSON, [1953], J. Chem. Phys., 21, p.366.
- LINDQVIST, [1952], Acta Cryst., 5, p.667.
- LINNETT, [1971], "Essays in Structural Chemistry", edited by DOWNES, LONG & STAVELY, MacMillan & Co., London.
- MAKI & FURNERIS, [1967], Spectrochim. Acta, 23A, p.867.
- MARTIN, [1932], J. Chem. Soc., p.2640.
- MEYER, [1902], Z. anorg. Chem., 30, p.113.
- MEYER, BARRETT & GEER, [1968], J. Chem. Phys., 49, p.1902.
- MEYERSTEIN & TREININ, [1963], Trans. Farad. Soc., 59, p.1114.
- MIGCHELSEN & VOS, [1966], Acta Cryst., 22, p.812.
- MIGCHELSEN & VOS, [1967], Acta Cryst., 23, p.796.
- MILLER, [1839], "A Treatise on Crystallography", J. & J.J. Deighton, Cambridge, U.K., (republished in expanded form in 1863 by Deighton, Bell & Co., Cambridge, U.K.).
- MINZER, [1949], Naturforsch., 49, p.11.
- MOONEY, [1935], Zeit. Krist., 90, p.143.
- MOONEY, [1937], Zeit. Krist., 98, p.377.
- MOONEY, [1940], J.A.C.S., 62, p.2995.
- MOONEY-SLATER, [1959], Acta Cryst., 12, p.187.
- MOORE & THOMAS, [1914], J.A.C.S., 36, p.192.

- NAUR, [1960], "Report on the Algorithmic Language ALGOL 60"
Regnecentralen, Copenhagen.
- NAUR, [1963], "Revised Report on the Algorithmic Language ALGOL 60",
Computer Journal, p.349.
- NOYES & LE BLANC, [1890], Z. physik Chem., 6, p.401.
- NUNN, [1964], Ph.D. Thesis, University of Tasmania.
- NYBERG, [1968], J. Chem. Phys., 48, p.4890.
- OCCAM, [1495], "Centiloquium theologicum", Lyons.
- OH, [1969], "The Direct Phasing Method", Internal Publication, School
of Chemistry, University of Sydney, NSW.
- PARSONS & CORCISS, [1910], J.A.C.S., 32, p.1367.
- PARSONS & WHITTIMORE, [1911], J.A.C.S., 33, p.1933.
- PATTERSON, [1934], Phys. Rev., 46, p.372.
- PATTERSON, [1935a], Zeit. Krist., 90, p.517.
- PATTERSON, [1935b], Zeit. Krist., 90, p.543.
- PAULING & SHAPPELL, [1930], Zeit. Krist., A75, p.128.
- PAULING, [1940], "The Nature of the Chemical Bond", Cornell University
Press, Ithica, New York.
- PELLETIER & CAVENTOU, [1819], Ann. chim., 10, p.164.
- PENFIELD & WHITE, [1959], Acta Cryst., 12, p.130.
- PERRIN, [1965], "Dissociation Constants of Organic Bases in Aqueous
Solution", I.U.P.A.C., Butterworths, London.
- PERSON, ANDERSON, FORDEMWALT, STAMMREICH & FORNERIS, [1961], J. Chem.
Phys., 35, p.908.
- PIMENTEL, [1951], J. Chem. Phys., 19, p.446.
- PLUMB & HORNIG, [1953], J. Chem. Phys., 21, p.366.
- PLUMB & HORNIG, [1955], J. Chem. Phys., 23, p.947.
- POPOV, [1967], "Halogen Chemistry", Volume 1, Academic Press, London &
New York.
- POST, [1964], International Union of Crystallography, Commission on
Crystallographic Apparatus, Bibliography 4.

- RAE, [1918], J. Chem. Soc., p.880.
- REDDY, KNOX & ROBIN, [1963], J. Chem. Phys., 40, p.1082.
- RIVETT & PACKER, [1927], J. Chem. Soc., p.1342.
- ROBIN, [1964], J. Chem. Phys., 40, p.3369.
- ROLLETT, [1965], "Computing Methods in Crystallography", Pergamon Press, Oxford.
- RØMMING, [1960], Acta Chem. Scand., 14, p.2145.
- ROSENBERG, [1964], J. Chem. Phys., 40, p.1707.
- ROUX & BOEYENS, [1969a], Acta Cryst., B25, p.1700.
- ROUX & BOEYENS, [1969b], Acta Cryst., B25, p.2395.
- RUNDLE, [1961], Acta Cryst., 14, p.585.
- RUNDLE, [1963], "Survey of Progress in Chemistry", Volume 1, Academic Press, London & New York.
- RUNSINK, SWEN-WALSTRA & MIGCHELSEN, [1972], Acta Cryst., B28, p.1331.
- SASANE, NAKAMURA & KUBO, [1967], J. Phys. Chem., 71, p.3249.
- SAYRE, [1952], Acta Cryst., 5, p.60.
- SCHWARTZENBACH & LUTZ, [1940], Helv. Chem. Acta, 23, p.1162.
- SHELL, [1959], Comm. A.C.M., 2, p.30.
- SHUGAM, AGRE & OBOZNENKO, [1967], Trudy Vsesoyuznogo Nauchno-Issledovatel'skogo Instituta Khimicheskikh Reaktivov (Transactions of the All-Union Institute concerning Chemical Reagents), 30, p.372.
- SIGWICK, [1950], "Chemical Elements and their Compounds", Volume 2, Oxford University Press.
- SKRABAL & FLACH, [1919], Monatshefte, 40, p.431.
- SLATER, [1959], Acta Cryst., 12, p.197.
- SOUTHWORTH, [1931], unpublished results cited by BANCROFT, SCHERER & GOULD, 1931.
- SNOOK, [1967], Thesis, University of Tasmania.
- STEPIN, PLYUSHCHEV & FAKKEEV, [1965], Russian Chemical Reviews, 34, p.811 (English Translation).

- STOUT & JENSEN, [1969], "X-Ray Structure Determination - a practical guide", Macmillan, Toronto.
- STRØMME, [1959], Acta Chem. Scand., 13, p.268.
- SUZUKI, YOKOYAMI & ITO, [1969], J. Chem. Phys., 50, p.3392.
- TASMAN & BOSWIJK, [1955], Acta Cryst., 8, p.59.
- THOMAS & UMEDA, [1957], J. Chem. Phys., 26, p.293.
- THOMAS, [1973], unpublished results, University of Tasmania.
- TILDEN, [1850], J. Chem. Soc., p.99.
- TOMAN, HONZL & JECNY, [1965], Acta Cryst., 18, p.673.
- TOPOL, [1967], Inorg. Chem., 7, p.451.
- TOWNES & DAILEY, [1952], J. Chem. Phys., 20, p.35.
- VAND & PEPINSKY, [1953], "The Statistical Approach to X-Ray Structural Analysis", State College, X-Ray & Crystal Analysis Laboratory of the Pennsylvania State University.
- VEDDER & HORNIG, [1961], J. Chem. Phys., 35, p.1560.
- WAGNER & HORNIG, [1950], J. Chem. Phys., 18, p.296.
- WEAST, [1967], "Handbook of Chemistry & Physics", 48th edition, Chemical Rubber Company, Cleveland, Ohio.
- WELLS & WHEELER, [1892], Am. J. Sci., 39, p.561.
- WELLS, WHEELER & PENFIELD, [1892a], Zeit. anorg. Chem., 1, p.442; and also Am. J. Sci., 44, p.475.
- WELLS, WHEELER & PENFIELD, [1892b], Zeit. anorg. Chem., 2, p.255; and also Am. J. Sci., 44, p.42.
- WELLS, [1962], "Structural Inorganic Chemistry", 3rd edition, Oxford University Press.
- WELLS, [1965], Acta Cryst., 19, p.173.
- WHEATLEY, [1960], Acta Cryst., 13, p.80.
- WIEBENGA, HAVINGA & BOSWIJK, [1961], Adv. inorg. Chem. & Radiochem., 3, p.133.
- WIEBENGA & KRACHT, [1969], Inorg. Chem., 8, p.738.
- WILKINSON, [1961], J. Assoc. Comp. Mach., 8, p.281.
- WILSON, [1942], Nature, 150, p.151.

WISE, [1971], Thesis, University of Tasmania.

WOOLFSON, [1961], "Direct Methods in Crystallography", Clarendon Press, Oxford.

WRINCH, [1938], Nature, 142, p.955.

WRINCH, [1939a], Phil. Mag., 27, p.98.

WRINCH, [1939b], Phil. Mag., 27, p.490.

WRINCH, [1950], Acta Cryst., 3, p.475.

WYCKOFF, [1924], "The Structure of Crystals", The Chemical Catalog Co., New York.

YAMASAKI, [1962], J. Phys. Soc. Japan., 17, p.1262.

ZACHARIESEN, [1952], Acta Cryst., 5, p.48.

ZASLOW & RUNDLE, [1957], J. Phys. Chem., 61, p.490.

Appendix A - Programming Details

	page
A - 1 Convention for representing ALGOL text	268
A - 2 Locally Introduced Standard Procedures in ALGOL F	268
A - 3 Least Squares Matrix Inversion in X24	269
A - 4 Index Permutation and Sorting in X16	273
A - 5 Listing of X16	276

A - 1 Convention for representing ALGOL text

Certain symbols employed by the ALGOL language are defined as being written in boldface text. As it is not normally possible to represent these symbols in boldface in a typewritten document, the convention of representing these symbols as underlined words has been followed.

A - 2 Locally Introduced Standard Procedures in ALGOL F

The standard procedures (that is, procedures which may be called without prior declaration) introduced locally into the Elliott ALGOL compiler fall into three classes:

- a) those intended to expand the set of numerical functions available to the programmer;
- b) those intended to facilitate input/output operations; and
- c) those designed to enable ALGOL programs resident in the Elliott 503 core to make use of the magnetic media bulk storage available on the PDP8/L machine.

Only those procedures which fall into the first class will be described here, the procedures in the other two classes did not materially affect the implementation of the numerical tasks required by the creation of the crystallographic suite, although they had some bearing on program organization. All the locally introduced standard procedures are documented in the Appendix to the 503 ALGOL Manual (reprinted by the University of Tasmania Photographic and Printing Service [1969]), the ALGOL F Reference Manual (Hydro-University Computing Centre [1972]), and in supplementary Bulletins issued by the Computer Centre.

The additional standard procedures included in class (a) above are:

integer procedure modulo(a,b); value a,b; integer a,b;

comment implements the following:

begin integer m;

if b<0 then print punch(3), \$MOD ERROR?, stop;

m:=a - (a div b) *b;

modulo:= if m<0 then m+b else m;

end;

boolean procedure even(i); value i; integer i;

comment takes the value true if i is even;

procedure clear(a); array a;

comment sets all the elements of array a to zero. Can be used to clear all types of arrays - the effect of clearing a boolean array is to set all elements false;

The sine and cosine routine has been replaced by a new routine which is faster (1 msec instead of 1.4 msec), more accurate (8 digits instead of 7) and which computes both sine and cosine at the same time. To take advantage of the last feature two new real procedures have been introduced:

real procedure sine;

comment yields the sine of the argument in the most recent call of sin, cos or tan;

real procedure cosine;

comment yields the cosine of the argument in the most recent call of sin, cos or tan;

A - 3 Least Squares Matrix Inversion in X24

The normal equations formed by the STRUCTURE FACTORS/LEAST SQUARES (X24) program can be written in matrix form (see Chapter 3, Section 3 - 10) as

$$A x = b$$

In this form, A is a symmetric positive definite coefficient matrix of order n , where n is the number of adjustable parameters in the least squares refinement. The inverse of this matrix is required, both for the calculation of the corrections to be applied to the adjustable parameters and also for the calculation of the parameter variances.

This matrix is symmetric, and as the accumulation of the matrix elements carries a greater penalty than does the inversion process, it is advantageous to build up only the $n(n+1)/2$ elements of the upper or lower triangle rather than the entire matrix. The time penalty is further reduced if the triangle elements are stored as elements of a one-dimensional vector instead of being held in a two-dimensional array. This is particularly relevant where ALGOL is used as the programming language, as array access time in this case is a sensitive function of the number of array subscripts. The Choleski process is usually favoured for the inversion of the normal equation matrix, as it has slightly greater precision in finite arithmetic than the process of Gaussian elimination (Wilkinson [1961]). As the original matrix is not required after inversion, the inversion routine does not need to build up the inverse in another array, but may make use of the storage used for the original matrix A for this purpose. Consequently, the matrix inversion routine employed by a crystallographic least squares refinement program is ideally one which will invert by the Choleski process either the upper or lower triangle of a symmetric positive definite matrix stored as a one-dimensional vector, preferably in its own space. The routine used in the X24 program is an ALGOL translation of a FORTRAN subroutine taken from the ancestral MONLS program. This routine meets the requirements indicated above, with the refinement that the algorithm required to map the two dimensional

matrix indices i, j into the one-dimensional vector index k is greatly simplified by storing the upper triangle elements in the vector in reverse order, i.e.

$V[1]$	contains	$A[n, n]$
$V[2]$	"	$A[n-1, n]$
$V[3]$	"	$A[n-1, n-1]$
$V[n(n+1)/2]$	"	$A[1, 1]$

This elegant matrix inversion routine was evidently written by Dr. J.B. White, formerly of Monash University. As this routine does not appear to have been published, it is presented here for reference in the form of an ALGOL procedure.

```

procedure symmetric matrix inversion(A,n,indic);
value n; integer n,indic; array A;
comment inverts the symmetric positive definite matrix held as an upper
triangle stored in reverse order in A[1:n]. The parameter indic=1 if
the matrix is found to be singular, otherwise 0. Written by J.B.White
in CDC 3200 FORTRAN, 503 ALGOL translation by A.J.T.Finnéy;
  begin integer nmi,i,j,loc,nrow,ncol,npiv,lpiv,npivm,np1;
    real amax,sinv;
    real array PCOL[1:n];
    boolean array ELIM[1:n];
    switch SS:=EX;

    nmi:=n-1; indic:=0;
    for i:=1 step 1 until n do ELIM[i]:=false;
    for i:=1 step 1 until n do
      begin amax:=0.0; loc:=1;
        for nrow:=1 step 1 until n do
          begin if abs(A[loc])>amax and
            not ELIM[nrow] then
            begin npiv:=nrow;
              lpiv:=loc;
              amax:=abs(A[loc])
            end;
            loc:=loc+nrow+1;
          end;
        if amax<10-12 then begin indic:=1; goto EX end;
        ELIM[npiv]:=true; sinv:=1.0/A[lpiv];
        if npiv≠n then
          begin loc:=lpiv+npiv;
            for nrow:=npiv step 1 until nmi do
              begin nrp1:=nrow+1;
                PCOL[nrp1]:=A[loc];
                PCOL[nrp1]:=-A[loc]*sinv;
                if ELIM[nrp1] then
                  PCOL[nrp1]:=-PCOL[nrp1];
                A[loc]:=0.0;
                loc:=loc+nrp1;
              end;
            end;
          end;
        end;
      end;
    end;
  
```

```

      if npiv#1 then
        begin loc:=lpiv-npiv+1;
              npivm:=npiv-1;
              for nrow:=1 step 1 until npivm do
                begin PCW[nrow]:=A[loc];
                      if ELIM[nrow] then
                        PCW[nrow]:=-PCW[nrow];
                        PCUL[nrow]:=-A[loc]*sinv;
                        A[loc]:=0.0; loc:=loc+1
                      end;
                end;
              A[lpiv]:=0.0; PCW[npiv]:=1.0; PCUL[npiv]:=sinv;
              loc:=1;
              for nrow:=1 step 1 until n do
                for ncol:=1 step 1 until nrow do
                  begin A[loc]:=A[loc]+PCW[nrow]*PCUL[ncol];
                        loc:=loc+1
                      end;
                end for n;
              end symmetric matrix inversion;
EX:

```

The matrix element index mapping algorithm is presented below as an ALGOL integer procedure; this algorithm is used in this form by the BOND LENGTHS & ANGLES (X26) program to extract from the least squares matrix inverse the elements which link positional parameters required in the computation of the estimated standard deviations of derived results.

```

integer procedure element(i,j,n); value i,j,n; integer i,j,n;
comment calculates the vector index k for the matrix element i,j of
the n*n matrix held as an upper triangle stored in reverse order in
a vector with bounds [1:n*(n+1)div2];
begin integer ij,ijd,k,jless;
      nm:=n*(n+1)div2;
      ij:=nm-i+1; ijd:=n-1; jless:=j-1;
      for k:=1 step 1 until jless do
        begin if k<i then
              begin ij:=ij-ijd; ijd:=ijd-1 end
            else ij:=ij-1;
          end;
      element:=ij
end element;

```

A typical call of this procedure would be:

$$x := V[\text{element}(i, j, n)];$$

the effect would be to access the element A_{ij} of the upper triangle of the $n \times n$ matrix A stored in reverse order in the vector $V[1 : n(n+1)/2]$, and then assign its value to the variable x .

A - 4 Index Permutation and Sorting in X16

The GENERAL FOURIER (X16) program is designed to allow the user to nominate the axis down which the synthesis sections will be calculated at selected intervals. This option makes necessary two operations which deserve further comment. The first operation concerns the permutation of the elements of the reflection index triple into a new order corresponding to the choice of section axis. This operation is a mandatory consequence of the structure of the algorithm used for the computation of the Fourier synthesis. The second operation, the sorting of a set of index triples into a sequence which reduces to a minimum the time taken for the calculation of a given section, is advantageous but not obligatory. During the development of the crystallographic suite, a number of programs used elsewhere were examined in some detail, and almost without exception those programs which incorporated these operations implemented them in an inefficient and sometime tortuous fashion. As the tasks incur a time penalty which may be significant when large data sets are being processed, the algorithms employed for their implementation in the X16 program are described.

The trivial task of permuting the index triple hkl into a specified order is accomplished in the X16 program using an indexing vector. The choice of the section axis which makes such a permutation necessary is made taking into account a number of considerations, including the cell

contents, the cell symmetry, the section area, the range of data, etc. Once the section axis is decided upon, the indices must be transposed so that the index associated with the section axis becomes the last element in the triple. The position of the remaining indices in the triple is left to the user to decide under the constraint of maintaining a right-handed axial system. The form in which the indexing vector is created is described below.

Let j_1, j_2, j_3 be three variables of type integer which refer to the three elements of the index triple, j_1 being associated with the first index position, j_2 with the second and j_3 with the last. The allowed values of j_1, j_2, j_3 are 1, 2 and 3, with the restriction that $j_1 \neq j_2 \neq j_3$. We employ the convention that the value 1 represents the index h , 2 represents the index k and 3 the index l . Thus to indicate the permutation of hkl to lkh , j_1, j_2, j_3 would have the values 3, 1, 2 respectively. Similarly the permutation of hkl to klh would be specified by the sequence 2, 3, 1.

The three j -values form part of the data for X16, and are referred to collectively as the 'permutation vector'. Internally they are held in an integer array $T [1 : 3]$, and are used to set up the inverse permutation vector held in a second integer array $PERM [1 : 3]$ by the execution of the statement

for $i := 1$ step 1 until 3 do $PERM [T[i]] := i;$

In the case of the first example given above, the two arrays will have the contents

T	3	1	2
PERM	2	3	1
	1	2	3

An example of the use of the inverse permutation vector to direct each element of n index triples into their correct positions in the integer

array INDEX [1 : n, 1 : 3] as they are read from the data tape is given below:

```

for i := 1 step 1 until n do
  for j := 1 step 1 until 3 do read INDEX [i, PERM[j]];

```

The tactic of creating the inverse permutation vector internally in the program has been found to reduce the number of mis-specifications of section axis made during data preparation (particularly by novice users) in contrast to the situation where it was left to the user to set up the inverse vector.

The second task, the sorting of index triples into a specified sequence, is undertaken to ensure that the Fourier synthesis algorithm is executed in minimum time. The execution time of the synthesis algorithm is minimized if the reflection data are sorted into blocks in which the leading index is constant, and within each block the data is arranged into sub-blocks in which the second index is constant. This arrangement of the data ensures that the last index changes most rapidly as the list of reflection data is processed, the intermediate index changes at an intermediate rate and the leading index changes most slowly. This arrangement of the data is accomplished by ordering the elements of a key vector into descending order of magnitude, ensuring that all operations performed on the key vector to achieve this end are also performed on the list of reflection data. The elements of the key vector consist of integers constructed from the index triple in two stages: first, the elements of the permuted index triple are made positive by the addition of a large positive integer to each, and second, the biased index triple elements are packed together into one computer word with the biased leading index occupying the most significant bit positions and the last index the least significant bit positions of the word. A key vector, made up of such elements, when sorted into ascending

or descending order, will arrange the reflection data in the desired sequence. The routine chosen for the sorting operation is the highly efficient algorithm developed by Shell (1959).

A - 5 X16 Listing

A photoreduction of a Flexowriter listing of the X16 program is reproduced on the following pages.

116 FUKUDA SYNTHESIS PROGRAM;

```

begin integer lines,i1,i2,i3, i,j,k,h,l,m,nx,ny,nz,px,py,ip,type,ireject,i1,i2,i3,icomu,freeino,preino,
funit,punit,lastsec,rcount;
real fzero,facale,scale,a,b,c,alpha,beta,gamm,mult,sthain,sthmax,rnom,conv,astar,betar,ctar,
alfstar,betstar,gamstar,calf,cbet,cgam,theta,nom,nomb,vol;
boolean cent,reject,paper,plot,supress,tape full;
real array TSM[1:3];
integer array PSM,IPSM[1:3],FLAL,PLUT[1:15],TITLE[1:10];
comment C85; integer array MULT[1:8],APARITY,SPAKITY[1:8,1:5],HULD,A,B,CUDE[1:2000];
switch 565:m1,J2,J3,J4,J5,J6,J7,J8,J9,UNSR;
switch KTYPE:m1,K2,K3,K4,K5;

procedure sendU(a,b); integer array a; array b;
begin integer array dum[1:1];
dum[1]:=size(b);
a[10]:=1; a[13]:=address(dum);
out4U(a);
a[10]:=dum[1]; a[13]:=address(b);
out4U(a);
end;

procedure get4U(a,b); integer array a; array b;
begin integer array dum[1:1];
a[10]:=1; a[13]:=address(dum);
in4U(a);
if dum[1]>size(b) then print '17TRANSFER TOO LARGE, ARRAY SIZE=7,digit(s),size(b),
' BULK SIZE=7,dum[1],'16??,atop;
a[10]:=dum[1]; a[13]:=address(b);
in4U(a);
end get4U;

procedure invert(a,b,c,alpha,beta,gamm,A,B,C,ALPHA,BETA,GAMMA,VUL); value a,b,c,alpha,beta,gamm;
real a,b,c,alpha,beta,gamm,A,B,C,ALPHA,BETA,GAMMA,VUL;
begin real vol,cosm,cosb,cosg,sinm,sinb,sing;
cosm:=cos(alpha); cosb:=cos(beta); cosg:=cos(gamm);
sinm:=sin(alpha); sinb:=sin(beta); sing:=sin(gamm);
vol:=1-U*cosm*cosm*cosb*cosb*cosg*cosg+2.U*cosm*cosb*cosg;
vol:=m*b*c*sqrt(vol);
ALPHA:=arccos((cosb*cosg*cosm)/sinb/sing);
BETA:=arccos((cosg*cosm*cosb)/sing/sinm);
GAMMA:=arccos((cosm*cosb*cosg)/sinm/sinb);
A:=m*c*sinm/vol; B:=m*a*sinb/vol; C:=m*b*sing/vol;
VUL:=vol;
end inversion;

procedure unpack(hkl,h,k,l); value hkl; integer hkl,h,k,l;
begin integer hh,kk,ll;
code 30 <+255> : 20 hh
20 kk : 16 ll
04 hkl : 23 ll
50 8 : 23 kk
50 8 : 23 hh
30 <+127> : 27 hh
27 kk : 27 ll;
h:=hh; k:=kk; l:=ll;
end;

integer procedure pack(h,k,l); value h,k,l; integer h,k,l;
begin code 30 h : 04 <+127>
55 8 : 16 h
04 k : 04 <+127>
04 h : 55 8
16 k : 04 l
04 <+127> : 04 k
16 pack :;
end pack;

procedure display(a); integer array a;
begin integer i,j,k,h; switch 56:m1,J2,J3;
switch TSM:m1,L2,L3,L4,L5,L6,L7,L8,KX;
for j:=0 step 1 until 7 do
begin print '127PARITY GRAP 7;
for k:=0 step -1 until 0 do
begin code 30 <+1> : 67 k
55 0 : 03 j
42 j1 : 40 j2;

```



```

J1:      print t17; goto J3;
J2:      print t07;
J3:
      end;
      print t177;
      for i:=1 step 1 until 6 do
        begin h:=c1*j+1; if h>0 then goto k2;
              goto TskMh1;
        L1:      print t-c117; goto k2;
        L2:      print t-c667; goto k2;
        L3:      print t-c67; goto k2;
        L4:      print t-c667; goto k2;
        L5:      print t-c167; goto k2;
        L6:      print t-c667; goto k2;
        L7:      print t-c667; goto k2;
        L8:      print t-c667; goto k2;
        k2:
          end;
      end for j;
      end display;

      sameline; lineprinter;

      comment read basic data;

      i:=1; instring(TITLE,i);
      read nx,ny,nz,yp,fzero,fscalo,scale,s,b,c,alpha,beta,gamm,mult,ip,type;
      cent:=p0;
      read ireject; reject:=reject0;
      if reject then
        begin goto KTYPE[ireject];
        K1:      read sthmx; goto K2;
        K2:      read sthmx; goto K2;
        K3:      read sthmx,sthmx; goto K2;
        K4:      read rnom;
        end;
      for i:=1 step 1 until 3 do read PNM[i];
      for i:=1 step 1 until 8 do read MULT[i];
      for i:=1 step 1 until 8 do for j:=1 step 1 until 8 do read APKITY[i,j];
      if not cent then for i:=1 step 1 until 8 do for j:=1 step 1 until 8 do read BPKITY[i,j];

      comment initializations;

      conv:=0.01745329;
      alpha:=alpha*conv; beta:=beta*conv; gamm:=gamm*conv;
      inver(a,b,c,alpha,beta,gamm,astar,betar,ctar,alfetar,betatar,gametar,vol);
      calf:=cos(alfetar); cbet:=cos(betar); cgam:=cos(gametar);
      TEMP[1]:=a; TEMP[2]:=b; TEMP[3]:=c;
      fscalo:=1.0/fscalo;
      fzero:=fzero*fscalo; xpimp=1; yp=yp-1;
      i1:=PNM[1]; i2:=PNM[2]; i3:=PNM[3];
      rnum:=1.0/2.0+1.0/3;
      for i:=1 step 1 until 3 do IPNM[i]:=PNM[i];
      i1:=IPNM[1]; i2:=IPNM[2]; i3:=IPNM[3];
      i:=i1; j:=i2;
      if i>j then begin i:=i2; j:=i1 end;
      if i=1 then begin if j=2 then theta:=gamm else theta:=beta end else theta:=alpha;
      nom:=TEMP[i]*(xp/nx); nomb:=TEMP[j]*(yp/ny);

      comment output synthesis type requested;

      tlines:=0;
      if type=1 then print 'CCT/PATTERSON ?' else
        begin if cent then print 'CCT/CENTRO ?' else print 'CCT/NUM.CENTRO?';
              print 'SYMMETRIC ?';
              if type=2 or type=3 then print 'C ?';
              if type=4 or type=5 then print 'VARIATION ?';
              if type=6 or type=7 then print 'DIFFERENCE ?';
              if type=8 or type=9 then print 'WEIGHTED DIFFERENCE ?';
        end;
      i:=1; print 'SYNTHESIS FIG. ?',instring(TITLE,i);

      comment read input/output media information;

      read ip, paper:=p0;
      print 'CCT/OUTPUT DATA INPUT FROM ?'; tlines:=tlines+1;

```

```

if paper then print SPAPIS TAPE? else
  print UDISK?;
read ip; plot:=pap;
print EEL76SECTION OUTPUT ON ?; tlines:=tlines+1;
if plot then
  print UDISK AND LINEPRINT?
  else print LINEPRINT ONLY?;
read ip; suppress:=pap;
if suppress then print EEL76NEGATIVE REGIONS OF OUTPUT SUPPRESSED?
  else print EEL76NO SUPPRESSION OF OUTPUT?; tlines:=tlines+1;

comment output orientation information;

print EEL76SECTION ORIENTATION AND INDEX PERMUTATIONS EEL76THE (VERTICAL) X-AXIS LENGTH IS ?,
  freopoint(4),nom,E ANGSTROM?;
  EEL76THE (HORIZONTAL) Y-AXIS LENGTH IS ?,nom,E ANGSTROM? EEL76THE INTERAXIAL ANGLE IS ?,
  theta/conv,E DEGREES?;
  EEL76THE SYNTHESIS WILL BE CALCULATED WITH SECTIONS DOWN THE ORIGINAL ?;
if i3=1 then print EA-? else if i3=2 then print EB-? else print EC-?; print EAXIS?;
print EEL76THE INDEX PERMUTATION IS FROM HKL TO ?;
for i:=1 step 1 until 3 do if iPERM[i]=1 then print EH? else if iPERM[i]=2 then print EK? else print EL?;
tlines:=tlines+3;

comment display trigonometric expression for A coefficients;

print EEL76A-COEFFICIENT TRIGONOMETRIC EXPRESSIONS EEL76;
display(APAKITY);
tlines:=tlines+12;
if cent then goto INK;

comment display trigonometric expression for B coefficients;

print EEL76B-COEFFICIENT TRIGONOMETRIC EXPRESSIONS EEL76;
display(BPAKITY);
tlines:=tlines+12;

comment display multiplicities;

print EEL76INDEX CLASS MULTIPLICITIES EEL76;
for j:=1 step 1 until 7 do
  begin print EEL76INDEX CLASS ?;
    for k:=2 step -1 until 0 do
      begin code 30 <+> : 67 k
        55 U : 03 J;
        42 J7 : 40 J8;
      J7: print EU7; goto J9;
      J8: if k=0 then print EL? else if k=1 then print EK? else print EH?;
      J9:
        end;
      print EEL76,digits(4),MULT[j+1],
    end;
  tlines:=tlines+12;

begin comment segment[1]..... subprogram to input, store and sort reflection data .....;
  integer ph,ph,pl,r,r,rl,rl,kl,m,t,t,az,a3,a4,b1,b2,b3;
  real modf,weight,w,alpha,mwifo,modfc,dol,sth1,t,t,t4;
  comment (B5); integer array hxy[1:2000]; real array PLATA[1:7];
  integer array ABITS,BBITS[1:4],INDEX[1:13];
  switch dd6:=MINXT,IIAST,SKIP;
  switch INPUT:=1,12,13,14,15,16,17,18,19,12;
  switch h3,M.T:=k1,k2,k3,k4,k2;
  switch SYNTH:=s1,s2,s3,s4,s5,s6,s7,s8,s9,s2;
  switch PAKJLT:=P1,P2,P3,P4,P2;

  real procedure Arctan(y)divided by:(x), value x,y; real x,y;
  begin comment finds angle in radians, in range 0 < Arctan < 2pi;
    real w,pi,piy4; Boolean yneg;
    pi:=3.141592654; piy4:=1.570796327;
    if y=0,0 then
      begin w:= (if abs(x)<abs(y) then piy4-arctan(x/y) else arctan(y/x));
        yneg:=y<0,0; x:=x*y;
        if x<0,0 or yneg then w:=w+pi;
        if x>0,0 and yneg then w:=w-pi;
      end
    else w:= (if x<0,0 then pi else 0,0);
    Arctan:=w;
  end Arctan;

```



```

K1:      if eth1>ethmx then begin rcr:=rcr+1; goto INXT and else goto K2;
K2:      if eth1<ethmn then begin rlcse:=rlcse+1; goto INXT and else goto K2;
K3:      if eth1>ethmx then begin rcr:=rcr+1; goto INXT and;
          if eth1<ethmn then begin rlcse:=rlcse+1; goto INXT and else goto K2;
K4:      t:=1+sin(2*0) then abs(dol)/modf also 0.20;
          if <rhom then begin rcr:=rcr+1; goto INXT and else goto K2;
          end rejection;

comment compute a,b for synthesis type;

K12:     if type=5 or type=7 or type=9 then alpha:=Arctan(b,a);
          if type=6 or type=8 then
              begin t1:=sin(alpha); t2:=t1*t1;
                  t3:=sin(alpha)*sin(alpha); t2:=t2*t2;
                  weight:=if (t2<t1) then 0.0 then 0.0 else t2/(t2+t1);
              end;
          goto SYNTH type;
S1:      a:=modf(modf; b:=0.0; goto S2;
S2:      a:=a; b:=0.0; goto S2;
S3:      a:=cos(alpha)*a; b:=sin(alpha)*a; goto S2;
S4:      a:=modf(a*sign(a); b:=0.0; goto S2;
S5:      a:=modf(a; goto S3;
S6:      a:=del*sign(a); b:=0.0; goto S2;
S7:      a:=abs(dol); goto S3;
S8:      a:=del*weight*sign(a); b:=0.0; goto S2;
S9:      a:=abs(dol)*weight; goto S3;
S12:     rcount:=rcount+1;
          if rcount>2000 then begin finalize; print 'C151377U MANY REFLECTIONS - RUN AXD01577,stop;end;

comment apply multiplicity. index class order is: 000,00L,00U,0KL,00U,0UL,00U,0KL;

j:=1;
j:=if h=0 then j else j+4;
j:=if h=0 then j else j+2;
j:=if l=0 then j else j+1;
a:=a*MULT[j]; b:=b*MULT[j];

comment permute a copy of the indices and store in KEY for sorting into synthesis order;

INDX[1]:=h; INDX[2]:=k; INDX[3]:=l;
ph:=INDX[1]; pk:=INDX[2]; pl:=INDX[3];
KEY[rcount]:=pack(ph,pk,pl); HULH[rcount]:=pack(h,k,l); A[rcount]:=a; B[rcount]:=b;
goto INXT;

comment output rejection statistics;

11A5T:   if not paper then close(PCAL);
          print 'C137REFLECTION SELECTIONS/27REFLECTIONS RETAINED/77,digits(4),rcount; tlines:=tlines+6;
          if not reject then print 'C137NO REFLECTIONS REJECTED? else
              begin print 'C137REFLECTION CRITERION IS ?;
                  goto PSECTI reject;
P1:      print 'C137REFLECTIONAL VECTOR >7,freepoint(4),ethmx; goto P2;
P2:      print 'C137REFLECTIONAL VECTOR <7,freepoint(4),ethmn; goto P2;
P3:      print 'C137REFLECTIONAL VECTOR <7,freepoint(4),ethmn,OR >7,ethmx; goto P2;
P4:      print 'C137REFLECTION K-FACTOR >7,freepoint(4),rhom*100.0;
P2:      tlines:=tlines+2;
          if rejected1 or rejected2 or rejected3 then
              begin print 'C137REFLECTIONS ABOVE UPPER THRESHOLD/77,digits(4),rcr; tlines:=tlines+1 end;
          if rejected2 or rejected3 then
              begin print 'C137REFLECTIONS BELOW LOWER THRESHOLD/77,digits(4),rlcse; tlines:=tlines+1 end;
          end;

comment sort indices on KEY;

for i:=1 step 1 until rcount do m:=2*-1;
for m:=m+2 while m<0 do
    begin k:=count-m;
        for j:=1 step 1 until k do
            begin for i:=j step -m until 1 do
                    begin if KEY[i+m]>KEY[i] then goto SKIP;
                        t:=KEY[i]; KEY[i]:=KEY[i+m]; KEY[i+m]:=t;
                        t:=HULH[i]; HULH[i]:=HULH[i+m]; HULH[i+m]:=t;
                        t:=A[i]; A[i]:=A[i+m]; A[i+m]:=t;
                        t:=B[i]; B[i]:=B[i+m]; B[i+m]:=t;
                    end;
                SKIP:
            end;
        end;
    end;
end;

```

present period indices are in synthonic order in KEY, unpresented indices and synthonic coefficients are not listed in the same order in HILL, AB respectively. Now compute the space group code word;

```

for i:=1 step 1 until count do
  begin unpack(HULL[i],h,t,i);
    j:=1;
    j:=if even(h) then j else j+4;
    j:=if even(k) then j else j+2;
    j:=if even(l) then j else j+1;

    comment parity group order is: eee,eee,eee,ooo,ooo,ooo,ooo,ooo, now pick up code word elements;

    t1:=0;
    for m:=1 step 1 until 8 do
      begin k:=BPAKITY[j,m];
        if k#0 then begin l:=if k>4 then BBITS[k-4] else ABITS[k]; t1:=t1+l end;
        if not cent then
          begin k:=BPAKITY[j,m];
            if k#0 then begin l:=if k>4 then BBITS[k-4] else ABITS[k]; t1:=t1+l end;
          end;
        end;
      CWD[i]:=t1;

    comment now replace unpermuted indices with permuted indices, so that KEY can be collapsed;

    HULL[i]:=KEY[i];

  end;
j:=61-tlines;
for k:=1 step 1 until j do print k*177;

end ***** subprogram to input, store and sort data *****

```

```

goto LL2;
LL3:  UA[apage]:=mp;  L1N5[apage]:=j;  poffset:=totaloff/apage;  offspaces:=mpoffset/(binterval/5.0);

      comment establish number of pages to span b-direction (across the page);

      i:=0;  bpage:=1;
LL4:  LB[bpage]:=i;  j:=offspaces;
LL5:  i:=i+1;
      if i>yp then goto LL6;
      j:=j+5;
      if j>100 then
        begin i:=i-1;  UB[bpage]:=i;
              bpage:=bpage+1;  goto LL4
        end;
      goto LL5;
LL6:  UB[bpage]:=yp;

      comment establish individual line offsets for a standard page of output;

margin:=7;  ua:=UA[1];
th:=if rect then 0 else (ainterval*ua*sin(phi))/(binterval/5.0);
margin:=margin+(100-(UB[1]*5+th))/5;  ua:=UA[1];
for i:=0 step 1 until ua do
  begin if rect then UF[i]:=margin else
        begin j:=if obtuse then ua-1 else 1;
              t:=interval*j*sin(phi);
              UF[i]:=margin+t/(binterval/5.0);
        end;
  end;

      comment output identification to disk;

if plot then
  begin PLUT[10]:=10;  send40(PLUT,TITLE);
        DIM[1]:=mp;  DIM[2]:=yp;
        PLUT[10]:=2;  send40(PLUT,DIM);
        SIZE[1]:=nom;  SIZE[2]:=theta;  SIZE[3]:=nom;
        PLUT[10]:=3;  send40(PLUT,SIZE);
        tape full:=false;
        code 30 <PLUT> : 16 i;
        PLUT[1]:=1;  PLUT[7]:=0;  open(PLUT);
        end identification;

      comment commence reading section numbers;

NEWSEC:  read secno;
if secno<0 then goto EXIT;
if plot then
  begin DIM[1]:=secno;  PLUT[10]:=1;  send40(PLUT,DIM) end;
clear(DEUM1);  clear(DEUM2);  clear(PAUR);  c1:=c2:=c3:=c4:=c5:=c6:=c7:=c8:=c9:=0;  marker:=0;
sint:=secno/ns;  count:=1;
unpack(HOLD[1],th,tk,tl);  a:=A[1];  b:=B[1];  cword:=UD[1];

      comment commence first summation;

SKIP:  h:=th;  k:=tk;  l:=tl;
BACK:  aarg:=sin(6.2831853*tl*sint);  carg:=cosine;
      ca:=a*aarg;  cb:=a*carg;  c1mb*carg;  cdmb*aarg;
      if a=0.0 then goto L4;
      code 30 <+1> : 03 cword
      42 L1 : ;
      c1:=c1+ca;  comment +Acce term;
      code 30 <+2> : 03 cword
      42 L2 : ;
      c2:=c2+cb;  comment -Acce term;
      code 30 <+4> : 03 cword
      42 L3 : ;
      c3:=c3+cb;  comment -Acce term;
      code 30 <+8> : 03 cword
      42 L4 : ;
      c4:=c4+ca;  comment +Acc term;
      if b=0.0 then goto L4;
      code 30 <+16> : 03 cword
      42 L5 : ;
      c1:=c1+cd;  comment +Bcca term;

```

```

L5:      code 30 <+34> : 03 cword
          42 L6 : ;
          c2:=c2+cc;      comment +Base term;
L6:      code 30 <+64> : 03 cword
          42 L7 : ;
          c3:=c3+cc;      comment +Base term;
L7:      code 30 <+128> : 03 cword
          42 L8 : ;
          c4:=c4+cc;      comment +Base term;
L8:      count:=count+1; if count>count then begin marker:=1; goto SUM2 end;
          unpack(HULL[count],th,tk,t1); a:=A[count]; b:=B[count]; cword:=CDD[count];
          if hath then goto SUM2; if k=tk then goto BACK;

          comment second summation;

SUM2:     code 26 yint : 26 j
          06 0 : 05 yp
          16 jcount : ;

LALUP:    arg:=sin(6.2831853*k*yint); carg:=cosine;
          code 30 arg : 63 c2
          16 arg : 04 carg
          63 c1 : 60 arg
          16 arg : 04 j
          04 DSUM1 : 20 p
          16 4 : 04 0
          60 arg : 67 p
          16 0 : 04 arg
          63 c4 : 16 arg
          04 carg : 63 c3
          60 arg : 16 arg
          04 DSUM2 : 04 j
          16 p : 67 p
          04 0 : 60 arg
          67 p : 16 0
          04 yi : 60 yint
          16 yint : 22 j
          32 jcount : 41 LALUP;

          code 26 c1 : 26 c2
          26 c3 : 26 c4
          30 marker : 05 <+1>
          42 SUM3 : 43 4;
          if hath then goto SKIP;

          comment third summation;

SUM3:     code 26 j : 06 0
          05 yp : 16 jcount;

JLALUP:    code 26 i : 06 0
          05 xp : 16 jcount
          26 xint : 04 j
          04 DSUM1 : 16 p
          67 p : 04 0
          16 ca : 04 j
          04 DSUM2 : 16 p
          67 p : 04 0
          16 cb : 43 9;

ILALUP:    arg:=sin(6.2831853*h*xint); carg:=cosine;
          code 30 ca : 63 carg
          16 arg : 04 cb
          63 arg : 60 arg
          16 arg : 02 yp
          52 i : 57 0
          04 FILL : 04 j
          16 q : 67 q
          04 0 : 60 arg
          67 q : 16 0
          04 xi : 60 xint
          16 xint : 22 i
          32 icount : 41 ILALUP
          22 j : 32 jcount
          41 JLALUP : 43 14;

          clear(DSUM1); clear(DSUM2); if marker=0 then goto SKIP;

```

```

comment scale synthesis section prior to output;

for i:=1 step 1 until xp do for j:=1 step 1 until yp do
  begin t:=FUK[i,j]; t:=(t+zero)*mult/vol; t:=t*scale;
    FUK[i,j]:=t;
  end;
if plot and not tape full then
  begin section out(xp,yp,tape full,total);
    if tape full then
      begin DIM[i]:=1; PLUT[10]:=1; send4U(PLUT,DIM) end
    else lastsec:=secno;
  end;

comment output section, and then return for the next;

for ia:=1 step 1 until apage do for ib:=1 step 1 until bpage do
  begin i:=1; print FFI2577,outstring(TITLE,i);
    la:=LA[ia]; lb:=LB[ib]; ua:=UA[ia]; ub:=UB[ib];
    print F SECTION AT 7,digits(3),special(1),leadzero(7),secno,E/7,nx,FFI177HORIZONTAL FROM 7,
    lb,E/7,ny,E TU 7,ub,E/7,ny,E sed7VERTICAL FROM 7,la,E/7,nx,E TU 7,ua,E/7,nx,FFI277;
    for i:=la step 1 until ua do
      begin k:=1; k:=KFF[k];
        for j:=1 step 1 until k do print F 7;
        for j:=lb step 1 until ub do
          begin f:=FUK[i,j];
            if supres then
              begin if f<0 then
                begin if i=la or i=ua or j=lb or j=ub then
                  print F *? else print F ?
                end
                else if f>999 then print F ****? else
                  print F 7,digits(3),f,j;
                end else if abs(f)>999 then print F ****? else print F 7,digits(3),f,j;
              end;
            if i=ua then for k:=1 step 1 until lines do print FFI77;
          end;
          k:=KLNES[ia]; j:=61-k;
          for i:=1 step 1 until j do print FFI77;
        end;
      goto NEW68;
EXIT: if plot and not tape full then
  begin DIM[i]:=1; PLUT[10]:=1; send4U(PLUT,DIM) end;

end ***** subprogram to compute synthesis *****;

if not paper or plot then finalize;
if plot then print FFI307LAST SECTION WRITTEN TO DISK WAS NUMBER 7,digits(3),lastsec,FFI2577;
end of program;

```


Appendix B - Density Determinations

	page
B - 1 Density Determinations	287
B - 2 Density Determination of RbI_3	289
B - 3 Density Determination of $\text{KI}_3 \cdot \text{H}_2\text{O}$	290

B - 1 Density Determinations

The determination of the density of crystalline solids by the pycnometric method depends upon measurement of the volume of liquid (the 'working fluid') displaced by a known weight of the solid material. The pycnometric vessels used in the determinations reported in this work were an adaption of the familiar specific gravity bottle. In place of the narrow stopper with its central capillary there is a wider solid ground glass stopper for ease of addition of solid. A separate vertical capillary side-arm communicates with the interior of the vessel (Figure B - 1). This pycnometer was designed by the writer with a view to facilitating the determination of the density of crystalline material by students involved in laboratory exercises which call for the characterization of inorganic preparations. In this context the design has proved to be very successful, as not only can good results be obtained with reasonable attention to technique, but also the pycnometers can be readily fabricated in quantity by a competent glassblower. There is also some pedagogic value in the fact that each pycnometer must be individually calibrated by the user.

The two pycnometers used for these determinations were calibrated with distilled water at 25.0°C; their calibrated volumes at this temperature are given below:

Pycnometer A (weight = 13.9421 gm)	Capacity at 25°C	11.3491 cc
Pycnometer B (weight = 14.5602 gm)	Volume at 25°C	9.6974 cc

The density of distilled water at 25°C was taken as 0.997044 gm/cc (Handbook of Chemistry and Physics, Weast [1967]). The slightly larger weight of Pycnometer B, which has the smaller volume, is due to its more massive stopper.

The steps in the procedure for the determination of the density of a sample of crystalline material are given below. The symbols used here also serve to identify the quantities recorded in the Tables which follow.

- (a) The pycnometer was cleaned, dried and weighed and its weight recorded (w_1).
- (b) It was then filled with the working fluid and suspended in a water thermostat and allowed to reach thermal equilibrium. Excess working fluid was removed from the top of the capillary side-arm by gentle wiping with the edge of a disk of filter paper. When the pycnometer had reached the bath temperature (25.0°C), it was removed and dried carefully with an absorbent tissue and reweighed (w_3). The difference between w_2 and w_1 gave the weight of the working fluid w_2 contained in the pycnometer, from which its density (ρ_1) could be calculated from the known volume of the vessel at the thermostat temperature.
- (c) Some of the working fluid was then carefully removed with a pipette, and the pycnometer was weighed again (w_4).
- (d) The solid was then added and the pycnometer placed in an upright position in a vacuum desiccator which was then partially evacuated to remove any air bubbles adhering to the crystals. When the crystals were judged to be free of attached air bubbles, the pycnometer was reweighed (w_5). The difference between w_5 and w_4 gave the weight of the crystals (w_6) added to the pycnometer.
- (e) The pycnometer was then refilled with the working fluid and returned to the thermostat. Upon equilibration it was removed, carefully dried as before and reweighed (w_7). The weight of displaced working fluid (w_8) contained in the pycnometer was then calculated as the difference:

$$w_8 = w_7 - (w_1 + w_6).$$

The weight of displaced working fluid could then be calculated as the difference between w_3 and w_8 :

$$w_9 = w_3 - w_8$$

The density of the crystals was then calculated from the relation:

$$\rho_2 = (w_6 \cdot \rho_1) / w_9$$

B - 2 Density Determination of RbI_3 (working fluid iodine-saturated paraffin oil)

Quantity	Determination 1	Determination 2	Determination 3	Determination 4
w_1 (gm)	13.9419	13.9420	14.5600	14.5604
w_2 (gm)	24.0358	24.0563	23.1994	23.2047
w_3 (gm)	10.0939	10.1143	8.6394	8.6433
ρ_1 (gm/cc)	0.8894	0.8912	0.8909	0.8913
w_4 (gm)	20.1778	18.3411	16.4175	20.8392
w_5 (gm)	21.1990	19.2024	17.1606	21.8429
w_6 (gm)	1.0212	0.8613	0.7431	1.0037
w_7 (gm)	24.8580	24.7501	23.7978	24.0118
w_8 (gm)	9.8949	9.9468	8.4947	8.4477
w_9 (gm)	0.1990	0.1675	0.1447	0.1956
ρ_2 (gm/cc)	4.563	4.583	4.577	4.573

Average value RbI_3 density = 4.574 gm/cc

B - 3 Density Determination of $KI_3 \cdot H_2O$

(Determinations 1 & 2 working fluid - iodine saturated
perfluorokerosene)

(Determinations 3, 4 & 5 working fluid - iodine saturated
paraffin oil)

Quantity	Determin- ation 1	Determin- ation 2	Determin- ation 3	Determin- ation 4	Determin- ation 5
w_1 (gm)	13.9423	14.5602	13.9423	14.5602	13.9421
w_2 (gm)	36.1253	33.5090	24.0544	23.2034	24.0553
w_3 (gm)	22.1832	18.9488	10.1121	8.6432	10.1132
ρ_1 (gm/cc)	1.9546	1.9540	0.8910	0.8913	0.8911
w_4 (gm)	31.6651	31.2155	18.3716	19.4318	20.0376
w_5 (gm)	32.1785	32.0223	19.1031	19.9622	20.8988
w_6 (gm)	0.5134	0.8068	0.7315	0.5304	0.8612
w_7 (gm)	36.3271	33.9052	24.6051	23.5870	24.7035
w_8 (gm)	21.8716	18.4844	9.9313	8.4963	9.9002
ρ_9 (gm)	0.3116	0.4644	0.1808	0.1309	0.2130
ρ_2 (gm/cc)	3.217	3.394	3.605	3.610	3.603

Average value Determinations 1 & 2 = 3.306*

Average value Determinations 3, 4 & 5 = 3.606 gm/cc

* This value is low due to the incomplete removal of attached air bubbles.
The relative merits of the two pycnometric fluids have been discussed in
Chapter 6, Section 6 - 3.

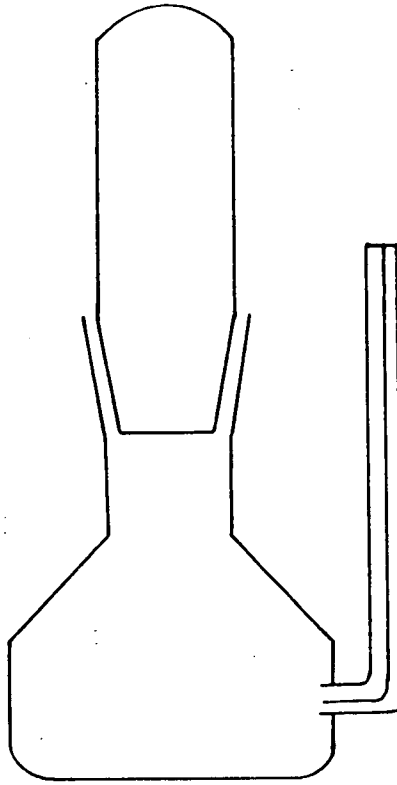


Figure B - 1. Diagram of the density bottle used for the pycnometric determination of crystal densities. Note the wide mouth for ease of addition of the sample.

Appendix C - The Derivation of the Unit Cell Constants of
 $\text{KI}_3 \cdot \text{H}_2\text{O}$.

C - 1 The derivation of the Unit Cell Constants of $\text{KI}_3 \cdot \text{H}_2\text{O}$

It is necessary in this detailed description of the derivation of the unit cell constants of $\text{KI}_3 \cdot \text{H}_2\text{O}$ to refer to geometrical information contained in specific X-ray photographs. At the suggestion of the author, all X-ray exposures made in this laboratory receive a unique alphanumeric code for purposes of identification. This code will be used here to nominate the exposures of interest; these are listed below:

- Orientation I :
- MG37 - oscillation photograph
 - MG38 - zero level weissenberg photograph
 - MG39 - first level weissenberg photograph
 - MG40 - second level weissenberg photograph
- Orientation II :
- MG17 - oscillation photograph
 - MG19 - zero level weissenberg photograph
 - MG20 - first level weissenberg photograph.

(As can be seen, the code consists of two alphabetic characters followed by a number; normally the first character of the code will remain constant throughout a study of a given compound but the remainder of the code will change). All directions and dimensions are expressed in terms of the reciprocal lattice and reciprocal lattice units unless otherwise indicated. To simplify discussion, only the axes of the final unit cell are labelled a^* , b^* , c^* - the axes of intermediate cells which do not coincide with those of the final cell are labelled differently, e.g. p^* , q^* .

Figure C - 1 is a perspective view of the reconstructed reciprocal lattice for $\text{KI}_3 \cdot \text{H}_2\text{O}$ in Orientation II (see Chapter 6, Section 5); this diagram also shows the relationship of the oscillation axis to the axial system of the lattice. The geometry of the $p^* a^*$ reciprocal net $a^* =$

0.170, $p^* = 0.105$, $\phi^* = 74^\circ$) was derived from polar plots of the zero and first level weissenberg photographs MG19 and MG20 respectively. The relative displacement of the nets was determined from a consideration of the axial row offsets on these photographs of adjacent levels (Buerger [1962]), taken together with the value of the layer line spacing $\zeta = 0.052$ measured from the oscillation photograph MG17.

Figure C - 2 presents the reconstructed reciprocal lattice for Orientation I viewed from the same direction as the lattice shown in Figure C - 1. As before, the oscillation axis direction is shown. The geometry of the b^*c^* reciprocal net ($b^* = 0.070$, $c^* = 0.078$, $\alpha^* = 90^\circ$) was determined from the weissenberg exposures MG38 and MG39. In Figure C - 3 an enlarged view of the relationship between the Orientation I and Orientation II cells is given. It can be seen that the p^* -axis of the Orientation II cell lies in the $\{0\bar{1}1\}$ direction of the Orientation II cell, thus forming a diagonal of the b^*c^* net. This is confirmed by a calculation of the reciprocal lengths involved; from Figure C - 3:

$$\begin{aligned} p^* &= (b^{*2} + c^{*2})^{1/2} \\ &= (0.070^2 + 0.078^2)^{1/2} \\ &= 0.10984^{1/2} \\ &= 0.1048 \approx 0.105 \text{ determined from MG19} \end{aligned}$$

The relative displacement of the b^*c^* planes as initially determined from the axial row offsets on the first level (MG39) and second level (MG40) weissenberg exposures gave a cell with a monoclinic angle of 88° , the a^* -axis of the Orientation II cell lying in the $\{101\}$ direction of the reciprocal cell defined by $q^*b^*c^*$ thus forming a diagonal of the q^*c^* net.

Although these two cells could be satisfactorily related to one another, so that the relationship of Orientation II with respect to

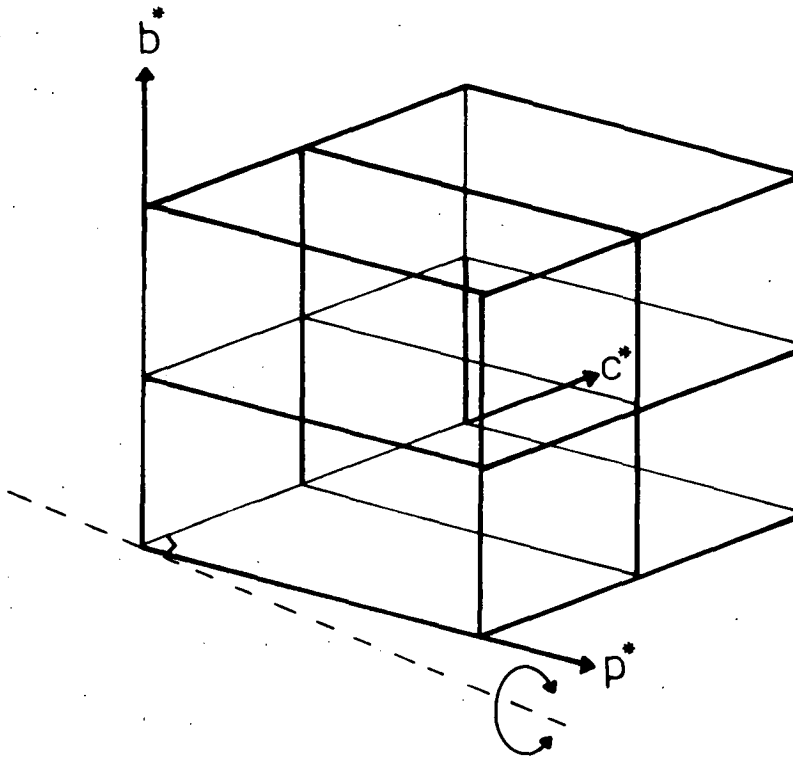


Figure C - 1. Reconstructed Orientation II reciprocal lattice.

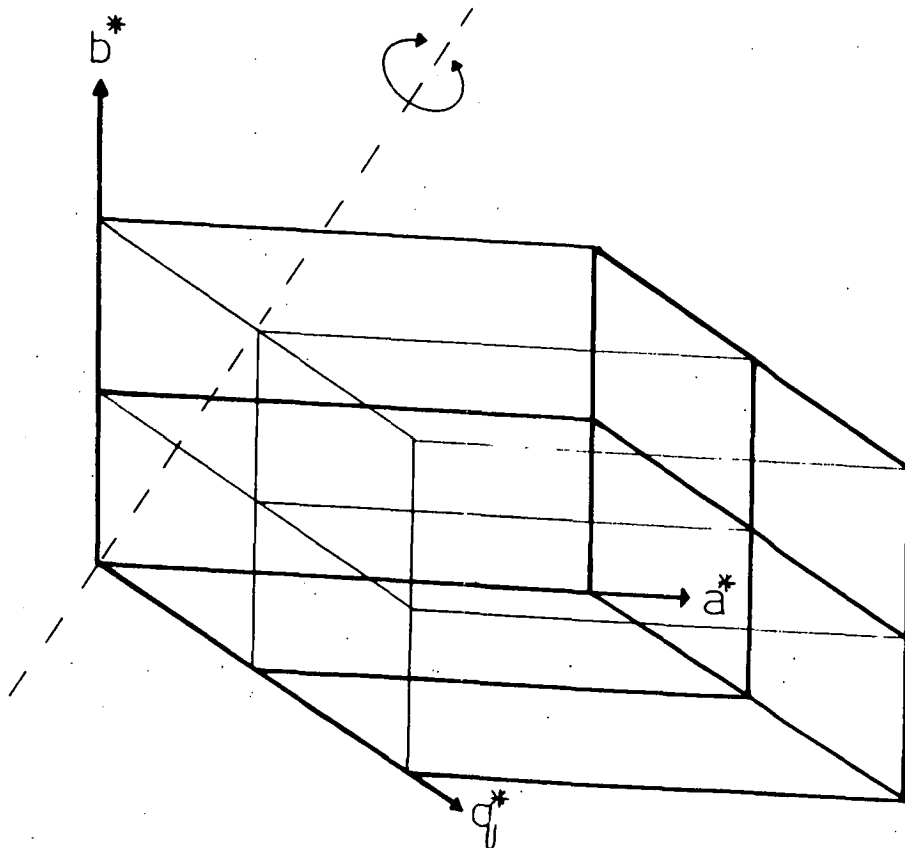


Figure C - 2. Reconstructed Orientation I reciprocal lattice.

Orientation I was effectively fixed; the monoclinic cell $q^* b^* c^*$ gave a systematic absence pattern in the $q^* c^*$ plane which did not correspond to an allowed absence pattern for a primitive monoclinic cell in the second setting. Also, a critical comparison of the intensities of equivalent reflections showed that spots which should have had equal intensity were in fact not equal. Although the reflections on the MG38 - MG40 exposures were affected by absorption, which was apparent as a decrease in intensity from the edge towards the centre of strong reflections, the effect was not sufficiently severe to vitiate this comparison. The peculiarity of the systematic absence pattern and the non-equivalence of what should have been equivalent reflections pointed to the mis-identification of the axial rows on the upper level photographs MG39 and MG40. By changing to the cell defined by $a^* b^* c^*$ (refer Figure C - 4) the absence pattern transformed to that required by the monoclinic space groups Pc , $P2/c$, and the equivalent reflections showed the correct intensity relationships about the now correctly identified axial rows.

The interaxial angle could now be calculated directly by making use of the $\zeta = 0.152_5$ calculated from the layer-line spacing of the oscillation photograph MG37, together with the previously determined length of the reciprocal interval a^* :

$$\begin{aligned}\sin \beta^* &= 0.1525/0.170 \\ &= 0.8971 \\ \beta^* &= 63.8^\circ\end{aligned}$$

The final direct cell parameters were calculated to be $a = 4.868$, $b = 10.152$, $c = 9.852 \text{ \AA}$ and $\beta = 116.2^\circ$. This unit cell does not possess the axial ratio or interaxial angle reported for $KI_3 \cdot H_2O$ by Wells, Wheeler and Penfield [1892], and it was not possible to derive a direct non-primitive cell which simultaneously possessed both

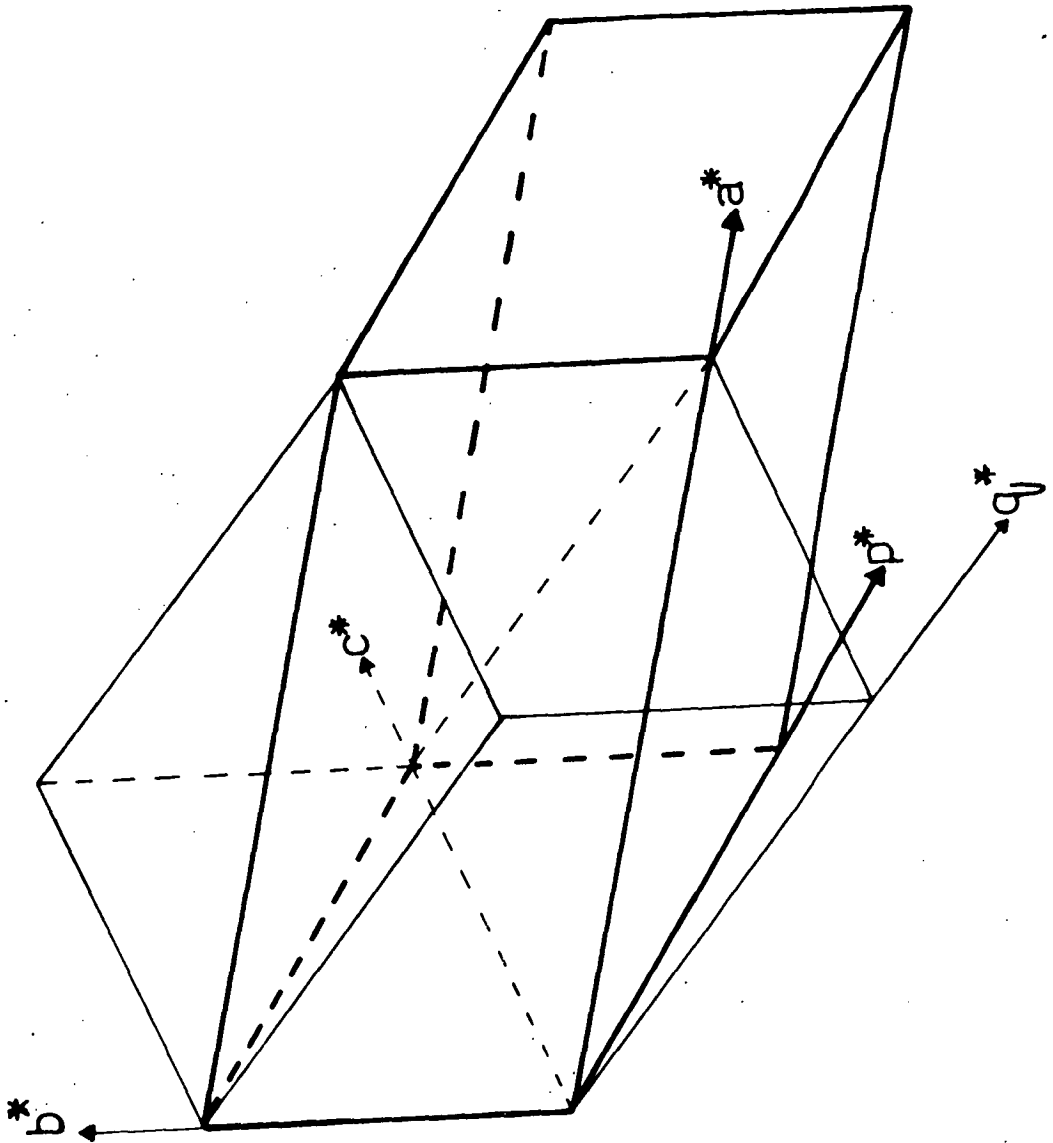


Figure C - 3. Inter-relationship of the Orientation I & Orientation II reciprocal cells.

properties. As the macroscopic crystallographic interpretations of these workers are reliable in other cases (e.g. CsI_3 , RbI_3 , etc.) it is concluded that their goniometric data are not accurate due to the experimental difficulties encountered when working with crystalline $\text{KI}_3 \cdot \text{H}_2\text{O}$ in the open laboratory.

Appendix D - I_3^- force constant Calculation

	page
D - 1 Overlap calculations	300
D - 2 Force Constant Calculation	300
D - 3 Disturbing Forces Calculation	304
D - 4 Estimation of pK_a for C_6H_5CN	305
D - 5 $[C_6H_5CNH^+]$ at the crystallization point of $HI_{3.4}(C_6H_5CN)$	310

D - 1 Overlap Calculations

The 5p σ overlap integrals for iodine used in Section 7 - 2 - 1 of Chapter 7 were calculated using an ALGOL F program which closely follows a GIER ALGOL program written by Johansen [1965] for the evaluation of overlaps between orbitals represented by linear combinations of Slater-type orbitals. The program evaluates the overlap integral where the orbital functions are centered respectively on centre a and centre b , and where the coordinate systems are given in the usual way with the x - and y -axes parallel and the z -axes pointing against each other (Ballhausen [1962]); the ϕ -dependencies are integrated out as ϕ is common ($\phi_a = \phi_b = \phi$) and the θ -dependencies are normalized Legendre polynomials in $\cos \theta_a$ and $\cos \theta_b$. A check on normalization is performed when the orbital functions are made up of more than one Slater type orbital. The program calculates the specified overlap for the given orbital functions over a range of r_{ab} , the upper and lower limits of this range and the intervals into which it is to be divided being set up by the user. For the $\langle p\sigma | p\sigma \rangle$ overlaps for iodine calculated here, the orbital functions were approximate by single Slater-type orbitals with an orbital exponent of $\zeta = 1.9$ and an effective principle quantum number of 4 (Nunn [1964]).

D - 2 Force Constant Calculation

The vibration frequencies recorded by Gabes and Gerding [1972] for solid Et_4NI_3 and Bu_4NI_3 are given in Table D - 1. From the simple nature of their spectra, Gabes and Gerding assume that both compounds contain linear symmetric anions. In the absence of any structural data for Bu_4NI_3 this assumption must stand on its merits; in the case of Et_4NI_3 it is only correct if the material studied crystallized in modification I. In Bu_4NI_3 the symmetric stretching

Table D - 1

Frequencies in cm^{-1} of symmetric I_3^- in Bu_4NI_3 , Et_4NI_3

W. Gabes and H. Gerding [1972]

Frequency	Bu_4NI_3		Et_4NI_3	
	IR	Raman	IR	Raman
ν_1	116 w	116	-	113.6 sh
	109 sh	109	-	112.8
ν_2	49	-	46	-
ν_3	134	-	135	-

w = weak
 sh = shoulder

Table D - 2

Frequencies in cm^{-1} used for force constant calculation

Frequency	Bu_4NI_3	Et_4NI_3
ν_1	112.5	113.2
ν_3	134	132.5

frequency, ν_1 , shows a departure from the strict selection rules for $D_{\infty h}$ symmetry by being infra-red active, presumably due to a lower site symmetry in the unit cell. Both compounds also show splittings (factor group splittings) due to interactions between the molecular groups in the unit cell (anion-anion interactions?). For the force constant calculation average frequencies were calculated; these are given in Table D - 2.

Using the formulae given in Chapter 7, Section 7 - 3 for the force constants, the average frequencies given in Table D - 2, a value of $4.745 \times 10^{21} \text{ gm}^{-1}$ for the reciprocal atomic mass of iodine and a value of $2.998 \times 10^{10} \text{ cm sec}^{-1}$ for the velocity of light, two simultaneous equations were set up and solved for k , k_{12} for both compounds.

For Bu_4NI_3 the result of this calculation gave

$$k = 0.4520 \text{ millidyne/A}^\circ$$

$$k_{12} = 0.3890 \text{ millidyne/A}^\circ;$$

and for Et_4NI_3

$$k = 0.6978 \text{ millidyne/A}^\circ$$

$$k_{12} = 0.2603 \text{ millidyne/A}^\circ.$$

Taking the average yielded

$$k = 0.575 \text{ millidyne/A}^\circ$$

$$k_{12} = 0.325 \text{ millidyne/A}^\circ.$$

The large positive value of k_{12} , indicating that the extension of one bond is accompanied by a considerable contraction of the other, is typical of the trihalides. In Table D - 3 the calculated k , k_{12} values for I_3^- are compared with values calculated by other workers for a number of trihalide anions.

Table D - 3

Force Constants for several trihalide ions

Anion	k (mdyne \AA^{-1})	k_{12} (mdyne \AA^{-1})	Reference
I_3^-	0.575	0.325	this work
Br_3^-	0.91	0.32	Person, Anderson, <i>et alii</i> [1961]
Cl_3^-	0.96	0.55	Evans and Lo [1966a]
IBr_2^-	0.91	0.30	Maki and Forneris [1967]
ICl_2^-	1.07	0.43	Person, Anderson, <i>et alii</i> [1961]
BrCl_2^-	1.09	0.47	Evans and Lo [1966b]

D - 3 Distorting Forces Calculation

Owing to the magnitude of the interaction force constant k_{12} it is necessary to use an iterative procedure to calculate the forces directed in the bond directions required to distort a linear anion with two equal bond lengths of 2.920 Å into another specified configuration. The effect of a non-negligible interaction constant can be expressed as a change of the force constant, k , for one bond which is proportional to the extension of the adjacent bond.

β is defined as the ratio of the stretching constant to the interaction constant, i.e.

$$\beta = k/k_{12}$$

then the changed force constant, k' , is given by

$$k' = k + \beta \Delta r$$

where Δr is the extension of the adjacent bond (Linnett [1971]).

When forces are applied simultaneously to each terminal atom, both bonds change in length, and consequently both force constants are modified.

These changes are described by the equations

$$\begin{aligned}\Delta r_i &= -\delta_i/k_i \\ r_j &= -\delta_j/k_j \\ k'_i &= k_i + \beta \Delta r_j \\ k'_j &= k_j + \beta \Delta r_i\end{aligned}$$

where δ_i, δ_j are the forces, and i, j label bonds. Trial calculations showed that k'_i, k'_j converged to stable values under iteration with constant δ_i, δ_j .

The forces required to reproduce a given geometrical configuration were calculated with the aid of a small program written in 4K-FOCAL and

run on a Digital Equipment Corporation PDP8/E computer. The bond lengths of the desired configuration were input as data to this program and arbitrary forces applied to the terminal atoms of the linear symmetric 'isolated' anion. The iterative calculation was then performed to determine the changed force constants and the bond extensions given by these forces. The differences between the bond lengths of the desired configuration and those generated by the arbitrary forces were then used to correct the applied forces. The calculation was then repeated as many times as was necessary to yield the desired configuration within 0.001 Å°.

A listing of the program is given in Figure D - 1, and the program output at each cycle for the CsI_3 calculation is shown in Figure D - 2. The trajectory taken by the course of the calculation is given in Figure D - 3 where δ_{12} is plotted against δ_{23} for each cycle.

D - 4 Estimation of pK_a for $\text{C}_6\text{H}_5\text{CN}$

The pK_a for benzonitrile can be estimated by making use of the known value of the pK_a of CH_3CN ($pK_a = -4.3$, Lemaire and Lucas [1951]) and determining from the pK_a data for analogous compounds the expected change in the pK_a caused by replacing the methyl with a benzyl group. The information used for the determination of the expected pK_a change is given in Table D - 4; from these data the average pK_a change is found to be approximately -1.0 pK_a units. The pK_a for benzonitrile is therefore estimated to be approximately -5.3, which does not appear to be unreasonable.

*WRITE ALL
C-FOCAL, 1969

```

01.01 T !! "I-I-I FORCE FIELD CALCULATION", !
01.02 A "BOND 12"S1, " BOND 23"S2
01.03 S M1=1; S M2=1; S P1=-1; S P2=-1; S C1=M1; S C2=M2
01.04 D 2
01.06 S B1=2.92+R1; S B2=2.92+R2
01.08 T %5.03, ! "BOND 12"B1, " BOND 23"B2
01.09 T %6.05, " F12"M1, " F23"M2
01.10 S D1=S1-B1; S D2=S2-B2
01.12 I (FABS(D1)-.0001) 1.20, 1.20, 1.14
01.14 I (FSGN(D1)-FSGN(P1)) 1.16, 1.18, 1.16
01.16 S P1=D1; S C1=C1*0.5
01.18 S M1=M1+FSGN(D1)*C1
01.20 I (FABS(D2)-.0001) 1.30, 1.30, 1.22
01.22 I (FSGN(D2)-FSGN(P2)) 1.24, 1.26, 1.24
01.24 S P2=D2; S C2=C2*0.5
01.26 S M2=M2+FSGN(D2)*C2
01.28 G 1.04
01.30 T ! "DONE", !; Q

02.01 S K1=0.5749; S K2=0.5749
02.02 S G1=1/K1; S G2=1/K2
02.04 S R1=G1*M1; S R2=G2*M2
02.06 S D1=0.5647*R2; S D2=0.5647*R1
02.08 I (FABS(D1)-.00001) 2.10, 2.10, 2.12
02.10 I (FABS(D2)-.00001) 2.14, 2.14, 2.12
02.12 S K1=0.5749+D1; S K2=0.5749+D2
02.14 R
*
```

Figure D - 1. Photo reproduction of the FOCAL program used to calculate the distorting forces.

Figure D - 2. Photo reproduction of the output for the CsI₃ anion.

*G0

1-1-1 FORCE FIELD CALCULATION
BOND 12:2.840 BOND 23:3.042

BOND 12=	4.660	BOND 23=	4.660	F12=	1.00000	F23=	1.00000
BOND 12=	2.920	BOND 23=	2.920	F12=	0.00000	F23=	0.00000
BOND 12=	1.181	BOND 23=	3.790	F12=-1.00000	F23=	0.50000	
BOND 12=	2.050	BOND 23=	3.355	F12=-0.50000	F23=	0.25000	
BOND 12=	2.920	BOND 23=	2.920	F12=	0.00000	F23=	0.00000
BOND 12=	2.485	BOND 23=	3.138	F12=-0.25000	F23=	0.12500	
BOND 12=	2.703	BOND 23=	3.029	F12=-0.12500	F23=	0.06250	
BOND 12=	2.920	BOND 23=	3.083	F12=	0.00000	F23=	0.09375
BOND 12=	2.811	BOND 23=	3.056	F12=-0.06250	F23=	0.07813	
BOND 12=	2.866	BOND 23=	3.029	F12=-0.03125	F23=	0.06250	
BOND 12=	2.839	BOND 23=	3.042	F12=-0.04688	F23=	0.07031	
BOND 12=	2.852	BOND 23=	3.036	F12=-0.03906	F23=	0.06641	
BOND 12=	2.845	BOND 23=	3.039	F12=-0.04297	F23=	0.06836	
BOND 12=	2.839	BOND 23=	3.042	F12=-0.04688	F23=	0.07031	
BOND 12=	2.842	BOND 23=	3.041	F12=-0.04492	F23=	0.06934	
BOND 12=	2.840	BOND 23=	3.042	F12=-0.04590	F23=	0.06983	
BOND 12=	2.839	BOND 23=	3.042	F12=-0.04688	F23=	0.07031	
BOND 12=	2.839	BOND 23=	3.042	F12=-0.04639	F23=	0.07007	
BOND 12=	2.840	BOND 23=	3.042	F12=-0.04590	F23=	0.07019	

DONE

*

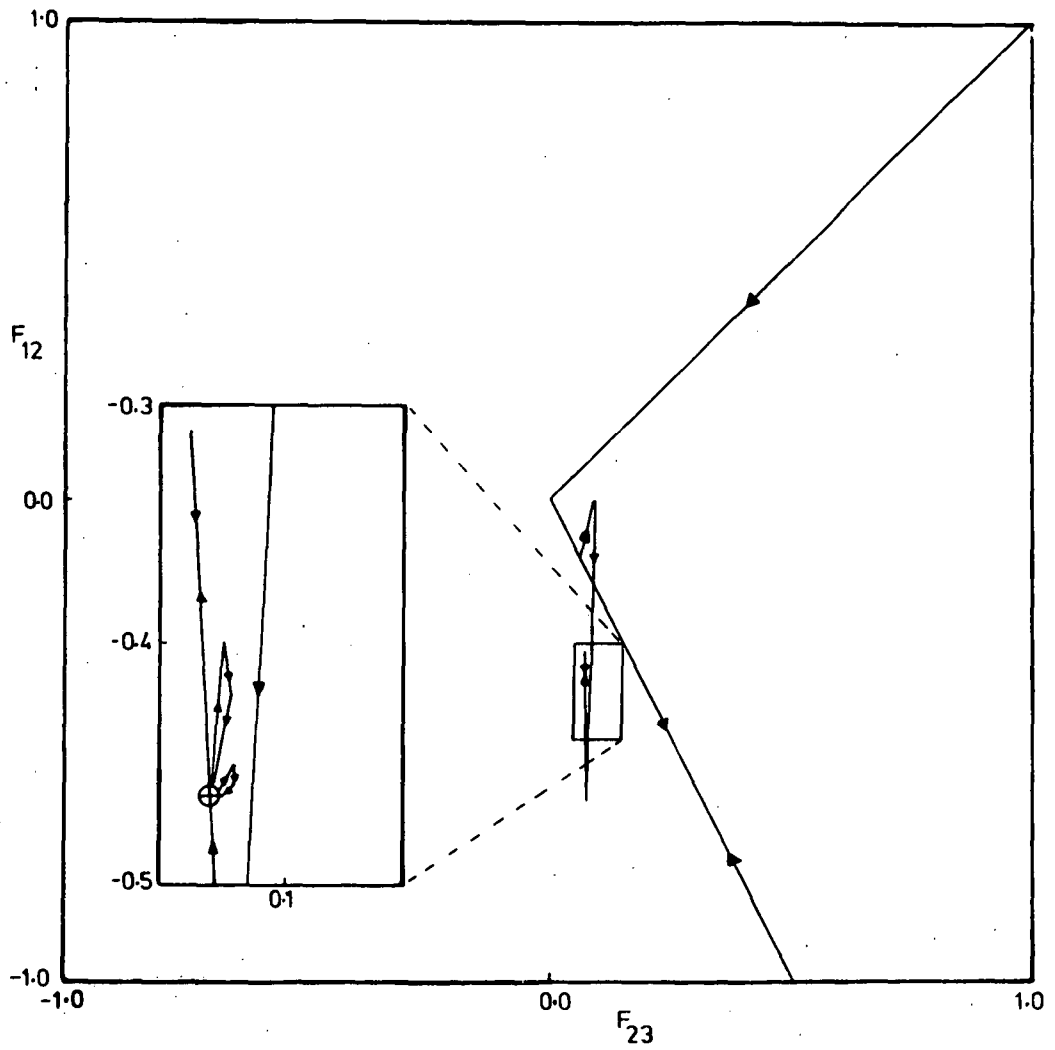


Figure D - 3. Trajectory of the distorting forces during iteration; the forces are initialized at the values represented by upper right corner.

Table D - 4

pK_a values for pairs of compounds analogous in structure to $\text{CH}_3\text{CN}/\text{C}_6\text{H}_5\text{N}$

Compound	pK_a value	Reference
CH_3COOH	-6.10	Goldfarb, Mele and Gutstein [1955]
$\text{C}_6\text{H}_5\text{COOH}$	-7.26	Flexser, Hammett and Dingwall [1935]
	$(\Delta pK_a = -1.16)$	
$\text{CH}_3\text{CNHNH}_2$	12.4	Schwartzbach and Lutz [1940]
$\text{C}_6\text{H}_5\text{CNHNH}_2$	11.2	Albert, Mills and Royer [1947]
	$(\Delta pK_a = -0.8)$	

Average $\Delta pK_a = -(1.16 + 0.8)/2 = -0.98 \approx -1.0$.

pK_a (benzonitrile) = pK_a (acetonitrile) + ΔpK_a (average)

= -4.3 - 1.0

= -5.3

D - 5 $[\text{C}_6\text{H}_5\text{CNH}^+]$ at the crystallization point of $\text{HI}_{3.4}(\text{C}_6\text{H}_5\text{CN})$

The molar concentration of H_3O^+ in aqueous HI can be calculated from the following data:

Composition of constant boiling HI(aq) = 57 w.w. %

Density 57 w.w. % HI(aq) = 1.70 gm cm^{-3}

Assuming complete dissociation $[\text{H}_3\text{O}^+] = (57 \times 1200)/(100 \times 127.91)$
 $= 7.57 \text{ mole litre}^{-1}$

Solubility of $\text{C}_6\text{H}_5\text{CN} \approx 0.1 \text{ mole litre}^{-1}$

$pK_a(\text{C}_6\text{H}_5\text{CN}) \approx -5.3$, $K_a \approx 2 \times 10^5$

Then, to an order of magnitude

$$[\text{C}_6\text{H}_5\text{CN}][\text{H}_3\text{O}^+]/[\text{C}_6\text{H}_5\text{CNH}^+] = 2 \times 10^5$$

$$[\text{C}_6\text{H}_5\text{CNH}^+] = [\text{C}_6\text{H}_5\text{CN}][\text{H}_3\text{O}^+] \times 0.5 \times 10^{-5}$$

$$= 1 \times 10^{-1} \times 7.6 \times 10^1 \times 0.5 \times 10^{-5}$$

$$= 3.8 \times 10^{-5}$$

$$\approx 10^{-5} \text{ mole l}^{-1}$$

Note that activities are assumed to be approximated by concentrations.

Appendix E - Publications

- E - 1 CHEESMAN, FINNEY & SNOOK, [1970], "Studies in Halogen-Halogen Bonding", Theo. chim. acta, 16, p.33.
- E - 2 CHEESMAN & FINNEY, [1970], "Unit-Cell Refinement by the Solution of an Overdetermined System of Linear Equations", J. Appl. Cryst., 3, p.399.
- E - 3 CHEESMAN & FINNEY, [1970], "Refinement of the Structure of Ammonium Tri-iodide, NH_4I_3 ", Acta Cryst., 1326, p.904.

Studies in Halogen-Halogen Bonding

I. The p - σ Model

G. H. CHEESMAN, A. J. T. FINNEY, and I. K. SNOOK

Chemistry Department, University of Tasmania

Received May 19, 1969

The VESCF-MO method is used to investigate the p - σ bonding model of halogen-halogen bonding. Procedures for estimating values of the core resonance integral, β , are discussed. It is found that if a semi-empirical procedure is used for estimating this integral, the model adequately predicts equilibrium bond-lengths for halogen-halogen molecules, but does not give an accurate description of the molecular wavefunction. The implicit assumptions of the semi-empirical approach are examined in some detail.

Mit Hilfe der VESCF-MO-Methode wird das p - σ -Bindungsmodell der Halogen-Halogen-Bindung untersucht. Verschiedene Verfahren für die Abschätzung des Kernresonanzintegrals β werden diskutiert. Legt man ein semi-empirisches Verfahren für die Abschätzung dieses Integrals zugrunde, so zeigt sich, daß das Modell die Gleichgewichtsbindungsabstände in Halogen-Halogen-Molekülen in guter Übereinstimmung mit dem experimentellen Befund wiedergibt. Für die Wellenfunktionen der Moleküle erhält man dagegen keine besonders genaue Beschreibung. Die implizierten Annahmen dieser semi-empirischen Näherung werden im Detail geprüft.

La méthode VESCF MO est utilisée pour étudier le modèle de liaison $p - \sigma$ pour la liaison halogène-halogène. Des procédés pour estimer les valeurs de l'intégrale de résonance de coeur β sont discutés. On trouve que si cette intégrale est évaluée par un procédé semi-empirique, le modèle prédit correctement les longueurs de liaison pour les molécules halogènes-halogène, mais ne fournit pas une description précise de la fonction d'onde moléculaire. Les hypothèses implicites dans l'approche semi-empirique sont examinées en détail.

A number of theoretical studies of halogen-halogen bonding in interhalogens and polyhalides has been made; these include studies based on simple electrostatic models [1–5], calculations and discussions using the valence-bond approach [6–9], inert pair theory [10], non-paired spatial orbitals [11], the method of maximum overlap [12] and Murrell's best-hybrid-orbital treatment [13]. Various molecular orbital treatments have been made ranging in complexity from the free electron approximation [14], through Hückel and extended Hückel calculations [2, 3, 8, 15–18], semi-empirical selfconsistent field (SCF) treatments [19, 20] to all-valence-electron SCF calculations [23, 24, 61–64]. Treatments employing Bloch orbitals have also been applied to both I_2 and I_3 in the solid state [25–28].

Most of the molecular orbital studies appear to indicate that d -orbitals are not involved to any extent in the bonding of these compounds, and in fact an adequate model of the bonding in the interhalogens can be developed by considering only the $p\sigma$ -orbitals of the valence shell as originally suggested by Pimentel [29] and subsequently discussed by others [17, 30, 31]. This bonding

model assumes that the only significant contribution to the interhalogen bond is made by the $p\sigma$ -electrons, the other electrons in the valence shell remaining non-bonding. This hypothesis appears to be supported by experimental data, notably the results of studies of nuclear quadrupole resonance [32-35], Raman and infra-red spectra [36-38]. However, for ionic species, in particular polyiodides, it has been shown theoretically [19-21] that this simple $p\sigma$ -electron bonding model must be modified to take into account the electrostatic perturbation due to the ionic environment. That this perturbation affects the properties of polyhalide ions is demonstrated by a variety of experimental data [39]: for example the dependence of nuclear quadrupole resonance frequencies of similar ions upon their crystalline environment. In fact, these ions, by virtue of their weak bonding and sensitivity to external fields, provide convenient tools for the exploration of environmental effects in the solid and perhaps the liquid state.

In view of this potential usefulness, this preliminary study was initiated in order to test the validity of the $p\sigma$ -bonding model. The ground state properties of diatomic halogen and interhalogen molecules were calculated by the VESCF method, and as we shall demonstrate, the $p\sigma$ -bonding model predicts the correct internuclear distances in the isolated molecules. Therefore, if the effect of the environment can be accurately included in the calculations, then the $p\sigma$ -model allows quite accurate investigations of the effect of environment on molecular geometry to be made. However, it turns out that the model has only limited power to predict those properties which depend upon charge distribution. This inadequacy in the model points to the fact that interactions between the non-bonding valence electrons of the bonded atoms cannot be neglected.

Method

The $p\sigma$ -electron bonding model can be formulated in a manner analogous to the typical semi-empirical SCF π -electron theory as currently applied to investigations of the electronic properties of planar unsaturated aromatic compounds. It is assumed that only one p -orbital per atom contributes to the σ -bonding molecular orbital set, the remaining occupied atomic orbitals forming an electronic core around each nucleus. The basic assumption is that of zero differential overlap (ZDO) [40]; this assumption in the case of diatomic interhalogen molecules reduces the problem to that of a two-electron system involving relatively simple integrals [40, 52]. In this study the calculations have been carried out using the variable electronegativity SCF procedure (VESCF method) [45-49], as this allows some optimization of orbital exponents to be made which improves the values calculated for some molecular properties [49].

In the calculations reported here, the one-centre electron repulsion integral, γ_{pp} , has been derived from a formula of the Paoloni type [19, 41]. The two-centre repulsion integral, γ_{pq} , was calculated from the Mataga-Nishimoto formula [42]: the approximation represented by the relation (1) has been suggested [20] as a more reliable one for $p\sigma$ -electrons on the grounds that in this case the Mataga-Nishimoto formula underestimates the value of this integral when compared with values calculated using Slater orbitals:

$$\gamma_{pq} \approx 1/r_{pq} \quad (1)$$

(where the subscripts p, q label orbitals). However, electron correlation studies [43, 44] indicate that this integral should be reduced from the value obtained using a Slater basis set. The low values of the integral calculated from the Mataga-Nishimoto formula make some semi-empirical allowance for electron correlation as the Paoloni formula does in γ_{pp} and γ_{qq} . For this reason the Mataga-Nishimoto approximation has been preferred to (1) which makes no such allowance and in fact overestimates the integral.

There are two main strategies which may be adopted for the selection of the core resonance integral β_{pq} , which in this treatment is assumed (as is usual) to be a bond property:

- (i) β_{pq} may be calculated in some theoretical fashion, or
- (ii) a semi-empirical approach may be used to derive a value of β_{pq} from some readily observed molecular property, *e.g.* electronic spectra.

These two strategies were compared by calculating potential energy curves for homonuclear halogen diatomic molecules, using the comparison between calculated and observed internuclear separation as a criterion of success. As the integrals for the fluorine molecule vary most sharply with internuclear separation, this molecule provides the most stringent test of the approximations used. The total valence electron energy at a given r_{pq} was calculated from the relationship [19]

$$E_{\text{total}} = -\frac{1}{2} \sum_{p,q} P_{pq}(H_{pq} + F_{pq}) + \frac{1}{2} \sum_{p,q} \frac{14.40}{r_{pq}} X_p X_q \quad (2)$$

where E_{total} is the total valence electron energy, the first summation represents the electronic energy due to the bonding electrons and the last summation the core-core repulsion energy, with the cores being treated as point charges¹.

For a diatomic molecule, β_{pq} may be expressed as

$$\beta_{pq} = (p | -\frac{1}{2} A | q) - X_p(p | 1/r_p | q) - X_q(p | 1/r_q | q). \quad (3)$$

Several theoretical methods were used to calculate β_{pq} ; these were

- (a) Slater orbital representation with the approximation [50]

$$(p | 1/r_p | q) = (p | 1/r_q | q) = \frac{1}{2} S_{pq} \gamma_{pq};$$

- (b) the Wolfsburg-Helmholtz-Mulliken approximation [54]

$$\beta_{pq} = \frac{1}{2} S_{pq}(H_{pp} + H_{qq});$$

- (c) the Cusach approximation [55]

$$\beta_{pq} = \frac{1}{2} S_{pq}(2 - |S_{pq}|)(H_{pp} + H_{qq});$$

- (d) the Ohno approximation [56]

$$\beta_{pq} = \frac{1}{2} S_{pq}(X_p + X_q)(\gamma_{pq} - 2.0 C/r_{pq})$$

(where C was taken as 0.85).

All approximations except (b) were also tried with orthogonality corrections [50], i.e.

$$\beta_{pq(\text{orthogonal})} = \beta_{pq} - \frac{1}{2} S_{pq}(H_{pp} + H_{qq}).$$

¹ The factor 14.40 appears in this equation to give E_{total} in electron volts when r_{pq} is measured in Angstrom units.

Table 1. *Halogen molecules*

Molecule	r_e (calc) Å	R_e (obs) Å
F ₂	0.71	1.42
Cl ₂	1.34	1.98
Br ₂	1.72	2.28
I ₂	2.34	2.66

Table 2. *Fluorine molecule*

	r_e calc (without orthog.)	r_e calc (with orthog.)
W.M.H.	1.0	— ^a
Cusack	0.85	1.1
Ohno	< 1.0	> 1.7

^a The orthogonality correction exactly cancels the approximation for β_{pq} .

The equilibrium internuclear separation, r_e , for the halogen molecules calculated using approximation (a) are presented in Table 1, and for the fluorine molecule calculated using approximations (b) (d) in Table 2. These results show that the calculated separations are seriously in error; we conclude that the discrepancy must be due to inadequacies in the $p\sigma$ -model itself, i.e. an inadequate representation of the core electrons and their interactions.

This same difficulty was experienced by Pohl, Rein, and Appel [52] in calculations of the ground-state properties of the hydrogen-halide molecules using a $p\sigma$ -model. To overcome this difficulty the core penetrations and interactions with non-bonding electrons in the halogen valence shell were represented by the Hartree-Fock potentials tabulated by Hermann and Skillman [53], that is

$$E_{\text{core-core}} = E_{\text{electrostatic}} + E_{\text{penetration}} \quad (4)$$

where $E_{\text{core-core}}$ is the total core interaction energy, $E_{\text{electrostatic}}$ is the total Coulomb repulsion between the charged cores and $E_{\text{penetration}}$ the total core penetration energy [52].

Although this remedy allowed Pohl *et al.* to calculate reasonable ground state properties for the hydrogen halides, it cannot be readily applied to calculations on diatomic halogen molecules [60], for in this case $E_{\text{penetration}}$ cannot be simply represented in terms of Hermann and Skillman's potentials. Further, the use of these potentials involves the implicit assumption that the charge distribution of all non-bonding electrons in the bonded atom is the same as that in the isolated atom. The measure of agreement between calculated and observed halogen halide [52] and interhalogen [60] bond lengths and dipole moments shows that this assumption is not entirely adequate.

The Core Resonance Integral – The Semi-Empirical Approach

The most successful application of this $p\sigma$ -model of the interhalogen bond using a value of β_{pq} derived from experimental data is that of Brown and Nunn [19]. In the following section we investigate the assumptions implicit in their

derivation. The derivation underlying their procedure is based on the Born-Oppenheimer approximation [40]

$$E_{\text{total}} = E_{\text{electronic}} + E_{\text{nuclear}} \quad (5)$$

This may be written

$$E_{\text{total}} = E_{\text{valence electron}} + E_{\text{core electron}} + E_{\text{electrostatic}} + E_{\text{penetration}} \quad (6)$$

where $E_{\text{valence electron}}$ is the energy of the valency electrons, $E_{\text{core electron}}$ is the electronic energy of the core electrons, and $E_{\text{electronic}}$ and $E_{\text{penetration}}$ have the same meaning as in Eq. (4). For a diatomic molecule with pure $p\sigma$ -bonding, the terms on the right hand side of Eq. (6) can be written:

$$E_{\text{valence electron}} = \frac{1}{2} \sum_{p,q=1}^2 P_{pq}(H_{pq} + F_{pq}), \quad (7)$$

$$E_{\text{electrostatic}} = X_1 X_2 14.4/r_{12}, \quad (8)$$

$$E_{\text{total}} = \frac{1}{2} \sum_{p,q=1}^2 P_{pq}(H_{pq} + F_{pq}) + X_1 X_2 14.4/r_{12} + E_{\text{core electron}} + E_{\text{penetration}} \quad (9)$$

As r_{12} tends to infinity, from Eqs. (6-9) we have

$$\begin{aligned} E_{\text{total}} &\rightarrow -P_{11}I_1 + P_{11}^2\gamma_{11} - P_{22}I_2 + P_{22}^2\gamma_{22} + E_{\text{core electron}}, \\ E_{\text{total}}(r) - E_{\text{total}}(\infty) &= -\{P_{11} - 1\}I_1 - \{P_{22} - 1\}I_2 \\ &\quad - P_{22}X_1\gamma_{12} - P_{11}X_2\gamma_{12} + \frac{1}{4}\{P_{11}^2 - 1\}\gamma_{11} \\ &\quad + \frac{1}{4}\{P_{22}^2 - 1\}\gamma_{22} + \frac{1}{2}P_{11}P_{12}\gamma_{12} + \frac{1}{2}P_{22}P_{12}\gamma_{12} \\ &\quad - \frac{1}{2}P_{12}\gamma_{12} + 2P_{12}\beta_{12} + 14.4/r_{12} + E_{\text{penetration}} \end{aligned}$$

for which the following assumptions have been made:

- (i) $E_{\text{core electron}}(r) = E_{\text{core electron}}(\infty)$.
- (ii) $I_1, I_2, \gamma_{11}, \gamma_{22}$ have the same value in the atoms as in the molecule.
- (iii) $P_{11}(\infty) = P_{22}(\infty) = 1$.
- (iv) $X_1 = X_2 = 1$.

The further assumption made by Brown and Nunn was

$$(v) P_{11} = P_{22} = P_{12} = P_{21} = 1$$

thus

$$\begin{aligned} \beta &= \left(\beta_{12} + \frac{1}{2P_{12}} E_{\text{penetration}} \right) \\ &= \left(\frac{1}{2P_{12}} \right) (E(r) - E(\infty)) + \frac{(P_{11} - 1)}{2P_{12}} I_1 + \frac{(P_{22} - 1)}{2P_{12}} I_2 \\ &\quad + \frac{P_{22}}{2P_{12}} \gamma_{12} + \frac{P_{11}}{2P_{12}} \gamma_{12} - \frac{(P_{11}^2 - 1)}{4P_{12}} \gamma_{11} - \frac{(P_{21}^2 - 1)}{4P_{12}} \gamma_{22} \\ &\quad - \frac{1}{4} P_{11}\gamma_{12} - \frac{1}{4} P_{22}\gamma_{12} + \frac{1}{4} P_{12}\gamma_{12} - \frac{7.1995}{P_{12}\gamma_{12}}. \end{aligned} \quad (10)$$

It follows therefore, with assumption (v) that

$$\beta_{12} = \{E(r) - E(\infty)\} + \frac{3}{4}\gamma_{12} - 7.2/r_{12} - \frac{1}{2}E_{\text{penetration}} \quad (11a)$$

or

$$\beta = (\beta_{12} + E_{\text{penetration}}) = \frac{1}{2}\{E(r) - E(\infty)\} + \frac{3}{4}\gamma_{12} - 7.2/r_{12}. \quad (11b)$$

That is, the β used in their calculations includes contributions from the core-core interactions. Although the inclusion of $E_{\text{penetration}}$ terms in β is not formally justified, their good results for calculated internuclear separations in the triiodide ion show that this is a workable method for including core-core interactions. This method also allows for problems related to orthogonality, in that Eq. (10) is derived from (9) using the ZDO approximation, that is, assuming an orthogonal basis set.

We performed calculations using Eq. (11b) for the homonuclear diatomic halogens in order to test assumptions (i) to (iii) since assumption (iv) holds for homonuclear molecules. The term $\frac{1}{2}\{E(r) - E(\infty)\}$ was calculated from Morse functions. Brown and Nunn [19] estimated the term $(E(\infty) - E(r))$ from the iodine dissociation curve; but as the corresponding curves are not as well defined for the other halogen and interhalogen diatomic molecules, Morse functions were used to estimate this term in the present study. This procedure would lead to false values of dissociation energies because the "experimental" curves do not coincide with those calculated from the MO model; but since in the present study (as in Brown and Nunn's study) it is only sought to determine the equilibrium interatomic separation, it is only required to locate the position of the minimum of the energy curve, and not its absolute value. It is therefore legitimate to use this modification of Brown and Nunn's procedure for estimating β and thence the interatomic distance.

The results are shown in Fig. 1, and the correct internuclear distances were predicted in all cases. This shows that assumptions (i) and (iii) hold: to test the validity of assumption (v), calculations were performed on the heteronuclear halogen diatomic molecules using both Eqs. (10) and (11). The results are presented in Fig. 2: once again the correct internuclear distances were predicted in all cases. It should be noted that although the calculated magnitude of the total energy depends upon whether Eq. (10) or (11) was used to estimate β , both equations give the same internuclear separation, as is shown in Fig. 3 for ICl. Further, the charge distributions, but not the bond order, depend upon which equation is used for the estimation of the core resonance integral. From the calculated charge distributions at the observed internuclear separations, the molecular dipole moments were calculated. These results are presented in Table 3, together with the calculated charge distribution. We draw attention to the result for IBr where in both cases the charge distribution is the reverse of that expected on the basis of the chemical behaviour of this compound [59]. It may be seen that the agreement with experimental is not outstandingly good, a point which further supports the conclusion that more than the $p\sigma$ -electrons must be included in calculations of the electronic structure of these molecules.

The fact that Brown and Nunn's [19] calculations would lead to incorrect values for the dissociation energy is not a serious criticism since the object was

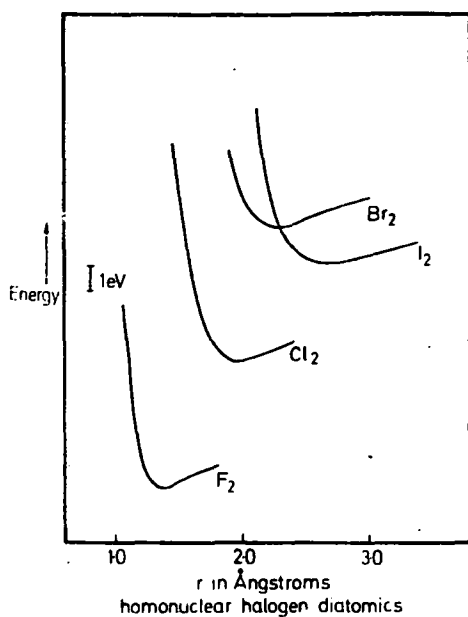


Fig. 1

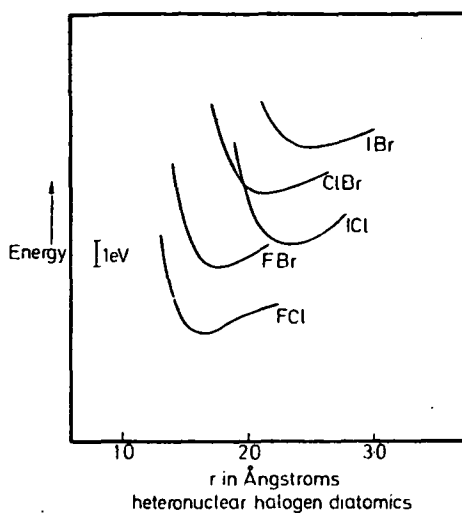


Fig. 2

Fig. 1. Total molecular energy curves for the homonuclear halogen diatomics

Fig. 2. Total molecular energy curves for the heteronuclear halogen diatomics

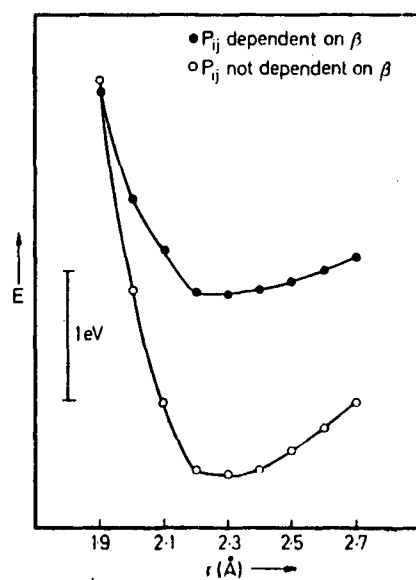


Fig. 3. Total molecular energy curves for the ICl molecule for the two cases, β dependent on P_{ij} (filled circles) and β not dependent on P_{ij} (unfilled circles)

Table 3. *Properties of interhalogens*

Molecule	Calculated charge on most electronegative atom		Calculated dipole moment (debye)		Observed dipole moment (debye)
	β not dependent on P_{pq}	β dependent on P_{pq}	β not dependent on P_{pq}	β dependent on P_{pq}	
ICl	-0.066	-0.071	0.505	0.535	0.88
EBr	-0.157	-0.178	1.285	1.450	1.29
BrCl	-0.113	0.123	1.140	1.240	
ICl	-0.106	-0.117	1.170	1.290	0.63
EBr	+0.103	0.110	1.235	1.320	1.26 (in solution)

The bond order was in all cases approximately 0.99.

primarily to predict the geometry of polyhalide ions. We conclude from the comparisons of our results with experimental values that their method can give correct geometries (*i.e.* the results were not fortuitous) but that it does not lead to very satisfactory estimates for the charge distribution in these cases.

A limited application of the same method was made by Migchelsen and Vos who derived their value of β from electronic spectra, that is, assuming a fixed nuclear framework, a method commonly used in semi-empirical π -electron theory. As they imply, this does not include contributions from electrons other than those directly involved in the bonding. In this context Migchelsen and Vos only discuss explicitly contributions from inner shells; our study would indicate that non-bonding valency electrons make a most significant contribution. If β estimated in this way is used in any study which involves variation of the internuclear distance, the problem of including or estimating $E_{\text{penetration}}$ would remain unsolved. The validity of using an integral calculated from an excited state for the investigation of groundstate properties is also questionable.

Conclusion

In the absence of an adequate theoretical method for estimating the contribution of the core overlap energy to the total energy, the semi-empirical approach was explored. We conclude that the VESCF $p\sigma$ -model using a value for the core resonance integral estimated in the manner of Brown and Nunn is satisfactory for predicting internuclear distances, and is therefore suitable for investigating the effect of lattice environment on the geometry of polyhalide ions. On the other hand the usefulness of the method for calculating charge distributions and properties derived from charge distributions is strictly limited and gives little insight into the electronic structure of the halogen-halogen bond. We are engaged in evaluating the usefulness of all electron models for this family of compounds and hope to present the results of these calculations in subsequent papers.

References

1. van Arkel, E., de Boer, T. H.: *Reçueil Trav. chim.* **47**, 593 (1928).
2. Havinga, E. E.: Ph. D. Thesis, Groningen, 1957.
3. —, Wiebenga, E. H.: *Reçueil Trav. chim.* **78**, 724 (1959).
4. Davies, M., Gwynne, L.: *J. Amer. chem. Soc.* **74**, 2748 (1952).
5. Meyerstein, D., Treinin, A.: *Trans. Farad. Soc.* **59**, 1114 (1963).
6. Pauling, L.: *Nature of the chemical bond*, 3rd ed. New York: Cornell University Press 1960.
7. Kimbal, G. E.: *J. chem. Physics* **8**, 188 (1940).
8. Havinga, E. E., Wiebenga, E. H., Boswijk, K. H.: *Advances inorg. Chem. Radiochem.* **3**, 133 (1961).
9. van Vleck, J. H., Sherman, A.: *Rev. mod. Physics* **7**, 167 (1935).
10. Sidgwick, N. V.: *Annual Reports of the Chemical Society (London)* **30**, 26 (1933).
11. Linnett, J. W.: *Electronic structure of molecules*, Methuen edition, New York: Wiley 1964.
12. Volkov, V. M., Dyatkina, M. E.: *Zh. Strukt. Khim.* **4**, 610 (1963).
13. Ali, M. A.: Unpublished work, quoted by Manne, R. (see Ref. [24]).
14. Müller, H.: *Theoret. chim. Acta (Berl.)* **6**, 445 (1966).
15. Rundle, R. E.: *Acta crystallogr.* **14**, 585 (1961).
16. Christie, K. O., Guertin, J. P.: *Inorg. Chem.* **4**, 905 (1965).
17. Coulson, C. A.: *J. chem. Soc. (London)* 1442 (1964).
18. Oakland, R. L., Duffy, G. H.: *J. chem. Physics* **46**, 19 (1967).
19. Brown, R. D., Nunn, E. K.: *Austral. J. Chem.* **19**, 1567 (1966).
20. Migchelsen, T., Vos, A.: *Acta crystallogr.* **23**, 796 (1967).
21. Mooney-Slater, R. C. L.: *Acta crystallogr.* **12**, 187 (1959).
22. Slater, J. C.: *Acta Crystallogr.* **12**, 197 (1959).
23. Santry, D. P., Segal, G. A.: *J. chem. Physics* **47**, 158 (1967).
24. Manne, R.: *Theoret. chim. Acta (Berl.)* **6**, 312 (1966).
25. Boersohn, R.: *J. chem. Physics* **36**, 3445 (1962).
26. Rosenberg, J. L.: *J. chem. Physics* **40**, 1707 (1964).
27. Yamasaki, R. S.: *J. physic. Soc. Japan* **17**, 1202 (1962).
28. Robin, M. B.: *J. chem. Physics* **40**, 3369 (1964).
29. Pimentel, G. C.: *J. chem. Physics* **19**, 446 (1951).
30. Hack, R. J., Rundle, R. E.: *J. Amer. chem. Soc.* **73**, 4321 (1951).
31. Pimentel, G. C., Spratley, R. D.: *J. Amer. chem. Soc.* **85**, 826 (1963).
32. Cornwell, C. D., Yamasaki, R. S.: *J. chem. Physics* **27**, 1060 (1957).
33. — — — *J. chem. Physics* **30**, 1265 (1959).
34. Kurita, Y., Nakamura, D., Hayakawa, N.: *J. chem. Soc. Japan, Pure Chemistry Section* **79**, 1093 (1958).
35. Evans, J. C., Lo, G. Y. S.: *J. physic. Chem.* **71**, 2730 (1967).
36. Stammreich, H.: *J. chem. Physics* **35**, 908 (1961).
37. Maki, A. G., Forneris, R.: *Spectrochim. Acta* **23A**, 867 (1967).
38. Christie, K. O., Sawodny, W.: *Inorg. Chem.* **6**, 313 (1967).
39. Snook, I. K.: Hons. Thesis, University of Tasmania, 1967.
40. Parr, R. G.: *Quantum theory of molecular electronic structure*, 1st ed. New York: Benjamin 1964.
41. Paoloni, L.: *Nuovo Cimento* **4**, 410 (1956).
42. Mataga, N., Nishimoto, K.: *Z. physik. Chem. NF*, **13**, 140 (1957).
43. Sinanoglu, O.: *Adv. Chem. Physics* **6**, 384 (1964).
44. Parr, R. G.: Reference 40, page 51.
45. Brown, R. D., Heffernan, M. L.: *Trans. Farad. Soc.* **54**, 757 (1958).
47. — — — *Austral. J. Chem.* **12**, 543 (1959).
48. — — — Harcourt, R. D.: *Austral. J. Chem.* **16**, 737 (1963).
49. — — — Coller, B. A. W.: *Theoret. chim. Acta (Berl.)* **7**, 259 (1967).
50. Tanaka, M., Nagakura, S.: *Theoret. chim. Acta (Berl.)* **6**, 320 (1966).
51. Fischer-Hjalmars, L.: *Ark. Fysik.* **21**, 123 (1962).
52. Pohl, H. A., Rein, R., Appel, K.: *J. chem. Physics* **41**, 3385 (1964).
53. Hermann, F., Skillman, S.: *Atomic structure calculations*, 1st ed. New Jersey: Prentice Hall 1963.
54. Ballhausen, C. J., Gray, H. B.: *Molecular orbital theory*, 1st ed. New York: Benjamin 1965.

- 55. Cusachs, L. C., Cusachs, B. B.: J. physic. Chem. **71**, 1060 (1967).
- 56. Ohno, K.: Theoret. chim. Acta (Berl.) **2**, 219 (1964).
- 57. Moffitt, W.: Proc. Roy. Soc. (London) A **210**, 224 (1951).
- 58. Pariser, R.: J. chem. Physics **21**, 568 (1953).
- 59. Cremer, H. W., Duncan, D. R.: J. chem. Soc. (London) 181 (1933).
- 60. Pohl, H. A., Ralf, L. M.: Int. J. Quantum Chem. **1**, 577 (1967).
- 61. Siegel, J. A., Whitehead, M. A.: Theoret. chim. Acta (Berl.) **11**, 220 (1968).
- 62. - - Theoret. chim. Acta (Berl.) **11**, 239 (1968).
- 63. - - Theoret. chim. Acta (Berl.) **11**, 254 (1968).
- 64. - - - - Theoret. chim. Acta (Berl.) **11**, 263 (1968).

Dr. G. H. Cheesman
Chemistry Department
University of Tasmania
Box 252 C, G.P.O., Hobart, Australia, 7001

J. Appl. Cryst. (1970). 3, 399**Unit-Cell Refinement by the Solution of an Overdetermined System of Linear Equations**

BY G. H. CHEESMAN AND A. J. T. FINNEY

Chemistry Department, University of Tasmania, G.P.O. Box 252C, Hobart, Tasmania 7001, Australia

(Received 15 January 1970)

A computer program which refines unit-cell parameters by solving the overdetermined system of linear equations obtained by indexing the powder pattern is described. The improved numerical stability of this treatment is reported.

Introduction

The usual method employed for improving unit-cell parameters derived from powder data is that of least-squares refinement. This method of treatment was initially proposed by Cohen (1935) and has been reviewed by Buerger (1966). The indices of the reflexions and the observed values of Q (or a related quantity) are used to establish a set of normal equations which are solved for refined values of the reciprocal-cell constants. This process may be applied in a cyclic fashion, the refined constants being used to re-index the pattern and hence to generate a new system of normal equations.

Experience has shown that when such a least-squares refinement process is carried out by a computer for the improvement of oblique cell parameters, the matrix-inversion routine used to solve the system of normal equations can in some cases fail on account of the development of a matrix singularity. It has been found that the formally equivalent procedure of treating the problem as the solution in the least-squares sense of a system of overdetermined linear equations (Golub, 1965) is less susceptible to numerical instability.

In the triclinic case the linear equation for Q_i , for the i th line in a powder pattern of m lines, can be written as:

$$Q_i = 1/d^2_{hkl} = s_{1j}e_j; \quad (j = 1, 2, \dots, 6)$$

where

$$\begin{array}{lll} s_{11} = h_1^2, & s_{12} = k_1^2, & s_{13} = l_1^2, \\ s_{14} = h_1k_1, & s_{15} = k_1l_1, & s_{16} = h_1l_1, \end{array}$$

and

$$\begin{array}{lll} e_1 = a^{*2}, & e_2 = b^{*2}, & e_3 = c^{*2}, \\ e_4 = 2a^*b^* \cos \gamma^*, & e_5 = 2b^*c^* \cos \alpha^*, & e_6 = 2a^*c^* \cos \beta^* \end{array}$$

When $m > 6$, these equations form an overdetermined system for which a least-squares solution can be found as described by Golub (1965). A computer program which implements this treatment for the cyclic refinement of the parameters of orthorhombic, monoclinic and triclinic cells has been written in Elliott ALGOL III for the Elliott 503 computer. Cells of higher symmetry can, of course, be treated as special cases within these classes.

Program description

The input to the program consists of the number of lines in the pattern; the X-ray wavelength at which the data was collected; a code specifying the crystal system; a tolerance related to the quality of the data; the limits between which the indices may range; the initial cell parameters and the list of observed $\sin^2 \theta$ values.

The observed $\sin^2 \theta$ values are converted to Q values on input, and a table of calculated Q values is built up from the initial reciprocal-cell parameters, with an entry for every index combination within the specified index ranges. Provision is made to reject from this table Q values corresponding to any index triple forbidden by the space group symmetry (when this is known). This table is then searched for correspondences between observed and calculated Q values which lie within the specified tolerance. The index triple for a given line is chosen from the set of such corresponding Q values by selecting the Q value which deviates least from the observed Q . When such an indexing can be made, the indices are used to add to the list of equations; otherwise a 'no index' message is recorded. If desired, some form of weighting may be introduced in forming the normal equations; in the present program weights proportional

Table 1. Details of the refinement of a pseudo-hexagonal monoclinic cell

Cycle number	Lines indexed	a	b	c	β	$\sigma Q_{\text{obs}} - Q_{\text{calc}} $
Initial input	26	14.5050 Å	9.6250 Å	14.5050 Å	120.0000°	0.000345
1	29	14.4509	9.6231	14.4832	119.6700	0.000371
2	29	14.4371	9.6236	14.4768	119.5692	0.000301
3	30	14.3987	9.6405	14.4775	119.5741	0.000348
4	30	14.3819	9.6508	14.4644	119.4797	0.000282
5	30	14.3769	9.6395	14.4614	119.4148	0.000250
6	30	14.3716	9.6348	14.4486	119.3471	0.000218
7	30	14.3583	9.6299	14.4418	119.2973	0.000184
8	30	14.3456	9.6305	14.4433	119.3005	0.000175
9	30	14.3396	9.6369	14.4385	119.2770	0.000168
10	30	14.3395	9.6373	14.4385	119.2774	0.000168
11	30	14.3395	9.6373	14.4385	119.2774	0.000168

to $\tan^2 \theta$ have been used following the treatment of Heavens & Cheesman (1950).

When the search routine has been completed, a test is made to establish that the system of equations is in fact overdetermined. If this proves to be the case, its solution is attempted using the algorithm developed by Businger & Golub (1965), incorporated in the program as an ALGOL procedure. A new reciprocal cell is derived from the solution vector, and from this a new table of calculated Q values is formed and the process repeated. The program will continue to cycle until the standard deviation of the difference between observed and calculated Q values remains unchanged from cycle to cycle. This criterion is somewhat arbitrary, but has been found to work well. The final output consists of the refined direct-cell constants. For each line it also shows the indices based on that cell, the observed and calculated Q values and the discrepancy between them, and also the reliability criterion of de Wolff (1961).

This program has now been in use in this laboratory for some months; in its present form it is capable of handling orthorhombic, monoclinic and triclinic cells, and during this period it has successfully refined tri-

clinic cells which resisted refinement by a program based on the inversion of the normal equation matrix; in fact, it was the failure of that method which prompted the development of the approach described here. Table 1 shows details of a typical refinement for a pseudo-hexagonal monoclinic cell, using thirty lines of the powder pattern. The number of cycles required to produce a refined cell naturally depends on the quality of the data, the size of the unit cell and the accuracy of the initial cell parameters; in this case the entire process took slightly more than six minutes to run through 11 cycles to completion. Copies of the program are available on request.

References

- BUERGER, M. J. (1966). *X-ray Crystallography*. New York: John Wiley.
 BUSINGER, P. & GOLUB, G. H. (1965). *Num. Math.* **7**, 269.
 COHEN, M. U. (1935). *Rev. Sci. Instrum.* **6**, 68.
 GOLUB, G. H. (1965). *Num. Math.* **7**, 206.
 HEAVENS, O. S. & CHEESMAN, G. H. (1950). *Acta Cryst.* **3**, 197.
 WOLFF, P. M. DE (1961). *Acta Cryst.* **14**, 579.

Acta Cryst. (1970). B26, 904

Refinement of the Structure of Ammonium Triiodide, NH_4I_3

BY G. H. CHEESMAN AND A. J. T. FINNEY

Chemistry Department, University of Tasmania, Hobart, Tasmania, Australia

(Received 5 May 1969)

A new study closely confirms the structure and dimensions ascribed by R.C.L. Mooney in 1935, but indicates the triiodide ion to be linear.

The initial investigation by Mooney (1935) into the structure of ammonium triiodide, NH_4I_3 , confirmed the assignment of this polyiodide to the orthorhombic system made by Groth (1908) on the basis of morphology. Mooney found that the unit cell contained four molecules and that the systematic absences were consistent with the space group $Pmcn$, limiting the atomic positions of the triiodide group to planes with x coordinates $x = \frac{1}{4}$ and $x = \frac{3}{4}$. The structural analysis was carried out through trial-and-error methods based on 144 qualitatively visually estimated intensities collected photographically by the oscillation method. She found the triiodide unit to be both non-linear (177°) and asymmetric with interiodine distances of 2.82 and 3.10 Å.

In view of the recent theoretical interest in crystalline polyiodides, in particular the work of Brown & Nunn (1966) on the configuration of the triiodide ion, it was considered worth while to attempt the refinement of this structure. In this connexion it was hoped that an examination of the thermal parameters of the triiodide iodine atoms would support their hypothesis that the asymmetric electrostatic environment of the anion stabilizes the asymmetric anion geometry.

This refinement confirms to a remarkable degree Mooney's structure for this compound.

Experimental

Crystals of ammonium triiodide suitable for X-ray analysis were prepared from a concentrated aqueous

solution of A.R. grade ammonium iodide and resublimed iodine. The composition of this solution was adjusted with reference to Briggs's (Briggs, Ballard, Alrich & Wikswo, 1940) phase diagram for the system iodine-ammonium iodide-water to ensure that the only solid phase formed on evaporation was the anhydrous triiodide. The crystals so prepared were freed from mother liquor by rapid suction filtration on a sintered glass disk and then rapidly transferred to a dry Lindemann glass tube which was then sealed. As ammonium triiodide readily decomposes with loss of iodine, a number of crystals were packed into the one tube and some of these intentionally destroyed during the sealing process in order to create a significant iodine partial pressure within the tube from the outset. It was found that specimens prepared in this way could be preserved intact out of the X-ray beam for periods in excess of one month. However, as Mooney observed, as soon as a small crystal was brought into the X-ray beam, decomposition began with free iodine being deposited on the tube walls adjacent to the crystal.

The cell dimensions as determined from single-crystal photographs agreed with those found by Mooney and the same systematic absences were observed. In Table 1 the cell dimensions measured in this study and those of Mooney are compared; for convenience in the subsequent refinement calculations the axial labelling has been changed to conform to *International Tables for X-ray Crystallography* (1952) standard orientation for space group $Pnma$.

Table 1. *Comparison of cell dimensions*

	This work	Mooney
<i>a</i>	10.819 Å	10.82 Å
<i>b</i>	6.640	6.64
<i>c</i>	9.662	9.66

Six levels of data about the *b* axis and the first level about the *a* axis were collected photographically using Zr-filtered Mo *K* radiation and a Nonius Weissenberg goniometer. All photographs used for intensity measurement were taken using multiple-film packs of four Ilford Industrial Type G films interleaved with tin foil. Intensities were measured by visual estimation against a calibrated strip and were brought to a common scale using the *a* axis data. The Lorentz-polarization correction was applied but no absorption correction was made as the instability of the compound in the X-ray beam necessitated the use of three separate crystals to record the 516 independent reflexions used in this refinement. The crystals used all had maximum dimensions less than 0.02 mm.

The refinement of the structure was carried out using a structure factors/least squares program developed for the Elliott 503 computer. The program makes use of the block-diagonal approximation to the full least-squares matrix and employs the Cruickshank, Pilling, Bujosa, Lovell & Truter (1961) weighting scheme. The scattering factor curves for iodine were taken from *International Tables for X-ray Crystallography* (1962), modified for the charge distribution of the triiodide unit and corrected for dispersion.

Refinement was commenced with the iodine atoms in the positions found by Mooney; at this stage the residual, $R = \sum (F_o - |F_c|) / \sum |F_o|$, stood at 0.32. Five least-square cycles were performed using isotropic temperature factors and a partial shift factor of 0.8. At this stage further refinement was attempted using anisotropic temperature factors, but no progress could be made until the contribution to the structure factors of the ammonium group nitrogen atom was included. A trial nitrogen position was assumed from the isomorphous compound CsI_3 , and after three further cycles with isotropic temperature factors, the refine-

ment with anisotropic factors progressed smoothly using a smaller partial shift factor at 0.5 to a final residual of 0.183. No attempt was made to refine the structure further by the inclusion of the ammonium group hydrogen atoms. The positional and temperature factor parameters of the ammonium group nitrogen atom and the triiodide anion iodine atoms are given in Table 2.

The positional parameters of the nitrogen atom are not very accurate as indicated by the estimated standard deviations. This not unexpected result is also reflected in the anisotropic temperature factors; the nitrogen atom values have an e.s.d. of 0.0175 as compared with 0.0024 for the iodine atoms. The significant interatomic distances and angles are given in Table 3.

Table 3. *Interatomic distances and angles*

I(1)–I(2)	3.1134 ± 0.0037, Å
I(2)–I(3)	2.7912 ± 0.0039
I(1)–I(2)–I(3)	180.0 ± 0.0022°
I(1)–N	3.624 ± 0.0678, 3.679 ± 0.0678 Å
I(3)–N	3.776 ± 0.0680, 3.875 ± 0.0680

Discussion

As stated above, this refinement supports the analysis made by Mooney in that it confirms her conclusions regarding the asymmetry of the triiodide ion.

However, the refinement gives no evidence for a nonlinear triiodide ion as reported by Mooney for this compound, and which others (Tasman & Boswijk, 1954; Mooney-Slater, 1959) have reported in the structures of other triiodides [CsI_3 and $(\text{C}_6\text{H}_5)_4\text{AsI}_3$]. It was thought at first that this discrepancy between this refinement and the previous work on ammonium triiodide and its analogues indicating an interbond angle of $\sim 176^\circ$ in the triiodide ion might be explained by the hypothesis that ammonium triiodide undergoes a phase transition in the temperature range 0–30°C. However, a preliminary survey of several physical properties of this compound, including nuclear quadrupole and nuclear magnetic resonances, has not yielded any evidence for such a transition. The struc-

Table 2. *Atomic parameters*

(a) Positional parameters (Å)

	<i>X</i>	<i>Z</i>
N	9.0356 ± 0.0637	4.5453 ± 0.0654
I(1)	1.6970 ± 0.0030	3.3540 ± 0.0025
I(2)	4.1242 ± 0.0027	5.3039 ± 0.0025
I(3)	6.2580 ± 0.0030	7.1033 ± 0.0029

Thermal parameters (Å²)

	<i>U</i> ₁₁	<i>U</i> ₂₂	<i>U</i> ₃₃	<i>U</i> ₁₂	<i>U</i> ₁₃	<i>U</i> ₂₃
N	0.0646	0.0614	0.0652	0.0	0.0	0.0
I(1)	0.0376	0.0306	0.0193	0.0	0.0	–0.0116
I(2)	0.0343	0.0317	0.0175	0.0	0.0	0.0
I(3)	0.0360	0.0392	0.0258	0.0	0.0	–0.0175

ture and crystallography of the tetraphenylarsonium triiodide (in which the bent triiodide ion is reported to have bonds of equal length) is sufficiently different from that of ammonium triiodide for environmental or packing effects to be responsible for differences in anion geometry. In the case of CsI_3 the structures are closely similar; a similar explanation can scarcely be envisaged. However, the most recent structural study (Tasman & Boswijk, 1954) was a refinement carried out by Fourier methods using 98 $0kl$ reflexions and we may question the reliability of the I-I-I interbond angle. In commencing our refinement with Mooney's positional parameters, the residual of 0.32 indicated clearly that her structure does not completely fit our observational data.

In the light of the studies made by Brown & Nunn on the effect of the crystalline environment on the configuration of the triiodide ion, the lattice field over the anion in ammonium triiodide is expected to be unsymmetrical, thus stabilizing the configuration with unequal interiodine bonds. This hypothesis is supported by the similarity of the thermal parameters of each of the three iodine atoms which together make up the anion. The short I-N distance of 3.624 Å may be evidence for a form of hydrogen bonding between the

ammonium group and the triiodide ion. This would raise the possibility of rotation or torsion of the cation about the $\text{N-H}\cdots\text{I}$ axis as is the case in NH_4I (Plumb & Hornig, 1953).

Copies of the observed and calculated structure factors listing are available from the authors upon request.

References

- BRIGGS, T. J., BALLARD, K. H., ALRICH, F. R. & WIKSWO, J. P. (1940). *J. Phys. Chem.* **44**, 325.
 BROWN, R. D. & NUNN, E. (1966). *Aust. J. Chem.* **19**, 1567.
 CRUICKSHANK, D. W. J., PILLING, D. E., BUJOSA, A., LOVELL, F. M. & TRUTER, M. R. (1961). *Intern. Tracts-Computer Sci. Technol. Appl.* Ed. PEPINSKY, ROBERTSON and SPEAKMAN, **4**, 32.
 GROTH, P. (1908). *Chemische Kristallographie*, Vol. 2. Leipzig: Engelmann.
International Tables for X-ray Crystallography (1952). Vol. I. Birmingham: Kynoch Press.
International Tables for X-ray Crystallography (1962). Vol. III. Birmingham: Kynoch Press.
 MOONEY, R. C. L. (1935). *Z. Kristallogr.* **90**, 143.
 MOONEY-SLATER, R. C. L. (1959). *Acta Cryst.* **12**, 187.
 PLUM, R. C. & HORNIG, D. F. (1953). *J. Chem. Phys.* **21**, 366.
 TASMAN, H. A. & BOSWIJK, K. H. (1955). *Acta Cryst.* **8**, 59.